Analysis Manual

DISCLAIMER

Developers and distributors assume no responsibility for the use of MIDAS Family Program (MIDAS CIVIL NX, MIDAS FEA, MIDAS FX+, MIDAS GEN NX, MIDAS Drawing, MIDAS SDS, MIDAS GTS, SoilWorks, MIDAS NFX ; hereinafter referred to as “MIDAS package”) or for the accuracy or validity of any results obtained from the MIDAS package.

Developers and distributors shall not be liable for loss of profit, loss of business, or financial loss which may be caused directly or indirectly by the MIDAS package, when used for any purpose or use, due to any defect or deficiency therein. Accordingly, the user is encouraged to fully understand the bases of the program and become familiar with the users manuals. The user shall also independently verify the results produced by the program.

INDEX

1. Numerical Analysis Model of MIDAS GEN NX

Numerical Analysis Model

The analysis model of a structure includes nodes (joints), elements and boundary conditions. Finite elements are used in data entry, representing members of the structure for numerical analysis, and nodes define the locations of such members. Boundary conditions represent the status of connections between the structure and neighboring structures such as foundations.

A structural analysis refers to mathematical simulations of a numerical analysis model of a structure. It allows the practicing structural engineers to investigate the behaviors of the structure likely subjected to anticipated eventual circumstances.

For a successful structural analysis, it should be premised that the structural properties and surrounding environmental conditions for the structure are defined correctly. External conditions such as loading conditions may be determined by applicable building codes or obtained by statistical approaches. **The structural properties, however, implicate a significant effect on the analysis results, as the results highly depend on modeling methods and the types of elements used to construct the numerical analysis model of the structure**. Finite elements, accordingly, should be carefully selected so that they represent the real structure as closely as possible. This can be accomplished by comprehensive understanding of the elements' stiffness properties that affect the behaviors of the real structure. However, it is not always easy and may be sometimes uneconomical to accurately reflect every stiffness property and material property of the structure in the numerical analysis model. Real structures generally comprise complex shapes and various material properties.

For practical reasons, the engineer may simplify or adjust the numerical analysis model as long as it does not deviate from the purpose of analysis. For example, the engineer may use beam elements for the analysis of shear walls rather than using planar elements (plate elements or plane stress elements) based on his/her judgment. In practice, modeling a shear wall as a wide column, represented by a beam element in lieu of a planar element, will produce reliable analysis results, if the height of the shear wall exceeds its width by five times. Also, in civil structures such as

bridges, it is more effective to use line elements (truss elements, beam elements, etc) rather than using planar elements (plate elements or plane stress elements) for modeling main girders, from the perspective of analysis time and practical design application.

The analysis model of a building structure can be significantly simplified if rigid diaphragm actions can be assumed for the lateral force analysis. In such a case, floors can be excluded from the building model by implementing proper geometric constraints without having to model the floors with finite elements.

Finite elements mathematically idealize the structural characteristics of members that constitute a structure. Nevertheless, the elements cannot perfectly represent the structural characteristics of all the members in all circumstances. As noted earlier, you are encouraged to choose elements carefully only after comprehensive understanding of the characteristics of elements. The boundaries and connectivities of the elements must reflect their behaviors related to nodal degrees of freedom.

Coordinate Systems and Nodes

MIDAS GEN NX provides the following coordinate systems:

- **Global Coordinate System (GCS)**
- **Element Coordinate System (ECS)**
- **Node local Coordinate System (NCS)**

The GCS (Global Coordinate System) uses capital lettered "X-Y-Z axes" in the conventional Cartesian coordinate system, following the right hand rule. The GCS is used for node data, the majority of data entries associated with nodes and all the results associated with nodes such as nodal displacements and reactions.

The GCS defines the geometric location of the structure to be analyzed, and its reference point (origin) is automatically set at the location, X=0, Y=0 and Z=0, by the program. Since the vertical direction of the program screen represents the Z-axis in MIDAS GEN NX, it is convenient to enter the vertical direction of the structure to be parallel with the Z-axis in the GCS. **The Element Coordinate System (ECS) uses lower case "x-y-z axes" in the conventional Cartesian coordinate system, following the right hand rule**. Analysis results such as element forces and stresses and the majority of data entries associated with elements are expressed in the local coordinate system.

See "Types of elements and important considerations" in Numerical analysis model in MIDAS GEN

The Node local Coordinate System (NCS) is used to define input data associated with nodal boundary conditions such as nodal constraints, nodal spring supports and specified nodal displacements, in an unusual coordinate system that does not coincide with the GCS. The NCS is also used for producing reactions in an arbitrary coordinate system. **The NCS uses lower case "x-y-z axes" in the conventional Cartesian coordinate system, following the right hand rule**.

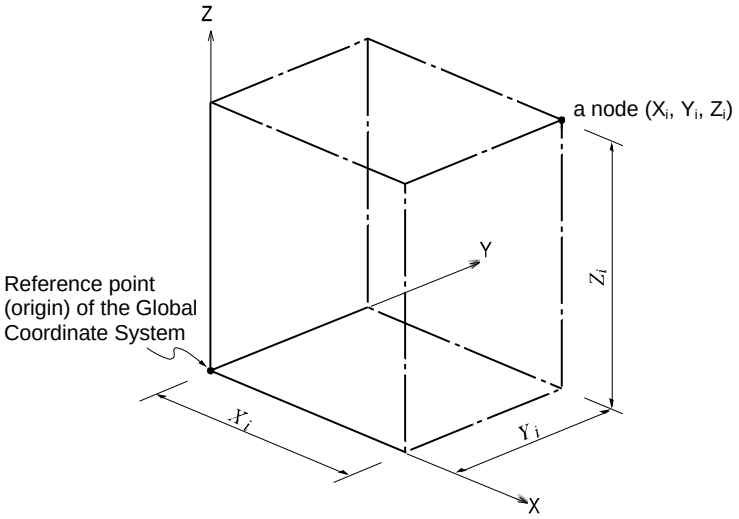

Figure 1.1 Global Coordinate System and Nodal Coordinates

Types of Elements and Important Considerations

The MIDAS GEN NX element library consists of the following elements:

- **Truss Element**
- **Tension-only Element (Hook and Cable function included)**
- **Compression-only Element (Gap function included)**
- **Beam Element/Tapered Beam Element**
- **Plane Stress Element**
- **Plate Element**
- **Two-dimensional Plane Strain Element**
- **Two-dimensional Axisymmetric Element**
- **Solid Element**
- **Wall Element**

Defining the types of elements, element material properties and element stiffness data completes data entry for finite elements. Connecting node numbers are then specified to define the locations, shapes and sizes of elements.

Truss Element

Introduction

A truss element is a two-node, uniaxial tension-compression three-dimensional line element. The element is generally used to model space trusses or diagonal braces. **The element undergoes axial deformation only**.

Element d.o.f. and ECS

All element forces and stresses are expressed with respect to the ECS. Especially, the ECS is consistently used to specify shear and flexural stiffness of beam elements.

Only the ECS x-axis is structurally significant for the elements retaining axial stiffness only, such as truss elements and tension-only/compression-only

elements. The ECS y and z-axes, however, are required to orient truss members' cross-sections displayed graphically.

MIDAS GEN NX uses the Beta Angle (β) conventions to identify the orientation of each cross-section. The Beta Angle relates the ECS to the GCS. The ECS x-axis starts from node N1 and passes through node N2 for all line elements (Figures 1.2 and 1.3). The ECS z-axis is defined to be parallel with the direction of "H" dimension of cross-sections (Figure 1.48). That is, the y-axis is in the strong axis direction. The use of the right-hand rule prevails in the process.

If the ECS x-axis for a line element is parallel with the GCS Z-axis, the Beta angle is defined as the angle formed from the GCS X-axis to the ECS z-axis. The ECS x-axis becomes the axis of rotation for determining the angle using the right-hand rule. If the ECS x-axis is not parallel with the GCS Z-axis, the Beta angle is defined as the right angle to the ECS x-z plane from the GCS Z-axis.

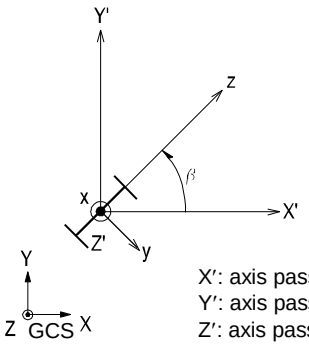

X′: axis passing through node N1 and parallel with the global X-axis
Y′: axis passing through node N1 and parallel with the global Y-axis
Z′: axis passing through node N1 and parallel with the global Z-axis

(a) Case of vertical members (ECS x-axis is parallel with the global Z-axis)

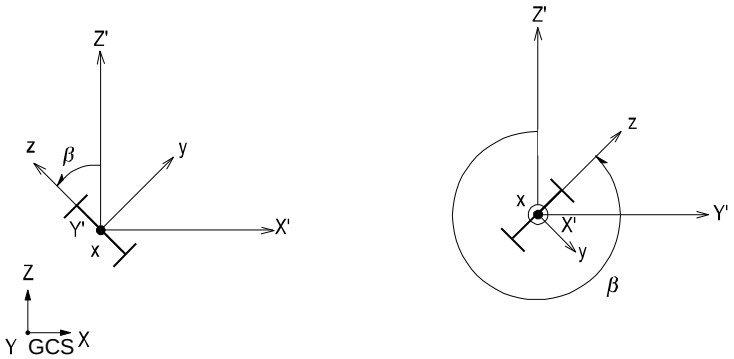

(b) Case of horizontal or diagonal members
(ECS x-axis is not parallel with the global Z-axis.)

Figure 1.2 Beta Angle Conventions

Functions related to the elements

Create Elements
Material: Material properties
Section: Cross-sectional properties
Pretension Loads

Output for element forces

The sign convention for truss element forces is shown in Figure 1.3. The arrows represent the positive (+) directions.

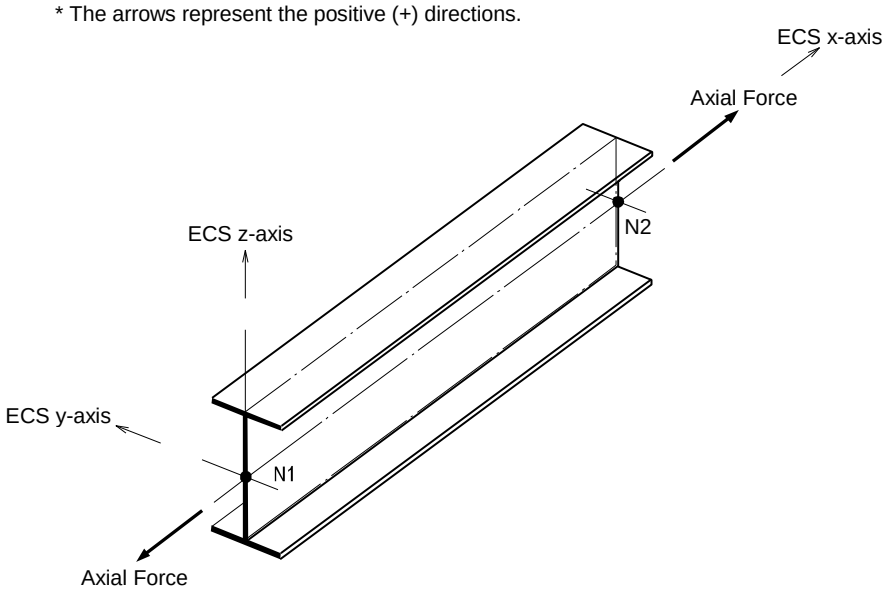

Figure 1.3 ECS of a truss element and the sign convention for element forces (or element stresses)

TRUSS ELEMENT FORCES DEFAULT PRINTOUT Unit System : kN , m

ELEM	MAT	SEC	LC	FORCE-I	FORCE-J
20	1	6	sLCB1	-22.81527	-22.77868
			sLCB2	-20.20131	-20.16994
			sLCB3	-27.16766	-27.13630
21	1	6	sLCB1	-42.00574	-41.93256
			sLCB2	-36.21717	-36.15445
			sLCB3	-49.17972	-49.11699
22	1	6	sLCB1	-43.48228	-43.37251
			sLCB2	-36.49496	-36.40087
			sLCB3	-50.08010	-49.98602

Figure 1.4 Sample Output for truss element forces

TRUSS ELEMENT STRESSES DEFAULT PRINTOUT Unit System : N , mm

ELEM	MAT	SEC	LC	STRESS-I	STRESS-J
20	1	6	sLCB1	-16.8006	-16.7737
			sLCB2	-14.8758	-14.8527
			sLCB3	-20.0056	-19.9825
21	1	6	sLCB1	-30.9321	-30.8782
			sLCB2	-26.6695	-26.6233
			sLCB3	-36.2148	-36.1686
22	1	6	sLCB1	-32.0194	-31.9385
			sLCB2	-26.8740	-26.8048
			sLCB3	-36.8778	-36.8086

Figure 1.5 Sample Output for truss element stresses

Tension-only Element

Introduction

Two nodes define a tension-only, three-dimensional line element. The element is generally used to model wind braces and hook elements. **This element undergoes axial tension deformation only**.

The tension-only elements include the following types:

Refer to"Analysis> Main Control Data" of On-line Manual.

Truss: A truss element transmits axial tension forces only.
Hook: A hook element retains a specified initial hook distance. The element stiffness is engaged after the tension deformation exceeds that distance.

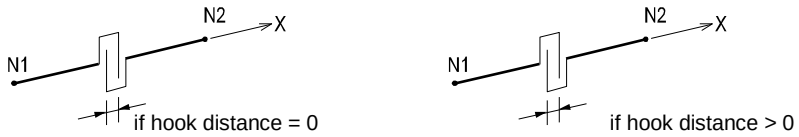

(a) Truss Type (b) Hook Type

Figure 1.6-1 Schematics of tension-only elements

Element d.o.f. and the ECS

The element d.o.f. and the ECS of a tension-only element are identical to that of a truss element.

Functions related to the elements

Main Control Data: Convergence conditions are identified for Iterative Analysis using tension-only elements.
Material: Material properties
Section: Cross-sectional properties
Pretension Loads

A nonlinear structural analysis reflects the change in stiffness due to varying member forces. The iterative analysis means to carry out the analysis repeatedly until the analysis results satisfy the given convergence conditions.

Output for element forces

Tension-only elements use the same sign convention as truss elements.

Cable Element

Introduction

Two nodes define a tension-only, three-dimensional line element, which is capable of transmitting axial tension force only. A cable element reflects the change in stiffness varying with internal tension forces.

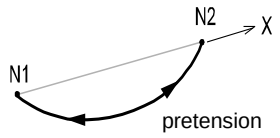

Figure 1.6-2 Schematics of a cable element

A cable element is automatically transformed into an equivalent truss element and an elastic catenary cable element in the cases of a linear analysis and a geometric nonlinear analysis respectively.

Equivalent truss element

The stiffness of an equivalent truss element is composed of the usual elastic stiffness and the stiffness resulting from the sag, which depends on the magnitude of the tension force. The following expressions calculate the stiffness:

$$K_{comb} = \frac{1}{1/K_{sag} + 1/K_{elastic}}$$

$$K_{comb} = \frac{EA}{L\left[1 + \frac{\omega^2 L^2 EA}{12T^3}\right]}$$

$$K_{elastic} = \frac{EA}{L}\ ,\ K_{sag} = \frac{12T^3}{\omega^2 L^3}$$

where, E: modulus of elasticity
A: cross-sectional area
L: length
w: weight per unit length
T: tension force

Elastic Catenary Cable Element

The tangent stiffness of a cable element applied to a geometric nonlinear analysis is calculated as follows:

Figure 1.6-3 illustrates a cable connected by two nodes where displacements Δ_1, Δ_2 & Δ_3 occur at Node i and Δ_4, Δ_5 & Δ_6 occur at Node j, and as a result the nodal forces F^0_1, F^0_2, F^0_3, F^0_4, F^0_5, F^0_6 are transformed into F_1, F_2, F_3, F_4, F_5, F_6 respectively. Then, the equilibriums of the nodal forces and displacements are expressed as follows:

$$F_4 = -F_1$$
$$F_5 = -F_2$$
$$F_6 = -F_3 - \omega_0 L_0 \quad \text{(except, } \omega_0 = \omega \text{ assumed)}$$
$$l_x = l_{x0} - \Delta_1 + \Delta_4 = f(F_1, F_2, F_3)$$
$$l_y = l_{y0} - \Delta_2 + \Delta_5 = g(F_1, F_2, F_3)$$
$$l_z = l_{z0} - \Delta_3 + \Delta_6 = h(F_1, F_2, F_3)$$

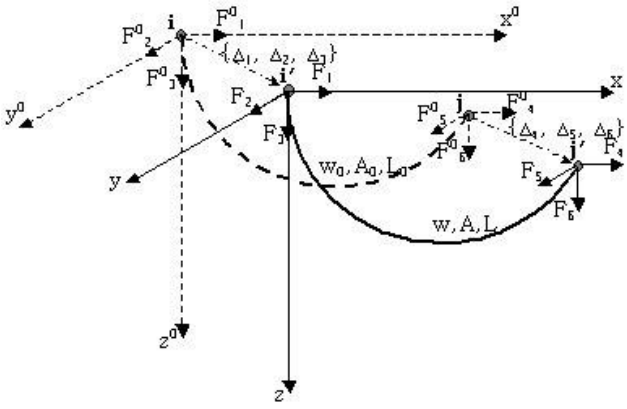

Figure 1.6-3 Schematics of tangent stiffness of an elastic catenary cable element

The differential equations for each directional length of the cable in the Global Coordinate System are noted below. When we rearrange the load-displacement relations we can then obtain the flexibility matrix, ([F]). The tangent stiffness, ([K]), of the cable can be obtained by inverting the flexibility matrix. The stiffness of the cable cannot be obtained immediately rather repeated analyses are carried out until it reaches an equilibrium state.

$$dl_x = \frac{\partial f}{\partial F_1} dF_1 + \frac{\partial f}{\partial F_2} dF_2 + \frac{\partial f}{\partial F_3} dF_3$$

$$dl_y = \frac{\partial g}{\partial F_1} dF_1 + \frac{\partial g}{\partial F_2} dF_2 + \frac{\partial g}{\partial F_3} dF_3$$

$$dl_z = \frac{\partial h}{\partial F_1} dF_1 + \frac{\partial h}{\partial F_2} dF_2 + \frac{\partial h}{\partial F_3} dF_3$$

$$\begin{Bmatrix} dl_x \\ dl_y \\ dl_z \end{Bmatrix} = [\mathbf{F}] \begin{Bmatrix} dF_1 \\ dF_2 \\ dF_3 \end{Bmatrix}, \quad \left([\mathbf{F}] = \begin{bmatrix} \frac{\partial f}{\partial F_1} & \frac{\partial f}{\partial F_2} & \frac{\partial f}{\partial F_3} \\ \frac{\partial g}{\partial F_1} & \frac{\partial g}{\partial F_2} & \frac{\partial g}{\partial F_3} \\ \frac{\partial h}{\partial F_1} & \frac{\partial h}{\partial F_2} & \frac{\partial h}{\partial F_3} \end{bmatrix} = \begin{bmatrix} f_{11} & f_{12} & f_{13} \\ f_{21} & f_{22} & f_{23} \\ f_{31} & f_{32} & f_{33} \end{bmatrix} \right)$$

$$\begin{Bmatrix} dF_1 \\ dF_2 \\ dF_3 \end{Bmatrix} = [\mathbf{K}] \begin{Bmatrix} dl_x \\ dl_y \\ dl_z \end{Bmatrix}, \quad (K = F^{-1})$$

The components of the flexibility matrix are expressed in the following equations:

$$f_{11} = \frac{\partial f}{\partial F_1} = -\frac{L_0}{EA_0} - \frac{1}{w}\left[\ln\{F_3 + wL_0 + B\} - \ln\{F_3 + A\}\right] - \frac{F_1^2}{w}\left[\frac{1}{B^2 + (F_3 + wL_0)B} - \frac{1}{A^2 + F_3 A}\right]$$

$$f_{12} = \frac{\partial f}{\partial F_2} = -\frac{F_1 F_2}{w}\left[\frac{1}{B^2 + (F_3 + wL_0)B} - \frac{1}{A^2 + F_3 A}\right]$$

$$f_{13} = \frac{\partial f}{\partial F_3} = -\frac{F_1}{w}\left[\frac{F_3 + wL_0 + B}{B^2 + (F_3 + wL_0)B} - \frac{F_3 + A}{A^2 + F_3 A}\right]$$

$$f_{21} = \frac{\partial g}{\partial F_1} = f_{12}$$

$$f_{22} = \frac{\partial g}{\partial F_2} = -\frac{L_0}{EA_0} - \frac{1}{w}\left[\ln\{F_3 + wL_0 + B\} - \ln\{F_3 + A\}\right] - \frac{F_2^2}{w}\left[\frac{1}{B^2 + (F_3 + wL_0)B} - \frac{1}{A^2 + F_3 A}\right]$$

$$f_{23} = \frac{\partial g}{\partial F_3} = \frac{F_2}{F_1} f_{13}$$

$$f_{31} = \frac{\partial h}{\partial F_1} = -\frac{F_1}{w}\left[\frac{1}{B} - \frac{1}{A}\right]$$

$$f_{32} = \frac{\partial h}{\partial F_2} = \frac{F_2}{F_1} f_{31}$$

$$f_{33} = \frac{\partial h}{\partial F_3} = -\frac{L_0}{EA_0} - \frac{1}{w}\left[\frac{F_3 + wL_0}{B} - \frac{F_3}{A}\right]$$

$$A = \left(F_1^2 + F_2^2 + F_3^2\right)^{1/2}, \quad B = \left(F_1^2 + F_2^2 + (F_3 + wL_0)^2\right)^{1/2}$$

$$\{d\mathbf{F}\} = \mathbf{K}_T \{d\Delta\}$$

(where, $\mathbf{K}_T = \begin{bmatrix} \frac{\partial F_1}{\partial \Delta_1} & \frac{\partial F_1}{\partial \Delta_2} & \frac{\partial F_1}{\partial \Delta_3} & \frac{\partial F_1}{\partial \Delta_4} & \frac{\partial F_1}{\partial \Delta_5} & \frac{\partial F_1}{\partial \Delta_6} \\ \frac{\partial F_2}{\partial \Delta_1} & \frac{\partial F_2}{\partial \Delta_2} & \frac{\partial F_2}{\partial \Delta_3} & \frac{\partial F_2}{\partial \Delta_4} & \frac{\partial F_2}{\partial \Delta_5} & \frac{\partial F_2}{\partial \Delta_6} \\ \frac{\partial F_3}{\partial \Delta_1} & \frac{\partial F_3}{\partial \Delta_2} & \frac{\partial F_3}{\partial \Delta_3} & \frac{\partial F_3}{\partial \Delta_4} & \frac{\partial F_3}{\partial \Delta_5} & \frac{\partial F_3}{\partial \Delta_6} \\ -\frac{\partial F_1}{\partial \Delta_1} & -\frac{\partial F_1}{\partial \Delta_2} & -\frac{\partial F_1}{\partial \Delta_3} & -\frac{\partial F_1}{\partial \Delta_4} & -\frac{\partial F_1}{\partial \Delta_5} & -\frac{\partial F_1}{\partial \Delta_6} \\ -\frac{\partial F_1}{\partial \Delta_1} & -\frac{\partial F_2}{\partial \Delta_2} & -\frac{\partial F_2}{\partial \Delta_3} & -\frac{\partial F_2}{\partial \Delta_4} & -\frac{\partial F_2}{\partial \Delta_5} & -\frac{\partial F_2}{\partial \Delta_6} \\ -\frac{\partial F_1}{\partial \Delta_1} & -\frac{\partial F_3}{\partial \Delta_2} & -\frac{\partial F_3}{\partial \Delta_3} & -\frac{\partial F_3}{\partial \Delta_4} & -\frac{\partial F_3}{\partial \Delta_5} & -\frac{\partial F_3}{\partial \Delta_6} \end{bmatrix} = \begin{bmatrix} \mathbf{F}_{ii} & \mathbf{F}_{ij} \\ -\mathbf{F}_{ii} & -\mathbf{F}_{ij} \end{bmatrix}$)

Compression-only Element

Introduction

Two nodes define a compression-only, three-dimensional line element. The element is generally used to model contact conditions and support boundary conditions. **The element undergoes axial compression deformation only**.

The compression-only elements include the following types:

Truss: A truss element transmits axial compression forces only.
Gap: A gap element retains a specified initial gap distance. The element stiffness is engaged after the compression deformation exceeds that distance.

Element d.o.f. and the ECS

See "Analysis> Main Control Data" of On-line Manual.

The element d.o.f. and the ECS of a compression-only element are identical to that of a truss element.

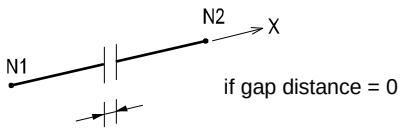

(a) Truss Type

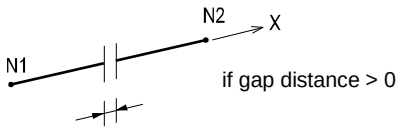

(b) Gap Type

Figure 1.7 Schematics of compression-only elements

Functions related to the elements

Main Control Data: Convergence conditions are identified for Iterative Analysis using tension/compression-only elements.
Material: Material properties
Section: Cross-sectional properties
Pretension Loads

Output for element forces

Compression-only elements use the same sign convention as truss elements.

Beam Element

Introduction

Two nodes define a Prismatic/Non-prismatic, three-dimensional beam element. Its formulation is founded on the **Timoshenko Beam theory taking into account the stiffness effects of tension/compression, shear, bending and torsional deformations**. In the Section Dialog Box, only one section is defined for a prismatic beam element whereas, two sections corresponding to each end are required for a non-prismatic beam element.

MIDAS GEN NX assumes linear variations for cross-sectional areas, effective shear areas and torsional stiffness along the length of a non-prismatic element. For moments of inertia about the major and minor axes, you may select a linear, parabolic or cubic variation.

See "Model> Properties>Section" of On-line Manual.

Element d.o.f. and the ECS

Each node retains three translational and three rotational d.o.f. irrespective of the ECS or GCS.

The ECS for the element is identical to that for a truss element.

Functions related to the elements

Create Elements
Material: Material properties
Section: Cross-sectional properties
Beam End Release: Boundary conditions at each end (end-release, fixed or hinged)
Beam End Offsets: Rigid end offset distance
Element Beam Loads: Beam loads (In-span concentrated loads or distributed loads)
Line Beam Loads: Beam loads within a specified range
Assign Floor Load: Floor loads converted into beam loads
Prestress Beam Load: Prestress or posttension loads
Temperature Gradient

Output for element forces

The sign convention for beam element forces is shown in Figure 1.8. The arrows represent the positive (+) directions. Element stresses follow the same sign convention. However, stresses due to bending moments are denoted by '+' for tension and '-' for compression.

* The arrows represent the positive (+) directions of element forces.

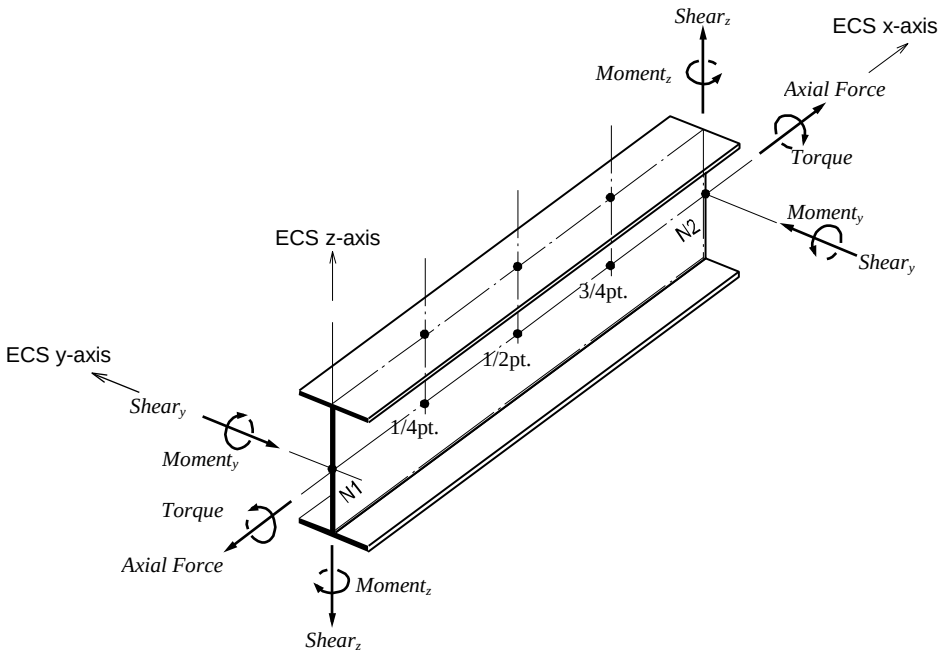

Figure 1.8 Sign convention for ECS and element forces (or stresses) of a beam element

BEAM ELEMENT FORCES & MOMENTS DEFAULT PRINTOUT Unit System : kN , m

ELEM	MAT	SEC	LC	PT	AXIAL	SHEAR-y	SHEAR-z	TORSION	MOMENT-y	MOMENT-z
1	1	1	sLCB1	I	-279.92428	4.87200	-12.40971	0.0000	0.0000	0.0000
				1/4	-279.24433	4.87200	-12.40971	0.0000	9.3073	-3.6540
				CNT	-278.56438	4.87200	-12.40971	0.0000	18.6146	-7.3080
				3/4	-277.88443	4.87200	-12.40971	0.0000	27.9219	-10.9620
				J	-277.20447	4.87200	-12.40971	0.0000	37.2291	-14.6160
			sLCB2	I	-504.10488	9.77588	-22.48581	0.0000	0.0000	0.0000
				1/4	-503.52207	9.77588	-22.48581	0.0000	16.8644	-7.3319
				CNT	-502.93925	9.77588	-22.48581	0.0000	33.7287	-14.6638
				3/4	-502.35643	9.77588	-22.48581	0.0000	50.5931	-21.9957
				J	-501.77362	9.77588	-22.48581	0.0000	67.4574	-29.3276
			sLCB3	I	-515.26489	9.78124	-23.07798	0.0000	0.0000	0.0000
				1/4	-514.68208	9.78124	-23.07798	0.0000	17.3085	-7.3359
				CNT	-514.09926	9.78124	-23.07798	0.0000	34.6170	-14.6719
				3/4	-513.51644	9.78124	-23.07798	0.0000	51.9254	-22.0078
				J	-512.93363	9.78124	-23.07798	0.0000	69.2339	-29.3437

Figure 1.8.1 Sample output of beam element forces

BEAM ELEMENT STRESSES DEFAULT PRINTOUT Unit System : N , mm

ELEM	MAT	SEC	LC	PT	AXIAL	SHEAR-y	SHEAR-z	(+y)-BENDING	(-y)	(+z)-BENDING	(-z)
1	1	1	sLCB1	I	-33.2768	1.4000	-4.2084	0.0000	0.0000	0.0000	0.0000
				1/4	-33.1959	1.4000	-4.2084	21.0000	-21.0000	-7.8542	7.8542
				CNT	-33.1151	1.4000	-4.2084	42.0000	-42.0000	-15.7085	15.7085
				3/4	-33.0343	1.4000	-4.2084	63.0000	-63.0000	-23.5627	23.5627
				J	-32.9535	1.4000	-4.2084	84.0000	-84.0000	-31.4170	31.4170
			sLCB2	I	-59.9269	2.8092	-7.6254	0.0000	0.0000	0.0000	0.0000
				1/4	-59.8576	2.8092	-7.6254	42.1374	-42.1374	-14.2315	14.2315
				CNT	-59.7883	2.8092	-7.6254	84.2748	-84.2748	-28.4630	28.4630
				3/4	-59.7190	2.8092	-7.6254	126.4122	-126.4122	-42.6946	42.6946
				J	-59.6497	2.8092	-7.6254	168.5496	-168.5496	-56.9261	56.9261
			sLCB3	I	-61.2536	2.8107	-7.8263	0.0000	0.0000	0.0000	0.0000
				1/4	-61.1843	2.8107	-7.8263	42.1605	-42.1605	-14.6063	14.6063
				CNT	-61.1150	2.8107	-7.8263	84.3210	-84.3210	-29.2126	29.2126
				3/4	-61.0457	2.8107	-7.8263	126.4816	-126.4816	-43.8189	43.8189
				J	-60.9764	2.8107	-7.8263	168.6421	-168.6421	-58.4253	58.4253

Figure 1.8.2 Sample output of beam element stresses

Plane Stress Element

Introduction

Three or four nodes placed in the same plane define a plane stress element. The element is generally used to model membranes that have a uniform thickness over the plane of each element. Loads can be applied only in the direction of its own plane.

This element is formulated according to the Isoparametric Plane Stress Formulation with Incompatible Modes. Thus, **it is premised that no stress components exist in the out-of-plane directions and that the strains in the out-of-plane directions can be obtained on the basis of the Poisson's effects**.

Element d.o.f. and the ECS

The element retains displacement d.o.f. in the ECS x and y-directions only.

The ECS uses x, y & z-axes in the Cartesian coordinate system, following the right hand rule. The directions of the ECS axes are defined as presented in Figure 1.9.

In the case of a quadrilateral (4-node) element, the thumb direction signifies the ECS z-axis. The rotational direction (**N1→N2→N3→N4**) following the right hand rule determines the thumb direction. The ECS z-axis originates from the center of the element surface and is perpendicular to the element surface. The line connecting the mid point of N1 and N4 to the mid point of N2 and N3 defines the direction of ECS x-axis. The perpendicular direction to the x-axis in the element plane now becomes the ECS y-axis by the right-hand rule.

For a triangular (3-node) element, the line parallel to the direction from N1 to N2, originating from the center of the element becomes the ECS x-axis. The y and z-axes are identically defined as those for the quadrilateral element.

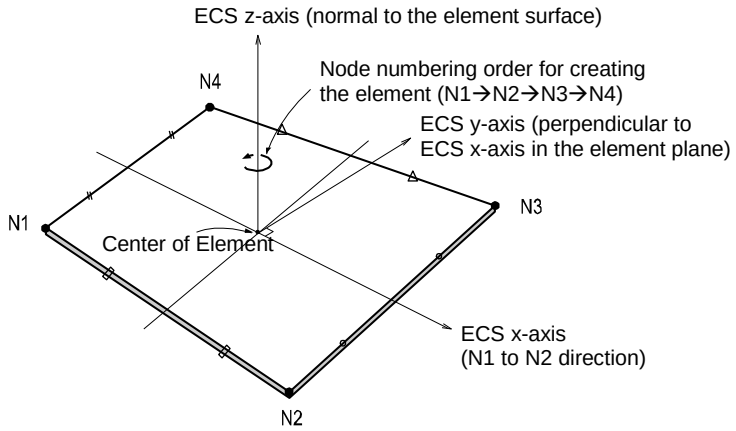

(a) ECS for a quadrilateral element

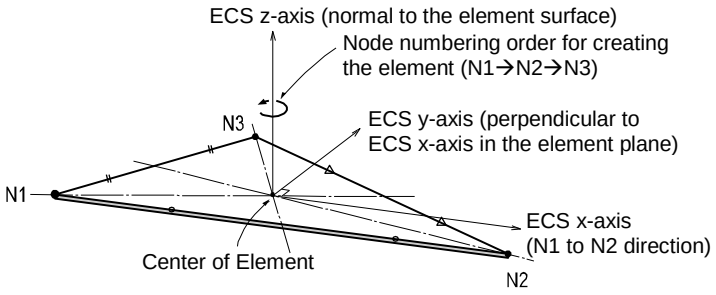

(b) ECS for a triangular element

Figure 1.9 Arrangement of plane stress elements and their ECS

Functions related to the elements

Create Elements
Material: Material properties
Thickness: Thickness of the element
Pressure Loads: Pressure loads acting normal to the edges of the element

Figure 1.10 illustrates pressure loads applied normal to the edges of a plane stress element.

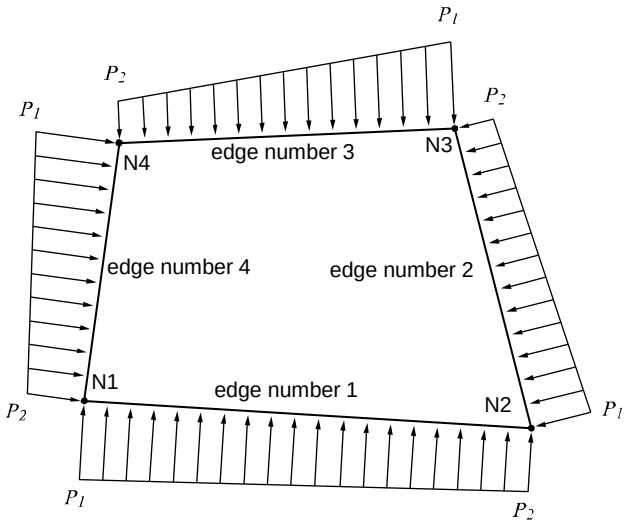

Figure 1.10 Pressure loads applied to a plane stress element

Output for element forces

The sign convention for element forces and element stresses is defined relative to either the ECS or GCS. The following descriptions are based on the ECS:

- **Output for element forces at connecting nodes**
- **Output for element stresses at connecting nodes and element centers**

At a connecting node, multiplying each nodal displacement component by the corresponding stiffness component of the element produces the element forces.

For stresses at the connecting nodes and element centers, the stresses calculated at the integration points (Gauss Points) are extrapolated.

- **Output for element forces**
  Figure 1.11 shows the sign convention for element forces. The arrows represent the positive (+) directions.

- **Output for element Stresses**
  Figure 1.12 shows the sign convention for element stresses. The arrows represent the positive (+) directions.

* Element forces are produced in the ECS and the arrows represent the positive (+) directions.

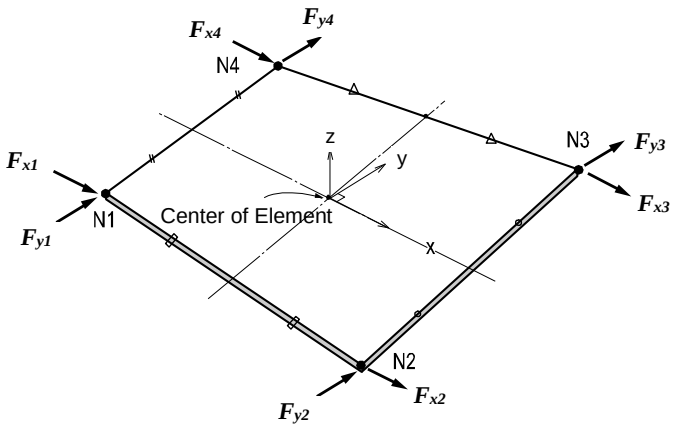

(a) Nodal forces for a quadrilateral element

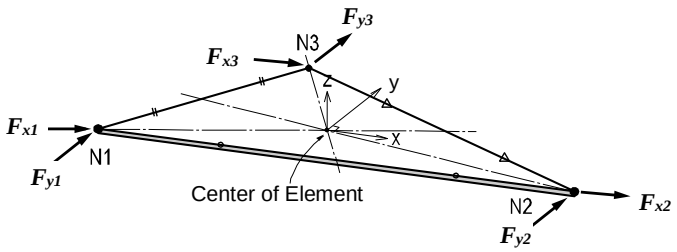

(b) Nodal forces for a triangular element

Figure 1.11 Sign convention for nodal forces at each node of plane stress elements

* Element stresses are produced in the ECS and the arrows represent the positive (+) directions.

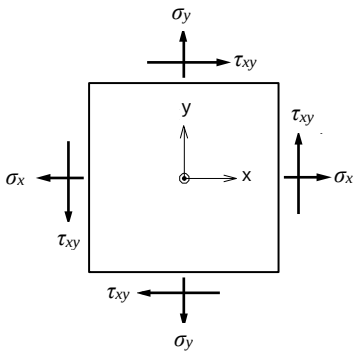

(a) Axial and shear stress components

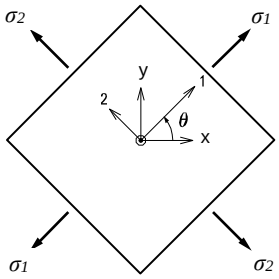

(b) Principal stress components

σ_x : Axial stress in the ECS x - direction

σ_x : Axial stress in the ECS y - direction

τ_{xy} : Shear stress in the ECS x - y plane

$$\sigma_1 : \textit{Maximum principal stress} = \frac{\sigma_x+\sigma_y}{2}+\sqrt{\left(\frac{\sigma_x-\sigma_y}{2}\right)^2+\tau_{xy}^2}$$

$$\sigma_2 : \textit{Minimum principal stress} = \frac{\sigma_x+\sigma_y}{2}-\sqrt{\left(\frac{\sigma_x-\sigma_y}{2}\right)^2+\tau_{xy}^2}$$

$$\tau_{xy} : \textit{Maximum shear stress} = \sqrt{\left(\frac{\sigma_x-\sigma_y}{2}\right)^2+\tau_{xy}^2}$$

θ : Angle between the x - axis and the principal axis, 1

$$\sigma_{eff} : \textit{von-Mises Stress} = \sqrt{(\sigma_1^{\,2}-\sigma_1\sigma_2+\sigma_2^{\,2})}$$

Figure 1.12 Sign convention for plane stress element stresses

PLANE STRESS ELEMENT FORCES(LOCAL) DEFAULT PRINTOUT Unit System : lbf , in

ELEM	MAT	SEC	LC	NODE	Fx	Fy
1	1	1	LCOMB1	1	0.25	1.25
				2	0.25	-1.25
				10	-0.25	-1.25
				9	-0.25	1.25
			LCOMB2	1	0.75	3.75
				2	0.75	-3.75
				10	-0.75	-3.75
				9	-0.75	3.75
2	1	1	LCOMB1	2	0.25	1.25
				3	0.25	-1.25
				11	-0.25	-1.25
				10	-0.25	1.25
			LCOMB2	2	0.75	3.75
				3	0.75	-3.75
				11	-0.75	-3.75
				10	-0.75	3.75

Figure 1.13 Sample output of plane stress element forces

PLANE STRESS ELEMENT STRESSES(LOCAL) DEFAULT OUTPUT Unit System : lbf , in

ELEM	MAT	SEC	LC	NODE	Sig-xx	Sig-yy	Sig-xy	Sig-MAX	Sig-MIN	ANGLE	Sig-EFF
1	1	1	LCOMB1	Cent	0.0000	0.0000	-0.0022	0.0022	-0.0022	-45.00	0.0038
				1	0.0000	0.0000	-0.0022	0.0022	-0.0022	-45.00	0.0038
				2	0.0000	0.0000	-0.0022	0.0022	-0.0022	-45.00	0.0038
				10	0.0000	0.0000	-0.0022	0.0022	-0.0022	-45.00	0.0038
				9	0.0000	0.0000	-0.0022	0.0022	-0.0022	-45.00	0.0038
			LCOMB2	Cent	0.0000	0.0000	-0.0067	0.0067	-0.0067	-45.00	0.0115
				1	0.0000	0.0000	-0.0067	0.0067	-0.0067	-45.00	0.0115
				2	0.0000	0.0000	-0.0067	0.0067	-0.0067	-45.00	0.0115
				10	0.0000	0.0000	-0.0067	0.0067	-0.0067	-45.00	0.0115
				9	0.0000	0.0000	-0.0067	0.0067	-0.0067	-45.00	0.0115
2	1	1	LCOMB1	Cent	0.0000	0.0000	-0.0022	0.0022	-0.0022	-45.00	0.0038
				2	0.0000	0.0000	-0.0022	0.0022	-0.0022	-45.00	0.0038
				3	0.0000	0.0000	-0.0022	0.0022	-0.0022	-45.00	0.0038
				11	0.0000	0.0000	-0.0022	0.0022	-0.0022	-45.00	0.0038
				10	0.0000	0.0000	-0.0022	0.0022	-0.0022	-45.00	0.0038
			LCOMB2	Cent	0.0000	0.0000	-0.0067	0.0067	-0.0067	-45.00	0.0115
				2	0.0000	0.0000	-0.0067	0.0067	-0.0067	-45.00	0.0115
				3	0.0000	0.0000	-0.0067	0.0067	-0.0067	-45.00	0.0115
				11	0.0000	0.0000	-0.0067	0.0067	-0.0067	-45.00	0.0115
				10	0.0000	0.0000	-0.0067	0.0067	-0.0067	-45.00	0.0115

Figure 1.14 Sample output of plane stress element stresses

Two-Dimensional Plane Strain Element

Introduction

2-D Plane Strain Element is a suitable element type to model lengthy structures of uniform cross-sections such as dams and tunnels. The element is formulated on the basis of Isoparametric Plane Strain Formulation with Incompatible Modes.

The element cannot be combined with other types of elements. It is only applicable for linear static analyses due to the characteristics of the element.

Elements are entered in the X-Z plane and their thickness is automatically given a unit thickness as shown in Figure 1.15.

Because the formulation of the element is based on its plane strain properties, it is premised that strains in the out-of-plane directions do not exist. Stress components in the out-of-plane directions can be obtained only based on the Poisson's Effects.

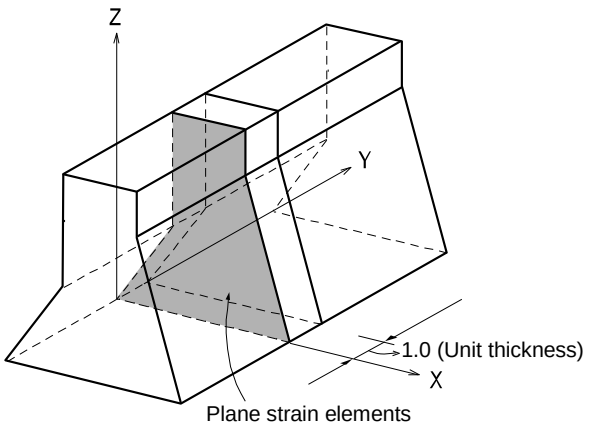

Figure 1.15 Thickness of two-dimensional plane strain elements

Element d.o.f. and the ECS

The ECS for plane strain elements is used when the program calculates the element stiffness matrices. Graphic displays for stress components are also depicted in the ECS in the post-processing mode.

The element d.o.f. exists only in the GCS X and Z-directions.

The ECS uses x, y & z-axes in the Cartesian coordinate system, following the right hand rule. The directions of the ECS axes are defined as presented in Figure 1.16.

In the case of a quadrilateral (4-node) element, the thumb direction signifies the ECS z-axis. The rotational direction (**N1→N2→N3→N4**) following the right hand rule determines the thumb direction. The ECS z-axis originates from the center of the element surface and is perpendicular to the element surface. The line connecting the mid point of N1 and N4 to the mid point of N2 and N3 defines the direction of ECS x-axis. The perpendicular direction to the x-axis in the element plane now becomes the ECS y-axis by the right-hand rule.

For a triangular (3-node) element, the line parallel to the direction from N1 to N2, originating from the center of the element becomes the ECS x-axis. The y and z-axes are identically defined as those for the quadrilateral element.

* Element forces are produced in the GCS and the arrows represent the positive (+) directions.

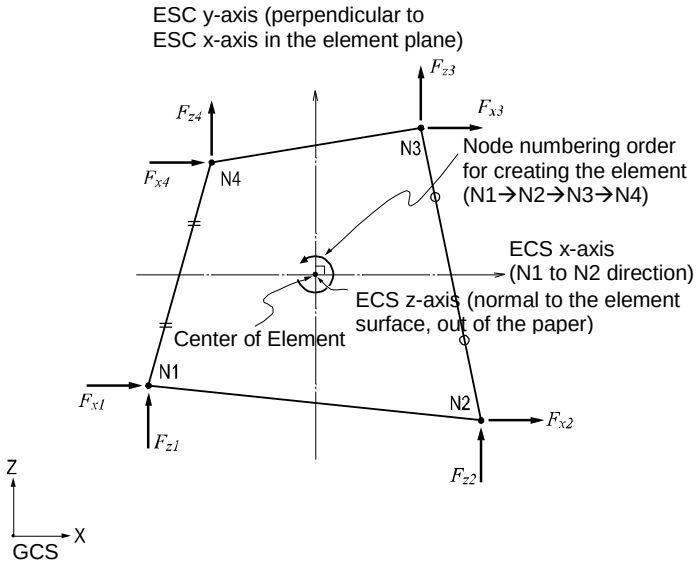

(a) Quadrilateral element

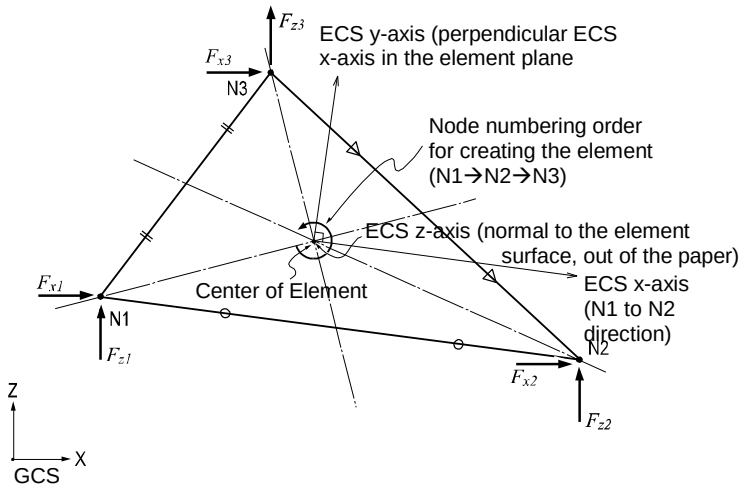

(b) Triangular element

Figure 1.16 Arrangement of plane strain elements, their ECS and nodal forces

Functions related to the elements

Create Elements
Material: Material properties
Pressure Loads: Pressure loads acting normal to the edges of the element

Figure 1.17 illustrates pressure loads applied normal to the edges of a plane strain element. The pressure loads are automatically applied to the unit thickness defined in Figure 1.15.

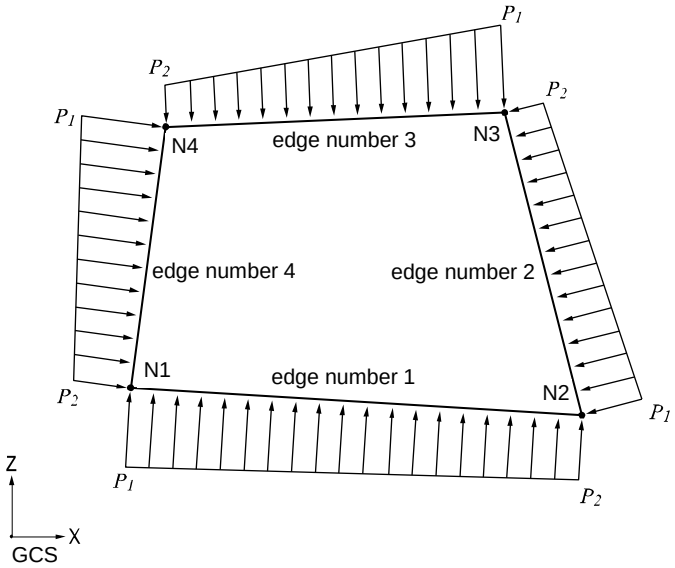

Figure 1.17 Pressure loads applied to a plane strain element

Output for element forces

The sign convention for plane strain element forces and stresses is defined relative to either the ECS or GCS. Figure 1.18 illustrates the sign convention relative to the ECS or principal stress directions of a unit segment.

- **Output for element forces at connecting nodes**
- **Output for element stresses at connecting nodes and element centers**

At a connecting node, multiplying each nodal displacement component by the corresponding stiffness component of the element produces the element forces.

For stresses at the connecting nodes and element centers, the stresses calculated at the integration points (Gauss Points) are extrapolated.

- **Output for element forces**
  Figure 1.16 shows the sign convention for element forces. The arrows represent the positive (+) directions.

- **Output for element stresses**
  Figure 1.18 shows the sign convention for element stresses. The arrows represent the positive (+) directions.

* Element stresses are produced in the ECS and the arrows represent the positive (+) directions.

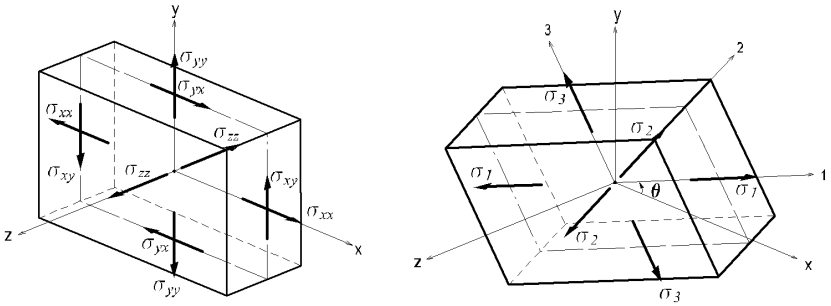

(a) Axial and shear stress components (b) Principal stress components

σ_{xx} : Axial stress in the ECS x-direction

σ_{yy} : Axial stress in the ECS y-direction

σ_{zz} : Axial stress in the ECS z-direction

$\sigma_{xy} = \sigma_{yx}$: Shear stress in the ECS x-y plane

$\sigma_1, \sigma_2, \sigma_3$: Principal stresses in the directions of the principal axes, 1,2 and 3

where, $\sigma^3 - I_1\sigma^2 - I_2\sigma - I_3 = 0$

$$I_1 = \sigma_{xx} + \sigma_{yy} + \sigma_{zz}$$

$$I_2 = -\begin{vmatrix} \sigma_{xx} & \sigma_{xy} \\ \sigma_{xy} & \sigma_{yy} \end{vmatrix} - \begin{vmatrix} \sigma_{xx} & \sigma_{xz} \\ \sigma_{xz} & \sigma_{zz} \end{vmatrix} - \begin{vmatrix} \sigma_{yy} & \sigma_{yz} \\ \sigma_{yz} & \sigma_{zz} \end{vmatrix}$$

$$I_3 = \begin{vmatrix} \sigma_{xx} & \sigma_{xy} & \sigma_{xz} \\ \sigma_{xy} & \sigma_{yy} & \sigma_{yz} \\ \sigma_{xz} & \sigma_{yz} & \sigma_{zz} \end{vmatrix}, \sigma_{xz} = \sigma_{zy} = 0$$

θ : Angle between the x-axis and the principal axis,1 in the ECS x-y plane

τ_{max} : Maximum shear stress $= max\left[\frac{\sigma_1 - \sigma_2}{2}, \frac{\sigma_2 - \sigma_3}{2}, \frac{\sigma_3 - \sigma_1}{2}\right]$

σ_{eff} : von-Mises Stress $= \sqrt{\frac{1}{2}\left[(\sigma_1 - \sigma_2)^2 - (\sigma_2 - \sigma_3)^2 - (\sigma_3 - \sigma_1)^2\right]}$

σ_{oct} : Octahedral Normal Stress $= \frac{1}{3}(\sigma_1 + \sigma_2 + \sigma_3)$

τ_{oct} : Octahedral Shear Stress $= \sqrt{\frac{1}{9}\left[(\sigma_1 - \sigma_2)^2 - (\sigma_2 - \sigma_3)^2 - (\sigma_3 - \sigma_1)^2\right]}$

Figure 1.18 Sign convention for plane strain element stresses

PLANE STRAIN ELEMENT FORCES(GLOBAL) DEFAULT OUTPUT Unit System : kN , m

ELEM	MAT	LC	NODE	FX	FZ
1	1	LCOMB1	1	0.00000	-792.25733
			2	-368.40881	-769.85496
			13	-434.10321	734.84737
			12	-69.04498	789.21492
		LCOMB2	1	0.00000	-1028.47676
			2	-352.46066	-978.32967
			13	-433.19898	947.23949
			12	-85.89736	1021.51694

Figure 1.19 Sample output of plane strain element forces

PLANE STRAIN ELEMENT STRESSES(GLOBAL) DEFAULT OUTPUT Unit System : N , mm

ELEM	MAT	LC	NODE	Sig-XX	Sig-YY	Sig-ZZ	Sig-XZ
1	1	LCOMB1	Cent	82.6287	0.0000	-1.9933	-3.7578
			1	82.3088	0.0000	-2.0162	-3.4446
			2	82.9937	0.0000	-2.0140	-3.4873
			13	82.9440	0.0000	-1.9716	-4.0557
			12	82.2564	0.0000	-1.9716	-4.0429

NODE	Sig-P1	Sig-P2	Sig-P3	MAX-SHR	Sig-EFF	Sig-Oct
Cent	82.7952	0.0000	-2.1599	42.4775	83.8960	39.5489
1	82.4492	0.0000	-2.1567	42.3030	83.5485	39.3851
2	83.1365	0.0000	-2.1568	42.6467	84.2356	39.7091
13	83.1373	0.0000	-2.1648	42.6511	84.2406	39.7114
12	82.4501	0.0000	-2.1652	42.3076	83.5537	39.3876

LC	NODE	Sig-XX	Sig-YY	Sig-ZZ	Sig-XZ
LCOMB2	Cent	82.6287	0.0000	-1.9933	-3.7578
	1	82.3088	0.0000	-2.0162	-3.4446
	2	82.9937	0.0000	-2.0140	-3.4873
	13	82.9440	0.0000	-1.9716	-4.0557
	12	82.2564	0.0000	-1.9716	-4.0429

NODE	Sig-P1	Sig-P2	Sig-P3	MAX-SHR	Sig-EFF	Sig-Oct
Cent	82.7952	0.0000	-2.1599	42.4775	83.8960	39.5489
1	82.4492	0.0000	-2.1567	42.3030	83.5485	39.3851
2	83.1365	0.0000	-2.1568	42.6467	84.2356	39.7091
13	83.1373	0.0000	-2.1648	42.6511	84.2406	39.7114
12	82.4501	0.0000	-2.1652	42.3076	83.5537	39.3876

Figure 1.20 Sample output of plane strain element stresses

Two-Dimensional Axisymmetric Element

Introduction

Two-Dimensional Axisymmetric Elements are suitable for modeling structures with a radial symmetry relative to geometries, material properties and loading conditions. Application examples may be pipes and cylindrical vessel bodies including heads. The elements are developed on the basis of the Isoparametric formulation theory. The element cannot be combined with other types of elements. It is only applicable for linear static analyses due to the characteristics of the element.

2-D axisymmetric elements are derived from 3-D axisymmetric elements by taking the radial symmetry into account. The GCS Z-axis is the axis of rotation. **The elements must be located in the global X-Z plane to the right of the global Z-axis**. In this case, the radial direction coincides with the GCS X-axis. The elements are modeled such that all the nodes retain positive X-coordinates ($X \geq 0$).

By default, the thickness of the element is automatically preset to a unit thickness (1.0 radian) as illustrated in Figure 1.21.

Because the formulation of the element is based on the axisymmetric properties, it is premised that circumferential displacements, shear strains (γ_{XY}, γ_{YZ}) and shear stresses (τ_{XY}, τ_{YZ}) do not exist.

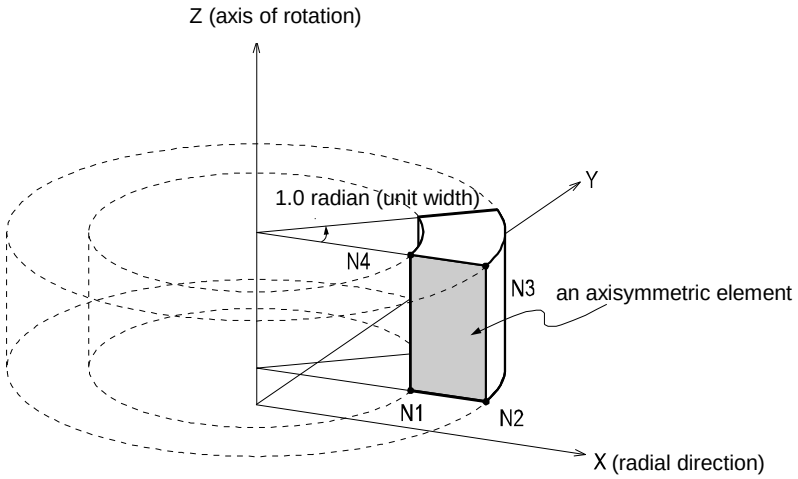

Figure 1.21 Unit width of an axisymmetric element

Element d.o.f. and the ECS

The ECS for axisymmetric elements is used when the program calculates the element stiffness matrices. Graphic displays for stress components are also depicted in the ECS in the post-processing mode.

The element d.o.f. exists only in the GCS X and Z-directions.

The ECS uses x, y & z-axes in the Cartesian coordinate system, following the right hand rule. The directions of the ECS axes are defined as presented in **Figure 1.22**.

In the case of a quadrilateral (4-node) element, the thumb direction signifies the ECS z-axis. The rotational direction (**N1→N2→N3→N4**) following the right hand rule determines the thumb direction. The ECS z-axis originates from the center of the element surface and is perpendicular to the element surface. The line connecting the mid point of N1 and N4 to the mid point of N2 and N3 defines the direction of ECS x-axis. The perpendicular direction to the x-axis in the element plane now becomes the ECS y-axis by the right-hand rule.

For a triangular (3-node) element, the line parallel to the direction from N1 to N2, originating from the center of the element becomes the ECS x-axis. The y and z-axes are identically defined as those for the quadrilateral element.

* Element stresses are produced in the GCS and the arrows represent the positive (+) directions.

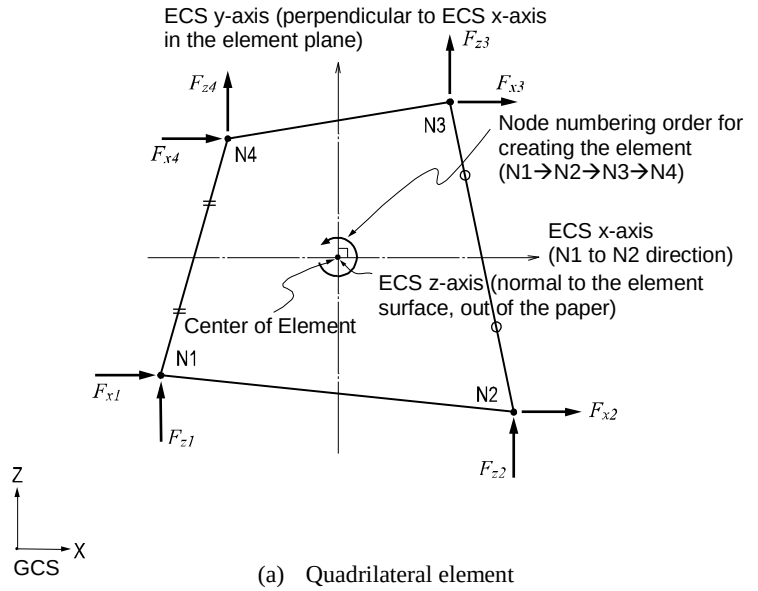

(a) Quadrilateral element

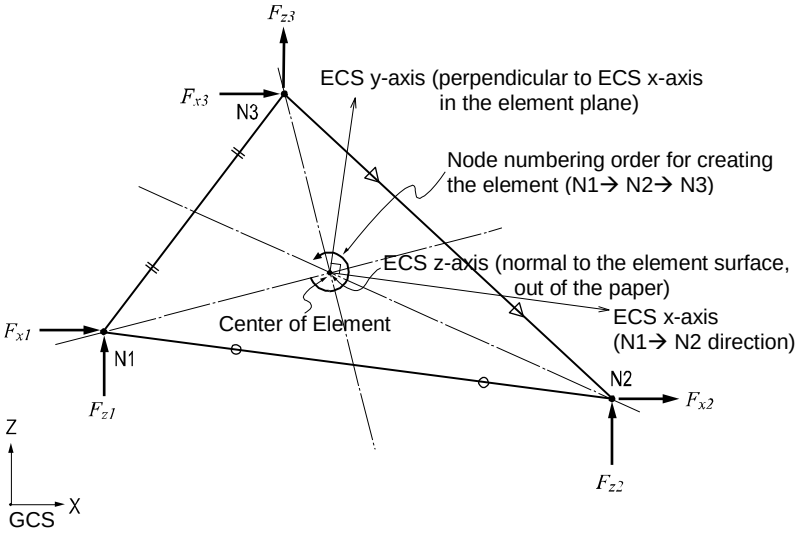

(b) Triangular element

Figure 1.22 Arrangement of axisymmetric elements, their ECS and nodal forces

Functions related to the elements

Create Elements
Material: Material properties
Pressure Loads: Pressure loads acting normal to the edges of the element

Figure 1.23 illustrates pressure loads applied normal to the edges of an axisymmetric element. The pressure loads are automatically applied to the width of 1.0 Radian as defined in Figure 1.21.

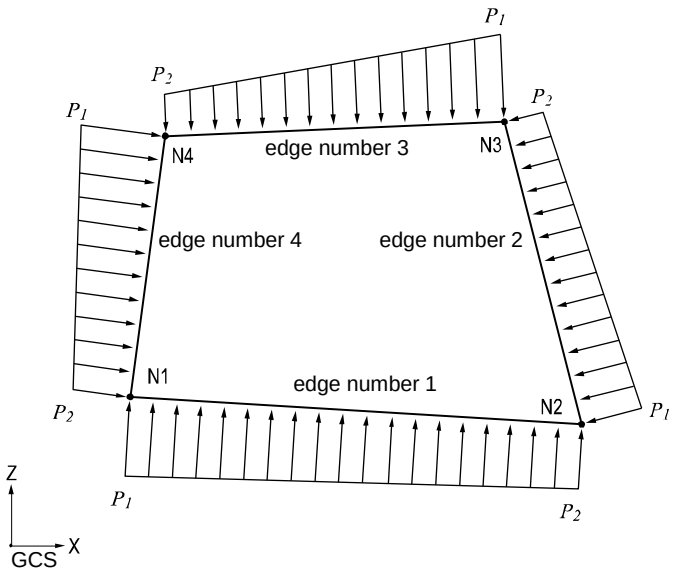

Figure 1.23 Pressure loads applied to an axisymmetric element

Output for element forces

The sign convention for axisymmetric element forces and stresses is defined relative to either the ECS or GCS. Figure 1.24 illustrates the sign convention relative to the ECS or principal stress directions of a unit segment.

- **Output for element forces at connecting nodes**
- **Output for element stresses at connecting nodes and element centers**

At a connecting node, multiplying each nodal displacement component by the corresponding stiffness component of the element produces the element forces.

For stresses at the connecting nodes and element centers, the stresses calculated at the integration points (Gauss Points) are extrapolated.

- **Output for element forces**
  Figure 1.22 shows the sign convention for element forces. The arrows represent the positive (+) directions.

- **Output for element stresses**
  Figure 1.24 shows the sign convention for element stresses. The arrows represent the positive (+) directions.

* Element stresses are produced in the ECS and the arrows represent the positive (+) directions.

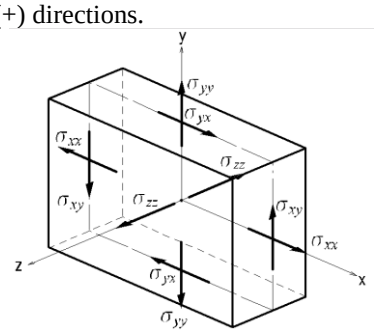

(a) Axial and shear stress components

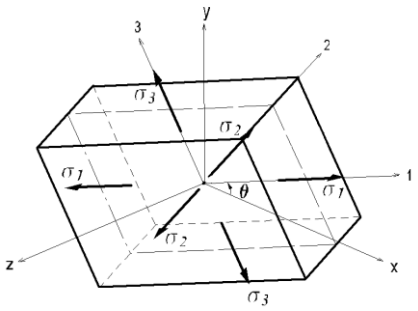

(b) Principal stress components

σ_{xx} : Axial stress in the ECS x - direction

σ_{yy} : Axial stress in the ECS y - direction

σ_{zz} : Axial stress in the ECS z - direction

$\sigma_{xy} = \sigma_{yx}$: Shear stress in the ECS x - y plane

$\sigma_1, \sigma_2, \sigma_3$: Principal stresses in the directions of the principal axes, 1, 2 and 3

where, $\sigma^3 - I_1\sigma^2 - I_2\sigma - I_3 = 0$

$$I_1 = \sigma_{xx} + \sigma_{yy} + \sigma_{zz}$$

$$I_2 = -\begin{vmatrix} \sigma_{xx} & \sigma_{xy} \\ \sigma_{xy} & \sigma_{yy} \end{vmatrix} - \begin{vmatrix} \sigma_{xx} & \sigma_{xz} \\ \sigma_{xz} & \sigma_{zz} \end{vmatrix} - \begin{vmatrix} \sigma_{yy} & \sigma_{yz} \\ \sigma_{yz} & \sigma_{zz} \end{vmatrix}$$

$$I_3 = \begin{vmatrix} \sigma_{xx} & \sigma_{xy} & \sigma_{xz} \\ \sigma_{xy} & \sigma_{yy} & \sigma_{yz} \\ \sigma_{xz} & \sigma_{yz} & \sigma_{zz} \end{vmatrix}, \quad \sigma_{yz} = \sigma_{zx} = 0$$

θ : Angle between the x - axis and the principal axis, 1 in the ECS x - y plane

τ_{max} : Maximum shear stress $= max\left[\frac{\sigma_1 - \sigma_2}{2}, \frac{\sigma_2 - \sigma_3}{2}, \frac{\sigma_3 - \sigma_1}{2}\right]$

σ_{eff} : von - Mises Stress $= \sqrt{\frac{1}{2}\left[(\sigma_1 - \sigma_2)^2 - (\sigma_2 - \sigma_3)^2 - (\sigma_3 - \sigma_1)^2\right]}$

σ_{oct} : Octahedral Normal Stress $= \frac{1}{3}(\sigma_1 + \sigma_2 + \sigma_3)$

τ_{oct} : Octahedral Shear Stress $= \sqrt{\frac{1}{9}\left[(\sigma_1 - \sigma_2)^2 - (\sigma_2 - \sigma_3)^2 - (\sigma_3 - \sigma_1)^2\right]}$

Figure 1.24 Sign convention for axisymmetric element stresses

AXISYMMETRIC ELEMENT FORCES(GLOBAL) DEFAULT OUTPUT Unit System : kN , m

ELEM	MAT	LC	NODE	FX	FZ
1	1	LCOMB1	1	0.00000	0.00000
			2	-42.26970	0.00000
			13	-42.26970	0.00000
			12	0.00000	0.00000
		LCOMB2	1	0.00000	-36.76077
			2	-42.26970	-38.83923
			13	-42.26970	0.00000
			12	0.00000	0.00000

Figure 1.25 Sample output of axisymmetric element forces

AXISYMMETRIC ELEMENT STRESSES(GLOBAL) DEFAULT OUTPUT Unit System : N , mm

ELEM	MAT	LC	NODE	Sig-XX	Sig-YY	Sig-ZZ	Sig-XZ
1	1	LCOMB1	Cent	-87.6928	154.4228	0.0000	0.0000
			1	-87.6928	166.1440	0.0000	0.0000
			2	-87.6928	143.0679	0.0000	0.0000
			13	-87.6928	143.0679	0.0000	0.0000
			12	-87.6928	166.1440	0.0000	0.0000

	NODE	Sig-P1	Sig-P2	Sig-P3	MAX-SHR	Sig-EFF	Sig-Oct
	Cent	154.4228	0.0000	-87.6928	121.0578	212.3162	100.0868
	1	166.1440	0.0000	-87.6928	126.9184	223.3013	105.2652
	2	143.0679	0.0000	-87.6928	115.3803	201.7535	95.1075
	13	143.0679	0.0000	-87.6928	115.3803	201.7535	95.1075
	12	166.1440	0.0000	-87.6928	126.9184	223.3013	105.2652

	LC	NODE	Sig-XX	Sig-YY	Sig-ZZ	Sig-XZ
	LCOMB2	Cent	-87.6928	154.4228	0.0000	0.0000
		1	-87.6928	166.1440	0.0000	0.0000
		2	-87.6928	143.0679	0.0000	0.0000
		13	-87.6928	143.0679	0.0000	0.0000
		12	-87.6928	166.1440	0.0000	0.0000

	NODE	Sig-P1	Sig-P2	Sig-P3	MAX-SHR	Sig-EFF	Sig-Oct
	Cent	154.4228	0.0000	-87.6928	121.0578	212.3162	100.0868
	1	166.1440	0.0000	-87.6928	126.9184	223.3013	105.2652
	2	143.0679	0.0000	-87.6928	115.3803	201.7535	95.1075
	13	143.0679	0.0000	-87.6928	115.3803	201.7535	95.1075
	12	166.1440	0.0000	-87.6928	126.9184	223.3013	105.2652

Figure 1.26 Sample output of axisymmetric element stresses

Plate Element

Introduction

Three or four nodes placed in the same plane define a plate element. **The element is capable of accounting for in-plane tension/compression, in-plane/out-of-plane shear and out-of-plane bending behaviors**.

The out-of-plane stiffness used in MIDAS GEN NX includes two types, DKT/DKQ (Discrete Kirchhoff element) and DKMT/DKMQ (Discrete Kirchhoff-Mindlin element). DKT and DKQ are developed on the basis of a thin plate theory, Kirchhoff Plate theory. Whereas, DKMT and DKMQ are developed on the basis of a thick plate theory, Mindlin-Reissner Plate theory, which exhibits superb performance for thick plates as well as thin plates by assuming appropriate shear strain fields to resolve the shear-locking problem. The in-plane stiffness is formulated according to the Linear Strain Triangle theory for the triangular element, and Isoparametric Plane Stress Formulation with Incompatible Modes is used for the quadrilateral element.

You may selectively enter separate thicknesses for the calculation of in-plane stiffness and out-of-plane stiffness. In general, the thickness specified for the in-plane stiffness is used for calculating self-weight and mass. When it is not specified, the thickness for the out-of-plane stiffness will be used.

Element d.o.f. and the ECS

The ECS for plate elements is used when the program calculates the element stiffness matrices. Graphic displays for stress components are also depicted in the ECS in the post-processing mode.

The element's translational d.o.f. exists in the ECS x, y and z-directions and rotational d.o.f. exists in the ECS x and y-axes.

The ECS uses x, y & z-axes in the Cartesian coordinate system, following the right hand rule. The directions of the ECS axes are defined as presented in Figure 1.27.

In the case of a quadrilateral (4-node) element, the thumb direction signifies the ECS z-axis. The rotational direction (**N1→N2→N3→N4**) following the right hand rule determines the thumb direction. The ECS z-axis originates from the center of the element surface and is perpendicular to the element surface. The line connecting the mid point of N1 and N4 to the mid point of N2 and N3 defines the direction of ECS x-axis. The perpendicular direction to the x-axis in the element plane now becomes the ECS y-axis by the right-hand rule.

For a triangular (3-node) element, the line parallel to the direction from N1 to N2, originating from the center of the element becomes the ECS x-axis. The y and z-axes are identically defined as those for the quadrilateral element.

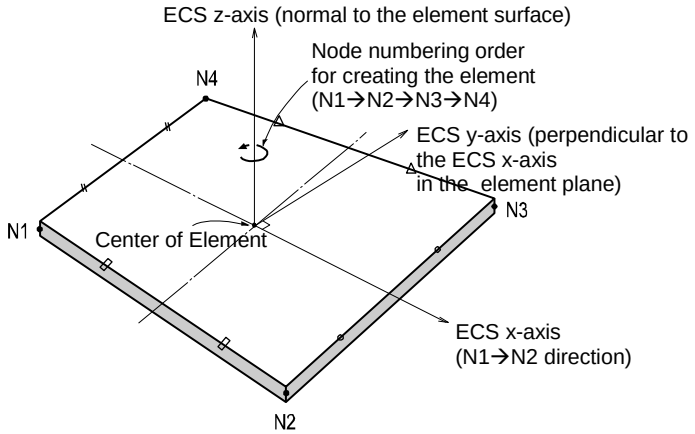

(a) ECS for a quadrilateral element

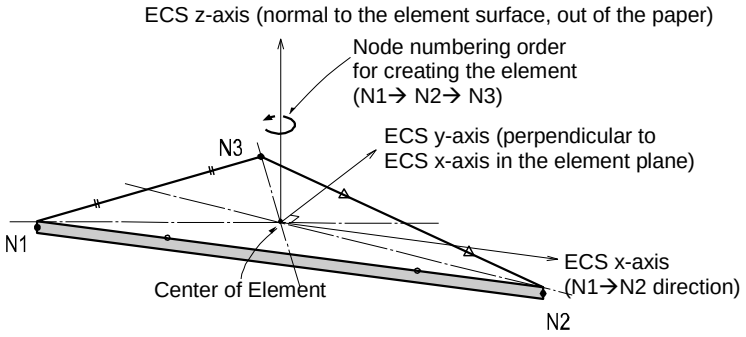

(b) ECS for a triangular element

Figure 1.27 Arrangement of plate elements and their ECS

Functions related to the elements

Create Elements
Material: Material properties
Thickness: thickness of the element
Pressure Loads: Pressure loads acting normal to the plane of the element
Temperature Gradient

Output for element forces

The sign convention for plate element forces and stresses is defined relative to either the ECS or GCS. The following descriptions are based on the ECS.

- **Output for element forces at connecting nodes**
- **Output for element forces per unit length at connecting nodes and element centers**
- **Output for element stresses at top and bottom surfaces at connecting nodes and element centers**

At a connecting node, multiplying each nodal displacement component by the corresponding stiffness component of the element produces the element forces.

In order to calculate element forces per unit length at a connecting node or an element center, the stresses are separately calculated for in-plane and out-of plane behaviors and integrated in the direction of the thickness.

The element forces per unit length can be effectively applied to the design of concrete members. For stresses at the connecting nodes and element centers, the stresses calculated at the integration points (Gauss Points) are extrapolated.

- **Output for element forces**
  Figure 1.28 shows the sign convention for element forces. The arrows represent the positive (+) directions.

- **Output for element forces per unit length**
  Figure 1.29 shows the sign convention for element forces per unit length at connecting nodes and element centers. The arrows represent the positive (+) directions.

- **Output for element stresses**
  Figure 1.30 (a) shows the top and bottom surface locations where element stresses are produced at connecting nodes and element centers. Figure 1.30 (b) shows the sign convention for element stresses.

* Element forces are produced in the ECS and the arrows represent the positive (+) directions.

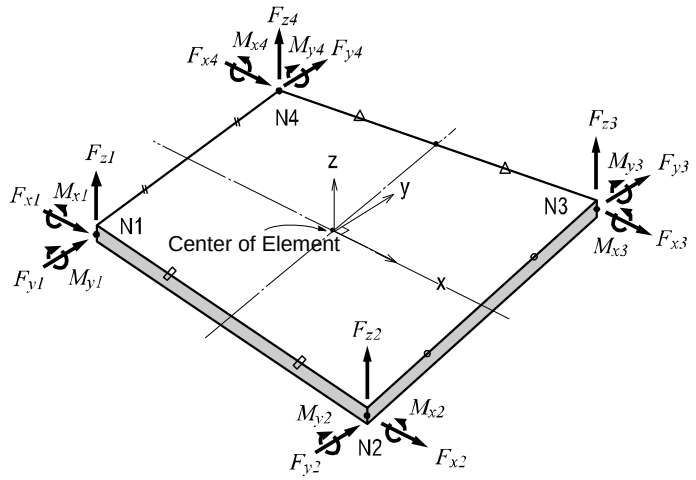

(a) Nodal forces for a quadrilateral element

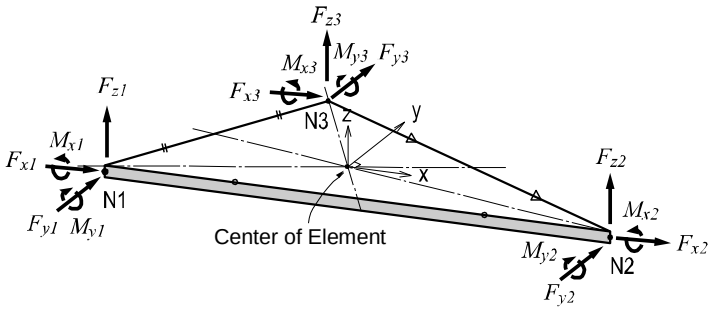

(b) Nodal forces for a triangular element

Figure 1.28 Sign convention for nodal forces at each node of plate elements

* Element forces are produced in the ECS and the arrows represent the positive (+) directions.

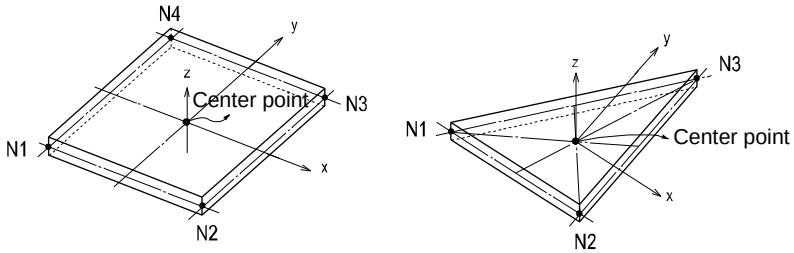

•: Out put locations of element forces per unit length

(a) Output locations of element forces

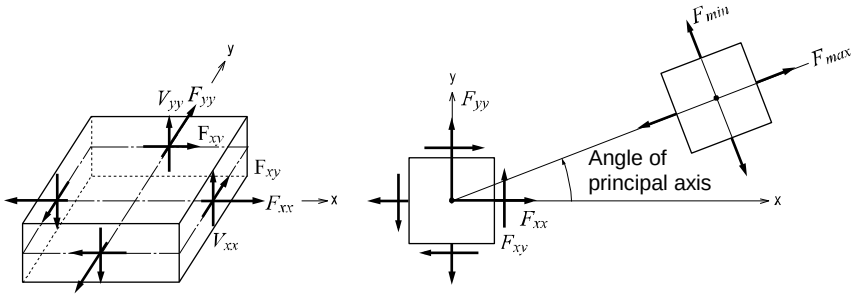

(b) Forces per unit length due to in-plane actions at the output locations

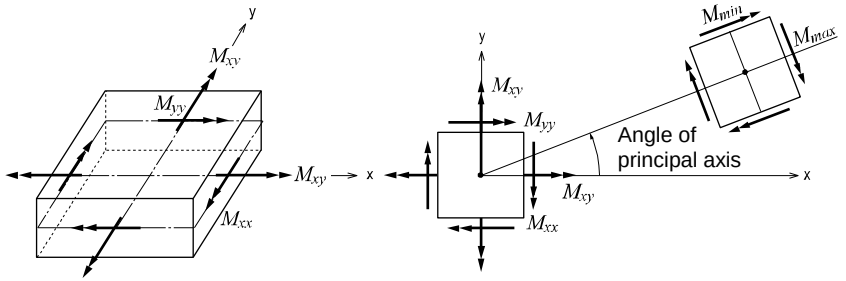

(c) Moments per unit length due to out-of-plane bending actions at the output locations

Figure 1.29 Output locations of plate element forces per unit length and the sign convention

* Element forces are produced in the ECS and the arrows represent the positive (+) directions.

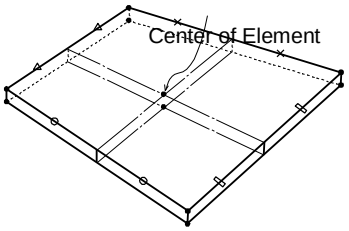

•: Output locations of the element stresses (at each connecting node and the center at top/bottom surfaces)

(a) Output locations of element stresses

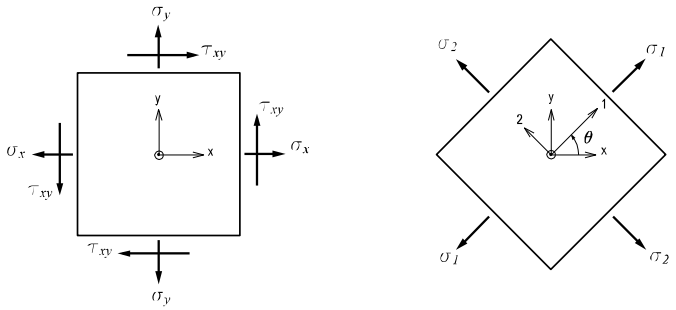

σ_x : Axial stress in the ECS x - direction

σ_x : Axial stress in the ECS y - direction

τ_{xy} : Shear stress in the ECS x - y plane

σ_1 : Maximum principal stress $= \frac{\sigma_x+\sigma_y}{2}+\sqrt{\left(\frac{\sigma_x-\sigma_y}{2}\right)^2+\tau_{xy}^2}$

σ_2 : Minimum principal stress $= \frac{\sigma_x+\sigma_y}{2}-\sqrt{\left(\frac{\sigma_x-\sigma_y}{2}\right)^2+\tau_{xy}^2}$

τ_{xy} : Maximum shear stress $= \sqrt{\left(\frac{\sigma_x-\sigma_y}{2}\right)^2+\tau_{xy}^2}$

θ : Angle between the x - axis and the principal axis,1

σ_{eff} : von - Mises Stress $= \sqrt{(\sigma_1^2-\sigma_1\sigma_2+\sigma_2^2)}$

(b) Sign convention for plate element stresses

Figure 1.30 Output locations of plate element stresses and the sign convention

PLATE ELEMENT FORCES(LOCAL) DEFAULT PRINTOUT Unit System : lbf , in

ELEM	MAT	SEC	LC	NODE	Fx	Fy	Fz	Mx	My	Mz
1	1	1	LCOMB1	1	6.66	-0.13	1.66	-0.0	-1.1	-0.0
				10	-7.51	0.12	0.25	-0.0	0.6	-0.0
				11	0.61	0.57	0.21	0.8	0.5	-0.0
				2	0.25	-0.56	-0.33	0.8	-0.8	-0.0

PLATE ELEMENT FORCES (LOCAL, UNIT LENGTH) PRINTOUT Unit System : lbf , in

ELEM	MAT	SEC	LC	NODE	Fxx	Fyy	Fxy	Fmax	Fmin	ANGLE
1	1	1	LCOMB1	Cent	-4.4	0.0	0.4	0.0	-4.5	84.41
				1	-18.3	-0.7	0.5	-0.6	-18.3	88.44
				10	-18.3	0.7	0.4	0.7	-18.3	88.80
				11	9.5	0.7	0.5	9.5	0.7	3.11
				2	9.5	-0.7	0.4	9.5	-0.7	2.24

NODE	Mxx	Myy	Mxy	Mmax	Mmin	ANGLE
Cent	-1.0	0.4	0.2	0.5	-1.0	80.73
1	-1.7	-0.0	0.2	-0.0	-1.7	84.30
10	-0.8	0.0	0.3	0.1	-0.9	70.89
11	-0.6	0.8	0.3	0.9	-0.6	79.31
2	-0.8	0.9	0.1	0.9	-0.8	85.99

NODE	Vxx	Vyy
Cent	-0.3	-0.5
1	-0.5	-0.4
10	-0.5	-0.5
11	-0.1	-0.5
2	-0.1	-0.4

Figure 1.31 Sample output of plate element forces

PLATE ELEMENT STRESSES(LOCAL) DEFAULT PRINTOUT Unit System : lbf , in

ELEM	SEC	LC	NODE	Sig-xx	Sig-yy	Sig-xy	Sig-MAX	Sig-MIN	ANGLE	Sig-EFF
1	1	LCOMB1	Cent T	3.5e+003	-1.5e+003	-847.4250	3.6e+003	-1.7e+003	-9.35	4.7e+003
			B	-3.7e+003	1.5e+003	869.3237	1.7e+003	-3.8e+003	80.81	4.9e+003
			1 T	5.8e+003	52.3091	-613.6626	5.9e+003	-12.2579	-6.01	5.9e+003
			B	-6.7e+003	-85.1531	637.6313	-24.5580	-6.8e+003	84.57	6.8e+003
			10 T	2.5e+003	-43.3576	-1.2e+003	3.0e+003	-511.7862	-21.37	3.3e+003
			B	-3.5e+003	77.5279	1.2e+003	455.6133	-3.8e+003	72.74	4.1e+003
			11 T	2.4e+003	-3.0e+003	-990.5796	2.5e+003	-3.2e+003	-10.17	4.9e+003
			B	-1.9e+003	3.0e+003	1.0e+003	3.2e+003	-2.1e+003	78.76	4.6e+003
			2 T	3.1e+003	-3.2e+003	-418.5579	3.1e+003	-3.3e+003	-3.76	5.5e+003
			B	-2.6e+003	3.2e+003	438.4212	3.2e+003	-2.7e+003	85.72	5.1e+003

Figure 1.32 Sample output of plate element stresses

Solid Element

Introduction

4, 6 or 8 nodes in a three-dimensional space define a solid element. The element is generally used to model solid structures or thick shells. A solid element may be a tetrahedron, wedge or hexahedron. **Each node retains three translational displacement d.o.f.**

The element is formulated according to the Isoparametric Formulation with Incompatible Modes.

Element d.o.f., ECS and Element types

The ECS for solid elements is used when the program calculates the element stiffness matrices. Graphic displays for stress components are also depicted in the ECS in the post-processing mode.

The element d.o.f. exists in the translational directions of the GCS X, Y and Z-axes.

The ECS uses x, y & z-axes in the Cartesian coordinate system, following the right hand rule. The origin is located at the center of the element, and the directions of the ECS axes are identical to those of the plate element, plane number 1.

There are three types of elements, i.e., 8-node, 6-node and 4-node elements, forming different shapes as presented in Figure 1.33. The nodes are sequentially numbered in an ascending order starting from N1 to the last number.

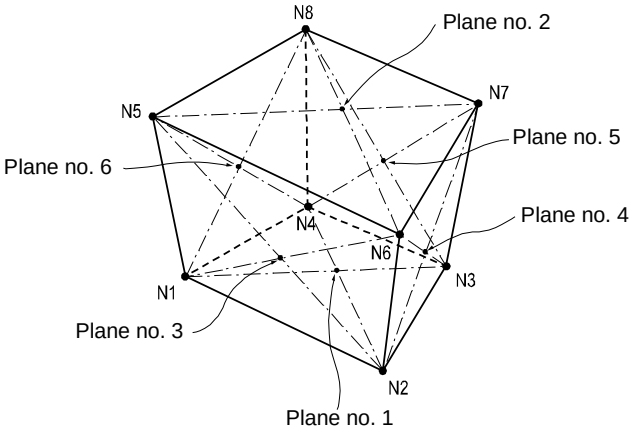

(a) 8-Node element (Hexahedron)

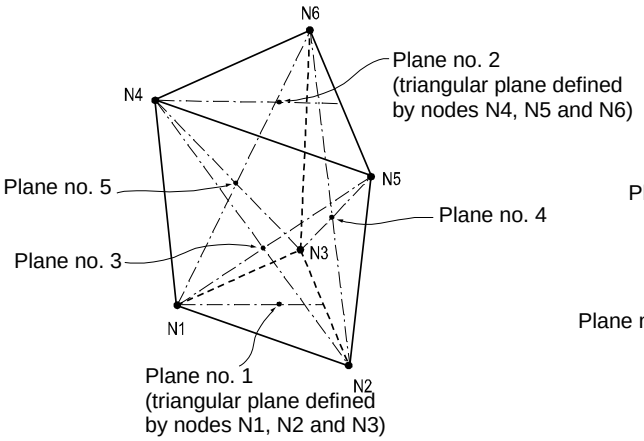

(b) 6-Node element (Wedge)

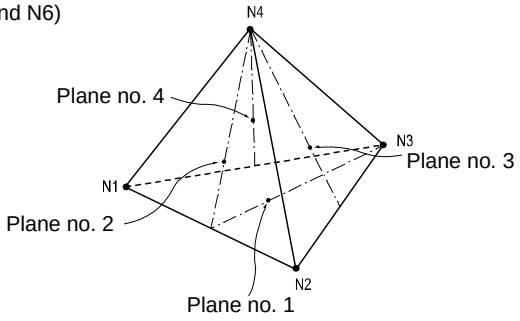

(c) 4-Node element (Tetrahedron)

Figure 1.33 Types of three-dimensional solid elements and node numbering sequence

Functions related to the elements

Create Elements
Material: Material properties
Pressure Loads: Pressure loads acting normal to the faces of the element

Loads are entered as pressure loads applied normal to each surface as illustrated in Figure 1.34.

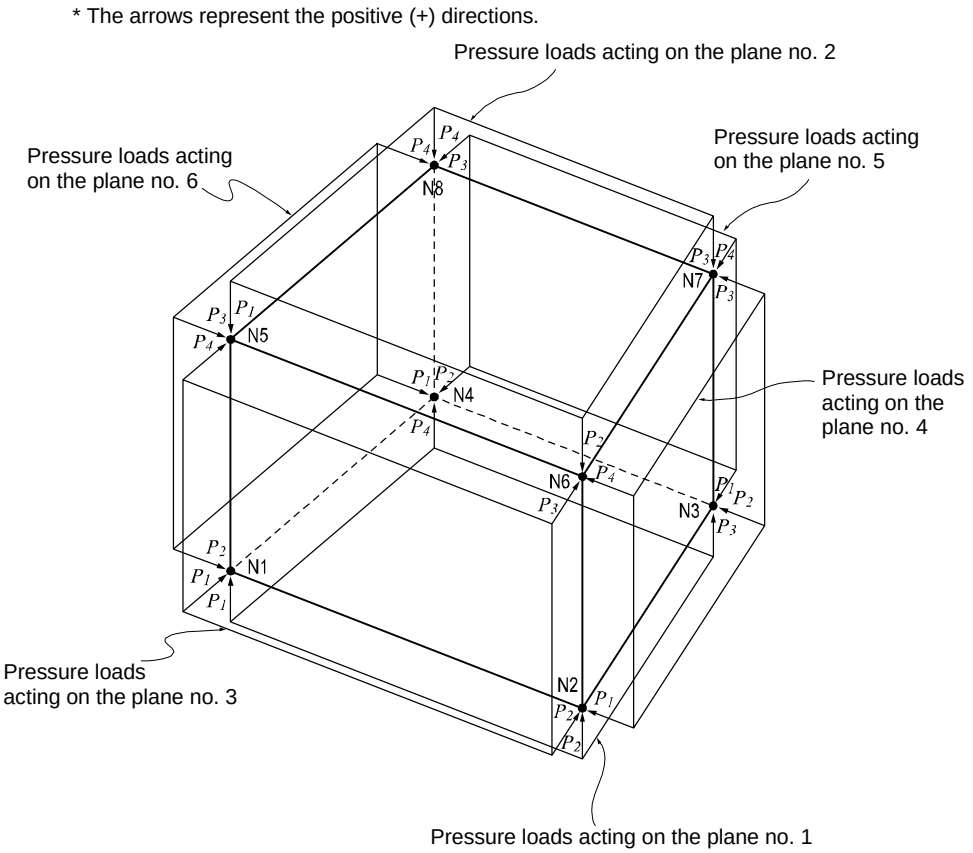

Figure 1.34 Pressure loads acting on the surfaces of a solid element

Output for element forces

The sign convention for solid element forces and stresses is defined relative to either the ECS or GCS.

- **Output for element forces at connecting nodes**
- **Output for three-dimensional element stress components at connecting nodes and element centers**

At a connecting node, multiplying each nodal displacement component by the corresponding stiffness component of the element produces the element forces.

For stresses at the connecting nodes and element centers, the stresses calculated at the integration points (Gauss Points) are extrapolated.

- **Output for element forces**
  Figure 1.35 shows the sign convention for element forces. The arrows represent the positive (+) directions.

- **Output for element stresses**
  Figure 1.36 shows the sign convention for element stresses. The arrows represent the positive (+) directions.

* Element forces are produced in the GCS and the arrows represent the positive (+) directions.

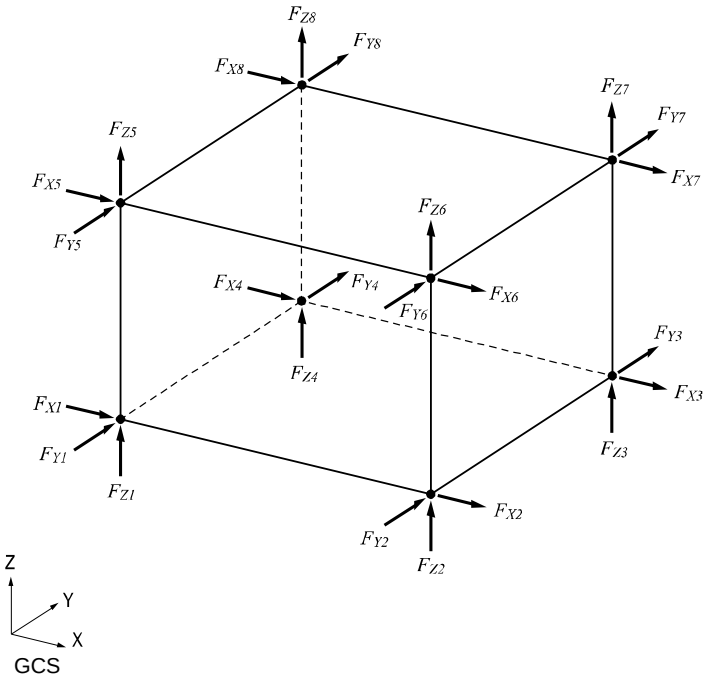

Figure 1.35 Sign convention for solid element forces at connecting nodes

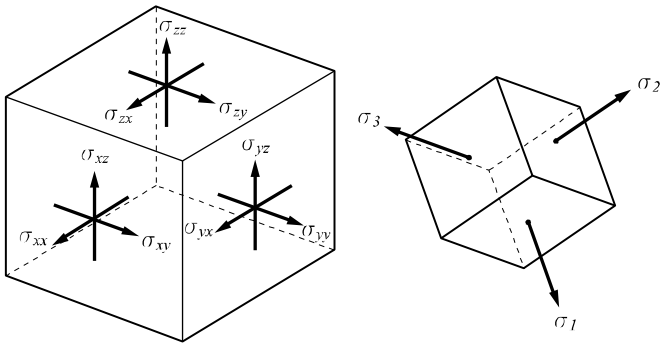

a) Axial and shear stress components (b) Principal stress components

σ_{xx} : Axial stress in the ECS x - direction

σ_{yy} : Axial stress in the ECS y - direction

σ_{zz} : Axial stress in the ECS z - direction

$\sigma_{xz} = \sigma_{zx}$: Shear stress in the ECS x - z direction

$\sigma_{xy} = \sigma_{yx}$: Shear stress in the ECS x - y direction

$\sigma_{yz} = \sigma_{zy}$: Shear stress in the ECS y - z direction

$\sigma_1,\ \sigma_2,\ \sigma_3$: Principal stresses in the directions of the principal axes, 1, 2 and 3

where, $\sigma^3 - I_1\sigma^2 - I_2\sigma - I_3 = 0$

$$I_1 = \sigma_{xx} + \sigma_{yy} + \sigma_{zz}$$

$$I_2 = -\begin{vmatrix}\sigma_{xx} & \sigma_{xy}\\ \sigma_{xy} & \sigma_{yy}\end{vmatrix} - \begin{vmatrix}\sigma_{xx} & \sigma_{xz}\\ \sigma_{xz} & \sigma_{zz}\end{vmatrix} - \begin{vmatrix}\sigma_{yy} & \sigma_{yz}\\ \sigma_{yz} & \sigma_{zz}\end{vmatrix}$$

$$I_3 = \begin{vmatrix}\sigma_{xx} & \sigma_{xy} & \sigma_{xz}\\ \sigma_{xy} & \sigma_{yy} & \sigma_{yz}\\ \sigma_{xz} & \sigma_{yz} & \sigma_{zz}\end{vmatrix}$$

τ_{max} : Maximum shear stress $= max\left[\frac{\sigma_1-\sigma_2}{2}, \frac{\sigma_2-\sigma_3}{2}, \frac{\sigma_3-\sigma_1}{2}\right]$

σ_{eff} : von - Mises Stress $= \sqrt{\frac{1}{2}\left[(\sigma_1-\sigma_2)^2-(\sigma_2-\sigma_3)^2-(\sigma_3-\sigma_1)^2\right]}$

σ_{oct} : Octahedral Normal Stress $= \frac{1}{3}(\sigma_1+\sigma_2+\sigma_3)$

τ_{oct} : Octahedral Shear Stress $= \sqrt{\frac{1}{9}\left[(\sigma_1-\sigma_2)^2-(\sigma_2-\sigma_3)^2-(\sigma_3-\sigma_1)^2\right]}$

Figure 1.36 Sign convention for solid element stresses at connecting nodes

SOLID ELEMENT FORCES(GLOBAL) DEFAULT OUTPUT Unit System : kN , m

ELEM	MAT	LC	NODE	FX	FY	FZ
1	1	LCOMB1	1	-2.45166	-0.28377	-0.28377
			5	2.45166	-0.07604	-0.07604
			6	2.45166	0.07604	-0.07604
			2	-2.45166	0.28377	-0.28377
			3	-2.45166	-0.28377	0.28377
			7	2.45166	-0.07604	0.07604
			8	2.45166	0.07604	0.07604
			4	-2.45166	0.28377	0.28377
		LCOMB2	1	-49.03325	-2.45166	-6.30239
			5	44.12992	2.45166	-0.98543
			6	-44.12992	2.45166	0.98543
			2	49.03325	-2.45166	6.30239
			3	-49.03325	-2.45166	6.30239
			7	44.12992	2.45166	0.98543
			8	-44.12992	2.45166	-0.98543
			4	49.03325	-2.45166	-6.30239

Figure 1.37 Sample output of solid element forces

SOLID ELEMENT STRESSES(GLOBAL) DEFAULT OUTPUT Unit System : N , mm

ELEM	MAT	LC	NODE	Sig-XX	Sig-YY	Sig-ZZ	Sig-XY	Sig-YZ	Sig-XZ
1	1	LCOMB1	Cent	0.0392	0.0029	0.0029	0.0000	0.0000	0.0000
			1	0.0392	0.0079	0.0079	0.0000	0.0000	0.0000
			5	0.0392	-0.0021	-0.0021	0.0000	0.0000	0.0000
			6	0.0392	-0.0021	-0.0021	0.0000	0.0000	0.0000
			2	0.0392	0.0079	0.0079	0.0000	0.0000	0.0000
			3	0.0392	0.0079	0.0079	0.0000	0.0000	0.0000
			7	0.0392	-0.0021	-0.0021	0.0000	0.0000	0.0000
			8	0.0392	-0.0021	-0.0021	0.0000	0.0000	0.0000
			4	0.0392	0.0079	0.0079	0.0000	0.0000	0.0000

		NODE	Sig-P1	Sig-P2	Sig-P3	MAX-SHR	Sig-EFF	Sig-Oct
		Cent	0.0392	0.0029	0.0029	0.0182	0.0363	0.0171
		1	0.0392	0.0000	0.0000	0.0196	0.0392	0.0185
		5	0.0392	-0.0021	-0.0021	0.0207	0.0413	0.0195
		6	0.0392	0.0000	0.0000	0.0196	0.0392	0.0185
		2	0.0392	0.0079	0.0079	0.0157	0.0314	0.0148
		3	0.0392	0.0079	0.0079	0.0157	0.0314	0.0148
		7	0.0392	-0.0021	-0.0021	0.0207	0.0413	0.0195
		8	0.0392	-0.0021	-0.0021	0.0207	0.0413	0.0195
		4	0.0392	0.0079	0.0079	0.0157	0.0314	0.0148

	LC	NODE	Sig-XX	Sig-YY	Sig-ZZ	Sig-XY	Sig-YZ	Sig-XZ
	LCOMB2	Cent	0.0000	0.0000	0.0000	0.0392	0.0000	0.0000
		1	2.2786	0.0426	0.3876	0.0392	0.0850	0.0850
		5	2.1933	-0.0426	-0.0378	0.0392	-0.0850	0.0850
		6	-2.1933	0.0426	0.0378	0.0392	-0.0850	-0.0850
		2	-2.2786	-0.0426	-0.3876	0.0392	0.0850	-0.0850
		3	2.2786	0.0426	0.3876	0.0392	-0.0850	-0.0850
		7	2.1933	-0.0426	-0.0378	0.0392	0.0850	-0.0850
		8	-2.1933	0.0426	0.0378	0.0392	0.0850	0.0850
		4	-2.2786	-0.0426	-0.3876	0.0392	-0.0850	0.0850

		NODE	Sig-P1	Sig-P2	Sig-P3	MAX-SHR	Sig-EFF	Sig-Oct
		Cent	0.0392	0.0000	-0.0392	0.0392	0.0679	0.0320
		1	2.2832	0.4030	0.0227	1.1303	2.0964	0.9883
		5	2.1971	0.0443	-0.1286	1.1628	2.2442	1.0579
		6	0.1286	-0.0443	-2.1971	1.1628	2.2442	1.0579
		2	-0.0227	-0.4030	-2.2832	1.1303	2.0964	0.9883
		3	2.2832	0.4030	0.0227	1.1303	2.0964	0.9883
		7	2.1971	0.0443	-0.1286	1.1628	2.2442	1.0579
		8	0.1286	-0.0443	-2.1971	1.1628	2.2442	1.0579
		4	-0.0227	-0.4030	-2.2832	1.1303	2.0964	0.9883

Figure 1.38 Sample output of solid element stresses

Wall Element

Introduction

Wall elements are used to model shear walls, which retain the shape of a rectangle or square. The direction of gravity must be set opposite to the direction of the GCS Z-axis. The elements retain in-plane tension/compression stiffness in the vertical direction, in-plane shear stiffness in the horizontal direction, out-of-plane bending stiffness and rotational stiffness about the vertical direction.

Two types of wall elements included in MIDAS GEN NX are:

- **Wall element type 1 (Membrane type):**
  in-plane stiffness + rotational stiffness about the vertical direction

- **Wall element type 2 (Plate type):**
  in-plane stiffness + rotational stiffness about the vertical direction + out-of-plane bending stiffness

Wall element type 1 (membrane type) is generally used to model shear walls being subjected to in-plane loads only. Whereas, Wall element type 2 (plate type) is suitable for modeling common walls intended to resist in-plane loads as well as out-of-plane bending moments.

Shear walls are generally modeled with 4-node plane stress elements, which best reflect the characteristics of shear walls. The plane stress elements included in most finite element programs, however, are not readily applicable for shear walls. This type of element does not have rotational stiffness about the axis perpendicular to the plane of the element at the connecting nodes. When flexural beams are connected to the wall element's nodes, incompatibility in degrees of freedom results. Moreover, additional transformation process is required for design because all element forces are produced in terms of nodal forces or stresses rather than wall member forces and moments.

In MIDAS GEN NX, a new improved algorithm is used to overcome the limitation described above. This algorithm, if necessary, allows you to select out-of-plane bending stiffness to be included in the analysis.

The procedure for modeling wall elements in MIDAS GEN NX is as follows:

See "Model> Building> Story" of On-line Manual.

1. **Enter the story data for the building.**
2. **Enter wall elements. Note that elements must be rectangles of squares. Only one wall element is permitted at a given story vertically, i.e., the height of an element is one story high**.
3. **Enter the wall (combination) ID and specify the type of elements, considering whether or not the out-of-plane bending stiffness is to be included**.

Walls in general structures are consisted of combinations of single (linear in plan) individual walls, thereby forming different geometric configurations. Each wall (group) is defined by entering individual unit wall elements. In order to reflect the true stiffness of combined walls individual wall elements are assigned with wall (combination) IDs.

Member forces of wall elements are produced for each story by wall IDs. If two or more wall elements at a given floor are numbered with a same wall ID, they are recognized as a single wall structure and each element force is combined together for the force output. However, wall elements assigned with an identical wall ID but located at different floors are recognized as distinct wall structures. Accordingly, it would be advisable to assign the same wall ID to all wall elements located in the same plan throughout all the floors in order to avoid confusion.

As illustrated in Figure 1.39 (b), 5 wall elements are required for modeling the wall structure shown in Figure 1.39 (a). Figure 1.39 (c) shows the output configuration when each element is assigned with different wall IDs to design them separately. The element forces are produced in the ECS of each element. Figure 1.39 (d) illustrates the output configuration for the case where 5 elements are designed as a single unit wall structure. In this case, all elements have the same wall ID. The forces for the assembled wall structure are produced at the centroid. The resulting forces are expressed in the ECS of the first element defined.

The stiffness of the combined wall, (a) is reflected in the structural analysis irrespective of wall ID numbering.

E# : Element number W# : Wall ID

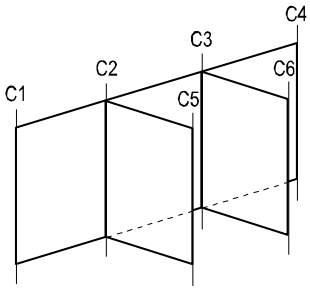

(a) Wall structure

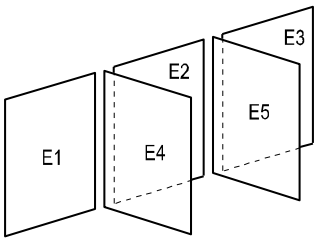

(b) Elements constituting the wall structure

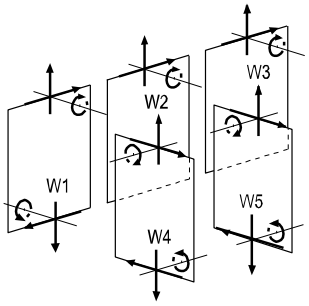

(c) Different wall IDs are assigned to each element

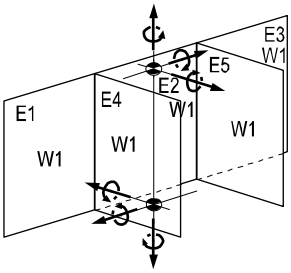

(d) Same wall ID is assigned to all elements

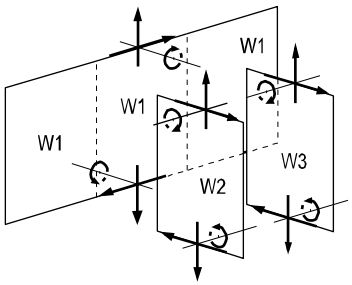

(e) W1 is assigned to Wall elements E1, E2 & E3. E4 and E5 are assigned with W2 and W3 respectively.

Figure 1.39 Element forces for different combinations of wall elements (Membrane Type)

Element d.o.f. and the ECS

Wall element type 1 (membrane type) retains displacement d.o.f in the ECS x and z-directions and rotational d.o.f. about the ECS y-axis. Whereas, Wall element type 2 (plate type) has three translational and three rotational d.o.f. (refer to Figure 1.40).

Shear$_y$ and Moment$_z$ are additional components produced only for wall elements with out-of-plane bending stiffness.

The ECS uses x, y and z-axes in the Cartesian coordinate system, following the right hand rule.

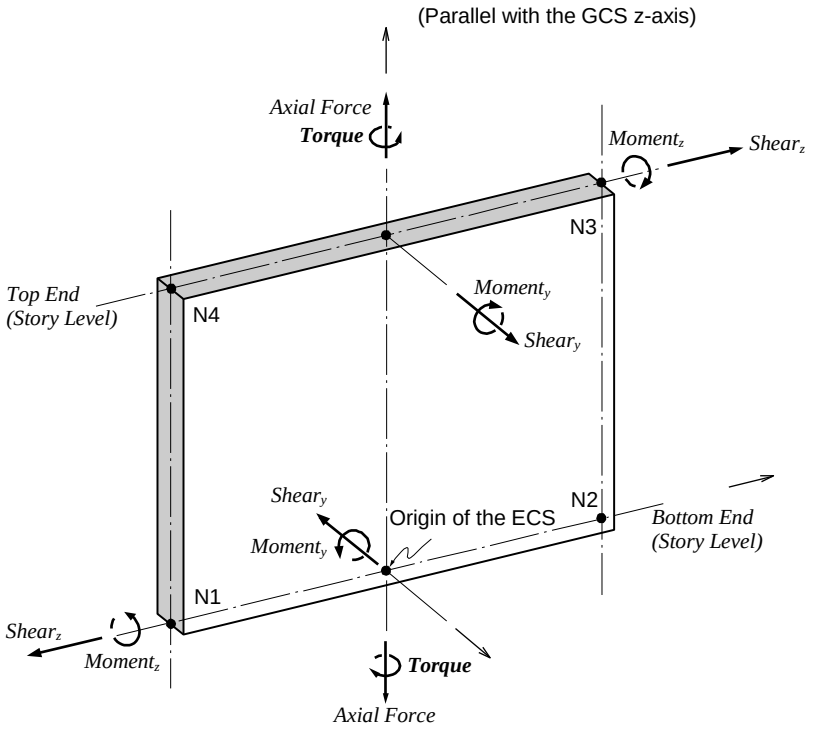

Figure 1.40 ECS and sign convention of a wall element assigned with a Wall ID

The ECS x-axis is set parallel with the GCS Z-axis by default. The ECS z-axis is determined by the direction defined from the first node (N1) to the second node (N2), which are in turn used to define the range of target elements for a given Wall ID (refer to Figure 1.40). The perpendicular axis to the x-z plane becomes the ECS y-axis.

When more than two wall elements are assigned with the same Wall ID number, the member forces are produced in the ECS of the first element (the element with the smallest element number). Refer to Figure 1.41.

Connecting nodes must be entered from the bottom up. The nodes at the top and bottom of an element must be located in a plane parallel to the global X-Y plane. All the nodes must lie in a single plane. You should exercise caution when defining elements, as the ECS is defined according to the node numbering order.

Functions related to the elements

Create Elements
Material: Material properties
Thickness: Thickness of the element

Output for element forces

The sign convention for element forces is shown in Figure 1.41. The arrows represent the positive (+) directions.

Element forces are produced for each story by Wall IDs.

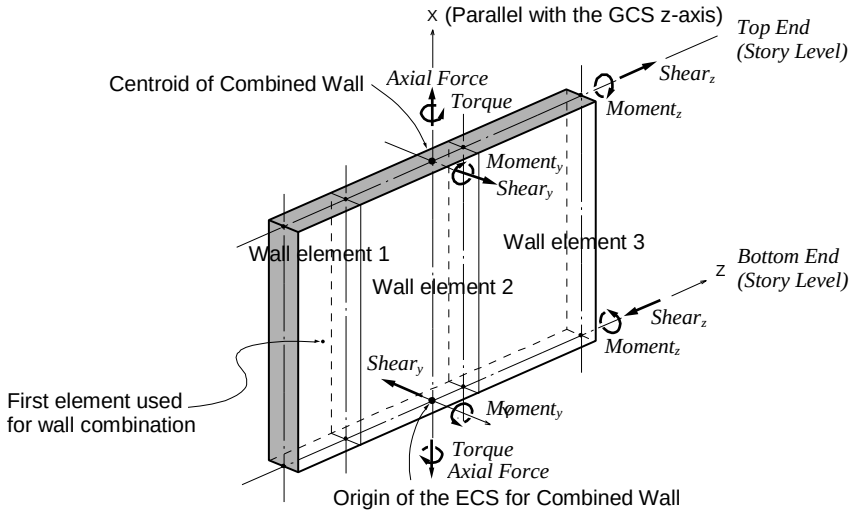

(a) When all wall elements of the same Wall ID is in the same plane

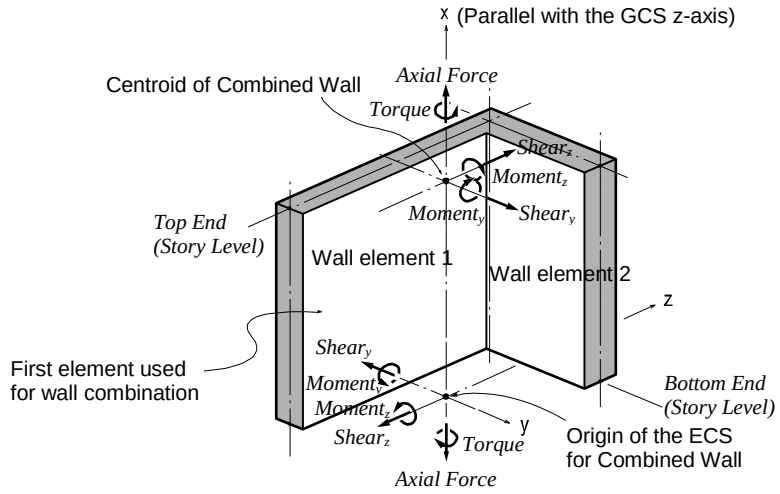

(b) When all wall elements of the same Wall ID are not in the same plane

Figure 1.41 ECS and sign convention of combined walls when two or more elements are assigned with the same Wall ID

WALL ELEMENT FORCES DEFAULT PRINTOUT Unit System : kN , m

WL.ID	STORY	HT	LC	PRT	AXIAL	SHEAR-y	SHEAR-z	TORSION	MOMENT-y	MOMENT-z
1	Roof	4	cLCB1	TOP	-809.20073	0.00000	30.45084	0.0000	-60.1482	-0.0000
				BOT	-998.99471	0.00000	30.45084	0.0000	61.6552	0.0000
			cLCB2	TOP	-681.95339	0.00000	35.25750	0.0000	-66.9998	0.0000
				BOT	-824.29887	0.00000	35.25750	0.0000	74.0302	-0.0000
1	11F	4	cLCB1	TOP	-1.77e+003	0.00000	41.68923	0.0000	-141.3230	-0.0000
				BOT	-1.96e+003	0.00000	41.68923	0.0000	25.4339	0.0000
			cLCB2	TOP	-1.46e+003	0.00000	39.27835	0.0000	-124.5366	0.0000
				BOT	-1.61e+003	0.00000	39.27835	0.0000	32.5768	-0.0000
1	10F	4	cLCB1	TOP	-2.70e+003	0.00000	35.25015	0.0000	-155.5649	-0.0000
				BOT	-2.89e+003	0.00000	35.25015	0.0000	-14.5643	0.0000
			cLCB2	TOP	-2.14e+003	0.00000	30.16766	0.0000	-130.0055	0.0000
				BOT	-2.28e+003	0.00000	30.16766	0.0000	-9.3348	-0.0000
1	9F	4	cLCB1	TOP	-3.65e+003	0.00000	28.37756	0.0000	-169.1732	-0.0000
				BOT	-3.84e+003	0.00000	28.37756	0.0000	-55.6629	0.0000
			cLCB2	TOP	-2.81e+003	0.00000	24.17009	0.0000	-141.2988	0.0000
				BOT	-2.95e+003	0.00000	24.17009	0.0000	-44.6184	-0.0000
1	8F	4	cLCB1	TOP	-4.60e+003	0.00000	26.28628	0.0000	-191.8974	-0.0000
				BOT	-4.79e+003	0.00000	26.28628	0.0000	-86.7523	0.0000
			cLCB2	TOP	-3.46e+003	0.00000	23.36327	0.0000	-160.3647	0.0000
				BOT	-3.60e+003	0.00000	23.36327	0.0000	-66.9116	-0.0000
1	7F	4	cLCB1	TOP	-5.54e+003	0.00000	23.61980	0.0000	-212.8816	-0.0000
				BOT	-5.73e+003	0.00000	23.61980	0.0000	-118.4024	0.0000
			cLCB2	TOP	-4.06e+003	0.00000	21.82310	0.0000	-175.2461	0.0000
				BOT	-4.20e+003	0.00000	21.82310	0.0000	-87.9536	-0.0000

Figure 1.42 Sample output of wall element forces

Important Aspects of Element Selection

The success of a structural analysis very much depends on how closely the selected elements and modeling represent the real structure.

Analysis objectives determine the selection of elements and the extent of modeling. For example, if the analysis is carried out for the purpose of design, then the structure needs to be divided into appropriate nodes and elements in order to obtain displacements, member forces and stresses that are required for design. It would be more efficient to select elements so that the member forces and stresses can be used directly for design without subsequent transformation. A comparatively coarse mesh model may be sufficient to obtain displacements or to perform eigenvalue analysis. In contrast, the model with fine mesh is more appropriate for computing element forces.

In the case of an eigenvalue analysis where the prime purpose is to observe the overall behavior of the structure, a simple model is preferable so as to avoid the occurrence of local modes. At times, idealizing the structure with beam elements having equivalent stiffness works better than a detailed model, especially in the preliminary design phase.

Important considerations for creating an analysis model are outlined below. Some of the factors to be considered for locating nodes in a structural model include the geometric shape of the structure, materials, section shapes and loading conditions. Nodes should be placed at the following locations:

- **Points where analysis results are required**
- **Points where loads are applied**
- **Points or boundaries where stiffness (section or thickness) changes**
- **Points or boundaries where material properties change**
- **Points or boundaries where stress concentrations are anticipated such as in the vicinity of an opening**
- **At the structural boundaries**
- **Points or boundaries where structural configurations change**

When line elements (truss elements, beam elements, etc.) are used, analysis results are not affected by the sizes of elements. Whereas, analyses using planar elements (plane stress elements, plane strain elements, axisymmetric elements and plate elements) or solid elements are heavily influenced by the sizes, shapes and arrangements of elements. Planar or solid elements should be sufficiently refined at the regions where stresses are expected to vary significantly or where detailed results are required. It is recommended that the elements be divided following the anticipated stress contour lines or stress distribution.

Fine mesh generations are generally required at the following locations:

- **Regions of geometric discontinuity or in the vicinity of an opening**
- **Regions where applied loadings vary significantly; e.g. points adjacent to relatively large magnitude concentrated loads are applied**
- **Regions where stiffness or material properties change**
- **Regions of irregular boundaries**
- **Regions where stress concentration is anticipated**
- **Regions where detailed results of element forces or stresses are required**

The factors to be considered for determining the sizes and shapes of elements are as follows:

- **The shapes and sizes of elements should be as uniform as possible.**
- **Logarithmic configurations should be used where element size changes are necessary.**
- **Size variations between adjacent elements should be kept to less than 1/2.**
- **4-Node planar elements or 8-node solid elements are used for stress calculations. An aspect ratio close to a unity (1:1) yields an optimum solution, and at least a 1:4 ratio should be maintained. For the purpose of transferring stiffness or calculating displacements, aspect ratios less than 1:10 are recommended.**
- **Corner angles near 90° for quadrilateral elements and near 60° for triangular elements render ideal conditions.**
- **Even where unavoidable circumstances arise, corner angles need to be kept away from the range of 45° and 135° for quadrilateral elements, and 30° and 150° for triangular elements.**
- **In the case of a quadrilateral element, the fourth node should be on the same plane formed by three nodes. That is, three points always form a plane and the remaining fourth point can be out of the plane resulting in a warped plane. It is recommended that the magnitude of warping (out-of–plane) be kept less than 1/100 of the longer side dimension.**

Truss, Tension-only and Compression-only Elements

These elements are generally used for modeling members that exert axial forces only such as space trusses, cables and diagonal members as well as for modeling contact surfaces.

For example, truss elements resisting axial tension and compression forces can be used to model a truss structure. Tension-only elements are suitable for modeling cables whose sagging effects can be neglected and for modeling diagonal members that are incapable of transmitting compression forces due to their large slenderness ratios, such as wind bracings. Compression-only elements can be used to model contact surfaces between adjacent structural members and to model ground support conditions taking into account the fact that tension forces cannot be resisted. Pretension loads can be used when members are prestressed.

Because these elements do not retain rotational degrees of freedom at nodes, Singular Errors can occur during the analysis at nodes where they are connected to the same type of elements or to elements without rotational d.o.f. MIDAS GEN NX prevents such singular errors by restraining the rotational d.o.f. at the corresponding nodes.

If they are connected to beam elements that have rotational degrees of freedom, this restraining process is not necessary.

As shown in Figure 1.43, you should exercise caution not to induce unstable structures when only truss elements are connected. The structure shown in Figure 1.43 (a) lacks rotational stiffness while being subjected to an external load in its plane, resulting in an unstable condition. Figures 1.43 (b) and (c) illustrate unstable structures in the loading direction (X-Z plane), even though the structures are stable in the Y-Z plane direction.

You should use tension-only and compression-only elements with care. Element stiffness may be ignored in the analysis depending on the magnitudes of loads; e.g., when compression loads are applied to tension-only elements.

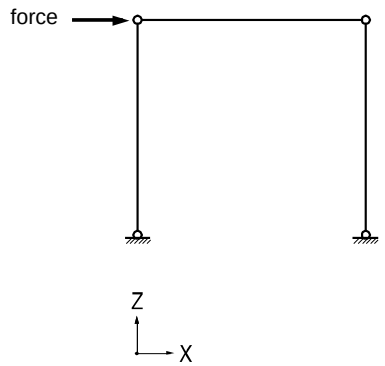

(a) When a force is applied in the X-direction on the X-Z plane

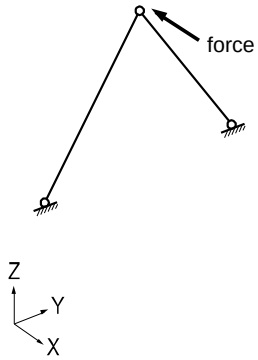

(b) When a force is applied in the X-direction perpendicular to the Y-Z plane

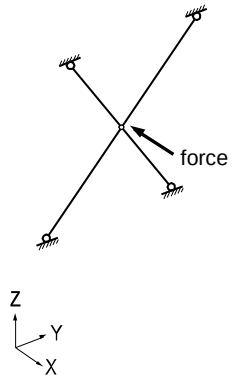

(c) When a force is applied in the X-direction perpendicular to the Y-Z plane

Figure 1.43 Typical examples of unstable structures that are composed of truss (tension-only & compression-only) elements

Beam Element

This element is typically used for modeling prismatic and non-prismatic tapered structural members that are relatively long compared to section dimensions. The element can be also used as load-transfer elements connecting other elements having differing numbers of d.o.f.

In-span concentrated loads, distributed loads, temperature gradient loads and prestress loads can be applied to beam elements.

A beam element has 6 d.o.f. per node reflecting axial, shear, bending and torsional stiffness. When shear areas are omitted, the corresponding shear deformations of the beam element are ignored.

The beam element is formulated on the basis of the Timoshenko beam theory (a plane section initially normal to the neutral axis of the beam remains plane but not necessarily normal to the neutral axis in the deformed state) reflecting shear deformations. If the ratio of the section depth to length is greater than 1/5, a fine mesh modeling is desirable because the effect of shear deformations becomes significant.

The torsional resistance of a beam element differs from the sectional polar moment of inertia (they are the same for circular and cylindrical sections). You are cautioned when the effect of torsional deformation is large, as the torsional resistance is generally determined by experimental methods.

Refer to Numerical Analysis Model in MIDAS GEN NX>Stiffness Data of

Beam and truss elements are idealized line elements, thus their cross-sections are assumed to be dimensionless. The cross-sectional properties of an element are concentrated at the neutral axis that connects the end nodes. As a result, the effects of panel zones between members (regions where columns and beams merge) and the effects of non-alignment of neutral axes are not considered. In order for those nodal effects to be considered, the beam end offset option or geometric constraints must be used.

Refer to Numerical Analysis Model in MIDAS GEN NX>Other Modeling Functions > Beam End Offset.

The tapered section may be used when the section of a member is non-prismatic. It may be desirable to use a number of beam elements to model a curved beam.

Refer to “Model> Properties>Section” of On-line Manual.

When members are connected by pins or slotted holes (Figure 1.44 (a) and (b)), the Beam End Release option is used.

Refer to “Model> Boundaries>Beam End Release” of On-line Manual.

Note that a singularity error can result in a case where a particular degree of freedom is released for all the elements joining at a node, resulting in zero stiffness associated with that degree of freedom. If it is inevitable, a spring element (or an elastic boundary element) having a minor stiffness must be added to the corresponding d.o.f.

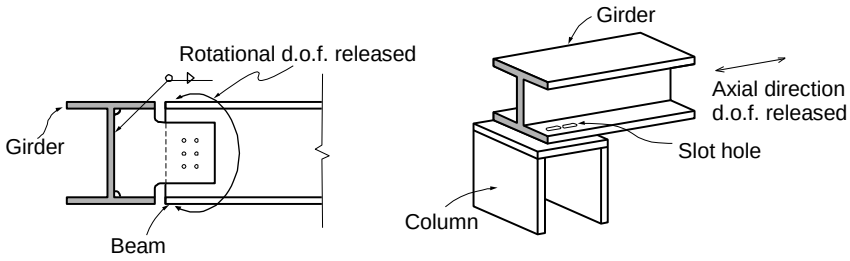

(a) Pin connection (b) Slot-hole connection

When several beam elements are pin connected at a node, the degree of freedom for at least one element must be maintained while the ends of all other elements are released in order to avoid singularity.

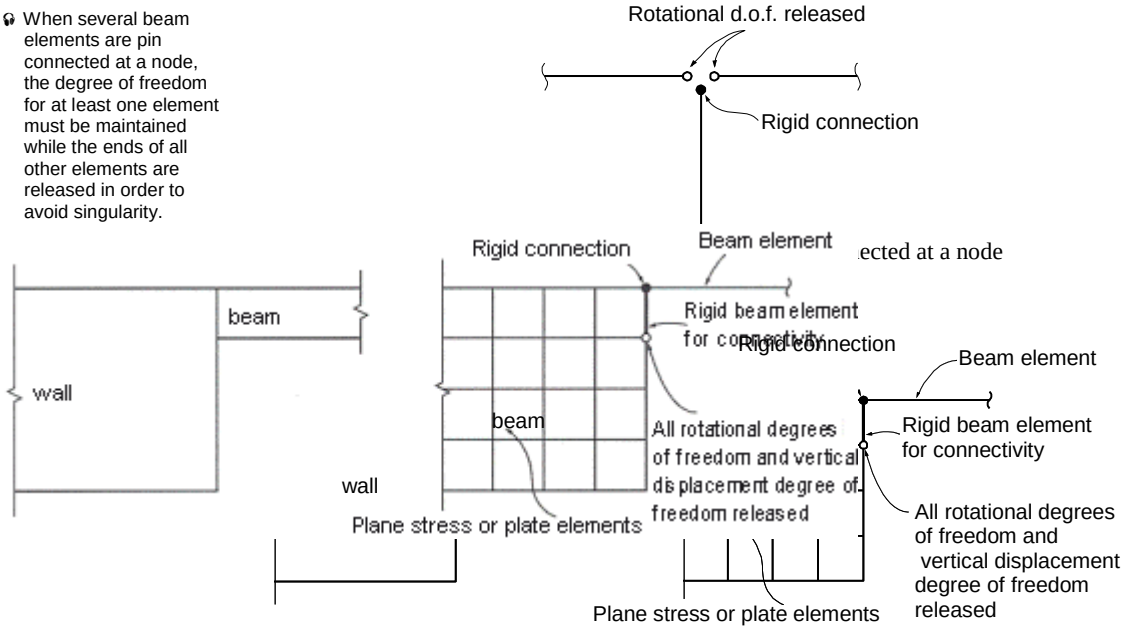

(d) When elements having different d.o.f. are connected

Figure 1.44 Examples of end-release application

The rigid beam element can be effectively used when elements having different degrees of freedom are connected. The rigid effect is achieved by assigning a large stiffness value relative to the contiguous beam elements. In general, a magnitude of $10^5 \sim 10^8$ times the stiffness of the neighboring elements provides an adequate result, avoiding numerical ill conditions.

Figure 1.44 (d) illustrates the case where a beam member is joined to a wall. The wall element may be a plane stress or plate element. The nodal in-plane moment corresponding to the beam element's rotational degree of freedom will not be transmitted to the planar element (plane stress or plate element) because the planar element has no rotational stiffness about the normal direction to the plane. The interface will behave as if the beam was pin connected. In such a case, a rigid beam element is often introduced in order to maintain compatible connectivity. All degrees of freedom of the rigid beam at the beam element are fully maintained while the rotational and axial displacement degrees of freedom are released at the opposite end.

Plane Stress Element

This element can be used for modeling membrane structures that are subjected to tension or compression forces in the plane direction only. Pressure loads can be applied normal to the perimeter edges of the plane stress element.

The plane stress element may retain a quadrilateral or triangular shape. The element has in-plane tension, compression and shear stiffness only.

Quadrilateral (4-node) elements, by nature, generally lead to accurate results for the computation of both displacements and stresses. On the contrary, triangular elements produce poor results in stresses, although they produce relatively accurate displacements. Accordingly, you are encouraged to avoid triangular elements at the regions where detailed analysis results are required, and they are recommended for the transition of elements only (Figure 1.45).

Singularity errors occur during the analysis process, where a plane stress element is joined to elements with no rotational degrees of freedom since the plane stress element does not have rotational stiffness. In MIDAS GEN NX, restraining the rotational degrees of freedom at the corresponding nodes prevents the singularity errors.

When a plane stress element is connected to elements having rotational stiffness such as beam and plate elements, the connectivity between elements needs to be preserved using the rigid link (master node and slave node) option or the rigid beam element option.

Appropriate aspect ratios for elements may depend on the type of elements, the geometric configuration of elements and the shape of the structure. However, aspect ratios close to unity (1:1) and 4 corner angles close to 90° are recommended. If the use of regular element sizes cannot be achieved throughout the structure, the elements should be square shaped at least at the regions where stress intensities are expected to vary substantially and where detailed results are required.

Relatively small elements result in better convergence.

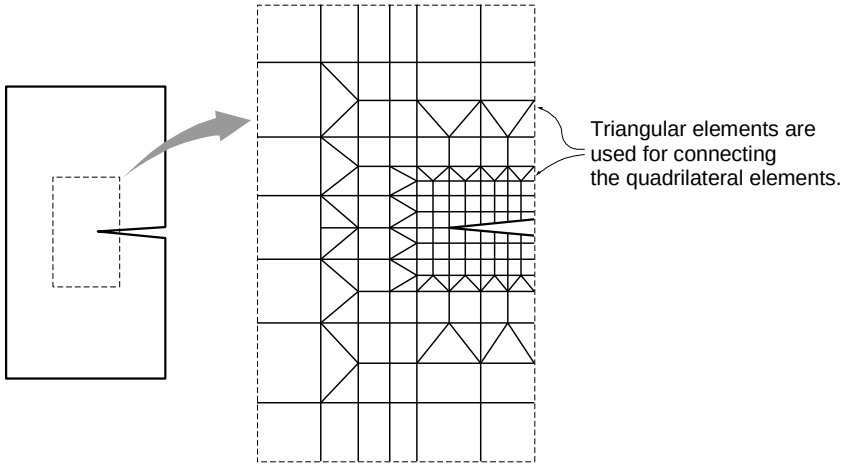

Figure 1.45 Crack modeling using quadrilateral/triangular elements

Plane Strain Element

This element can be used to model a long structure, having a uniform cross section along its entire length, such as dams and tunnels. The element cannot be used in conjunction with any other types of elements.

Pressure loads can be applied normal to the perimeter edges of the plane strain element.

Because this element is formulated on the basis of its plane strain properties, it is applicable to linear static analyses only. Given that no strain is assumed to exist in the thickness direction, the stress component in the thickness direction can be obtained through the Poisson's effect.

The plane strain element may retain a quadrilateral or triangular shape. The element has in-plane tension, compression and shear stiffness, and it has tension and compression stiffness in the thickness direction.

Similar to the plane stress element, quadrilateral elements are recommended over the triangular elements, and aspect ratios close to unity are recommended for modeling plane strain elements.

Refer to "Plane Stress Element".

Axisymmetric Element

This element can be used for modeling a structure with axis symmetry relative to the geometry, material properties and loading conditions, such as pipes, vessels, tanks and bins. The element cannot be used in conjunction with any other types of elements.

Pressure loads can be applied normal to the circumferential edges of the axisymmetric element.

Because this element is formulated on the basis of its axisymmetric properties, it is applicable to linear static analyses only. It is assumed that circumferential displacements, shear strains and shear stresses do not exist.

Similar to the plane stress element, quadrilateral elements are recommended over the triangular elements, and aspect ratios close to unity are recommended for modeling axisymmetric elements.

Refer to "Plane Stress Element".

Plate Element

This element can be used to model the structures in which both in-plane and out-of-plane bending deformations are permitted to take place, such as pressure vessels, retaining walls, bridge decks, building floors and mat foundations.

Pressure loads can be applied to the surfaces of the elements in either the GCS or ECS.

A plate element can be either quadrilateral or triangular in shape where its stiffness is formulated in two directions, in-plane direction axial and shear stiffness and out-of-plane bending and shear stiffness.

The out-of-plane stiffness used in MIDAS GEN NX includes two types of elements, DKT/DKQ (Discrete Kirchhoff elements) and DKMT/DKMQ (Discrete Kirchhoff-Mindlin elements). DKT/DKQ were developed on the basis of the Kirchhoff Thin Plate theory. Whereas, DKMT/DKMQ were developed on the basis of the Mindlin-Reissner Thick Plate theory, which results in superb performances on thick plates as well as thin plates by incorporating appropriate shear strain fields to resolve the shear-locking problem. The in-plane stiffness of the triangular element is formulated in accordance with the Linear Strain Triangle (LST) theory, whereas the Isoparametric Plane Stress Formulation with Incompatible Modes is used for the quadrilateral element.

The user may separately enter different thicknesses for an element for calculating the in-plane stiffness and the out-of-plane stiffness. In general, the self-weight and mass of an element are calculated from the thickness specified for the in-plane stiffness. However, if only the thickness for the out-of-plane stiffness is specified, they are calculated on the basis of the thickness specified for the out-of-plane stiffness.

Similar to the plane stress element, the quadrilateral element type is recommended for modeling structures with plate elements. When modeling a curved plate, the angles between two adjacent elements should remain at less than 10°. Moreover, the angles should not exceed 2~3° in the regions where precise results are required.

It is thus recommended that elements close to squares be used in the regions where stress intensities are expected to vary substantially and where detailed results are required.

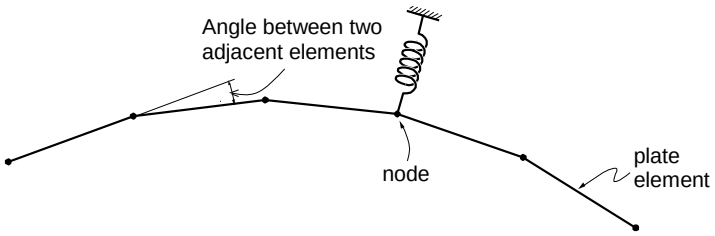

Figure 1.46 Example of plate elements used for a circular or cylindrical modeling

Solid Element

This element is used for modeling three-dimensional structures, and its types include tetrahedron, wedge and hexahedron.

Pressure loads can be applied normal to the surfaces of the elements or in the X, Y, and Z-axes of the GCS.

The use of hexahedral (8-node) elements produces accurate results in both displacements and stresses. On the other hand, using the wedge (6-node) and tetrahedron (4-node) elements may produce relatively reliable results for displacements, but poor results are derived from stress calculations. It is thus recommended that the use of the 6-node and 4-node elements be avoided if precise analysis results are required. The wedge and tetrahedron elements, however, are useful to join hexahedral elements where element sizes change.

Solid elements do not have stiffness to rotational d.o.f. at adjoining nodes. Joining elements with no rotational stiffness will result in singular errors at their nodes. In such a case, MIDAS GEN NX automatically restrains the rotational d.o.f. to prevent singular errors at the corresponding nodes.

When solid elements are connected to other elements retaining rotational stiffness, such as beam and plate elements, introducing rigid links (master node and slave node feature in MIDAS GEN NX) or rigid beam elements can preserve the compatibility between two elements.

An appropriate aspect ratio of an element may depend on several factors such as the element type, geometric configuration, structural shape, etc. In general, it is recommended that the aspect ratio be maintained close to 1.0. In the case of a hexahedral element, the corner angles should remain at close to 90°. It is particularly important to satisfy the configuration conditions where accurate analysis results are required or significant stress changes are anticipated. It is also noted that smaller elements converge much faster.

Element Stiffness Data

Material property and section (or thickness) data are necessary to compute the stiffnesses of elements. Material property data are entered through ***Model>Properties>Material***, and section data are entered through ***Model> Properties>Section*** or ***Thickness***.

Table 1.1 shows the relevant commands for calculating the stiffnesses of various elements.

Element	Material property data	Section or thickness data	Remarks
Truss element	***Material***	***Section***	Note 1
Tension-only element	***Material***	***Section***	Note 1
Compression-only element	***Material***	***Section***	Note 1
Beam element	***Material***	***Section***	Note 2
Plane stress element	***Material***	***Thickness***	Note 3
Plate element	***Material***	***Thickness***	Note 3
Plane strain element	***Material***	-	Note 4
Axisymmetric element	***Material***	-	Note 4
Solid element	***Material***	-	Note 5
Wall element	***Material***	***Thickness***	Note 3

Table 1.1 Commands for computing element stiffness data

Note

1. For truss elements, only cross-sectional areas are required for analysis. However, the section shape data should be additionally entered for the purposes of design and graphic display of the members.

2. When a beam element is used to model a Steel-Reinforced Concrete (SRC) composite member, the program automatically calculates the equivalent stiffness reflecting the composite action.

3. Thickness should be specified for planar elements.

4. No section/thickness data are required for plane strain and axisymmetric elements as the program automatically assigns the unit width (1.0) and unit angle (1.0 rad) respectively.

5. The program determines the element size from the corner nodes, and as such no section/thickness data are required for solid elements.

Definitions of section properties for line elements and their calculation methods are as follows:

The user may directly calculate and enter the section properties for line elements such as truss elements, beam elements, etc. However, cautions shall be exercised as to their effects of the properties on the structural behavior. In some instances, the effects of corrosions and wears may be taken into account when computing section properties.

MIDAS GEN NX offers the following three options to specify section properties:

1. MIDAS GEN NX automatically computes the section properties when the user simply enters the main dimensions of the section.

2. The user calculates and enters all the required section properties.

3. The user specifies nominal section designations contained in the database of AISC, BS, Eurocode3, JIS, etc.

In specifying section properties, you can assign individual ID numbers for prismatic, tapered, combined and composite sections. In the case of a construction section, two separate predefined sections are used in combination. Section properties for composite construction sections composed of steel and reinforced concrete vary with construction stages reflecting the concrete pour and maturity.

The following outlines the methods of calculating section properties and the pertinent items to be considered in the process:

Area (Cross-Sectional Area)

The cross-sectional area of a member is used to compute axial stiffness and stress when the member is subjected to a compression or tension force. Figure 1.47 illustrates the calculation procedure.

Cross-sectional areas could be reduced due to member openings and bolt or rivet holes for connections. MIDAS GEN NX does not consider such reductions. Therefore, if necessary, the user is required to modify the values using the option 2 above and his/her judgment.

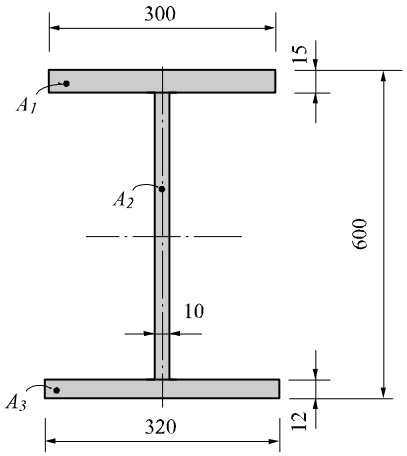

$$\text{Area} = \int dA = A_1 + A_2 + A_3$$

$$= (300 \times 15) + (573 \times 10) + (320 \times 12)$$

$$= 14070$$

Figure 1.47 Example of cross-sectional area calculation

Effective Shear Areas (A_{sy}, A_{sz})

The effective shear areas of a member are used to formulate the shear stiffness in the y and z-axis directions of the cross-section. If the effective shear areas are omitted, the shear deformations in the corresponding directions are neglected.

When MIDAS GEN NX computes the section properties by the option 1 or 3, the corresponding shear stiffness components are automatically calculated. Figure 1.48 outlines the calculation methods.

$\boldsymbol{A_{sy}}$: Effective shear area in the ECS y-axis direction
$\boldsymbol{A_{sz}}$: Effective shear area in the ECS z-axis direction

Section Shape	Effective Shear Area	Section Shape	Effective Shear Area
1. *Angle* 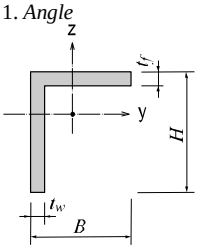	$A_{sy} = \frac{5}{6} B \times t_f$ $A_{sz} = \frac{5}{6} H \times t_w$	2. *Channel* 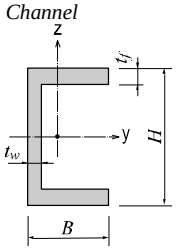	$A_{sy} = \frac{5}{6}(2 \times B \times t_f)$ $A_{sz} = H \times t_w$
3. *I-Section* 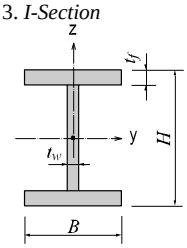	$A_{sy} = \frac{5}{6}(2 \times B \times t_f)$ $A_{sz} = H \times t_w$	4. *Tee* 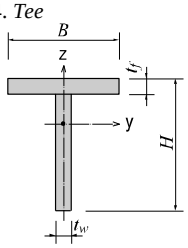	$A_{sy} = \frac{5}{6}(B \times t_f)$ $A_{sz} = H \times t_w$
5. *Thin Walled Tube* 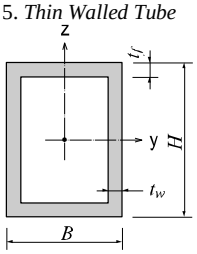	$A_{sy} = 2 \times B \times t_f$ $A_{sz} = 2 \times H \times t_w$	6. *Thin Walled Pipe* 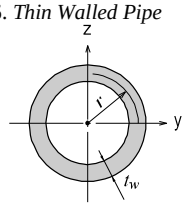	$A_{sy} = \pi \times r \times t_w$ $A_{sz} = \pi \times r \times t_w$
7. *Solid Round Bar* 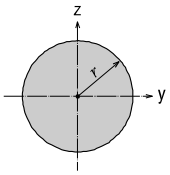	$A_{sy} = 0.9\pi r^2$ $A_{sz} = 0.9\pi r^2$	8.*Solid Rectangular Bar* 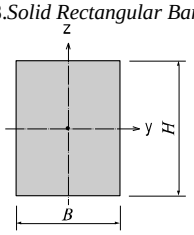	$A_{sy} = \frac{5}{6} BH$ $A_{sz} = \frac{5}{6} BH$

Figure 1.48 Effective shear areas by section shape

Torsional Resistance (I_{xx})

Torsional resistance refers to the stiffness resisting torsional moments. It is expressed as

<Eq. 1>

$$I_{xx} = \frac{T}{\theta}$$

where,

I_{xx}: Torsional resistance
T: Torsional moment or torque
θ: Angle of twist

The torsional stiffness expressed in <Eq. 1> must not be confused with the polar moment of inertia that determines the torsional shear stresses. However, they are identical to one another in the cases of circular or thick cylindrical sections.

No general equation exists to satisfactorily calculate the torsional resistance applicable for all section types. The calculation methods widely vary for open and closed sections and thin and thick thickness sections.

For calculating the torsional resistance of an open section, an approximate method is used; the section is divided into several rectangular sub-sections and then their resistances are summed into a total resistance, I_{xx}, calculated by the equation below.

<Eq. 2>

$$I_{xx} = \sum i_{xx}$$

$$i_{xx} = ab^3\left[\frac{16}{3} - 3.36\frac{b}{a}\left(1 - \frac{b^4}{12a^4}\right)\right] \quad \text{for } a \geq b$$

where,

i_{xx}: Torsional resistance of a (rectangular) sub-section
$2a$: Length of the longer side of a sub-section
$2b$: Length of the shorter side of a sub-section

Figure 1.49 illustrates the equation for calculating the torsional resistance of a thin walled, tube-shaped, closed section.

<Eq. 3>

$$I_{xx} = \frac{4A^2}{\int d_s t}$$

where,

A: Cross-sectional area of tube

d_S: Infinitesimal length of thickness centerline at a given point

t: Thickness of tube at a given point

For those sections such as bridge box girders, which retain the form of thick walled tubes, the torsional stiffness can be obtained by combining the above two equations, <Eq. 1> and <Eq. 3>.

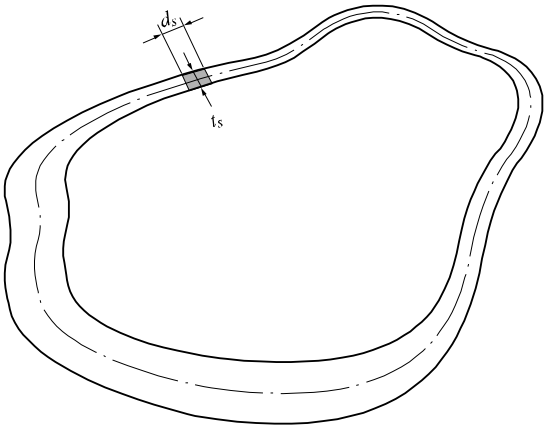

Torsional resistance: $I_{xx} = \frac{4A^2}{\int d_s / t_s}$

Shear stress at a given point: $\tau_T = \frac{T}{2At_s}$

Thickness of tube at a given point: t_s

Figure 1.49 Torsional resistance of a thin walled, tube-shaped, closed section

<table>
<tr><th>Section Shape</th><th>Torsional Resistance</th><th>Section Shape</th><th>Torsional Resistance</th></tr>
<tr><td>1. Solid Round Bar
 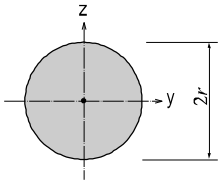
</td><td>$I_{xx} = \frac{1}{2}\pi r^2$</td><td>2. Solid Square Bar
 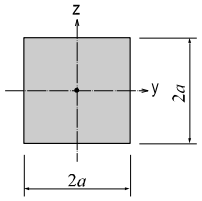
</td><td>$I_{xx} = 2.25a^4$</td></tr>
<tr><td>3. Solid Rectangular Bar
 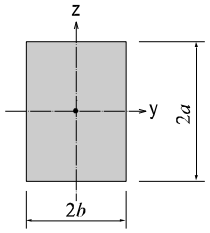
</td><td colspan="3">$I_{xx} = ab^3\left[\frac{16}{3} - 3.36\frac{b}{a}\left(I - \frac{b^4}{12a^4}\right)\right]$
$(where,\ a \geq b)$</td></tr>
</table>

Figure 1.50 Torsional resistance of solid sections

<table>
<tr><th>Section Shape</th><th>Torsional Resistance</th><th>Section Shape</th><th>Torsional Resistance</th></tr>
<tr><td>1. Rectangular Tube (Box)
 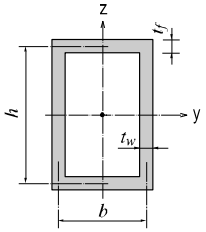
</td><td>$I_{xx} = \frac{2(b \times h)^2}{\left(\frac{b}{t_f} + \frac{h}{t_w}\right)}$</td><td>2. Circular Tube (Pipe)
 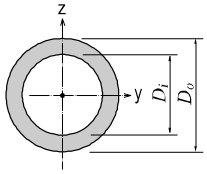
</td><td>$I_{xx} = \frac{1}{2}\pi\left[\left(\frac{D_o}{2}\right)^4 - \left(\frac{D_i}{2}\right)^4\right]$</td></tr>
</table>

Figure 1.51 Torsional resistance of thin walled, closed sections

Section Shape	Torsional Resistance
1. *Angle* 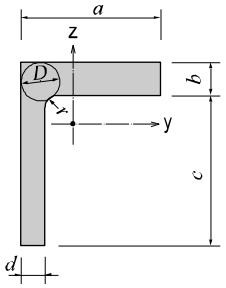 	$I_{xx} = I_1 + I_2 + \alpha D^4$ $I_1 = ab^3\left[\frac{1}{3} - 0.21\frac{b}{a}\left(1 - \frac{b^4}{12a^4}\right)\right]$ $I_2 = cd^3\left[\frac{1}{3} - 0.105\frac{d}{c}\left(1 - \frac{d^4}{192c^4}\right)\right]$ $\alpha = \frac{d}{b}\left(0.07 + 0.076\frac{r}{b}\right)$ $D = 2\left[d + b + 3r - \sqrt{2(2r+b)(2r+d)}\right]$ *(where, b < 2(d + r))*
2. *Tee* 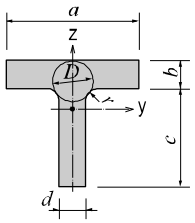 *IF b<d : t=b, t_1=d* *IF b>d : t=d, t_1=b*	$I_{xx} = I_1 + I_2 + \alpha D^4$ $I_1 = ab^3\left[\frac{1}{3} - 0.21\frac{b}{a}\left(1 - \frac{b^4}{12a^4}\right)\right]$ $I_2 = cd^3\left[\frac{1}{3} - 0.105\frac{d}{c}\left(1 - \frac{d^4}{192c^4}\right)\right]$ $\alpha = \frac{t}{t_1}\left(0.15 + 0.10\frac{r}{b}\right)$ $D = \frac{(b+r)^2 + rd + \frac{d^2}{4}}{(2r+b)}$ *(where, d < 2(b + r))*
3. *Channel* 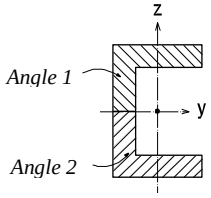 	Sum of torsinal stiffnesses of 2 angles
4. *I-Section* 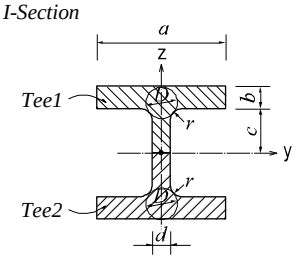 *IF b<d : t=b, t_1=d* *IF b>d : t=d, t_1=b*	$I_{xx} = 2I_1 + I_2 + 2\alpha D^4$ $I_1 = ab^3\left[\frac{1}{3} - 0.21\frac{b}{a}\left(1 - \frac{b^4}{12a^4}\right)\right]$ $I_2 = \frac{1}{3}cd^3$ $\alpha = \frac{t}{t_1}\left(0.15 + 0.10\frac{r}{b}\right)$ $D = \frac{(b+r)^2 + rd + \frac{d^2}{4}}{(2r+b)}$ *(where, d < 2(b + r))*

Figure 1.52 Torsional resistance of thick walled, open sections

Section Shape	Torsional Resistance
1. *Angle* 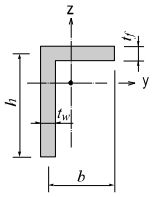	$I_{xx}=\frac{1}{3}\left(h\times t_w^3+b\times t_f^3\right)$
2. *Channel* 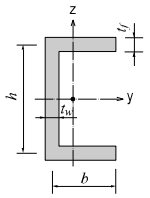	$I_{xx}=\frac{1}{3}\left(h\times t_w^3+2\times b\times t_f^3\right)$
3. *I-Section* 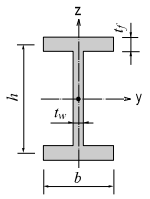	$I_{xx}=\frac{1}{3}\left(h\times t_w^3+2\times b\times t_f^3\right)$
4. *Tee* 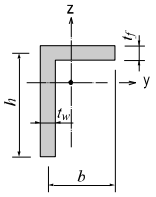	$I_{xx}=\frac{1}{3}\left(h\times t_w^3+b\times t_f^3\right)$
5. *I-Section* 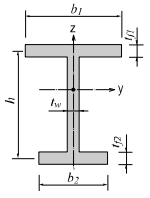	$I_{xx}=\frac{1}{3}\left(h\times t_w^3+b_1\times {t_{f1}}^3+b_2\times {t_{f2}}^3\right)$

Figure 1.53 Torsional resistance of thin walled, open sections

In practice, combined sections often exist. A combined built-up section may include both closed and open sections. In such a case, the stiffness calculation is performed for each part, and their torsional stiffnesses are summed to establish the total stiffness for the built-up section.

For example, a double I-section shown in Figure 1.54 (a) consists of a closed section in the middle and two open sections, one on each side.

-The torsional resistance of the closed section (hatched part)

<Eq. 4>

$$I_c = \frac{2(b_1 \times h_1)^2}{\left(\frac{b_1}{t_f} + \frac{h_1}{t_w} \right)}$$

-The torsional resistance of the open sections (unhatched parts)

<Eq. 5>

$$I_o = 2\left[\frac{1}{3}(2b - b_1 - t_w) \times t_w{}^3 \right]$$

-The total resistance of the built-up section

<Eq. 6>

$$I_{xx} = I_c + I_o$$

Figure 1.54 (b) shows a built-up section made up of an I-shaped section reinforced with two web plates, forming two closed sections. In this case, the torsional resistance for the section is computed as follows:

If the torsional resistance contributed by the flange tips is negligible relative to the total section, the torsional property may be calculated solely on the basis of the outer closed section (hatched section) as expressed in <Eq. 7>.

<Eq. 7>

$$I_{xx} = \frac{2(b_1 \times h_1)^2}{\left(\frac{b_1}{t_f} + \frac{h_1}{t_s} \right)}$$

If the torsional resistance of the open sections is too large to ignore, then it should be included in the total resistance.

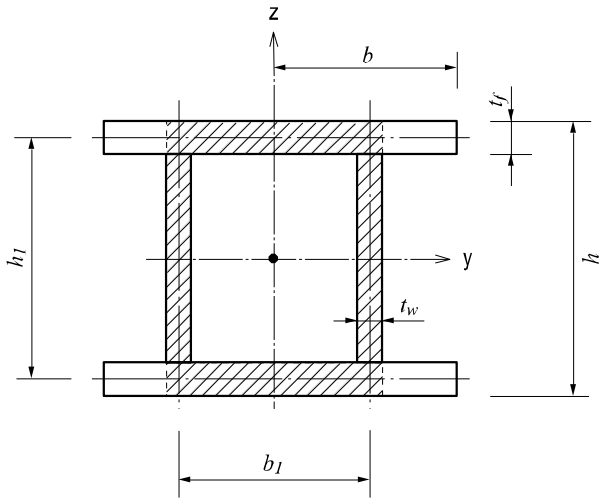

(a) Section consisted of closed and open sections

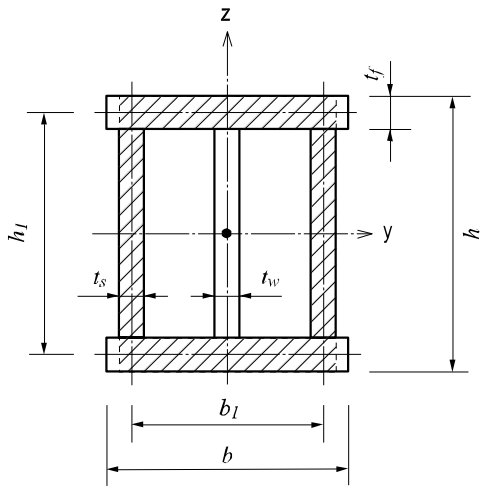

(b) Section consisted of two closed sections

Figure 1.54 Torsional resistance of built-up sections

Area Moment of Inertia (I_{yy}, I_{zz})

The area moment of inertia is used to compute the flexural stiffness resisting bending moments. It is calculated relative to the centroid of the section.

-Area moment of inertia about the ECS y-axis

<Eq. 8>

$$I_{yy} = \int z^2 dA$$

-Area moment of inertia about the ECS z-axis

<Eq. 9>

$$I_{zz} = \int y^2 dA$$

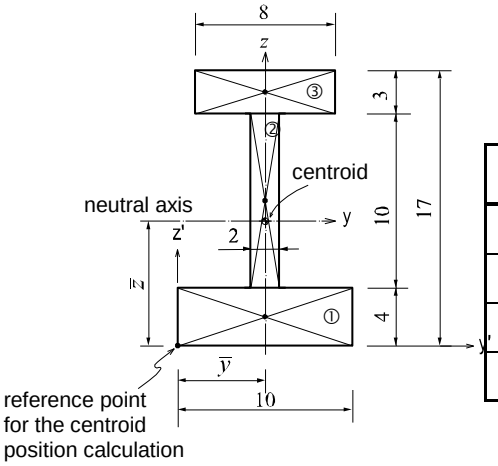

Section Element	b	h	A_i	$\bar{z}_i$	Q_{yi}	$\bar{y}_i$	Q_{zi}
①	10	4	40	2	80	5	200
②	2	10	20	9	180	5	100
③	8	3	24	15.5	372	5	120
Total	-	-	84	-	632	-	420

A_i : area

$\bar{z}_i$: distance from the reference point to the centroid of the section element in the z′-axis direction

$\bar{y}_i$: distance from the reference point to the centroid of the section element in the y′-axis direction

Q_{yi} : first moment of area relative to the reference point in the y′-axis direction

Q_{zi} : first moment of area relative to the reference point in the z′-axis direction

➢ ***Calculation of neutral axes ($\bar{Z}, \bar{Y}$)***

$$\bar{Z} = \frac{\int \bar{z} dA}{Area} = \frac{Q_y}{Area} = \frac{632}{84} = 7.5238$$

$$\bar{Y} = \frac{\int \bar{y} dA}{Area} = \frac{Q_z}{Area} = \frac{420}{84} = 5.0000$$

➢ ***Calculation of area moments of inertia (Iyy, Izz)***

Section Element	A_i	$\bar{Z} - \bar{z}_i$	I_{y1}	I_{y2}	I_{yy}	$\bar{Y} - \bar{y}_i$	I_{z1}	I_{z2}	I_{zz}
①	40	5.5328	1224.5	53.3	1277.8	0	0	333.3	333.3
②	20	1.4672	43.1	166.7	209.8	0	0	6.7	6.7
③	24	7.9762	1526.9	18.0	1544.9	0	0	128.0	128.0
Total			2976.5	238.0	3032.5		0	468.0	468.0

$$I_{y1} = A_i \times (\bar{Z} - \bar{z}_i)^2, \quad I_{y2} = \frac{bh^3}{12}, \quad I_{yy} = I_{y1} + I_{y2}$$

$$I_{z1} = A_i \times (\bar{Y} - \bar{y}_i)^2, \quad I_{z2} = \frac{hb^3}{12}, \quad I_{zz} = I_{z1} + I_{z2}$$

Figure 1.55 Example of calculating area moments of inertia

Area Product Moment of Inertia (I_{yz})

The area product moment of inertia is used to compute stresses for non-symmetrical sections, which is defined as follows:

<Eq. 10>

$$I_{yz} = \int y \cdot z dA$$

Sections that have at least one axis of symmetry produce $I_{yz}=0$. Typical symmetrical sections include I, pipe, box, channel and tee shapes, which are symmetrical about at least one of their local axes, y and z. However, for non-symmetrical sections such as angle shaped sections, where $I_{yz}\neq 0$, the area product moment of inertia should be considered for obtaining stress components.

The area product moment of inertia for an angle is calculated as shown in Figure 1.56.

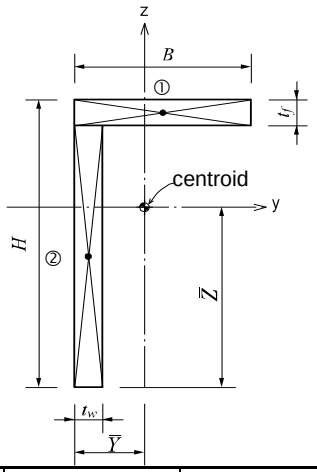

Section Element	A_i	e_{yi}	e_{zi}
①	$B \times t_f$	$B/2-\bar{Y}$	$(H-t_f/2)-\bar{Z}$
②	$(H-t_f)\times t_w$	$t_w/2-\bar{Y}$	$(H-t_f/2)-\bar{Z}$

$$\begin{aligned} I_{yz} &= \sum A_i \times e_{yi} \times e_{zj} \\ &= (B \times t_f) \times (B/2-\bar{Y}) \times \{(H-t_f/2)-\bar{Z}\} \\ &\quad +\{(H-t_f) \times t_w\} \times \{t_w/2-\bar{Y}) \times \{(H-t_f/2)-\bar{Z}\} \end{aligned}$$

Figure 1.56 Area product moment of inertia for an angle

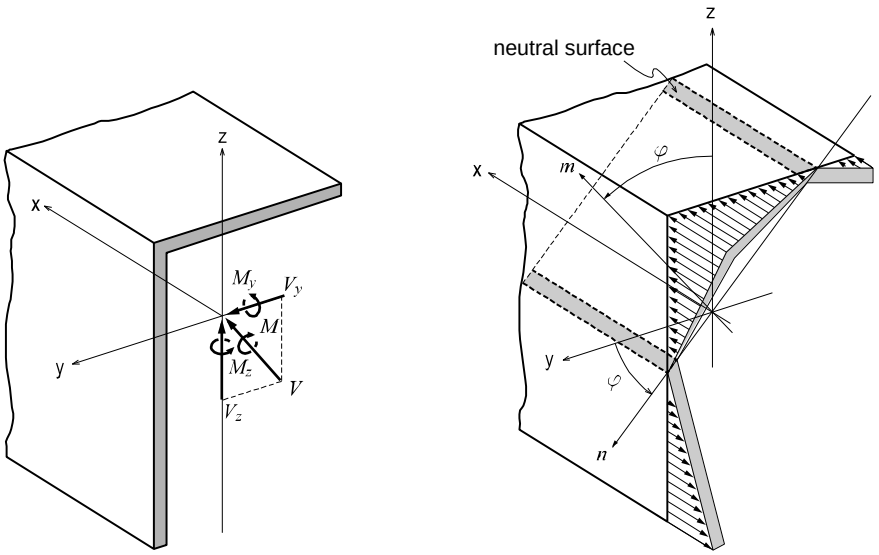

Figure 1.57 Bending stress distribution of a non-symmetrical section

The neutral axis represents an axis along which bending stress is 0 (zero). As illustrated in the right-hand side of Figure 1.57, the n-axis represents the neutral axis, to which the m-axis is perpendicular. Since the bending stress is zero at the neutral axis, the direction of the neutral axis can be obtained from the relation defined as

<Eq. 11>

$$(M_y \times I_{zz} + M_z \times I_{yz}) \times z - (M_z \times I_{yy} + M_y \times I_{yz}) \times y = 0$$

$$\tan\phi = \frac{y}{z} = \frac{M_y \times I_{zz} + M_z \times I_{yz}}{M_z \times I_{yy} + M_y \times I_{yz}}$$

The following represents a general equation applied to calculate the bending stress of a section:

<Eq. 12>

$$f_b = \frac{M_y - M_z(I_{yz}/I_{zz})}{I_{yy} - (I_{yz}{}^2/I_{zz})} \cdot z + \frac{M_z - M_y(I_{yz}/I_{yy})}{I_{zz} - (I_{yz}{}^2/I_{yy})} \cdot y$$

In the case of an I shaped section, I_{yz}=0, hence the equation can be simplified as:

<Eq. 13>

$$f_b = \frac{M_y}{I_{yy}} \cdot z + \frac{M_z}{I_{zz}} \cdot y = f_{by} + f_{bx}$$

where,

I_{yy}: Area moment of inertia about the ECS y-axis
I_{zz}: Area moment of inertia about the ECS z-axis
I_{yz}: Area product moment of inertia
y: Distance from the neutral axis to the location of bending stress calculation in the ECS y-axis direction
z: Distance from the neutral axis to the location of bending stress calculation in the ECS z-axis direction
M_y: Bending moment about the ECS y-axis
M_z: Bending moment about the ECS z-axis

The general expressions for calculating shear stresses in the ECS y and z-axes are:

<Eq. 14>

$$\tau_y = \frac{V_y}{b_z \times (I_{yy} \cdot I_{zz} - I_{yz}^{\,2})} \times (I_{yy} \cdot Q_z - I_{yz} \cdot Q_y) = \left(\frac{I_{yy} \cdot Q_z - I_{yz} \cdot Q_y}{I_{yy} \cdot I_{zz} - I_{yz}^{\,2}} \right) \times \left(\frac{V_y}{b_z} \right)$$

<Eq. 15>

$$\tau_x = \frac{V_z}{b_y \times (I_{yy} \cdot I_{zz} - I_{yz}^{\,2})} \times (I_{zz} \cdot Q_y - I_{yz} \cdot Q_z) = \left(\frac{I_{zz} \cdot Q_y - I_{yz} \cdot Q_z}{I_{yy} \cdot I_{zz} - I_{yz}^{\,2}} \right) \times \left(\frac{V_z}{b_y} \right)$$

where,

V_y: Shear force in the ECS y-axis direction
V_z: Shear force in the ECS z-axis direction
Q_y: First moment of area about the ECS y-axis
Q_z: First moment of area about the ECS z-axis
b_y: Thickness of the section at which a shear stress is calculated, in the direction normal to the ECS z-axis
b_z: Thickness of the section at which a shear stress is calculated, in the direction normal to the ECS y-axis

First Moment of Area (Q_y, Q_z)

The first moment of area is used to compute the shear stress at a particular point on a section. It is defined as follows:

<Eq. 16>

$$Q_y = \int z dA$$

<Eq. 17>

$$Q_z = \int y dA$$

When a section is symmetrical about at least one of the y and z-axes, the shear stresses at a particular point are:

<Eq. 18>

$$\tau_y = \frac{V_y \cdot Q_z}{I_{zz} \cdot b_z}$$

<Eq. 19>

$$\tau_z = \frac{V_z \cdot Q_y}{I_{yy} \cdot b_y}$$

where,

V_y: Shear force acting in the ECS y-axis direction
V_z: Shear force acting in the ECS z-axis direction
I_{yy}: Area moment of inertia about the ECS y-axis
I_{zz}: Area moment of inertia about the ECS z-axis
b_y: Thickness of the section at the point of shear stress calculation in the ECS y-axis direction
b_z: Thickness of the section at the point of shear stress calculation in the ECS z-axis direction

Shear Factor for Shear Stress (Q_{yb}, Q_{zb})

The shear factor is used to compute the shear stress at a particular point on a section, which is obtained by dividing the first moment of area by the thickness of the section.

<Eq. 20>

$$\tau_y = \frac{V_y \cdot Q_z}{I_{zz} \cdot b_z} = \frac{V_y}{I_{zz}}\left(\frac{Q_z}{b_z}\right) = \frac{V_y}{I_{zz}} Q_{zb} \ , \ Q_{zb} = \frac{Q_z}{b_z}$$

<Eq. 21>

$$\tau_z = \frac{V_z \cdot Q_y}{I_{yy} \cdot b_y} = \frac{V_z}{I_{yy}}\left(\frac{Q_y}{b_y}\right) = \frac{V_z}{I_{yy}} Q_{yb} \ , \ Q_{yb} = \frac{Q_y}{b_y}$$

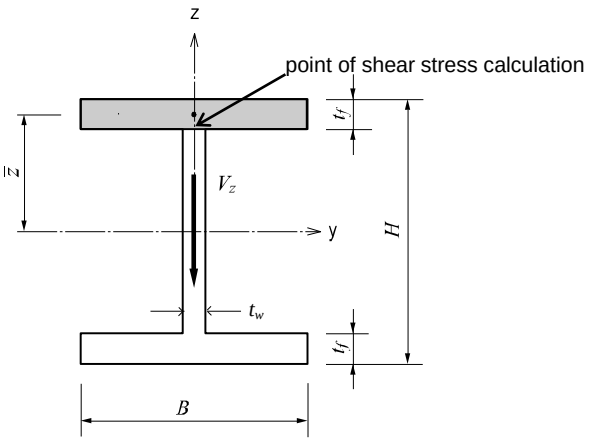

$$\tau_z = \frac{V_z Q_y}{I_{yy} b_y} = \frac{V_z}{I_{yy}} Q_{yb}$$

$$Q_y = \int z dA = (B \times t_f) \times \bar{z}$$

$$b_y = t_w$$

$$Q_{yb} = \{(B \cdot t_f) \times \bar{z}\} / t_w$$

Figure 1.58 Example of calculating a shear factor

Stiffness of Composite Sections

MIDAS GEN NX calculates the stiffness for a full composite action of structural steel and reinforced concrete. Reinforcing bars are presumed to be included in the concrete section. The composite action is transformed into equivalent section properties.

The program uses the elastic moduli of the steel (E_s) and concrete (E_c) defined in the SSRC79 (Structural Stability Research Council, 1979, USA) for calculating the equivalent section properties. In addition, the E_c value is decreased by 20% in accordance with the EUROCODE 4.

- **Equivalent cross-sectional area**

$$Area_{eq} = A_{st1} + \frac{0.8E_c}{E_s} A_{con} = A_{st1} + 0.8\frac{A_{con}}{REN}$$

- **Equivalent effective shear area**

$$As_{eq} = As_{st1} + \frac{0.8E_c}{E_s} As_{con} = As_{st1} + 0.8\frac{As_{con}}{REN}$$

- **Equivalent area moment of inertia**

$$I_{eq} = I_{st1} + \frac{0.8E_c}{E_s} I_{con} = I_{st1} + 0.8\frac{I_{con}}{REN}$$

where,

A_{st1}: Area of structural steel
A_{con}: Area of concrete
As_{st1}: Effective shear area of structural steel
As_{con}: Effective shear area of concrete
I_{st1}: Area moment of inertia of structural steel
I_{con}: Area moment of inertia of concrete
REN: Modular ratio (elasticity modular ratio of the structural steel to the concrete, E_s/E_c)

Boundary Conditions

Boundary Conditions

Boundary conditions are distinguished by nodal boundary conditions and element boundary conditions.

- **Nodal boundary conditions:**
  Constraint for degree of freedom
  Elastic boundary element (Spring support)
  Elastic link element (Elastic Link)

- **Element boundary conditions:**
  Element end release
  Rigid end offset distance (Beam End Offset)
  Rigid link

Constraint for Degree of Freedom

The constraint function may be used to constrain specific nodal displacements or connecting nodes among elements such as truss, plane stress and plate elements, where certain degrees of freedom are deficient.

Refer to "Model> Boundaries>Supports" of On-line Manual.

Nodal constraints are applicable for 6 degrees of freedom with respect to the Global Coordinate System (GCS) or the Node local Coordinate System (NCS).

Figure 1.59 illustrates a method of specifying constraints on the degrees of freedom of a planar frame model. Since this is a two dimensional model with permitted degrees of freedom in the GCS X-Z plane, the displacement d.o.f. in the GCS X-direction and the rotational d.o.f. about the GCS X and Z axes need to be restrained at all the nodes, using ***Model>Boundaries>Supports***.

For node **N1**, which is a fixed support, the ***Supports*** function is used to additionally restrain the displacement d.o.f. in the GCS X and Z-directions and the rotational d.o.f. about the GCS Y-axis.

Use the function "Model>Structure Type" for convenience when analyzing two-dimensional problems.

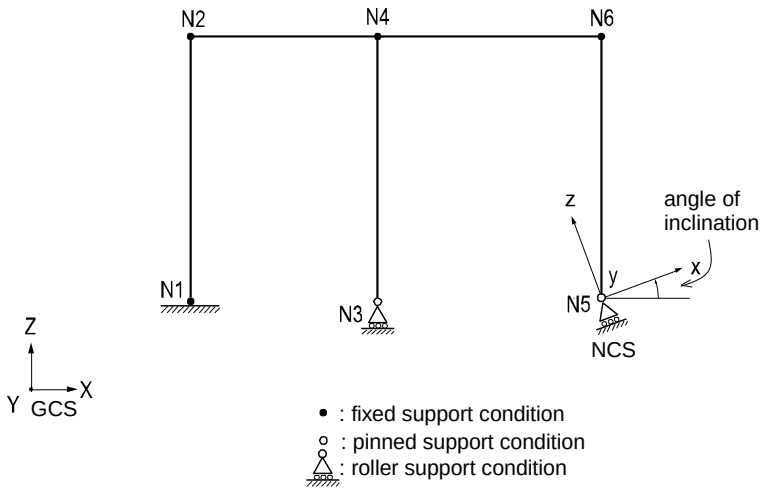

Figure 1.59 Planar frame model with constraints

For node **N3**, which is a roller support, the displacement d.o.f. in the GCS Z direction is additionally restrained.

For node **N5,** which is a roller support in a NCS, the NCS is defined first at an angle to the GCS X-axis. Then the corresponding displacement degrees of freedom are restrained in the NCS using ***Supports***.

Refer to "Model> Boundaries>Node Local Axis" of On-line Manual.

Nodal constraints are assigned to supports where displacements are truly negligible. When nodal constraints are assigned to a node, the corresponding reactions are produced at the node. Reactions at nodes are produced in the GCS, or they may be produced in the NCS if defined.

Figure 1.60 shows examples of constraining deficient degrees of freedom of elements using ***Supports***.

In Figure 1.60 (a), the displacement d.o.f. in the X-axis direction and the rotational d.o.f. about all the axes at the connecting node are constrained because the truss elements have the axial d.o.f. only.

Figure 1.60 (b) represents an I-beam where the top and bottom flanges are modeled as beam elements and the web is modeled with plane stress elements. The beam elements have 6 d.o.f. at each node, and as such where the plane stress elements are connected to the beam elements, no additional nodal constraints are required. Whereas, the out-of-plane displacement d.o.f. in the Y direction and the rotational d.o.f. in all directions are constrained at the nodes where the plane stress elements are connected to one another. Plane stress elements retain the in-plane displacement degrees of freedom only.

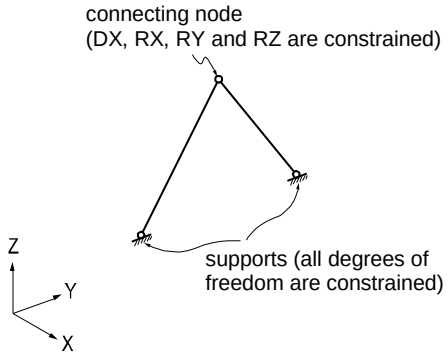

(a) Connection of truss elements

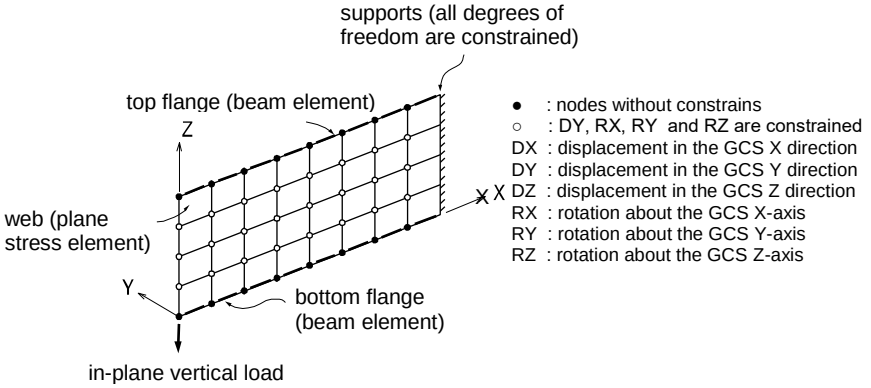

(b) Modeling of an I-shaped cantilever beam, top/bottom flanges modeled as beam elements, and web modeled as plane stress elements

Figure 1.60 Examples of constraints on degrees of freedom

Elastic Boundary Elements (Spring Supports)

Elastic boundary elements are used to define the stiffness of adjoining structures or foundations. They are also used to prevent singular errors from occurring at the connecting nodes of elements with limited degrees of freedom, such as truss, plane stress, plate element, etc.

Refer to "Model> Boundaries>Point Spring Supports" of On-line Manual.

Spring supports at a node can be expressed in six degrees of freedom, three translational and three rotational components with respect to the Global Coordinate System (GCS). The translational and rotational spring components are represented in terms of unit force per unit length and unit moment per unit radian respectively.

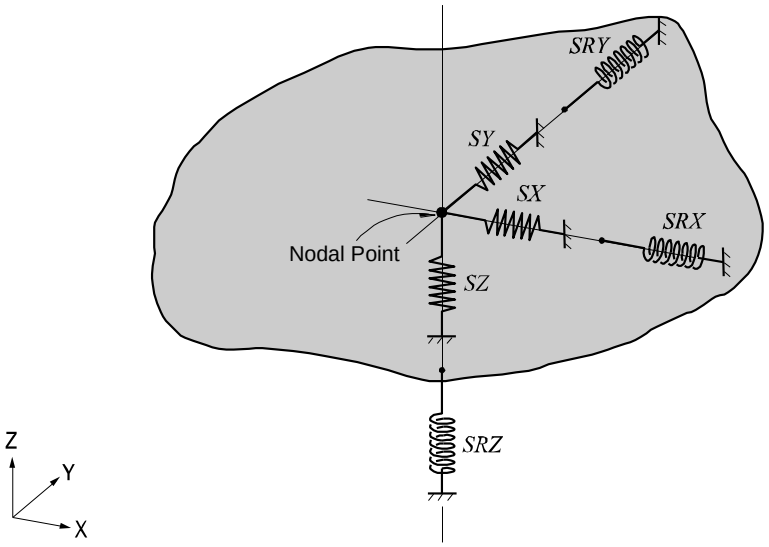

(a) Modeling of boundary condition using point spring supports

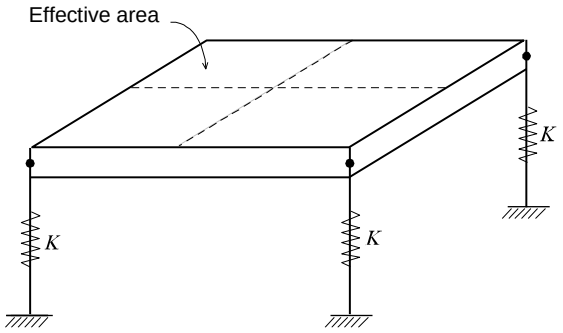

K = modulus of subgrade reaction x effective area

(b) Modeling of boundary conditions using surface spring supports

Figure 1.61 Modeling examples of spring supports

Spring supports are readily applied to reflect the stiffness of columns, piles or soil conditions. When modeling sub-soils for foundation supports, the modulus of subgrade reaction is multiplied by the tributary areas of the corresponding nodes. In this case, it is cautioned that soils can resist compressions only.

MIDAS GEN NX provides ***Surface Spring Supports*** to readily model the boundary conditions of the subsurface interface. The Point Spring is selected in ***Model>Boundaries>Surface Spring Supports*** and the modulus of subgrade reaction is specified in each direction. The soil property is then applied to the effective areas of individual nodes to produce the nodal spring stiffness as a boundary condition. In order to reflect the true soil characteristics, which can sustain compression only, Elastic Link (compression-only) is selected and the modulus of subgrade reaction is entered for the boundary condition.

Refer to "Model> Boundaries>Surface Spring Supports" of On-line Manual.

Table 1.2 summarizes moduli of subgrade reaction for soils that could be typically encountered in practice. It is recommended that both maximum and minimum values be used separately, and conservative values with discretion be adopted for design.

The axial stiffness of spring supports for columns or piles can be calculated by *EA/H*, where E is the modulus of elasticity for columns or piles, A is Effective cross-sectional area, and H is Effective length.

Reference "Foundation Analysis and Design" by Joseph E. Bowles 4th Edition

Soil Type	Modulus of subgrade reaction (KN/m^3)
Soft clay	12000 ~ 24000
Medium stiff clay	24000 ~ 48000
Stiff clay	48000~ 112000
Loose sand	4800 ~ 16000
Medium dense sand	9600 ~ 80000
Silty medium dense sand	24000 ~ 48000
Clayey gravel	48000 ~ 96000
Clayey medium dense sand	32000 ~ 80000
Dense sand	64000 ~ 130000
Very dense sand	80000~ 190000
Silty gravel	80000~ 190000

Table 1.2 Typical values of moduli of subgrade reaction for soils

Rotational spring components are used to represent the rotational stiffness of contiguous boundaries of the structure in question. If the contiguous boundaries are columns, the stiffness is calculated by $\alpha EI/H$, where α is a rotational stiffness coefficient, I is Effective moment of inertia, and H is Effective length.

Generally, boundary springs at a node are entered in the direction of each d.o.f. For more accurate analyses, however, additional coupled stiffness associated with other degrees of freedom needs to be considered. That is, springs representing coupled stiffness may become necessary to reflect rotational displacements accompanied by translational displacements. For instance, it may be necessary to model pile foundation as boundary spring supports. More rigorous analysis could be performed by introducing coupled rotational stiffness in addition to the translational stiffness in each direction.

Refer to “Model> Boundaries>General Spring Supports” of On-line Manual.

Boundary springs specified at a node, in general, follows the GCS unless an NCS is specified, in which case they are defined relative to the NCS.

Singular errors are likely to occur when stiffness components in certain degrees of freedom are deficient subsequent to formulating the stiffness. If the rotational stiffness components are required to avoid such singular errors, it is recommended that the values from 0.0001 to 0.01 be used. The range of the values may vary somewhat depending on the unit system used. To avoid such singular errors, MIDAS GEN NX

thus provides a function that automatically assigns stiffness values, which are insignificant to affect the analysis results.

Refer to "Analysis> Main Control Data" of On-line Manual.

Elastic Link Element

An elastic link element connects two nodes to act as an element, and the user defines its stiffness. Truss or beam elements may represent elastic links.

However, they are not suitable for providing the required stiffness with the magnitudes and directions that the user desires. An elastic link element is composed of three translational and three rotational stiffnesses expressed in the ECS.

The translational and rotational stiffnesses of an elastic link element are expressed in terms of unit force per unit length and unit moment per unit radian respectively. Figure 1.62 presents the directions of the ECS axes. An elastic link element may become a tension-only or compression-only element, in which case the only directional stiffness can be specified is in the ECS x-axis.

Examples for elastic link elements include elastic bearings of a bridge structure, which separate the bridge deck from the piers. Compression-only elastic link elements can be used to model the soil boundary conditions. The rigid link option connects two nodes with an "infinite" stiffness.

Refer to "Model> Boundaries>Elastic Link" of On-line Manual.

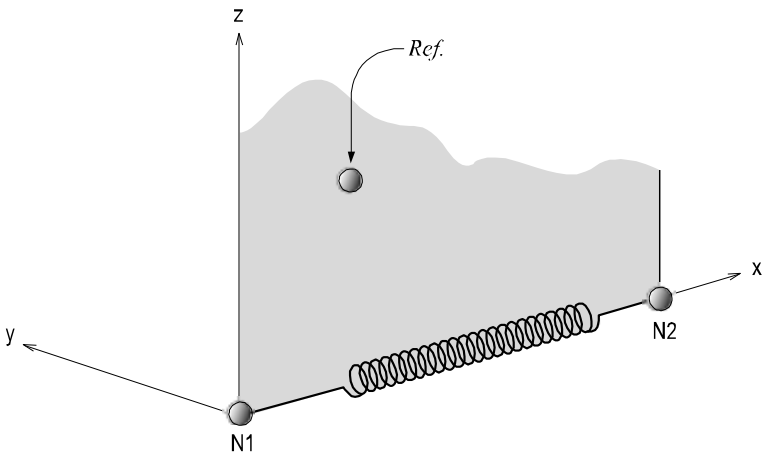

Figure 1.62 The ECS of an elastic link element connecting two nodes

General Link Element

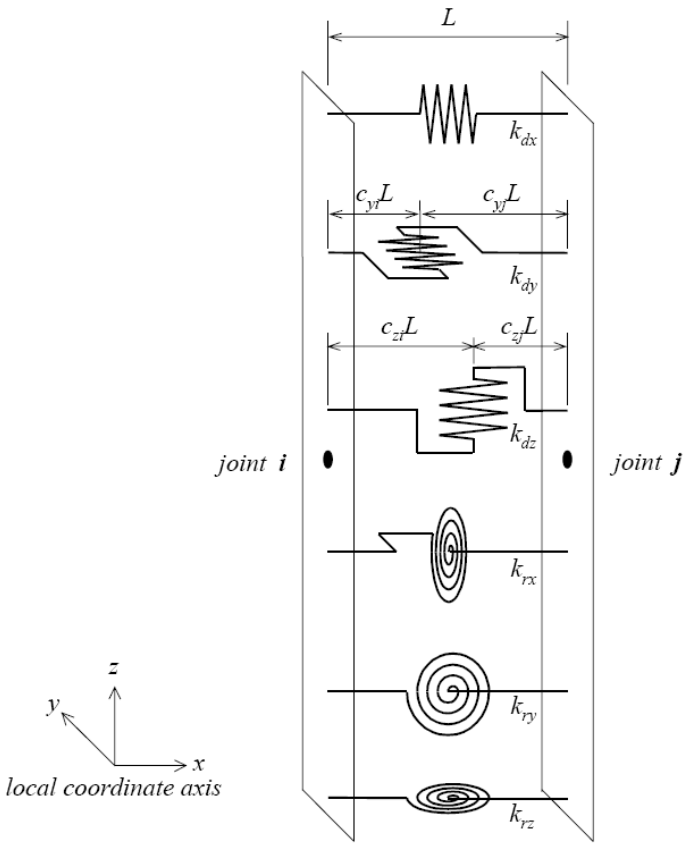

Figure 1.63 Composition of General Link Element

The General Link element is used to model dampers, base isolators, compression-only element, tension-only element, plastic hinges, soil springs, etc. The 6 springs individually represent 1 axial deformation spring, 2 shear deformation springs, 1 torsional deformation spring and 2 bending deformation springs as per Figure 1.63. Among the 6 springs, only selective springs may be partially used, and linear and nonlinear properties can be assigned. The general link can be thus used as linear and nonlinear elements.

The General Link element can be largely classified into Element type and Force type depending on the method of applying it to analysis. The Element type general link element directly reflects the nonlinear behavior of the element by renewing the element stiffness matrix. The Force type on the other hand, does not renew the stiffness matrix, but rather reflects the nonlinearity indirectly by

converting the member forces calculated based on the nonlinear properties into external forces.

First, the Element type general link element provides three types, Spring, Dashpot and Spring and Dashpot. The Spring retains linear elastic stiffness for each of 6 components, and the Dashpot retains linear viscous damping for each of 6 components. The Spring and Dashpot is a type, which combines Spring and Dashpot. All of the three types are analyzed as linear elements. However, the Spring type general link element can be assigned inelastic hinge properties and used as a nonlinear element. This can be mainly used to model plastic hinges, which exist in parts in a structure or nonlinearity of soils. However, this can be used as a nonlinear element only in the process of nonlinear time history analysis by direct integration. Also, viscous damping is reflected in linear and nonlinear time history analyses only if "Group Damping" is selected for damping for the structure.

The Force type general link element can be used for dampers such as Viscoelastic Damper and Hysteretic System, seismic isolators such as Lead Rubber Bearing Isolator and Friction Pendulum System Isolator, Gap (compression-only element) and Hook (tension-only element). Each of the components retains effective stiffness and effective damping. You may specify nonlinear properties for selective components.

The Force type general link element is applied in analysis as below. First, it is analyzed as a linear element based on the effective stiffness while ignoring the effective damping in static and response spectrum analyses. In linear time history analysis, it is analyzed as a linear element based on the effective stiffness, and the effective damping is considered only when the damping selection is set as "Group Damping". In nonlinear time history analysis, the effective stiffness acts as virtual linear stiffness, and as indicated before, the stiffness matrix does not become renewed even if it has nonlinear properties.

Also, because the nonlinear properties of the element are considered in analysis, the effective damping is not used. This is because the role of effective damping indirectly reflects energy dissipation due to the nonlinear behavior of the Force type general link element in linear analysis. The rules for applying the general link element noted above are summarized in Table 1.3.

When the damping selection is set as "Group Damping", the damping of the Element type general link element and the effective damping of the Force type general link element are reflected in analysis as below. First, when linear and nonlinear analyses are carried out based on modal superposition, they are reflected in the analyses through modal damping ratios based on strain energy.

On the other hand, when linear and nonlinear analyses are carried out by direct integration, they are reflected through formulating the element damping matrix.

If element stiffness or element-mass-proportional damping is specified for the general link element, the analysis is carried out by adding the damping or effective damping specified for the properties of the general link element.

General Link Element		Element Type		Force Type	
Properties		**Elastic**	**Damping**	**Effective Stiffness**	**Effective Damping**
Static analysis		Elastic	X	Elastic	X
Response spectrum analysis		Elastic	X	Elastic	X
Linear Time History Analysis	Model Superposition	Elastic	Linear	Elastic	Linear
	Direct Integration	Elastic	Linear	Elastic	Linear
Nonlinear Time History Analysis	Modal Superposition	Elastic	Linear	Elastic (virtual)	X
	Direct Integration	Elastic & Inelastic	Linear	Elastic (virtual)	X

Table 1.3 Rules for applying general link element (Damping and effective damping are considered only when the damping option is set to "Group Damping".)

The locations of the 2 shear springs may be separately specified on the member. The locations are defined in ratios by the distances from the first node relative to the total length of the member. If the locations of the shear springs are specified and shear forces are acting on the nonlinear link element, the bending moments at the ends of the member are different. The rotational deformations also vary depending on the locations of the shear springs. Conversely, if the locations of the shear springs are unspecified, the end bending moments always remain equal regardless of the presence of shear forces.

The degrees of freedom for each element are composed of 3 translational displacement components and 3 rotational displacement components regardless of the element or global coordinate system. The element coordinate system follows the convention of the truss element. Internal forces produced for each node of the element consist of 1 axial force, 2 shear forces, 1 torsional moment and 2 bending moments. The sign convention is identical to that of the beam element. In calculating the nodal forces of the element, the nodal forces due to damping or effective damping of the general link element are found based on Table1.3.However,the nodal forces due to the element mass or element stiffness-proportional damping are ignored.

Element End Release

When two elements are connected at a node, the stiffness relative to the degrees of freedom of the two elements is reflected. Element End Release can release such stiffness connections. This function can be applied to beam and plate elements, and the methods of which are outlined below.

Beam End Release is applicable for all the degrees of freedom of the two nodes of an element. Using partial fixity coefficients can create partial stiffness of elements. If all three rotational degrees of freedom are released at both ends of a beam element, then the element will behave like a truss element.

Refer to "Model> Boundaries>Beam End Release" of On-line Manual.

Similarly, Plate End Release is applicable for all the degrees of freedom of three or four nodes constituting a plate element. Note that the plate element does not retain the rotational degree of freedom about the axis normal to the plane of the element. If all the out-of-plane rotational d.o.f. are released at the nodes of a plate element, this element then behaves like a plane stress element.

Refer to "Model> Boundaries>Plate End Release" of On-line Manual.

The end releases are always specified in the Element Coordinate System (ECS). Cautions should be exercised when stiffness in the GCS is to be released. Further, the change in stiffness due to end releases could produce singular errors, and as such the user is encouraged to specify end releases carefully through a comprehensive understanding of the entire structure.

Figure 1.63 shows boundary condition models depicting the connections between a pier and bridge decks, using end releases for beam and plate elements.

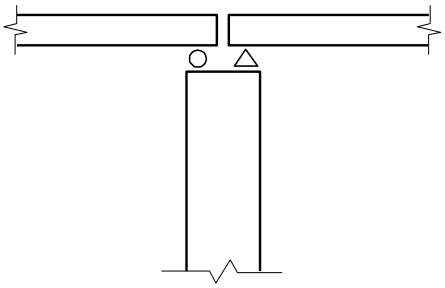

(a) Connection of a pier and bridge decks

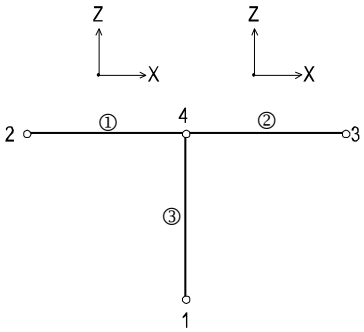

Element 1 – Node 4 end release of F_x & M_y
Element 2 – Node 4 end release of M_y

(b) Modeling of beam elements

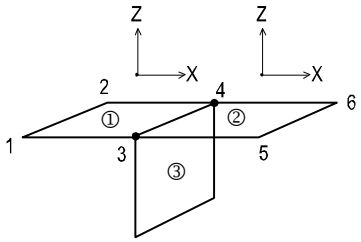

Element 1 – Node 3 & 4 end release of F_x & M_y
Element 2 – Node 3 & 4 end release of M_y

(c) Modeling of plate elements

Figure 1.63 Modeling of end releases using beam and plate elements

Rigid End Offset Distance

Frame members of civil and building structures are typically represented by element centerlines. Whereas, physical joint sizes (panel zones) actually do exist at the intersections of the element centerlines. Ignoring such panel zones in an analysis will result in larger displacements and moments. In order to account for element end eccentricities and panel zone effects at beam-column connections, MIDAS GEN NX provides the following two methods: Note that the terms, beams and girders are interchangeably used in this section. (See Figure 1.64)

Refer to "Model> Boundaries>Panel Zone Effects" of On-line Manual.

1. MIDAS GEN NX automatically calculates rigid end offset distances for all panel zones where column and beam members intersect.

Refer to "Model> Boundaries>Beam End Offsets" of On-line Manual.

2. The user directly defines the rigid end offset distances at beam-ends.

Rigid end offset distances are applicable only to beam elements, including tapered beam elements, in MIDAS GEN NX.

Automatic consideration of panel zone stiffness

If the bending and shear deformations in the panel zones are ignored, the effective length for member stiffness can be written as:

$$L_1 = L - (R_i + R_j)$$

where, L is the length between the end nodes, and R_i and R_j are the rigid end offset distances at both ends. If the element length is simply taken as L_1, the result will contain some errors by ignoring the actual rigid end deformations. MIDAS GEN NX, therefore, allows the user to alleviate such errors by introducing a compensating factors for rigid end offset distances (Offset Factors).

$$L_1 = L - Z_F\ (R_i + R_j)$$

where, Z_F is an offset factor for rigid end offset distance.

The value of the offset factor for rigid end offset distance varies from 0 to 1.0. The user's discretion is required for determining the factor as it depends on the shapes of connections and the use of reinforcement.

The rigid end offset factor does not affect the calculation of axial and torsional deformations. The entire element length (L) is used for such purposes.

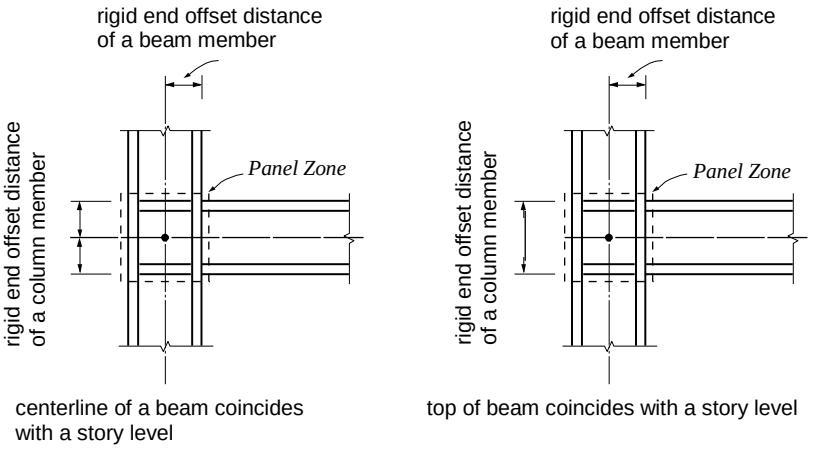

(a) Formation of Rigid panel zones at beam-column connections

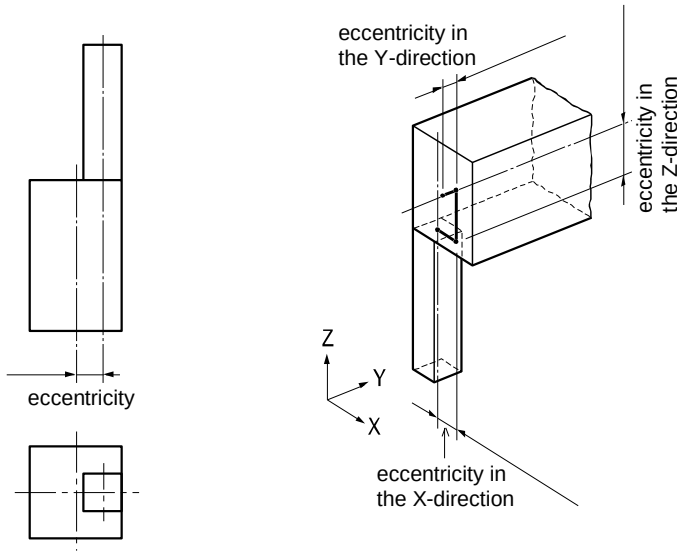

(b) Column connection with eccentricity (c) Beam-column connection with eccentricity

Figure 1.64 Examples of end offsets due to discordant neutral axes between beam elements

Using ***Model>Boundaries>Panel Zone Effects*** in MIDAS GEN NX, the GCS Z-axis is automatically established opposite to the gravity direction, and the rigid end offset distances of the panel zones are automatically considered. Note that the rigid end offset distances are applicable only to the beam–column connections. The columns represent the elements parallel to the GCS Z-axis, and the beams represent the elements parallel to the GCS X-Y plane.

Refer to "Model> Structure Type" of On-line Manual.

When the ***Panel Zone Effects*** function is used to calculate the rigid end offset distances automatically, the user may select the "Offset Position" for the "Output Position". In that case, the element stiffness, applications of self-weight and distributed loads, and the output locations of member forces vary with the offset locations adjusted by the offset factor. If "Panel Zone" is selected, the offset factor is reflected in the element lengths for the element stiffness only. The locations for applying self-weight and distributed loads and the output locations of member forces are determined on the basis of the boundaries of the panel zones, i.e., column faces for beams and beam faces for columns.

Selecting "Offset Position" with an offset factor, 1.0 for "Output Position" in ***Panel Zone Effects*** is tantamount to selecting "Panel Zone" with an offset factor of 1.0. Conversely, selecting "Offset Position" with an offset factor of 0.0 for "Output Position" becomes equivalent to a case where no rigid end offset distances are considered.

When rigid end offset distances are to be automatically calculated by using ***Panel Zone Effects***, "Output Position" determines the way in which self-weight and distributed loads are applied and the output locations of member forces.

- **Element stiffness calculation**

  In calculating the axial and torsional stiffnesses of an element, the distance between the end nodes is used. Whereas, an adjusted length, $L_1=L-Z_F\ (R_i+R_j)$, which reflects the offset factor, is used for the calculation of the shear and bending stiffnesses, regardless of the selection of the location for member force output (See Figure 1.65).

- **Calculation of distributed loads**

  If "Panel Zone" is selected for "Output Position", any distributed load within a rigid end offset distance is transferred to the corresponding node. The remaining distributed loads are converted to shear forces and moments as shown in Figure 1.66. If "Offset Position" is selected for "Output Position", the above forces are calculated relative to the rigid end offset locations that reflect the offset factor.

- **Length considered for the self-weight**

  The self-weight of a column member is calculated for the full element length without the effect of rigid end offset distances. For the self-weight of a beam, the full nodal distance less the rigid end offset distances, $L_1=L-(R_i+R_j)$, is used when "Panel Zone" is selected for "Output Position". If "Offset Position" is selected for "Output Position", the full nodal distance is reduced by the adjusted rigid end offset distances, $L_1=L-Z_F(R_i+R_j)$. The self-weight calculated in this manner is converted into shear forces and moments using the load calculation method described above.

- **Output position of member forces**

  If "Panel Zone" is selected for "Output Position", the member forces for columns and beams are produced at the ends of the panel zones and the quarter points of the net lengths between the panel zones. If "Offset Position" is selected for "Output Position" in the case of beams, the results are produced at the similar positions relative to the adjusted rigid end offset distances. Note that the output positions for the "Panel Zone" are identical to the case where "Offset Position" is selected for "Output Position" with an offset factor of 1.0.

- **Rigid end offset distance when the beam end release is considered**

  If one or both ends of a column or a beam are released to form pinned connections, the rigid end offset distances for the corresponding nodes will not be considered.

- **Calculation of rigid end offset distances in column members**

  The full length of a column member is taken as a story-height between adjoining floors. In calculating the length, two assumptions are made in MIDAS GEN NX; (1) the centerlines of beam sections coincide with the story level line, and (2) the tops of beam sections are flush with the story level line. The rigid end offset distances of columns vary with the two assumptions. If the first assumption is made, the end offsets are calculated at both top and bottom ends of the columns. Meanwhile, with the second assumption, the end offsets are considered only at the tops of the columns (See Figure 1.65)[1].

[1] Refer to "Align Top of Beam Section to Floor (X-Y Plane) for Panel Zone Effect/Display in Model>Structure Type".

At a connection point of a column member and beam (girder) members, the rigid end offset distances of the column is calculated on the basis of the depths and directions of the connected beams. In the case of a beam-column connection as shown in Figure 1.67, the rigid end offset distances of the column are calculated separately for the ECS y and z-axes.

When multi-directional beam members are connected to a column, the rigid end offset distance in each direction is calculated as follows: (See Figure 1.68)

$RC_y = BD \times \cos^2\theta \qquad RC_z = BD \times \sin^2\theta$
RC_y: Rigid end offset distance about the ECS y-axis of the column top
RC_z: Rigid end offset distance about the ECS z-axis of the column top
BD: Depth of a beam (girder) connected to the column
θ: Angle of a beam (girder) orientation to the ECS z-axis of the column

The largest value of the end offsets calculated for the beam members is selected for the rigid end offset distance of the column in each direction.

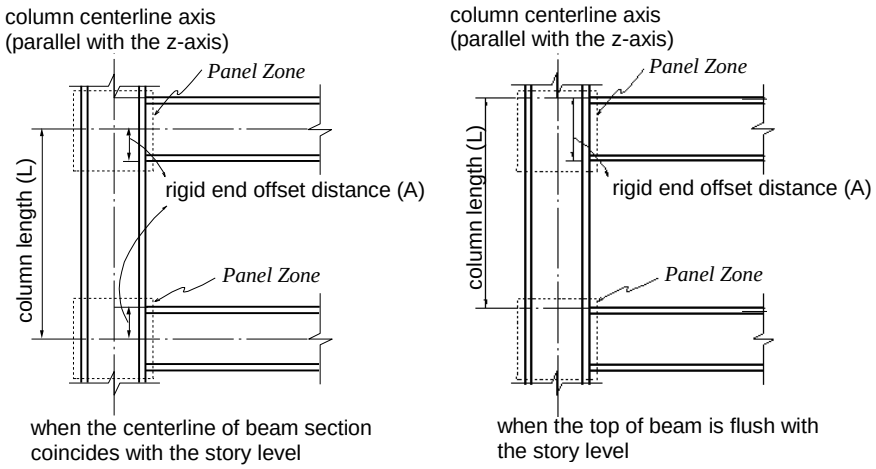

(a) Rigid end offset distances of column

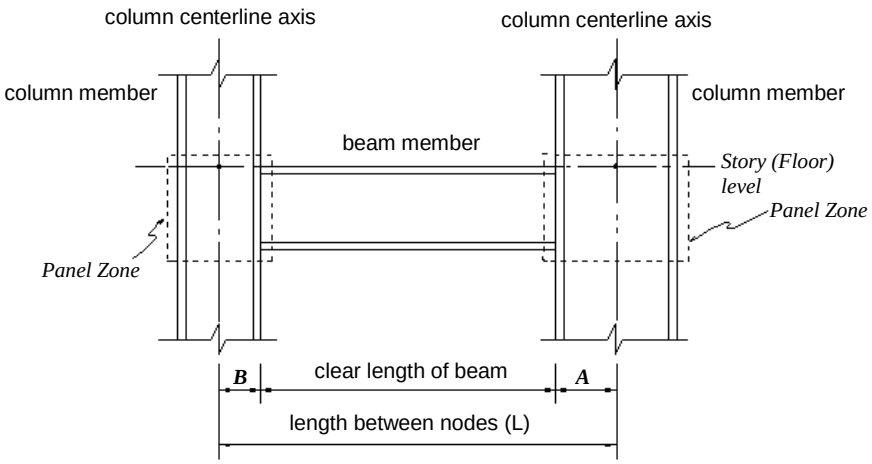

(b) Panel zones of a beam

Offset Factor	effective length for stiffness calculation
1.00	$L - 1.00 \times (A + B)$
0.75	$L - 0.75 \times (A + B)$
0.50	$L - 0.50 \times (A + B)$
0.25	$L - 0.25 \times (A + B)$
0.00	$L - 0.00 \times (A + B)$

Offset Factor: rigid end offset factor entered in “Panel Zone Effects”

(c) Effective lengths for stiffness calculation (B=0 for columns)

Figure 1.65 Effective lengths used to calculate bending/shear stiffness when “Panel Zone Effects” is used for the rigid end offset distances

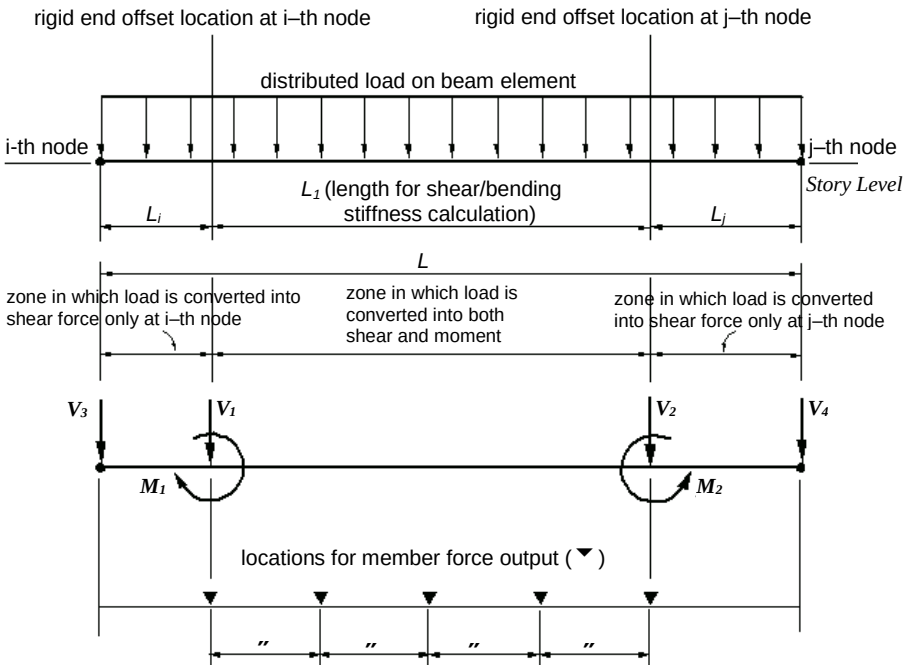

$L_i = 1.0 \times R_i$		"Panel Zone" is selected for the locations of member force output.
$L_i = Z_F \times R_i$		"Offset Position" is selected for the locations of member force output.
$L_j = 1.0 \times R_j$		"Panel Zone" is selected for the locations of member force output.
$L_j = Z_F \times R_j$		"Offset Position" is selected for the locations of member force output.
R_i	:	rigid end offset distance at i-th node
R_j	:	rigid end offset distance at j-th node
Z_F	:	rigid end Offset Factor
V_1, V_2	:	shear forces due to distributed load between the offset ends
M_1, M_2	:	moments due to distributed load between the offset ends
V_3, V_4	:	shear forces due to distributed load between the offset ends and the nodal points

(a) Beam member

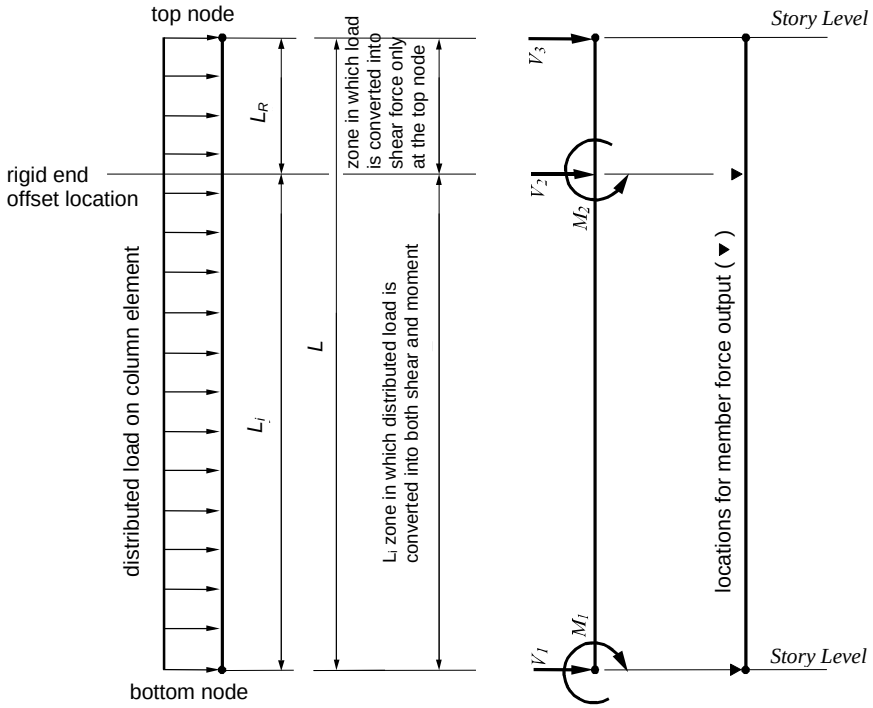

$L_R = 1.0 \times R$ (“Panel Zone” is selected for the location of member force output.)

$L_R = Z_F \times R$ (“Offset Position” is selected for the locations of member force output.)

Where, R is the rigid end offset factor

V_1, V_2 : shear forces due to distributed load between the offset end and the bottom node)

M_1, M_2 : moments due to distributed load between the offset end and the bottom node

V_3 : shear force due to distributed load between the offset end and the top node

(b) Column member

Figure 1.66 Load distribution and locations of member force output when “Panel Zone Effects” is used to consider rigid end offset distances

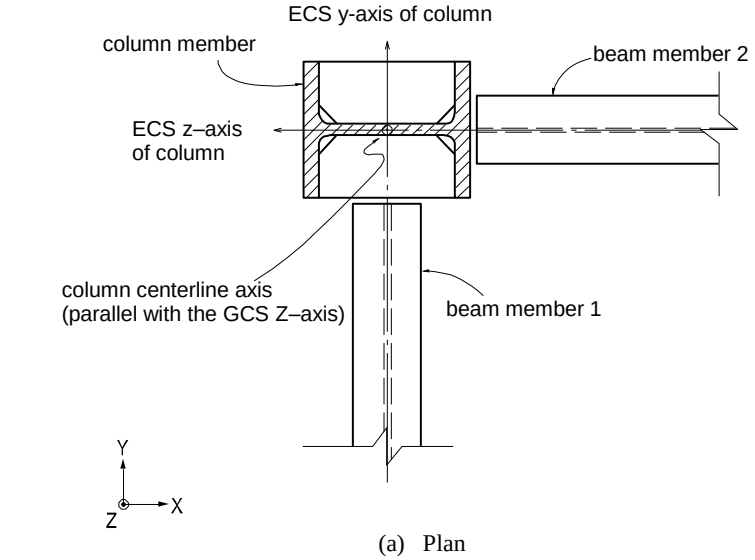

(a) Plan

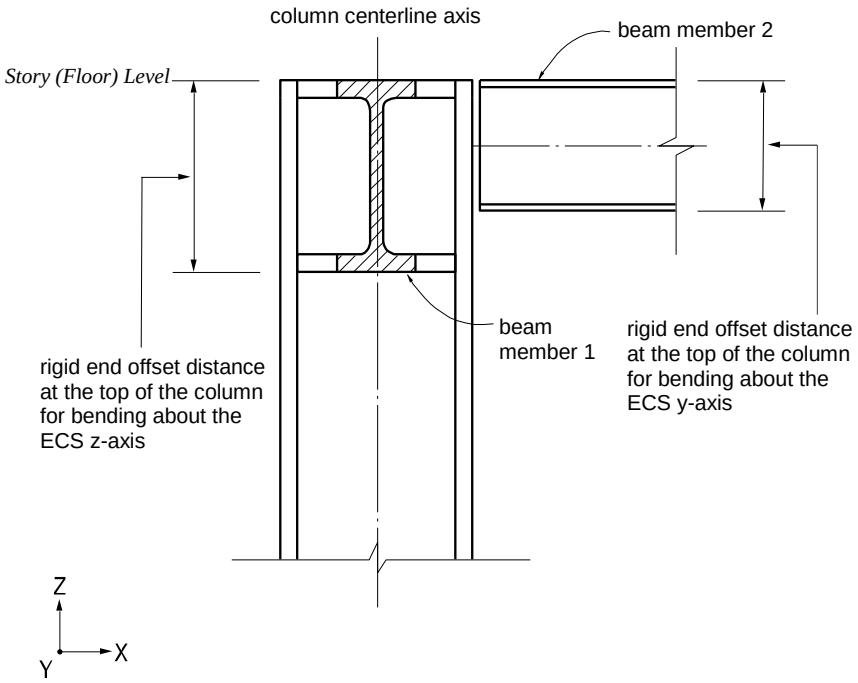

(b) Sectional Elevation

Figure 1.67 Rigid end offset distance of a column using "Panel Zone Effects"

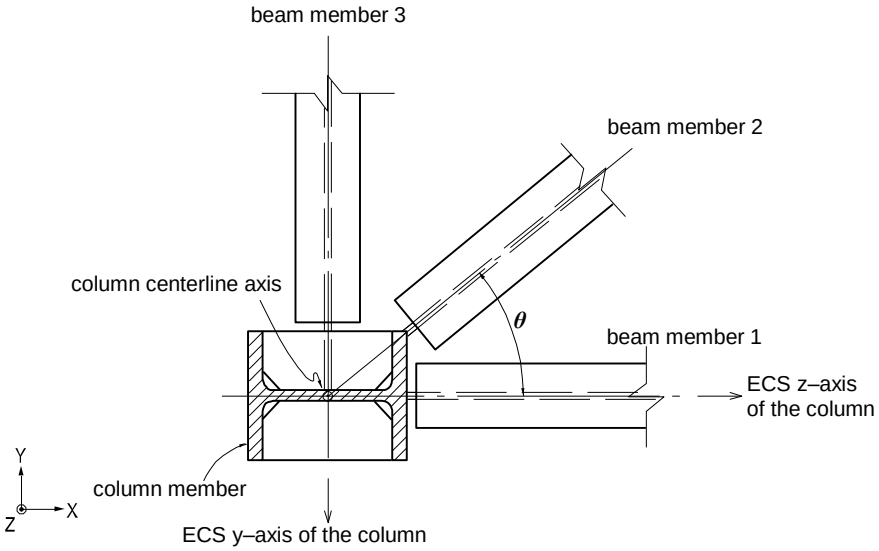

$beam\ member1: BD = 250 \quad \theta = 0^\circ \quad RC_z = 250 \times sin^2 0^\circ = 0.0 \quad RC_y = cos^2 0^\circ = 250.0$

$beam\ member2: BD = 200 \quad \theta = 40^\circ \quad RC_z = 200 \times sin^2 40^\circ = 82.6 \quad RC_y = 200 \times cos^2 0^\circ = 117.4$

$beam\ member3: BD = 150 \quad \theta = 90^\circ \quad RC_z = 150 \times sin^2 90^\circ = 150 \quad RC_y = 150 \times cos^2 90^\circ = 0.0$

rigid end offset distance of the column

$RC_y = \mathrm{MAX}(250.0, 117.4, 0.0) = 250.0 \qquad RC_z = \mathrm{MAX}(0.0, 82.6, 150.0) = 150.0$

where, BD : beam depth
RC_z : rigid end offset distance for bending about the minor axis
RC_y : rigid end offset distance for bending about the major axis

Figure 1.68 Example for calculating rigid end offset distances of a column using "Panel Zone Effects"

- **Method of calculating rigid end offset distances of beam (girder) members.**

  The rigid end offset distance of a beam (girder) member at a column is based on the depth and width of the column member at the beam-end and calculated as follows:

  Formula for calculating rigid end offset distance in each direction (See Figure 1.69)

$$RB = \frac{Depth \times \cos^2\theta}{2} + \frac{Width \times \sin^2\theta}{2}$$

  Depth: dimension of the column section in the ECS z-axis direction
  Width: dimension of the column section in the ECS y-axis direction
  θ: Angle of the beam (girder) orientation to the ECS z-axis of the column

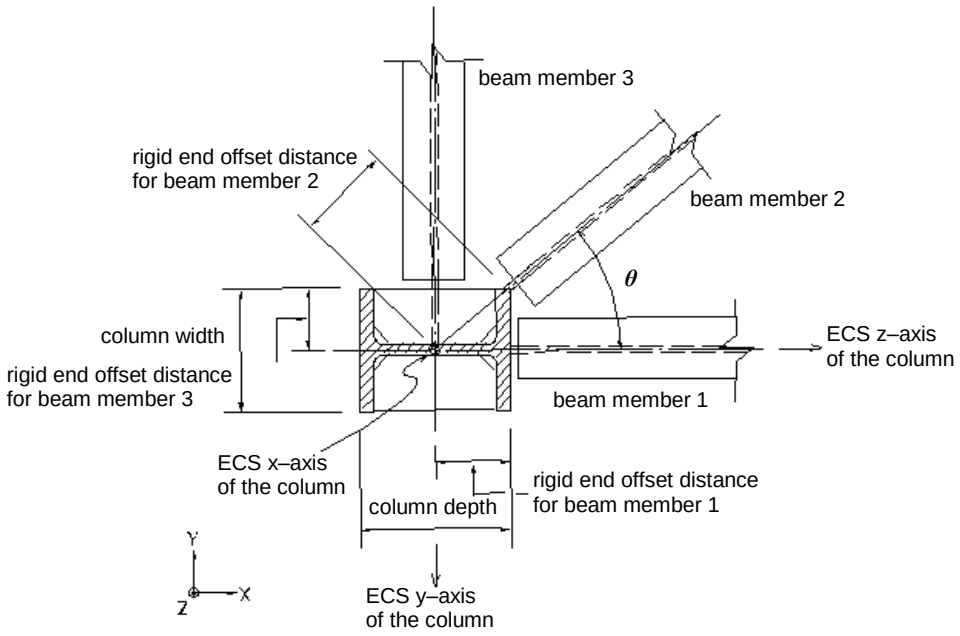

Figure 1.69 Rigid end offset distances of beam (girder) members using "Panel Zone Effects"

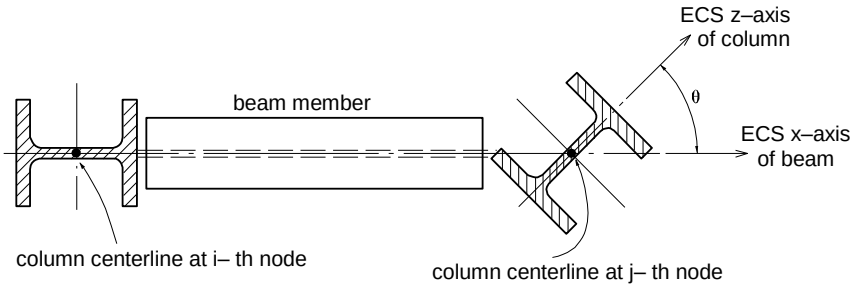

depth of column section = 150, width of column section=100, for $\theta = 40^{\circ}$

rigid end offset distance at i-th node = $\frac{150 \times cos^2 0^{\circ}}{2} + \frac{100 \times sin^2 0^{\circ}}{2} = 75.0$

rigid end offset distance at j-th node = $\frac{150 \times cos^2 40^{\circ}}{2} + \frac{100 \times sin^2 40^{\circ}}{2} = 64.7$

Figure 1.70 Example for calculating rigid end offset distances of a beam using "Panel Zone Effects"

Method by which the user directly specifies the rigid end offset distances at both ends of beams using "*Beam End Offsets*"

"***Beam End Offsets***" allows the user to specify rigid end offset distances using the following two methods.

Refer to "Model> Boundaries>Beam End Offsets of On-line Manual.

1. Offset distances at both ends are specified in the X, Y and Z-axis direction components in the GCS
2. Offset distances at both ends are specified in the ECS x-direction

The first method is generally used to specify eccentricities at connections. In this case, the length between the end offsets is used to calculate element stiffness, distributed load and self-weight. The locations for member force output and the end releases are also adjusted relative to the end offsets (See Figures 1.64 (b) & (c)).

The second method is used to specify eccentricities in the axial direction. It produces identical element stiffness, force output locations and end release conditions to the case where "***Panel Zone***" with an offset factor, 1.0 is selected in ***Panel Zone Effects***. However, the full length between two nodes is used for distributed loads, instead of the adjusted length.

Master and Slave Nodes (Rigid Link Function)

The rigid link function specified in ***Model>Boundaries>Rigid Link*** constrains geometric, relative movements of a structure.

Geometric constraints of relative movements are established at a particular node to which one or more nodal degrees of freedom (d.o.f.) are subordinated. The particular reference node is called a Master Node, and the subordinated nodes are called Slave Nodes.

The rigid link function includes the following four connections:

1. Rigid Body Connection
2. Rigid Plane Connection
3. Rigid Translation Connection
4. Rigid Rotation Connection

Rigid Body Connection constrains the relative movements of the master node and slave nodes as if they are interconnected by a three dimensional rigid body. In this case, relative nodal displacements are kept constant, and the geometric relationships for the displacements are expressed by the following equations:

$$U_{Xs} = U_{Xm} + R_{Ym}\Delta Z - R_{Zm}\Delta Y$$
$$U_{Ys} = U_{Ym} + R_{Zm}\Delta X - R_{Xm}\Delta Z$$
$$U_{Zs} = U_{Zm} + R_{Xm}\Delta Y - R_{Ym}\Delta X$$
$$R_{Xs} = R_{Xm}$$
$$R_{Ys} = R_{Ym}$$
$$R_{Zs} = R_{Zm}$$

where, $\Delta X = X_m - X_s$, $\Delta Y = Y_m - Y_s$, $\Delta Z = Z_m - Z_s$

The subscripts, m and s, in the above equations represent a master node and slave nodes respectively. U_X, U_Y and U_Z are displacements in the Global Coordinate System (GCS) X, Y and Z directions respectively, and R_X, R_Y and R_Z are rotations about the GCS X, Y and Z-axes respectively. X_m, Y_m and Z_m represent the coordinates of the master node, and X_s, Y_s and Z_s represent the coordinates of a slave node. This feature may be applied to certain members whose stiffnesses are substantially larger than the remaining structural members such that their deformations can be ignored. It can be also used in the case of a stiffened plate to interconnect its plate and stiffener.

Rigid Plane Connection constrains the relative movements of the master node and slave nodes as if a planar rigid body parallel with the X-Y, Y-Z or Z-X plane interconnects them. The distances between the nodes projected on the plane in question remain constant. The geometric relationships for the displacements are expressed by the following equations:

- **Rigid Plane Connection assigned to X-Y plane**

  $U_{Xs} = U_{Xm} - R_{Zm}\Delta Y$
  $U_{Ys} = U_{Ym} + R_{Zm}\Delta X$
  $R_{Zs} = R_{Zm}$

- **Rigid Plane Connection assigned to Y-Z plane**

  $U_{Ys} = U_{Ym} - R_{Xm}\Delta Z$
  $U_{Zs} = U_{Zm} + R_{Xm}\Delta Y$
  $R_{Xs} = R_{Xm}$

- **Rigid Plane Connection assigned to Z-X plane**

  $U_{Zs} = U_{Zm} - R_{Ym}\Delta X$
  $U_{Xs} = U_{Xm} + R_{Ym}\Delta Z$
  $R_{Ys} = R_{Ym}$

This feature is generally used to model floor diaphragms whose relative in-plane displacements are negligible.

Rigid Translation Connection constrains relative translational movements of the master node and slave nodes in the X, Y or Z-axis direction. The geometric relationships for the displacements are expressed by the following equations:

- **Displacement constraint in the X-axis direction**

  $U_{Xs} = U_{Xm}$

- **Displacement constraint in the Y-axis direction**

  $U_{Ys} = U_{Ym}$

- **Displacement constraint in the Z-axis direction**

  $U_{Zs} = U_{Zm}$

Rigid Rotation Connection constrains the relative rotational movements of the master node and slave nodes about the X, Y or Z-axis. The geometric relationships for the displacements are expressed by the following equations:

- **Rotational constraint about the X-axis**

  $R_{Xs} = R_{Xm}$

- **Rotational constraint about the Y-axis**

  $R_{Ys} = R_{Ym}$

- **Rotational constraint about the Z-axis**

  $R_{Zs} = R_{Zm}$

The following illustrates an application of ***Rigid Plane Connection*** to a building floor diaphragm to help the user understand the concept of the rigid link feature.

When a building is subjected to a lateral load, the relative horizontal deformation at any point in the floor plane is generally negligible compared to that from other structural members such as columns, walls and bracings. This rigid diaphragm action of the floor slab can be implemented by constraining all the relative in-plane displacements to behave as a unit. The movements consist of two in-plane translational displacements and one rotational displacement about the vertical direction.

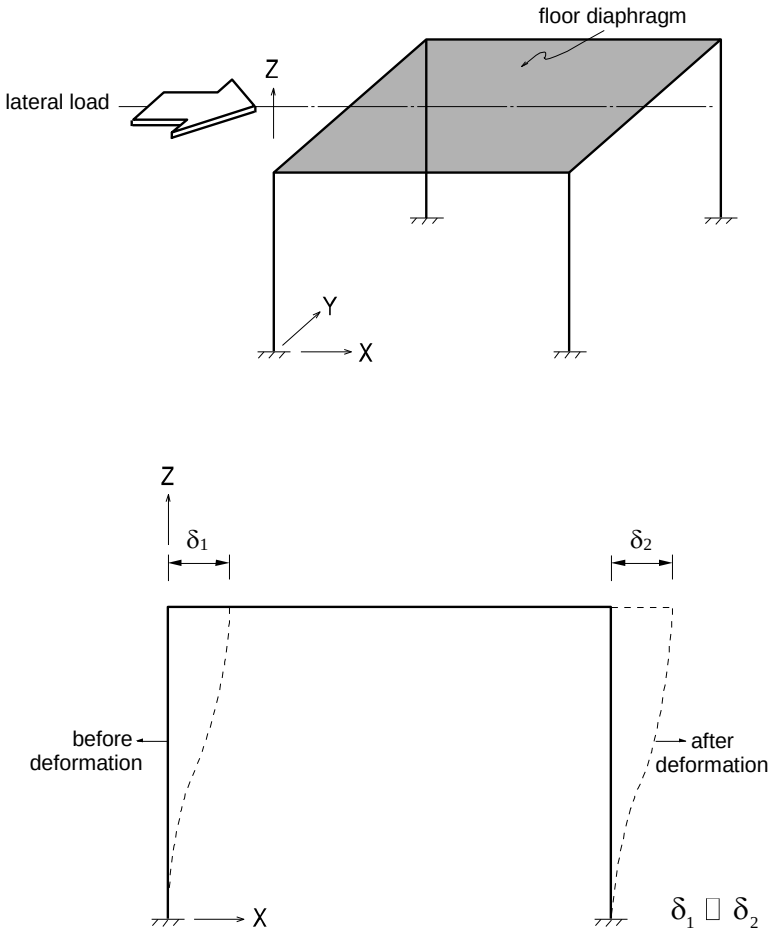

Figure 1.71 Typical structure with floor diaphragm subjected to a lateral load

As illustrated in Figure 1.71, when a structure is subjected to a lateral load and the in-plane stiffness of the floor is significantly greater than the horizontal stiffness of the columns, the in-plane deformations of the floor can be ignored. Accordingly, the values of δ_1 and δ_2 may be considered equal.

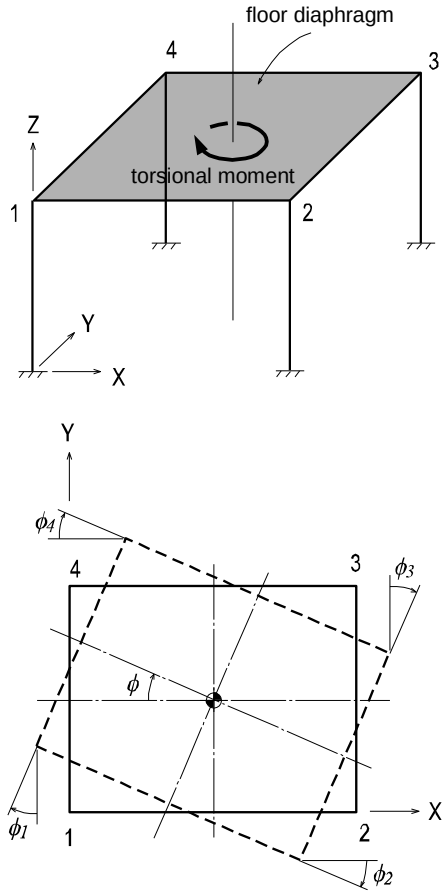

$$\Phi_1 \simeq \Phi_2 \simeq \Phi_3 \simeq \Phi_4 \simeq \Phi_5$$

Figure 1.72 Single story structure with a floor diaphragm subjected to a torsional moment about the vertical axis

When a single-story structure, as illustrated in Figure 1.72, is subjected to a torsional moment about the vertical direction and the in-plane stiffness of the floor is significantly greater than the horizontal stiffness of the columns, the entire floor diaphragm will be rotated by ϕ, where, $\phi = \phi_1 = \phi_2 = \phi_3 = \phi_4$. Accordingly, the four degrees of freedom can be reduced to a single degree of freedom.

Figure 1.73 shows a process in which a total of 24 (6×4) degrees of freedom are compressed to 15 d.o.f. within the floor plane, considering its diaphragm actions.

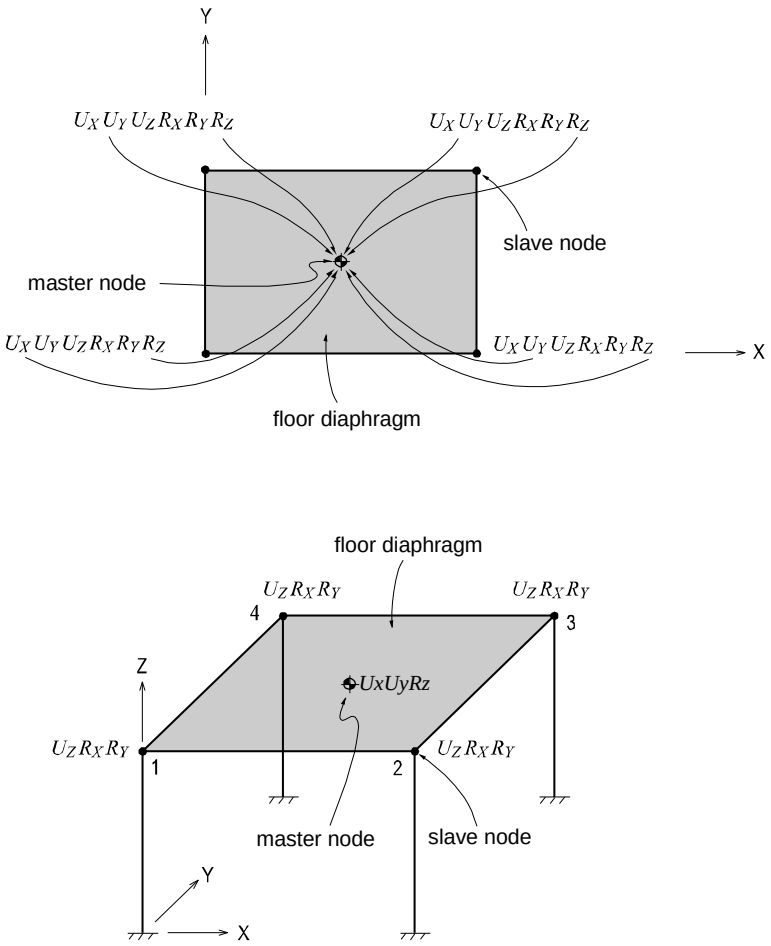

U_X : displacement degree of freedom in the X-direction at the corresponding node
U_Y : displacement degree of freedom in the Y-direction at the corresponding node
U_Z : displacement degree of freedom in the Z-direction at the corresponding node
R_X : rotational degree of freedom about the X-axis at the corresponding node
R_Y : rotational degree of freedom about the Y-axis at the corresponding node
R_Z : rotational degree of freedom about the Z-axis at the corresponding node

Figure 1.73 Reduction of d.o.f. for floor diaphragm of significant in-plane stiffness

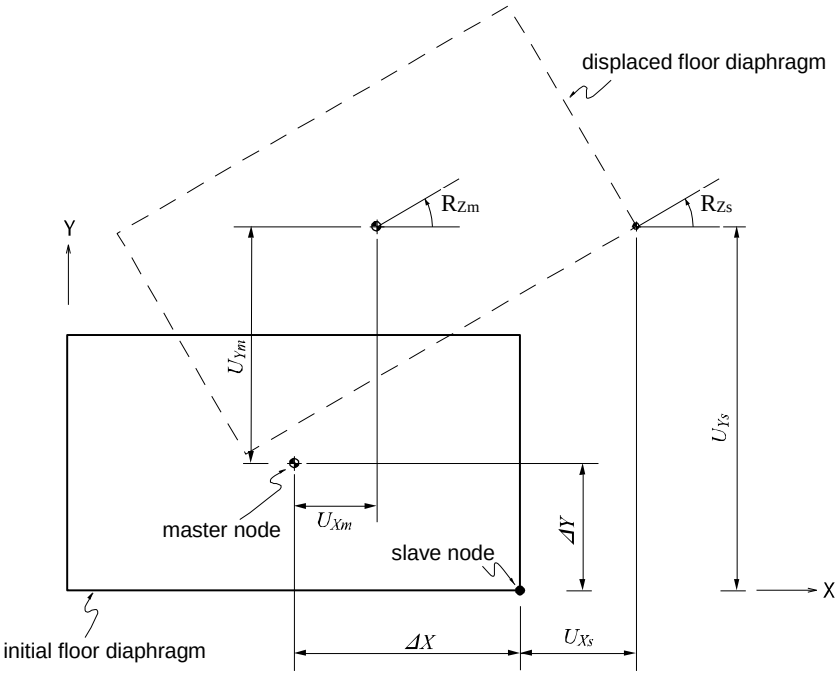

U_{Xm} : X-direction displacement of master node
U_{Ym} : Y-direction displacement of master node
R_{Zm} : rotation about Z-axis at master node
U_{Xs} : X-direction displacement of slave node
U_{Ys} : X-direction displacement of slave node
R_{Zs} : rotation about Z-axis at slave node

Figure 1.74 Displacements of an infinitely stiff floor diaphragm due to horizontal loads

As illustrated in Figure 1.74, if translational and rotational displacements take place simultaneously in an infinitely stiff floor diaphragm due to a lateral load, the displacements of a point on the floor plane can be obtained by:

$$U_{Xs} = U_{Xm} - R_{Zm}\Delta Y$$
$$U_{Ys} = U_{Ym} + R_{Zm}\Delta X$$
$$R_{Zs} = R_{Zm}$$

Reducing number of degrees of freedom by geometric constraints can significantly reduce the computational time for analysis. For instance, if a building structure is analyzed with the floors modeled as plate or plane stress elements, the number of nodes will increase substantially. Each additional node represents 3 additional degrees of freedom even if one considers d.o.f in lateral directions only. A large number of nodes in an analysis can result in excessive program execution time, or it may even surpass the program capacity. In general, solver time required is proportional to the number of degrees of freedom to the power of 3. It is, therefore, recommended that the number of degrees of freedom be minimized as long as the accuracy of the results is not compromised.

Figure 1.75 shows applications of ***Rigid Body Connection*** and ***Rigid Plane Connection***. Figure 1.75 (a) illustrates an application of ***Rigid Link*** using ***Rigid Body Connection***. Here a rectangular tube is modeled with plate elements in the region where a detail review is required, beyond which a beam element represents the tube. Then, Rigid Body Connection joins the two regions.

Figure 1.75 (b) shows an application of ***Rigid Plane Connection*** for a column offset in a two-dimensional plane. Whenever Rigid Link is used in a plane, geometric constraints must be assigned to two translational displacement components and one rotational component about the perpendicular axis to the plane.

If a structural analysis model includes geometric constraints and is used for a dynamic analysis, the location of the master node must coincide with the mass center of all the masses pertaining to the slave nodes. This condition also applies to the masses converted from self-weights.

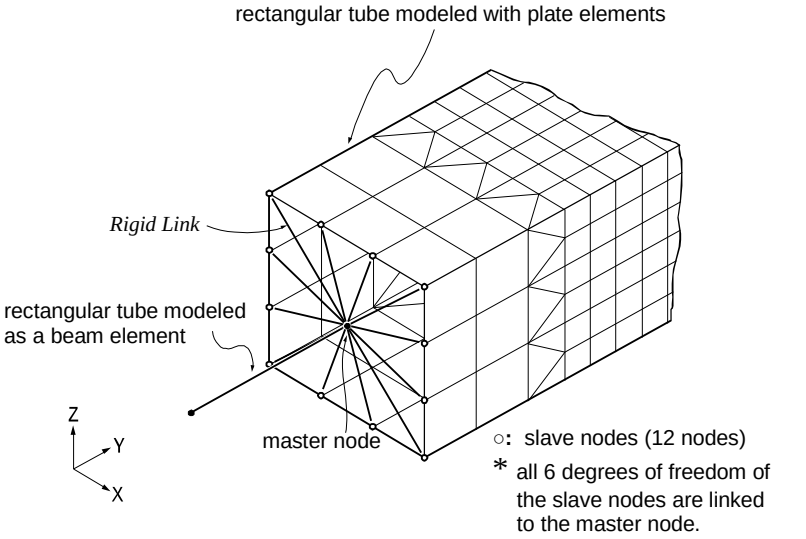

(a) A tube modeled using a beam element and plate elements, and connected by Rigid Body Connection

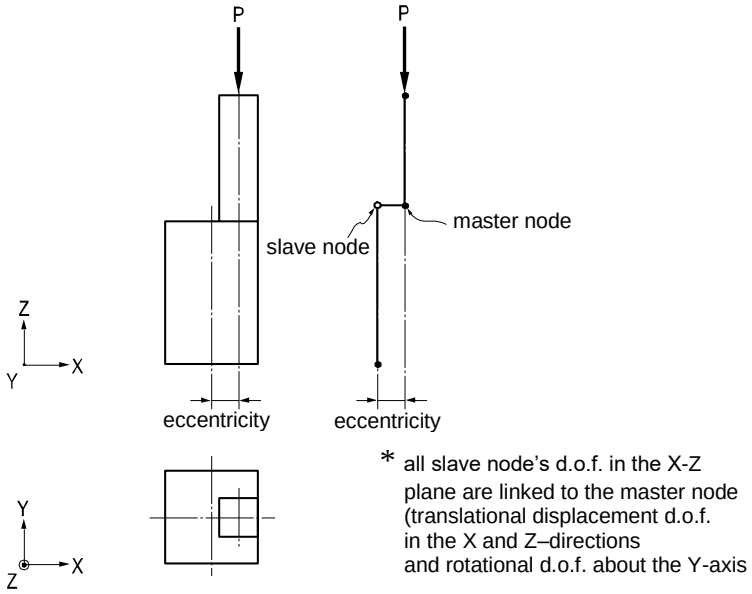

(b) Eccentricity of an offset-column linked by Rigid Plane Connection

Figure 1.75 Application examples of geometric constraints

Specified Displacements of Supports

"Specified Displacements of Supports" is used to examine structural behaviors under the condition where displacements for restrained degrees of freedom are known in advance. It is also commonly referred to as "Forced Displacements".

Refer to "Load> Specified Displacements of Supports" of On-line Manual.

In practice, this functio In practice, this function is effectively used in the following cases:

- **Detail safety assessment of an existing building, which has experienced post-construction deformations.**
- **Detail analyses of specific parts of a main structure. Displacements obtained from the analysis of a total structure form the basis of boundary conditions for analyzing specific parts.**
- **Analyses of existing buildings for foundation support settlements.**
- **Analyses of bridges reflecting support settlements.**

MIDAS GEN NX allows you to define Specified Displacements of Supports by individual load cases. If Specified Displacements of Supports are assigned to unrestrained nodes, the program automatically restrains the corresponding degrees of freedom of the nodes. A separate data file is required if the analysis results of unrestrained degrees of freedom are desired.

Entering accurate values for Specified Displacements of Supports may become critical since structural behaviors are quite sensitive to even a slight variation. Thus, whenever possible, specifying all six degrees of freedom is recommended. In the case of analyzing an existing structure for safety evaluation, a deformed shape analysis may be required. However, it is typically not possible to measure in-situ rotational displacements. In such a case, only translational displacements are specified for an approximate analysis, but the resulting deformations must be reviewed against the deformations of the total structure.

When the displacements are obtained from the initial analysis of a total structure and subsequently used for a detailed analysis of a particular part of the structure, all the 6 nodal degrees of freedom must be specified at the boundaries. In addition, all the loads present in the detail model must be specified.

Specified Displacements generally follow the GCS unless NCS are previously defined at the corresponding nodes.

Figure 1.76 illustrates a procedure for analyzing a beam-corner column connection in detail.

1. As shown on the left-hand side of Figure 1.76 (a), an initial analysis is performed for the entire structure, from which the displacements at the connection nodes and boundaries are extracted for a detail analysis.

2. A total of 24 displacement components (6 d.o.f. per node) extracted from the 4 boundary nodes are assigned to the model, as shown to the right of Figure 1.76 (a). A master node is created at the centroid of each boundary section, and slave nodes are created and connected to the master node by Rigid Link at each section. The nodal displacements at the boundary sections from the analysis results of the entire structure are applied to the master nodes. Boundary sections should be located as far as possible from the zone of interest for detail analysis in order to reduce errors due to the effects of using Rigid Link.

Refer to "Master and Slave Nodes" in Model>Boundaries> Rigid Link of On-line Manual.

3. All the loads (applied to the entire structure model) that fall within the range of the detail analysis model are entered for a subsequent detail analysis.

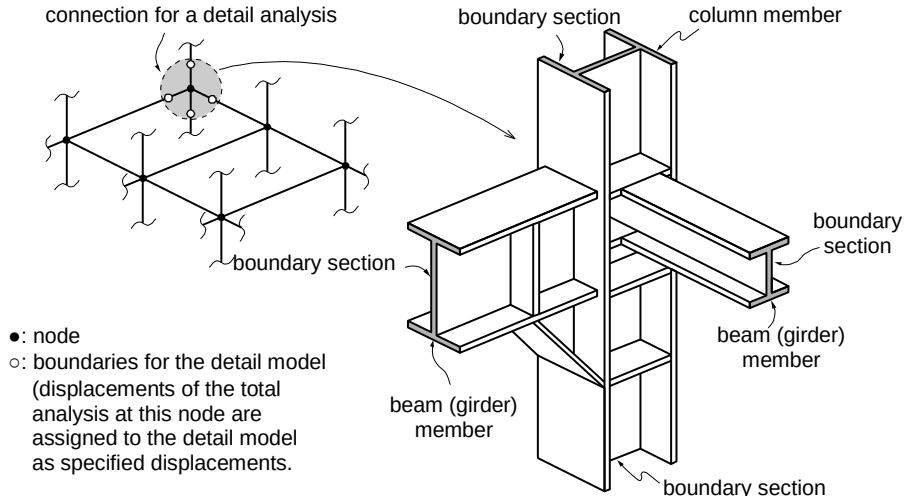

(a) Total structure and connection detail

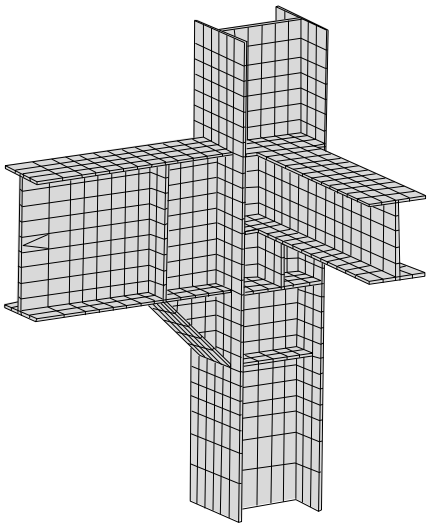

Rigid links (master and slave nodes) are assigned to the boundary sections, and the specified displacements, the displacements obtained from the initial analysis for the entire structure, are assigned to the master node at the centroid of each section.

(b) Detail FEM model of a joint

Figure 1.76 Detail analysis of a joint specified displac

2. MIDAS GEN NX Analysis Options

Analysis Options

When a structure is subjected to external loads, the corresponding structural response may exhibit material nonlinearity to a certain extent. However, in most structural analyses for design purposes, structures behave almost linearly provided that the member stresses remain within the limits of design codes. Material nonlinearity thus is rarely considered in practice.

MIDAS GEN NX is formulated on the basis of linear analysis, but it is also capable of carrying out geometric nonlinear analyses. MIDAS GEN NX implements nonlinear elements (tension or compression-only), P-Delta and large displacement analyses, etc.

The structural analysis features of MIDAS GEN NX include basic linear analysis and nonlinear analysis in addition to various analysis capabilities required in practice.

The following outlines some of the highlights of the analysis features:

- **Linear Static Analysis**

- **Linear Dynamic Analysis**
  Eigenvalue Analysis
  Response Spectrum Analysis
  Time History Analysis

- **Linear Buckling Analysis**

- **Nonlinear Static Analysis**
  P-Delta Analysis
  Large Displacement Analysis
  Nonlinear Analysis with Nonlinear Elements

- **Other analysis options**
  Construction Sequence Analysis
  Steel Box Bridge Analysis reflecting Pre- and Post-composite Action
  Analysis of Unknown Loads Using Optimization Technique

MIDAS GEN NX permits a multi-functional analysis incorporating more than one feature from the above simultaneously. However, response spectrum and time history analyses cannot be executed together.

Linear Static Analysis

The basic equation adopted in MIDAS GEN NX for linear static analysis is as follows:

$$[K]\{U\} = \{P\}$$

where,

$[K]$: Stiffness matrix

$\{U\}$: Displacement vector

$\{P\}$: Load vector

MIDAS GEN NX allows unlimited numbers of static load cases and load combinations.

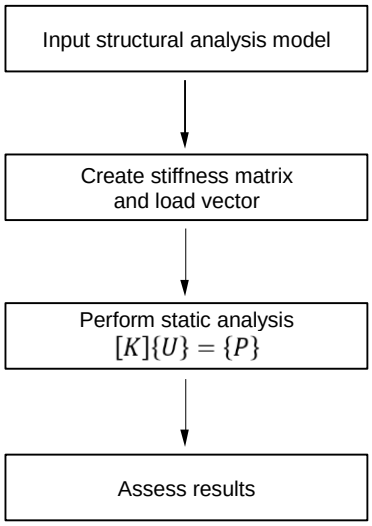

Figure 2.1 Flow chart for Linear Static Analysis in MIDAS GEN NX

Free Vibration Analysis

Eigenvalue Analysis

Mode shapes and natural periods of an undamped free vibration are obtained from the characteristic equation below.

Refer to “Analysis> Eigenvalue Analysis Control” of On-line Manual.

$$[K]\{\Phi_n\} = \omega_n{}^2 [M]\{\Phi_n\}$$

where,

$[K]$: Stiffness matrix

$[M]$: Mass matrix

ω_n^2 : n-th mode eigenvalue

$\{\Phi_n\}$: n-th mode eigenvector (mode shape)

Eigenvalue analysis is also referred to as “free vibration analysis” and used to analyze the dynamic characteristics of structures.

The dynamic characteristics obtained by an eigenvalue analysis include vibration modes (mode shapes), natural periods of vibration (natural frequencies) and modal participation factors. They are determined by the mass and stiffness of a structure.

Vibration modes take the form of natural shapes in which a structure freely vibrates or deforms. The first mode shape or natural vibration shape is identified by a shape that can be deformed with the least energy or force. The shapes formed with increases in energy define the subsequent higher modes.

Figure 2.2 shows the vibration modes of a cantilever beam arranged in the order of their energy requirements for deflected shapes, starting from the shape formed by the least energy.

A natural period of vibration is the time required to complete one full cycle of the free vibration motion in the corresponding natural mode.

The following describes the method of obtaining the natural period of a single degree of freedom (SDOF) system: Assuming zero damping and force in the governing motion equation of a SDOF system, we can obtain the 2nd order linear differential equation <Eq. 1> representing a free vibration.

<Eq. 1>

$$m\ddot{u} + c\dot{u} + ku = p(t)$$

$$m\ddot{u} + k\dot{u} = 0$$

Since u is the displacement due to vibration, if we simply assume u = Acosωt, where, A is a constant related to the initial displacement, <Eq. 1> can be written as

<Eq. 2>

$$(-m\omega^2 + k)A\cos\omega t = 0$$

In order to satisfy the <Eq. 2>, the value of the parenthesis must be zero, which leads to <Eq. 3>.

<Eq. 3>

$$\omega^2 = \frac{k}{m},\ \omega = \sqrt{\frac{k}{m}},\ f = \frac{\omega}{2\pi},\ T = \frac{1}{f}$$

where, ω^2, ω, f and T are eigenvalue, rotational natural frequency, natural frequency and natural period respectively.

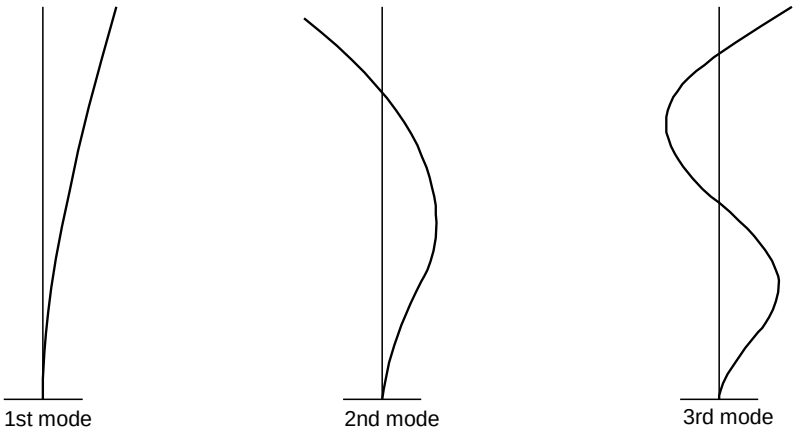

(a) Mode shapes

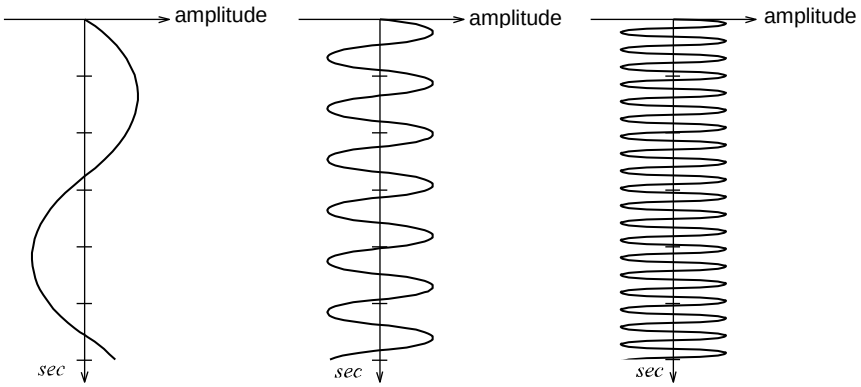

λ_1=1.87510407
T_1=1.78702 sec

λ_2=4.69409113
T_2=0.28515 sec

λ_3=7.85475744
T_3=0.10184 sec

$$T_i = \frac{2\pi}{\lambda_i^2}\left(\frac{mL^4}{EI}\right)^{1/2}$$: natural period of a slender cantilever beam

where, L = 100, E = 1000000, I = 0.1, m = 0.001

(b) Natural periods

Figure 2.2 Mode shapes and corresponding natural periods of a prismatic cantilever beam

The modal participation factor is expressed as a contribution ratio of the corresponding mode to the total modes and is written as

<Eq. 4>

$$\Gamma_m = \frac{\sum M_i \varphi_{im}}{\sum M_i \varphi_{im}^2}$$

where,

Γ_m : Modal participation factor

m : Mode number

M_i : Mass at location i

φ_{im} : m-th mode shape at location i

In most seismic design codes, it is stipulated that the sum of the effective modal masses included in an analysis should be greater than 90% of the total mass. This will ensure that the critical modes that affect the results are included in the design.

<Eq. 5>

$$M_m = \frac{\left[\sum \varphi_{im} M_i\right]^2}{\sum \varphi_{im}^2 M_i}$$

where, M_m: Effective modal mass

If certain degrees of freedom of a given mass become constrained, the mass will be included in the total mass but excluded from the effective modal mass due to the restraints on the corresponding mode vectors. **Accordingly, when you attempt to compare the effective modal mass with the total mass, the degrees of freedom pertaining to the mass components must not be constrained**.

For instance, when the lateral displacement d.o.f. of a building basement are constrained, it is not necessary to enter the lateral mass components at the corresponding floors.

In order to analyze the dynamic behavior of a structure accurately, the analysis must closely reflect the mass and stiffness, which are the important factors to determine the eigenvalues. In most cases, finite element models can readily estimate the stiffness components of structural members. In the case of mass, however, you are required to pay a particular attention for an accurate estimate. The masses pertaining to the self-weights of structural components are relatively small compared to the total mass. It is quite important that an eigenvalue analysis accounts for all mass components in a structure, such as floor slabs and claddings among other masses.

Mass components are generally specified as 3 translational masses and 3 rotational mass moments of inertia consistent with 6 degrees of freedom per node. The rotational mass moments of inertia pertaining to rotational mass inertia do not directly affect the dynamic response of a structure. Only translational ground accelerations are typically applied in a seismic design. However, when the structure is of an irregular shape, where the mass center does not coincide with the stiffness center, the rotational mass moments of inertia indirectly affect the dynamic response by changing the mode shapes.

Mass components are calculated by the following equations: (See Figure 2.3)

- **Translational mass**

$$\int dm$$

- **Rotational mass moment of inertia**

$$\int r^2 dm$$

where, r is the distance from the total mass center to the center of an infinitesimal mass.

The units for mass and rotational mass moment of inertia are defined by the unit of weights divided by the gravitational acceleration, ***W(T2/L)*** and the unit of masses multiplied by the square of a length unit, ***W(T2/L)×L2*** respectively. Here,W, T and L represent weight, time and length units respectively. In the case of anMKS or English unit system, the mass is determined by the weight divided by the gravitational acceleration. The masses in an SI unit system directly use the weights in the MKS units, whereas the stiffness or loads in the MKS units are multiplied by the gravitational acceleration for the SI unit system.

MIDAS GEN NX uses lumped masses in analyses for efficiency. Mass data can be entered in the main menu through ***Model>Masses>Nodal Masses, Floor Diaphragm Masses or Loads to Masses***.

MIDAS GEN NX adopts the subspace iteration method for the solution of an eigenvalue analysis, which is suitable for the analyses of large structures.

ρ : mass per unit area : mass center

shape	translation mass	rotational mass moment of inertia
rectangular shape 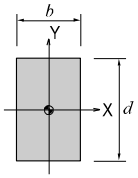	$M = \rho bd$	$I_m = \rho\left(\frac{bd^3}{12} + \frac{db^3}{12}\right)$ $= \frac{M}{12}\left(b^2 + d^2\right)$
triangular shape 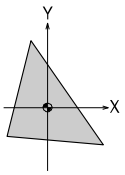	$M = \rho \times$ area of triangle	$I_m = \rho\left(I_x + I_y\right)$
circular shape 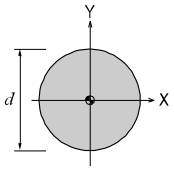	$M = \rho\left(\frac{\pi d^2}{4}\right)$	$I_m = \rho\left(\frac{\pi d^4}{32}\right)$
general shape 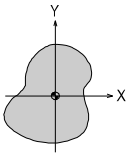	$M = \rho \times \int dA$	$I_m = \rho\left(I_x + I_y\right)$
linear shape 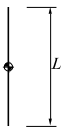	$\rho_L =$ mass per unit lengh $M = \rho_L \times L$	$I_m = \rho_L\left(\frac{L^3}{12}\right)$
eccentric mass 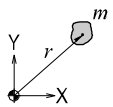	eccentric mass: m $M = m$	rotational mass moment of inertia about its mass center: I_o $I_m = I_o + mr^2$

Figure 2.3 Calculations for Mass data

Ritz Vector Analysis

Ritz vector analysis is an approach, which finds natural frequencies and mode shapes representing the dynamic properties of a structure. The use of Ritz vectors is known to be more efficient than using Eigen vector analysis for calculating such dynamic properties. This method is an extension of the Rayleigh-Ritz approach, which finds a natural frequency by assuming a mode shape of a multi-degree of freedom structure and converting it into a single degree of freedom system.

We now assume that the displacement vector in the equation of motion for a structure of n – degrees of freedom can be expressed by combining p number of Ritz vectors. Here, p is smaller than or equal to n.

$$M\ddot{u}(t)+C\dot{u}(t)+Ku(t)=p(t) \quad (1)$$

$$u(t)=\sum_{i=1}^{p}\psi_i z_i(t)=\Psi z(t) \quad (2)$$

where,

M : Mass matrix of the structure

C : Damping matrix of the structure

K : Stiffness matrix of the structure

$u(t)$: Displacement vector of the structure with n – degrees of freedom

$z(t)$: Generalized coordinate vector

$p(t)$: Dynamic load vector

ψ_i : i - th Ritz vector

$z_i(t)$: i - th Generalized coordinate

$\Psi=\left[\psi_1\cdots\psi_i\cdots\psi_p\right]^T$: Ritz vector matrix

From the above assumption, the equation of motion of n – degrees of freedom can be reduced to the equation of motion of p – degrees of freedom.

$$\tilde{M}\ddot{z}(t)+\tilde{C}\dot{z}(t)+\tilde{K}z(t)=\tilde{p}(t) \quad (3)$$

where,

$\tilde{M}=\Psi^T M\Psi$: Mass matrix of the reduced equation of motion

$\tilde{C}=\Psi^T C\Psi$: Damping matrix of the reduced equation of motion

$\tilde{K}=\Psi^T K\Psi$: Stiffness matrix of the reduced equation of motion

$\tilde{p}(t)=\Psi^T p(t)$: Dynamic load vector of the reduced equation of motion

The following eigenvalue is formulated and analyzed for the reduced equation of motion:

$$\tilde{K}\tilde{\varphi}_i = \tilde{\omega}_i^2 \tilde{M}\tilde{\varphi}_i \quad (4)$$

where,

$\tilde{\varphi}_i$: Mode shape of the reduced equation of motion

$\tilde{\omega}_i$: Natural frequency of the reduced equation of motion

Using the above eigenvalue solution and assuming the classical damping matrix, the reduced equation of motion can be decomposed into the equation of motion for a single degree of freedom for each mode as follows:

$$\ddot{q}_i(t) + 2\xi_i\tilde{\omega}_i\dot{q}_i(t) + \tilde{\omega}_i^2 q(t) = \frac{\Psi^T \tilde{p}_i(t)}{\Psi^T M \Psi} \quad (5)$$

$$z(t) = \sum_{i=1}^{p} \tilde{\varphi}_i q_i(t) \quad (6)$$

Where

$q_i(t)$: $i-th$ mode coordinate

ξ_i : $i-th$ mode damping ratio

The eigenvalue solution of the reduced equation of motion, $\tilde{\omega}_i$, represents an approximate solution for the natural frequency of the original equation of motion.

$$\omega_i = \tilde{\omega}_i \quad (7)$$

where,

ω_i : Approximate solution for *i- th* mode shape

A mode shape of a structure is a vector, which defines the mapping relationship between the displacement vector of the equation of motion and the mode coordinate. The approximate mode shape obtained by Ritz vector analysis is thus defined by the relationship between the displacement vector of the original equation of motion, $u(t)$, and the mode coordinate, $q_i(t)$, as noted below.

$$u(t) = \Psi z(t) = \sum_{i=1}^{p} \left[\Psi\tilde{\varphi}_i\right] q_i(t) \quad (8)$$

Accordingly, the approximate solution for the *i – th* mode shape is defined as

$$\varphi_i = \Psi\tilde{\varphi}_i \quad (9)$$

where,

φ_i : Approximate solution for the *i – th* mode shape

The approximate mode shape vector in Ritz vector analysis retains orthogonality

for the original mass and stiffness matrices similar to that for eigenvalue analysis.

The approximate solution for natural frequencies and mode shapes in Ritz vector analysis is used for calculating modal participation factors and effective modal masses similar to a conventional eigenvalue analysis.

When a time history analysis is carried out by modal superposition on the basis of the results of Ritz vector analysis, the above equation of motion (5) is used.

The Ritz vector, which assumes the deformed shape of a structure, is generally created by repeatedly calculating the displacement due to loads applied to the structure. The user first specifies the initial load vector. The basic assumption here is that the dynamic loading changes with time, but the spatial distribution for each degree of freedom follows the initial load vector specified by the user. Next, the first Ritz vector is obtained by performing the first static analysis for the specified initial load vector.

$$K\psi^{(1)} = r^{(1)}$$

$$\psi^{(1)} = K^{-1}r^{(1)}$$

where,

K : Stiffness matrix of the structure

$\psi^{(1)}$: First Ritz vector

$r^{(1)}$: User specified initial load vector

The first Ritz vector thus obtained is assumed as the structural displacement However, the above static analysis ignores the effect of the inertia force developed by the dynamic response of the structure. Accordingly, the displacement due to the inertia force is calculated through additional repeated calculations. The distribution of acceleration for the structure is assumed to follow the displacement vector calculated before, which is the first Ritz vector. The inertia force generated by the acceleration is calculated by multiplying the mass vector. The inertia force is then assumed to act as a loading, which induces additional displacement in the structure, and static analysis is carried out again.

$$K\psi^{(2)} = M\psi^{(1)}$$

$$\psi^{(2)} = K^{-1}M\psi^{(1)}$$

where,

M : Mass matrix of the structure

$\psi^{(2)}$: Second Ritz vector

The second Ritz vector thus obtained in the above equation also reflects a static equilibrium only. Assuming the above equation is expressed without considering

the acceleration distribution, the above process is repeated in order to calculate the number of Ritz vectors specified by the user.

The user may specify a multiple number of initial load vectors. The number of Ritz vectors to be generated can be individually specified for each initial load vector. However, the total number of Ritz vectors to be generated can not exceed that of real modes, which exist in the equation of motion. Also, those Ritz vectors already generated in the repetitive process are deleted once linearly dependent Ritz vectors are calculated. For this reason, the generation cycle ends if linearly independent Ritz vectors can not be calculated any longer. This means that the initial load vectors specified by the user alone can not find the specified number of modes.

The initial load vectors that can be specified in the MIDAS programs are an inertia force due to ground acceleration in the global X, Y or Z direction, a userdefined static load case and a nonlinear link force vector. The inertia force due to ground acceleration in the global X, Y or Z direction is mainly used to find the Ritz vector related to the displacement resulting from the ground acceleration in the corresponding direction.

The user-defined static load case is used to find the Ritz vectors for a dynamic load with specific distribution. A common static load case (dead load, live load, wind load, etc.) may be used, or an artificially created static load case may be used to generate Ritz vectors.

The member force vectors of nonlinear link elements are used to generate Ritz vectors. The member forces generated in each nonlinear link element are applied to the structure as a load vector. For only the degrees of freedom checked by the user among the 6 degrees of freedom in an element, initial load vectors having unit forces individually are composed and used for generating the Ritz vectors. However, the member force vectors of link elements do not have to be used in the analysis of a structure, which contains nonlinear link elements. The user specifies initial load vectors at his/her discretion, which should adequately reflect the structural deformed shape under the given analysis condition.

When compared with eigenvalue analysis, Ritz vector analysis has the following advantages:

Ritz vectors are founded on static analysis solutions for real loads. Even if smaller number of modes are calculated in Ritz vector analysis, the effects of higher modes are automatically reflected. For example, the first mode shape in a Ritz vector analysis can be different from that in an eigenvalue analysis, which is attributed to representing the effects of higher modes. Also, Ritz vector analysis finds only the mode shapes pertaining to the loads acting on the structure, thereby eliminating the calculations for unnecessary modes. Ritz vector analysis

thus reduces the number of modes for finding accurate results. Ritz vector analysis requires a less number of modes to attain sufficient modal mass participation compared to eigenvalue analysis.

Consideration of Damping

Overview of Damping

Structural damping in a dynamic analysis can be largely classified into the following:

- Modal damping
  - Proportional damping
    - Mass proportional type
    - Stiffness proportional type
    - Rayleigh type
    - Caughey type
  - Non-proportional damping
    - Energy proportional type
- Viscous damping (Voigt model & Maxwell model)
- Hysteretic damping
- Friction damping
  - Internal friction damping (Material damping)
  - External friction damping
  - Sliding friction damping
- Radiation damping

Among the many different ways of expressing damping phenomena above, modal damping is most frequently used in numerical analyses of structures. The values for modal damping are determined for each modal natural frequency of a vibration system. The modal damping can be classified into proportional and non-proportional damping. The MIDAS programs provide proportional damping, which includes mass proportional, stiffness proportional and Rayleigh type damping.

In order to calculate the non-proportional damping matrix of a structure, which includes materials with different damping properties or artificial damping devices, the damping properties are individually evaluated first. And then, its damping matrix is obtained. In real structures, however, damping mechanisms

are complex, and it is thus impractical to determine the damping matrix in this manner for most cases.

Accordingly, proportional damping (also referred to as classical damping) is generally used to account for the effects of damping. In order to obtain the damping matrix of a structure, the damping properties of the major modes from an eigenvalue analysis of the structure are formulated into a proportional damping matrix. A diagonal damping matrix can be obtained when the damping matrix is multiplied left and right by the corresponding mode vectors. Then the modal damping ratios can be further obtained with a simple mathematical modification to the diagonal damping matrix. Note that the orthogonal property of eigen-vectors with respect to the proportional damping matrix is utilized in computing the modal damping ratios.

When non-proportional damping is under consideration, it is not possible to obtain modal damping ratios as the eigen-vectors are not orthogonal with respect to the non-proportional damping matrix. Based on the mode shapes calculated from an eigenvalue analysis, the strain energy concept is applied to obtain the modal damping ratios.

In MIDAS GEN NX, the damping method can be specified in the Response Spectrum Load Cases menu for a response spectrum analysis, and in the Time History Load Cases menu for a time history analysis. Depending on the type of dynamic analysis, possible options to assign the damping method are as follows:

- In response spectrum analysis and in time history analysis using modal superposition
  - Modal
  - Mass & Stiffness Proportional
    - Mass Proportional Type
    - Stiffness Proportional Type
    - Rayleigh Damping Type
  - Strain Energy Proportional

- In time history analysis using a direct integration method
  - Modal
  - Mass & Stiffness Proportional
    - Mass Proportional Type
    - Stiffness Proportional Type
    - Rayleigh Damping Type
  - Strain Energy Proportional
  - Element Mass & Stiffness Proportional
    - Rayleigh Damping Type

In addition, the Kelvin model can be implemented by assigning a linear viscous damper (damping or effective damping) in the General Link menu. In response spectrum and modal superposition analyses, Strain Energy Proportional must be selected in the damping method to reflect the modal damping ratios in calculation. In a time history analysis using a direct integration method, Mass & Stiffness Proportional or Element Mass & Stiffness Proportional must be selected for the damping method such that the damping ratios are directly applied in analysis through the element damping matrices. Note that when Strain Energy Proportional is selected in the damping method, the modal damping ratios are indirectly applied in analysis.

The method of reflecting damping in modal superposition and direct integration methods will be explained next. The equation of motion of a structure is presented below.

$$M\ddot{u}(t) + C\dot{u}(t) + Ku(t) = p(t) \tag{1}$$

where,

M	: Mass Matrix
C	: Damping Matrix
K	: Stiffness Matrix
$u(t)$, $\dot{u}(t)$, $\ddot{u}(t)$	: Nodal displacement, velocity & acceleration
$p(t)$	: Dynamic Force

In response spectrum analysis and vibration analysis by modal superposition, the solutions to the equations of motions of individual modes are superimposed. Equation (1) is decomposed into individual modes as expressed in Equation (2) using the orthogonality of the modal vectors. Accordingly, an eigenvalue analysis must precede.

$$\ddot{q}_i(t) + 2\xi_i\omega_i\dot{q}_i(t) + \omega_i^2 q(t) = \frac{\phi_i^T p(t)}{\phi_i^T M \phi_i} \tag{2}$$

where, ϕ_i : i-th mode eigenvector (mode shape)

ξ_i	: i –th mode damping ratio
ω_i	: i –th mode natural frequency
$q_i(t)$, $\dot{q}_i(t)$, $\ddot{q}_i(t)$	: i–th mode generalized displacement, velocity, acceleration

Regardless of the type of damping method selected for vibration analysis by response spectrum and modal superposition analyses, damping is considered by the assigned modal damping ratios, ξ_i .

Time history analysis by a direct integration method directly solves the equation of motion in a matrix form obtained from the dynamic equilibrium (Equation (1)). This method thus requires a damping matrix in formulating the equation of motion.

The following sections describe the methods of formulating the damping ratio (ξ_i) and the damping matrix (C) pertaining to each analysis method and damping method.

Proportional Damping

Mass-proportional damping accounts for the effects of external viscous damping such as air resistance, which assumes that the damping matrix is proportional to the mass matrix. Stiffness-proportional damping on the other hand can be explained as an energy dissipated model. Because the effects of radiation damping (effects of emitting vibration energy into the ground) cannot be directly expressed, the effects are assumed to be proportional to the stiffness, which may lead to an overestimation of damping for high modes.

The general form of a proportional damping matrix is defined by Caughey.

$$C = M\{\sum_{j=0}^{N-1} a_j (M^{-1}K)^j\} \tag{3}$$

where,

j, *N*: Nodal degrees of freedom of nodes, Nth mode (Mode number)

From Equation (1), $M^{-1}K$ can be obtained from the free vibration of an undamped system as follows:

$$M\{y\} + K\{y\} = 0 \tag{4}$$

$$\{y\} = \{u\}e^{i\alpha x} \tag{5}$$

Equation (5) is assumed and substituted into Equation (4), which becomes,

$$(-\omega^2 M + K)\{u\} = \{0\} \tag{6}$$

$M^{-1}K = \omega^2$ is then obtained from Equation (6). As many number of ω^2 as the number of modes exist, which are expressed as ω_s^2 considering the order of the modes.

Substituting $M^{-1}K$ obtained from Equations (4)-(6) into Equation (3), and multiplying $\{u_s\}^T$ on the left and $\{u_s\}$ on the right, Equation (3) then becomes,

$$\{u_s\}^T C \{u_s\} = C_s = \sum_{j=0}^{N-1} a_j \cdot \omega_s^{2j} \cdot \{u_s\}^T M \{u_s\} = \sum_{j=0}^{N-1} a_j \cdot \omega_s^{2j} \cdot M_s \tag{7}$$

Also, damping constant (ξ_s) for the s-th mode can be expressed as,

$$C_s = 2\xi_s \cdot \omega_s \cdot M_s \tag{8}$$

Damping constant, ξ_s for N number of modes can be calculated in Equations (7) and (8).

$$\xi_s = \frac{C_s}{2\omega_s \cdot M_s} = \frac{1}{2\omega_s}\sum a_j \cdot \omega_s^{2j}$$
$$= \frac{1}{2}\left(\frac{a_0}{\omega_s} + a_1 \cdot \omega_s + a_2 \cdot \omega_s^3 + \cdots + a_{N-1} \cdot \omega_s^{2N-3} \right), \quad s = 1 - N \tag{9}$$

Damping constants and matrices for the mass proportional type and stiffness proportional type are expressed as follows:

$$\xi_s = \frac{a_0}{2\omega_s}, \quad C = a_0 M = 2\xi_s \omega_s M \quad : \text{ Mass proportional type} \tag{10}$$

$$\xi_s = \frac{a_1 \cdot \omega_s}{2}, \quad C = a_1 K = \frac{2\xi_s}{\omega_s} K \quad : \text{ Stiffness proportional type} \tag{11}$$

In the Response Spectrum Load Cases menu or the Time History Load Cases menu, Mass & Stiffness Proportional is selected first for the damping method. Then, Mass Proportional and Stiffness Proportional can be selected. The detailed selection method will be discussed in the following Rayleigh Damping section.

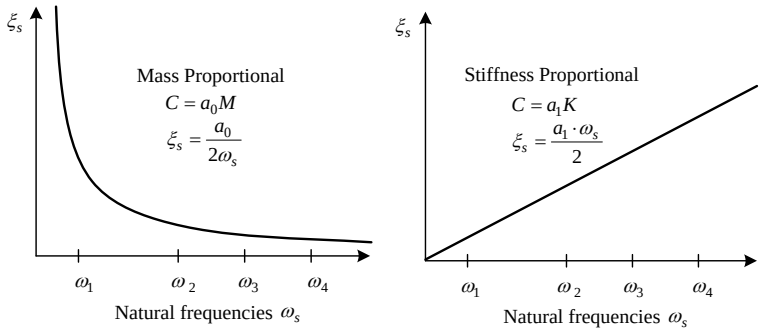

(a) Mass Proportional Damping (b) Stiffness Proportional Damping

Figure 2.4.1 Modal damping ratios

Rayleigh Damping

Rayleigh damping is a modified version of the stiffness-proportional damping by correcting the damping ratios of high modes. As shown in Figure 2.4.2(b), the damping matrix is formulated by linearly combining the mass-proportional damping and stiffness-proportional damping matrices. Given the damping ratios and natural frequencies of the i-th and j-th modes, the Rayleigh damping matrix is determined by Equations (12), (13), (14) and (15) below. Note that the i-th and j-th modes represent two major modes.

$$C = a_0 M + a_1 K \tag{12}$$

$$\xi_s = \frac{1}{2}\left(\frac{a_0}{\omega_s} + a_1 \cdot \omega_s \right) \tag{13}$$

where,

$$a_0 = \frac{2 \cdot \omega_i \cdot \omega_j \left(\xi_i \cdot \omega_j - \xi_j \cdot \omega_i \right)}{\left(\omega_j^2 - \omega_i^2 \right)} \tag{14}$$

$$a_1 = \frac{2\left(\xi_j \cdot \omega_j - \xi_i \cdot \omega_i \right)}{\left(\omega_j^2 - \omega_i^2 \right)} \tag{15}$$

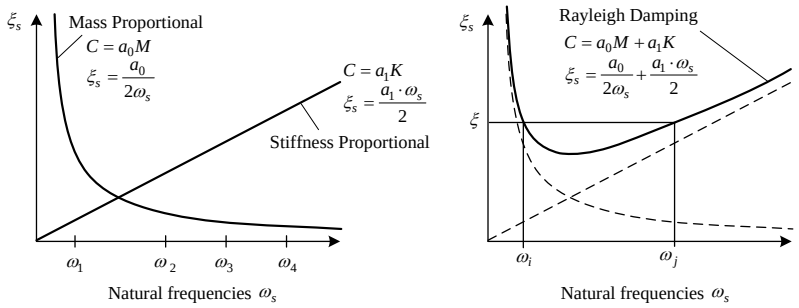

(a) Mass Proportional Damping and Stiffness Proportional Damping

(b) Rayleigh Damping

Figure 2.4.2 Relationship between modal damping and frequencies

a_0 and a_1 can be assigned in the Response Spectrum Load Cases menu or the Time History Load Cases menu in the following manner:

1. Direct Specification

   The values of a_0 and a_1 are directly defined by the user.

2. Calculate from Modal Damping

   Damping ratios for the i-th and j-th modes are defined by the user. Using the damping ratios with the natural frequencies or natural periods obtained from an eigenvalue analysis, a_0 and a_1 are then automatically calculated in MIDAS GEN NX.

   For example, if the frequencies and damping ratios for the i-th and j-th modes are $f_i = 1.0Hz$, $f_j = 1.25Hz$, $\xi_i = 0.05$ and $\xi_j = 0.05$ respectively, then the values of a_0 and a_1 are obtained as follows:

   - Natural frequency

     $$\omega_1 = \frac{2\pi}{1.0} = 6.28,\ \omega_2 = \frac{2\pi}{0.8} = 7.85$$

   - Calculations of a_0 and a_1, using Equations (14) and (15)

     $$a_0 = \frac{2 \cdot 6.28 \cdot 7.85(0.05 \cdot 7.85 - 0.05 \cdot 6.28)}{7.85^2 - 6.28^2} = 0.349$$

     $$a_1 = \frac{2(0.05 \cdot 7.85 - 0.05 \cdot 6.28)}{7.85^2 - 6.28^2} = 0.007$$

   - Automatic calculations of a_0 and a_1 performed in MIDAS GEN NX

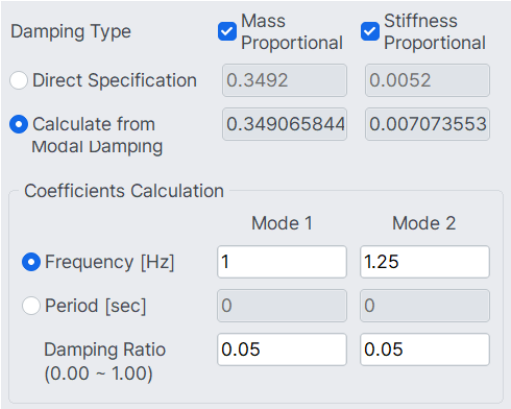

Rayleigh damping can be used in a response spectrum analysis and a time history analysis by the direct integration or modal superposition method. In the Response Spectrum Load Cases menu or the Time History Load Cases menu, Mass & Stiffness Proportional is selected first for the damping method. Then, both Mass Proportional and Stiffness Proportional are selected in the damping type. The method of considering damping for each analysis type will be discussed in the next two sections.

Rayleigh Damping in Response Spectrum and Modal Superposition Analyses

In a response spectrum analysis or the modal superposition method in a vibration analysis, the equation of motion for the structure is decomposed into N number of equations of motion (N modes defined by the user). The equations are individually calculated and the results of all the modes are combined. When the Rayleigh damping is used, the a_0 and a_1 values obtained from the two major modes are used in Equation (13) to obtain the damping ratios for all the modes being used.

The following explains how MIDAS GEN NX calculates modal damping ratios, using the values of a_0 and a_1 obtained from the two major modes.

For example, if the first three modes are considered with $a_0 = 0.35$ and $a_1 = 0.005$, the modal damping ratio, ξ_s is computed as follows. Assume $\omega_1 = 4.59215$, $\omega_2 = 9.81814$ and $\omega_3 = 14.57793$.

- Damping ratio calculations for the first three modes

$$\xi_s = \frac{1}{2}\left(\frac{a_0}{\omega_s} + a_1 \cdot \omega_s\right)$$

$$\xi_1 = \frac{1}{2}\left(\frac{1}{4.59215}0.35 + 0.005 \cdot 4.59215\right) = 0.04959$$

$$\xi_2 = \frac{1}{2}\left(\frac{1}{9.81814}0.35 + 0.005 \cdot 9.81814\right) = 0.04237$$

$$\xi_3 = \frac{1}{2}\left(\frac{1}{14.57793}0.35 + 0.005 \cdot 14.57793\right) = 0.04845$$

- Damping ratio calculations for the first three modes

RAYLEIGH DAMPING COEFFICIENT, TIME LOADCASE = 1

MASS COEFFICIENT. : 0.35000
STIFFNESS COEFFICIENT. : 0.00500

MODE NO.	FREQUENCY [RAD/SEC]	DAMPING RATIO
1	4.59215E+00	**4.95889E-02**
2	9.81814E+00	**4.23695E-02**
3	1.45779E+01	**4.84493E-02**

Exception: if $\xi_s > 1$ or $\xi_s < 0$, then ξ_s is considered as 0.9999 or 0.0 respectively.

Rayleigh Damping in Direct Integration Method

The Rayleigh damping in a direct integration method also uses the values of a_0 and a_1 determined by only two major modes, which are incorporated in $C = a_0 M + a_1 K$ to compute a damping matrix. With the equation of motion in a matrix format, direct integration is executed for each time step.

In a nonlinear time history analysis using the direct integration method, the damping effects can be overestimated when the structure undergoes inelastic deformations beyond the elastic limit and the initial stiffness, *K* is maintained in $C = a_0 M + a_1 K$.

MIDAS GEN NX automatically updates the stiffness of members beyond the yielding point extending into the zone of stiffness degradation, which in turn becomes reflected in the composition of the damping matrix. The renewal of stiffness is applicable only when Mass & Stiffness Proportional or Element Mass & Stiffness Proportional is selected for the damping method, both of which constitute a damping matrix based on the Rayleigh damping.

In order to execute the analysis, the user must specify the following in the Time History Load Cases menu:

1. Nonlinear is selected for the analysis type.
2. Direct integration is selected for the analysis method.
3. Mass & Stiffness Proportional or Element Mass & Stiffness Proportional is selected for the damping method.
4. “Yes” is selected for the damping matrix update.

Note that when “No” is selected, the initial stiffness matrix is used for the entire time history analysis irrespective of the condition of the structure.

Modal Damping Based on Strain Energy

Overview

In real structures, damping properties are different for different materials, and sometimes damping devices are locally installed. MIDAS GEN NX enables the user to specify different damping characteristics for different elements by using Element Mass & Stiffness Proportional. However, the damping matrices of such structures generally are of non-classical damping, and their modes cannot be decomposed. Accordingly, modal damping ratios are calculated on the basis of the concept of strain energy in order to reflect different damping properties by elements in response spectrum analysis and modal superposition in dynamic analysis.

The modal damping based on strain energy can be performed in time history analysis by the response spectrum, modal superposition and direct integration methods. Strain Energy Proportional is selected for the damping method in the Response Spectrum Load Cases menu and the Time History Load Cases menu. However, when the strain energy based modal damping is considered in time history analysis by the direct integration, the damping matrix becomes a full matrix, which demands an excessive time for analysis compared to that required for modal superposition.

The damping ratio of a single degree of vibration system having viscous damping can be defined by a ratio of dissipated energy in a harmonic motion to the strain energy of the structure.

$$\xi = \frac{E_D}{4\pi E_S} \tag{16}$$

where,

E_D : Dissipated energy
E_S : Strain energy

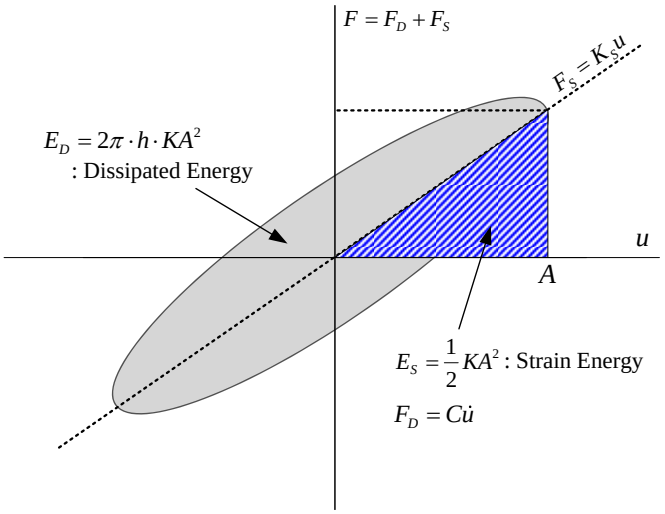

Figure 2.4.3 Dissipated Energy and Strain Energy

In a structure with multi-degrees of freedom, the dynamic behavior of a particular mode can be identified by the dynamic behavior of the single degree of freedom system of the corresponding natural frequency. For this, two assumptions are made to calculate the dissipated energy and strain energy pertaining to a particular element. First, the deformation of the structure is assumed to be proportional to the mode shapes. The element nodal displacement and velocity vectors of the structure in a harmonic motion based only on the *i*-th mode of the corresponding natural frequency can be written as,

$$\begin{aligned} \mathbf{u}_{i,n} &= \boldsymbol{\varphi}_{i,n} \sin\left(\omega_i t + \theta_i\right) \\ \dot{\mathbf{u}}_{i,n} &= \omega_i \boldsymbol{\varphi}_{i,n} \cos\left(\omega_i t + \theta_i\right) \end{aligned} \tag{17}$$

where,

$\mathbf{u}_{i,n}$: Nodal displacement of the *n*-th element due to the *i*-th mode of vibration

$\dot{\mathbf{u}}_{i,n}$: Nodal velocity of the *n*-th element due to the *i*-th mode of vibration

$\varphi_{i,n}$: *i*-th Mode shape corresponding to the *n*-th element's degree of freedom

ω_i : Natural frequency of the *i*-th mode

θ_i : Phase angle of the *i*-th mode

Second, the element's damping is assumed to be viscous damping, which is proportional to the element's stiffness.

$$\mathbf{C}_n = \frac{2h_n}{\omega_i}\mathbf{K}_n \tag{18}$$

where,

$\mathbf{C}_n$: Damping matrix of the *n*-th element
$\mathbf{K}_n$: Stiffness matrix of the *n*-th element
h_n : Damping ratio of the *n*-th element

The dissipated energy and strain energy can be expressed as below under the above assumptions.

$$\begin{aligned} E_D(i,n) &= \pi \mathbf{u}_{i,n}^T \mathbf{C}_n \dot{\mathbf{u}}_{i,n} = 2\pi h_n \boldsymbol{\varphi}_{i,n}^T \mathbf{K}_n \boldsymbol{\varphi}_{i,n} \\ E_S(i,n) &= \frac{1}{2}\mathbf{u}_{i,n}^T \mathbf{K}_n \mathbf{u}_{i,n} = \frac{1}{2}\boldsymbol{\varphi}_{i,n}^T \mathbf{K}_n \boldsymbol{\varphi}_{i,n} \end{aligned} \tag{19}$$

where,

$E_D(i, n)$: Dissipated energy of the *n*-th element due to the *i*-th mode of vibration
$E_S(i, n)$: Strain energy of the *n*-th element due to the *i*-th mode of vibration

The damping ratio of the *i*-th mode for the entire structure can be calculated by summing the energy for all the elements corresponding to the *i*-th mode.

$$\xi_i = \frac{\sum_{n=1}^{N} E_D(i,n)}{4\pi \cdot \sum_{n=1}^{N} E_S(i,n)} = \frac{\sum_{n=1}^{N} h_n \boldsymbol{\varphi}_{n,i}^T \mathbf{K}_n \boldsymbol{\varphi}_{n,i}}{\sum_{n=1}^{N} \boldsymbol{\varphi}_{n,i}^T \mathbf{K}_n \boldsymbol{\varphi}_{n,i}} \tag{20}$$

Set-up and Calculation of Modal Damping Based on Strain Energy

In order to define the modal damping based on strain energy in MIDAS GEN NX, the elements and boundaries need to be grouped in Group such that each group has the same damping properties. Then the Damping Ratios are individually specified for the element groups and boundary groups in Strain Energy Proportional Damping within Damping Ratio for Specified Elements and Boundaries of Group Damping. For those elements and boundaries, which have not been grouped, the Damping Ratios are defined in Strain Energy Proportional Damping within Default Values for Unspecified Elements and Boundaries.

Using the Damping Ratios of the element and boundary groups defined thus far, the individual modal damping ratios are calculated based on the strain energy upon the execution of eigenvalue analysis. The results can be then found in Modal Damping Ratio of Modal Damping Ratio based on Group Damping. When Calculated Only When Used is checked on in Group Damping (shown at the bottom of the left figure below), the modal damping will be calculated only under the damping condition of Strain Energy Proportional in time history analysis.

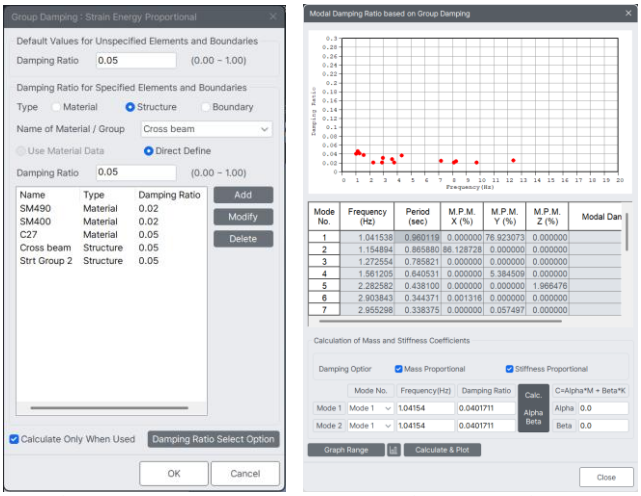

(a) Defining Damping Ratios for Each Element and Boundary Groups *(b) Calculation of Damping Ratio for Each Mode based on strain Energy*

Figure 2.4.4 Definition of Strain Energy Damping and Modal Damping

In response spectrum and modal superposition analyses, the equation of motion for the structure is decomposed into a set of modal equations of motion. These

modal equations of motion are then solved using the modal damping ratios, ξ_s obtained on the basis of strain energy.

In a time history analysis with the direct integration method, the damping matrix constituting the equation of motion for the entire structure is formulated by using the strain energy based modal damping ratios (ξ_s), natural frequencies (ω_i) and modal matrices. Formulating the damping matrix for this particular case will be discussed separately.

Modal Damping

Modal damping ratios can be directly defined by the user. Modal responses are then computed based on the defined modal damping ratios. Modal damping can be utilized in response spectrum, modal superposition and direct integration analyses. However, when modal damping is used in a time history analysis by the direct integration method, the damping matrix becomes unsymmetrical, which demands an excessive calculation time compared to that required for the modal superposition method.

Modal damping can be defined in the Response Spectrum Load Cases menu and the Time History Load Cases menu. Modal is selected for the Damping Method, and then modal damping ratios can be assigned within Modal Damping Overrides. Damping ratios for modes, which have not been assigned, can be entered in Damping Ratio for All Modes.

For response spectrum and modal superposition analyses, the equation of motion of the structure is decomposed into a set of modal equations of motion. Each of the modal equations of motion is then solved with the corresponding user-defined modal damping ratio (ξ_s).

In a time history analysis with the direct integration method, the damping matrix constituting the equation of motion for the entire structure is formulated by using the pre-defined modal damping ratios (ξ_s), natural frequencies (ω_s) and modal matrices. Formulating the damping matrix for this particular case will be discussed separately.

Rayleigh Damping by Elements

Rayleigh Damping by Elements enables the user to apply different damping ratios for different members and/ or boundaries constituting a structure. This helps the user effectively model a structure composed of different materials, vibration control devices or vibration isolation devices.

When damping is considered individually for each element, the damping matrix becomes non-proportional damping, which cannot be decomposed by modes. Accordingly, the Rayleigh Damping by Elements can be only applicable to a time history analysis using a direct integration method in which damping matrix is directly created. Element Mass & Stiffness Proportional needs to be selected for the damping method in the Time History Load Cases menu.

In order to reflect different damping properties for different elements in response spectrum and modal superposition analyses, damping ratios need to be assigned in the Specified Element and Boundaries within the Group Damping menu. Modal damping ratios based on the strain energy concept are then calculated based on the results of an eigenvalue analysis.

The Rayleigh damping by elements in MIDAS GEN NX is defined as follows:

1. Group elements and boundaries that will have the same damping properties.
2. For individual groups of elements and boundaries,
   Group Damping → Damping Ratio for Specified Elements and Boundaries → Element Mass & Stiffness Proportional Damping → Assign values for Mass Coefficient (α) and Stiffness Coefficient (β).
3. For the elements and boundaries, which have not been grouped,
   Group Damping → Default Values for Unspecified Elements and Boundaries → Element Mass & Stiffness Proportional Damping → Assign values for Mass Coefficient and Stiffness Coefficient.

Using the values of α and β for each element group, the damping matrix for each element is computed with $C = \alpha M + \beta K$ and the equation of motion can be obtained. Since the Rayleigh Damping by Elements is based on the Rayleigh damping, α_n and β_n for the member *n* are calculated in the same manner as the Rayleigh Damping.

Currently, MIDAS GEN NX does not support Mass Coefficient (α), so it will be treated as stiffness proportional damping by elements.

Formulation of Damping Matrix

In a time history analysis using the direct integration method, the damping matrix becomes a full matrix when Modal or Strain Energy Proportional is selected for the damping method. The damping matrix for the entire structure can be obtained through the assigned modal damping ratios (ξ_s), natural frequencies (ω_i) and modal matrices.

The damping matrix of the entire structure is formulated as below.

$$\mathbf{C} = \mathbf{M}\mathbf{\Phi}\begin{bmatrix} \ddots & & \\ & 2\xi_i\omega_i & \\ & & \ddots \end{bmatrix}\mathbf{\Phi}^T\mathbf{M}$$

where,

C : Damping matrix of the entire structure
M : Mass matrix of the entire structure
ξ_i : Damping ratio of the i-th mode of the entire structure
Φ : Mode shape
$\Phi = \{\Phi_1 \quad \Phi_2 \quad .... \quad \Phi_i \quad .... \quad \Phi_{nf}\}$
nf : number of modes used

Consideration of Linear Damping in General Link Element

General Link Element is used to model vibration damping devices, vibration isolation devices, compression only elements, tension only elements, inelastic hinges and foundation springs. It consists of six springs, which connects two nodes. General Link Element can be used to model an additionally installed damper by specifying the linear viscous damping.

In case the linear viscous damping of a general link is of the Element Type, it can be defined by selecting Linear Dashpot and Spring and Linear Dashpot through Damping of Linear Properties. In the case of Force Type, it can be defined through Effective Damping of Linear Properties.

The details of the linear viscous damping of a general link element are separately addressed in the general link element section. Below explains the method of obtaining modal damping ratios considering the linear viscous damping of a general link element when modal damping based on strain energy is used.

Damping or Effective Damping of linear viscous damping of a general link element is assumed as follows:

$$C_{eff} = \frac{2\xi_{eff}}{\omega_{eff}} K_{eff}$$

where,

C_{eff} : Damping or Effective Damping

K_{eff} : Stiffness of General Link Element

ξ_{eff} : Damping Ratio of General Link Element

ω_{eff} : Frequency of General Link Element

Based on the above equation, the damping ratio of the i-th mode, which reflects the linear viscous damping at the time of calculating the strain energy of a general link, can be expressed as below.

$$\xi_i = \frac{\sum_{n=1}^{N} E_D(i,n)}{4\pi \cdot \sum_{n=1}^{N} E_S(i,n)} = \frac{\sum_{n=1}^{N} \left(h_n \phi_{n,i}^T K_n \phi_{n,i} + 0.5\omega_i \phi_{n,i}^T C_{eff} \phi_{n,i} \right)}{\sum_{n=1}^{N} \phi_{n,i}^T K_n \phi_{n,i}}$$

The modal damping ratios calculated with the above equation are identically applied to response spectrum analysis and time history analysis using the modal superposition and direct integration methods.

Response Spectrum Analysis

The dynamic equilibrium equation for a structure subjected to a ground motion used in a response spectrum analysis can be expressed as follows:

Refer to “Analysis> Response Spectrum Analysis Control" of On-line Manual.

$$[M]\ddot{u}(t)+[C]\dot{u}(t)+[K]u(t)=-[M]w_g(t)$$

where,

$[M]$: Mass matrix

$[C]$: Damping matrix

$[K]$: Stiffness matrix

$w_g(t)$: Ground acceleration

and, $u(t)$, $\dot{u}(t)$ and $\ddot{u}(t)$ are relative displacement, velocity and acceleration respectively.

Response spectrum analysis assumes the response of a multi-degree-of-freedom (MDOF) system as a combination of multiple single-degree-of-freedom (SDOF) systems. A response spectrum defines the peak values of responses corresponding to and varying with natural periods (or frequencies) of vibration that have been prepared through a numerical integration process. Displacements, velocities and accelerations form the basis of a spectrum. Response spectrum analyses are generally carried out for seismic designs using the design spectra defined in design standards.

To predict the peak design response values, the maximum response for each mode is obtained first and then combined by an appropriate method. For seismic analysis, the displacement and inertial force corresponding to a particular degree of freedom for the *m*-th mode are expressed as follows:

<Eq. 1>

$$d_{xm}=\Gamma_m\varphi_{xm}S_{dm},\ F_{xm}=\Gamma_m\varphi_{xm}S_{am}W_x$$

where,

Γ_m : *m*-th modal participation factor

φ_{xm} : *m*-th modal vector at location x

S_{dm} : Normalized spectral displacement for *m*-th mode period

S_{am} : Normalized spectral acceleration for *m*-th mode period

W_x : Mass at location x

In a given mode, the spectral value corresponding to the calculated natural period is searched from the spectral data through linear interpolation. It is therefore recommended that spectral data at closer increments of natural periods be provided at the locations of curvature changes (refer to Figure 2.5). The range of natural periods for spectral data must be sufficiently extended to include the maximum and minimum natural periods obtained from the eigenvalue analysis. Some building codes indirectly specify the seismic design spectral data by means of Dynamic coefficient, Foundation factor, Zoning factor, Importance factor, etc. MIDAS GEN NX can generate the design spectrum using these seismic parameters. However, Ductility factor (or Response modification factor or Seismic response factor) is typically applied at the member design stage.

Response spectrum analyses are allowed in any direction on the Global X-Y plane and in the vertical Global Z direction. You may choose an appropriate method of modal combination for analysis results such as the Complete Quadratic Combination (CQC) method or the Square Root of the Sum of the Squares (SRSS) method.

You may reinstate the signs lost during the modal combination process and apply them to the response spectrum analysis results. For details, refer to "Analysis> Response Spectrum Analysis Control" of On-line Manual.

The following describes the methods of modal combination:

- **SRSS (Square Root of the Sum of the Squares)**
  <Eq. 2>

$$R_{\max} = [R_1^{\ 2} + R_2^{\ 2} + \cdots R_n^{\ 2}]^{1/2}$$

- **ABS (Absolute Sum)**
  <Eq. 3>

$$R_{\max} = |R_1| + |R_2| + \cdots + |R_n|$$

- **CQC (Complete Quadratic Combination)**
  <Eq. 4>

$$R_{\max} = \left[\sum_{i=1}^{N} \sum_{j=1}^{N} R_i \rho_{ij} R_j \right]^{1/2}$$

where,

$$\rho_{ij} = \frac{8\xi^2(1+r)r^{3/2}}{(1-r^2)^2 + 4\xi^2 r(1+r)^2}\ ,\ r = \frac{\omega_j}{\omega_i}$$

R_{max}: Peak response
R_i : Peak response of i-th mode
r : Natural frequency ratio of i-th mode to j-th mode
ξ : Damping ratio

In <Eq. 4>, when $i = j$, then $\rho_{ij} = 1$ regardless of the damping ratio. If the damping ratio (ξ) becomes zero (0), both CQC and SRSS methods produce identical results.

The ABS method produces the largest combination values among the three methods. The SRSS method has been widely used in the past, but it tends to overestimate or underestimate the combination results in the cases where the values of natural frequencies are close to one another. **As a result, the use of the CQC method is increasing recently as it accounts for probabilistic inter-relations between the modes**.

If we now compare the displacements of each mode for a structure having 3 DOF with a damping ratio of 0.05, the results from the applications of SRSS and CQC are as follows:

- **Natural frequencies**

$$\omega_1 = 0.46\ ,\ \omega_2 = 0.52\ ,\ \omega_3 = 1.42$$

- **Maximum modal displacements: D_{ij} (displacement components of i-th degree of freedom for j-th mode)**

$$D_{ij} = \begin{vmatrix} 0.036 & 0.012 & 0.019 \\ -0.012 & 0.044 & -0.005 \\ 0.049 & 0.002 & -0.017 \end{vmatrix}$$

- **If SRSS is applied to compute the modal combination for each degree of freedom,**

$$R_{\max} = \left[R_1^2 + R_2^2 + R_3^2 \right]^{1/2} = \{0.042, 0.046, 0.052\}$$

- **If CQC is applied,**

$$\rho_{12} = \rho_{21} = 0.3985$$
$$\rho_{13} = \rho_{31} = 0.0061$$

$$R_{\max} = [R_1^{\,2} + R_2^{\,2} + R_3^{\,2} + 2\rho_{12}R_1R_2 + 2\rho_{13}R_1R_3 + 2\rho_{23}R_2R_3]^{1/2}$$
$$= \{0.046, 0.041, 0.053\}$$

Comparing the two sets of displacements for each degree of freedom, we note that the SRSS method underestimates the magnitude for the first degree of freedom overestimates the value for the second degree of freedom relative to those obtained by CQC. Thus, the SRSS method should be used with care when natural frequencies are close to one another.

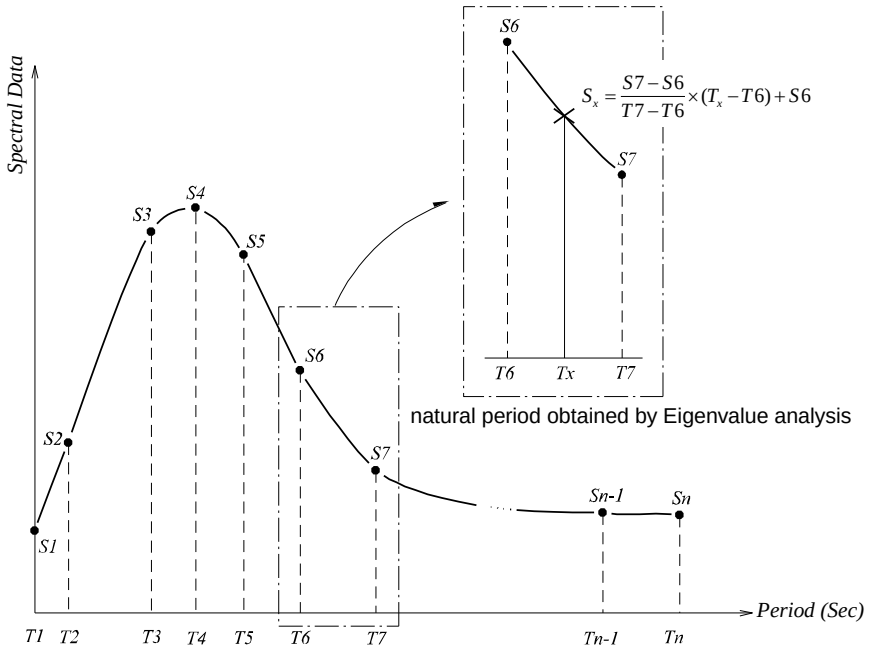

Figure 2.5 Response spectrum curve and linear interpolation of spectral data

Time History Analysis

The dynamic equilibrium equation for time history analysis is written as

Refer to "Load>Time History Analysis Data" of On-line manual.

$$[M]\ddot{u}(t)+[C]\dot{u}(t)+[K]u(t)=p(t)$$

where,

$[M]$: Mass matrix

$[C]$: Damping matrix

$[K]$: Stiffness matrix

$p(t)$: Dynamic load

and, $u(t)$, $\dot{u}(t)$ and $\ddot{u}(t)$ are displacement, velocity and acceleration respectively.

Time history analysis seeks out a solution for the dynamic equilibrium equation when a structure is subjected to dynamic loads. It calculates a series of structural responses (displacements, member forces, etc.) within a given period of time based on the dynamic characteristics of the structure under the applied loads. MIDAS GEN NX uses the Modal Superposition Method for time history analysis.

Modal Superposition Method

The displacement of a structure is obtained from a linear superposition of modal displacements, which maintain orthogonal characteristics to one another. This method premises on the basis of that the damping matrix is composed of a linear combination of the mass and stiffness matrices as presented below.

<Eq. 1>

$$[C]=[\alpha M]+[\beta K]$$

<Eq. 2>

$$\Phi^T M\Phi\ddot{q}(t)+\Phi^T C\Phi\dot{q}(t)+\Phi^T K\Phi q(t)=\Phi^T F(t)$$

<Eq. 3>

$$m_i\ddot{q}_i(t)+c_i\dot{q}_i(t)+k_i q_i(t)=P_i(t) \qquad (i=1,2,3,...,m)$$

<Eq. 4>

$$u(t) = \sum_{i=1}^{m} \Phi_i q_i(t)$$

<Eq. 5>

$$q_i(t) = e^{-\xi_i \omega_i t}[q_i(0)\cos\omega_{Di}t + \frac{\xi_i \omega_i q_i(0) + \dot{q}_i(0)}{\omega_{Di}}\sin\omega_{Di}t]$$

$$+ \frac{1}{m_i \omega_{Di}} \int_0^t P_i(\tau) e^{-\xi_i \omega_i (t-\tau)} \sin\omega_{Di}(t-\tau) d\tau$$

where,

<Eq. 6>

$$\omega_{Di} = \omega_i \sqrt{1-\xi_i^{\,2}}$$

α, β : Rayleigh coefficients
ζ_i : Damping ratio for *i*-th mode
ω_i : Natural frequency for *i*-th mode
Φ_i : *i*-th mode shape
$q_i(t)$: Solution for *i*-th mode SDF equation

When a time history analysis is carried out, the displacement of a structure is determined by summing up the product of each mode shape and the solution for the corresponding modal equation as expressed in <Eq. 4>. Its accuracy depends on the number of modes used. This modal superposition method is very effective and, as a result, widely used in linear dynamic analyses for large structures. However, this method cannot be applied to nonlinear dynamic analyses or to the cases where damping devices are included such that the damping matrix cannot be assumed as a linear combination of the mass and stiffness matrices.

The following outlines some precautions for data entries when using the modal superposition method:

- **Total analysis time (or Iteration number)**

- **Time step**
  Time step can affect the accuracy of analysis results significantly. The increment must be closely related to the periods of higher modes of the structure and the period of the applied force. The time step directly influences the integral in <Eq. 5>, and as such specifying an improper time step may lead to inaccurate results. In general, one-tenth of the highest modal period under consideration is reasonable for the time step. In addition, the time step should be smaller than that of the applied load.

$$\Delta t = \frac{T_p}{10}$$

where, T_p = the highest modal period being considered

- **Modal damping ratios (or Rayleigh coefficients)**
  Values for determining the energy dissipation (damping) properties of a structure, which relate to either the total structure or individual modes.

- **Dynamic loads**
  Dynamic loads are directly applied to nodes or foundation of a structure, which are expressed as a function of time. The change of loadings must be well represented in the forcing function. A loading at an unspecified time is linearly interpolated.

Figure 2.6 shows an idealized system to illustrate the motion of a SDOF structural system. The equilibrium equation of motion subjected to forces exerting on a SDOF system is as follows:

<Eq. 7>

$$f_I(t) + f_D(t) + f_E(t) = f(t)$$

$f_I(t)$ is an inertia force, which represents a resistance to the change of velocity of a structure. The inertia force acts in the opposite direction to the acceleration, and its magnitude is $m\ddot{u}(t)$. $f_E(t)$ is an elastic force by which the structure restores its configuration to the original state when the structure undergoes a deformation. This force acts in the opposite direction to the displacement, and its magnitude is $ku(t)$. $f_D(t)$ is a damping force, which is a fictitious internal force dissipating kinetic energy and thereby decreasing the amplitude of a motion. The damping force may come in a form of internal frictions. It acts in the opposite direction to the velocity, and its magnitude is $c\dot{u}(t)$.

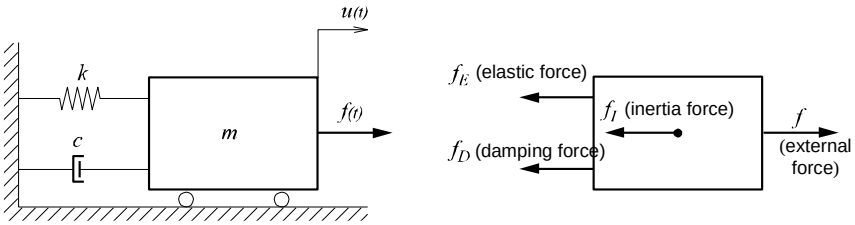

(a) Idealized model (b) State of equilibrium

Figure 2.6 Motion of SDOF System

The above forces are now summarized as

<Eq. 8>

$$f_I = m\ddot{u}(t)$$

$$f_D = c\dot{u}(t)$$

$$f_E = ku(t)$$

where, m, c and k represent mass, damping coefficient and elastic coefficient respectively. From the force equilibrium shown in Figure 2.6 (b), we can obtain the equation of motion for a SDOF structural system.

<Eq. 9>

$$m\ddot{u}(t) + c\dot{u}(t) + k(u) = f(t)$$

<Eq. 9> becomes the equation of damped free vibration by letting *f(t)=0*, and it becomes the equation of undamped free vibration if the condition of *c=0* is additionally imposed on the damped free vibration. If *f(t)* is assigned as a seismic loading (or displacements, velocities, accelerations, etc.) with varying time, the equation then represents a forced vibration analysis problem. The solution can be found by using either Modal Superposition Method or Direction Integration Method.

Buckling Analysis

Linear buckling analysis is used to determine Critical Load Factors and the corresponding Buckling Mode Shapes of a structure, which is composed of truss, beam or plate elements. The static equilibrium equation of a structure at a deformed state is expressed as

<Eq. 1>

$$[K]\{U\}+[K_G]\{U\}=\{P\}$$

Refer to "Analysis>Buckling Analysis Control" of On-line Manual.

where,

$[K]$: Elastic stiffness matrix

$[K_G]$: Geometric stiffness matrix

$\{U\}$: Total displacement of the structure

$\{P\}$: Applied load

The geometric stiffness matrix of a structure can be obtained by summing up the geometric stiffness matrix of each element. The geometric stiffness matrix in this case represents a change in stiffness at a deformed state and is directly related to the applied loads. For instance, a compressive force on a member tends to reduce the stiffness, and conversely a tensile force tends to increase the stiffness.

$$[K_G]=\sum[k_G]$$

$$[k_G]=F[\bar{k}_G]$$

where,

$[\bar{k}_G]$: Standard geometric stiffness matrix of an element

F : Member force (axial force for truss and beam elements)

➢ **Standard geometric stiffness matrix of a truss element**

$$[\bar{k}_G] = \begin{bmatrix} 0 & & & & & \\ 0 & \frac{1}{L} & & & \textit{symm.} & \\ 0 & 0 & \frac{1}{L} & & & \\ 0 & 0 & 0 & 0 & & \\ 0 & -\frac{1}{L} & 0 & 0 & \frac{1}{L} & \\ 0 & 0 & -\frac{1}{L} & 0 & 0 & \frac{1}{L} \end{bmatrix}$$

➢ **Standard geometric stiffness matrix of a beam element**

$$[\bar{k}_G] = \begin{bmatrix} 0 & & & & & & & & & & & \\ 0 & \frac{6}{5L} & & & & & & & & & & \\ 0 & 0 & \frac{6}{5L} & & & & & & & & & \\ 0 & 0 & 0 & 0 & & & & & & & & \\ 0 & 0 & -\frac{1}{10} & 0 & \frac{2L}{15} & & & & & & & \\ 0 & \frac{1}{10} & 0 & 0 & 0 & \frac{2L}{15} & & & & & & \\ 0 & 0 & 0 & 0 & 0 & 0 & 0 & & & & & \\ 0 & -\frac{6}{5L} & 0 & 0 & 0 & -\frac{1}{10} & 0 & \frac{6}{5L} & & & & \\ 0 & 0 & -\frac{6}{5L} & 0 & \frac{1}{10} & 0 & 0 & 0 & \frac{6}{5L} & & & \\ 0 & 0 & 0 & 0 & 0 & 0 & 0 & 0 & 0 & 0 & & \\ 0 & 0 & -\frac{1}{10} & 0 & -\frac{L}{30} & 0 & 0 & 0 & \frac{1}{10} & 0 & \frac{2L}{15} & \\ 0 & \frac{1}{10} & 0 & 0 & 0 & -\frac{L}{30} & 0 & -\frac{1}{10} & 0 & 0 & 0 & \frac{2L}{15} \end{bmatrix}$$

- **Geometric stiffness matrix of a plate element**

$$[k_G] = \int_v [G]^T \begin{bmatrix} s & 0 & 0 \\ 0 & s & 0 \\ 0 & 0 & s \end{bmatrix} [G] dV$$

$[G]$: Matrix of strain-displacement relationship

$$[S] = \begin{bmatrix} \sigma_{xx} & \sigma_{xy} & \sigma_{zx} \\ \sigma_{xy} & \sigma_{yy} & \tau_{yz} \\ \sigma_{zx} & \sigma_{yz} & \sigma_{zz} \end{bmatrix}$$: Element stress matrix

The geometric stiffness matrix can be expressed in terms of the product of the load factor and the geometric stiffness matrix of a structure being subjected to input loads. It is written as

<Eq. 2>

$$[K_G] = \alpha[\bar{K}_G]$$

where,

α : Load scale factor

$\left[\bar{K}_G\right]$: Geometric stiffness matrix of a structure being subjected to external loads

<Eq. 3>

$$[K + \lambda K_G]\{U\} = \{P\}$$

$$[K_{eq}] = [K + \lambda K_G]$$

In order for a structure to become unstable, the above equilibrium equation must have a singularity. That is, buckling occurs when the equivalent stiffness matrix becomes zero.

$\left|[K_{eq}]\right| < 0 \quad (\lambda > \lambda_{cr})$: Unstable equilibrium state

$\left|[K_{eq}]\right| = 0 \quad (\lambda = \lambda_{cr})$: Unstable state

$\left|[K_{eq}]\right| > 0 \quad (\lambda < \lambda_{cr})$: Stable state

Therefore, the buckling analysis problem in <Eq. 3> can be narrowed to an eigenvalue analysis problem.

<Eq. 4>

$$\left|[K]+\lambda_i[K_G]\right|=0$$

where, λ_i : eigenvalue (critical load factor)

This can be now solved by the same method used in “Eigenvalue Analysis”.

From the eigenvalue analysis, eigenvalues and mode shapes are obtained, which correspond to critical load factors and buckling shapes respectively. **A critical load is obtained by multiplying the initial load by the critical load factor. The significance of the critical load and buckling mode shape is that the structure buckles in the shape of the buckling mode when the critical load exerts on the structure**. For instance, if the critical load factor of 5 is obtained from the buckling analysis of a structure subjected to an initial load in the magnitude of 10, this structure would buckle under the load in the magnitude of 50. Note that the buckling analysis has a practical limit since buckling by and large occurs in the state of geometric or material nonlinerity with large displacements.

As stated earlier, the linear buckling analysis feature in MIDAS GEN NX is applicable for truss, beam and plate elements. The analysis is carried out in two steps according to the flow chart shown in Figure 2.7.

1. Linear static analysis is performed under the user-defined loading condition. The geometric stiffness matrices corresponding to individual members are then formulated on the basis of the resulting member forces or stresses.

2. The eigenvalue problem is solved using the geometric and elastic stiffness matrices obtained in Step 1.

The eigenvalues and mode shapes obtained from the above process now become the critical load factors and buckling shapes respectively.

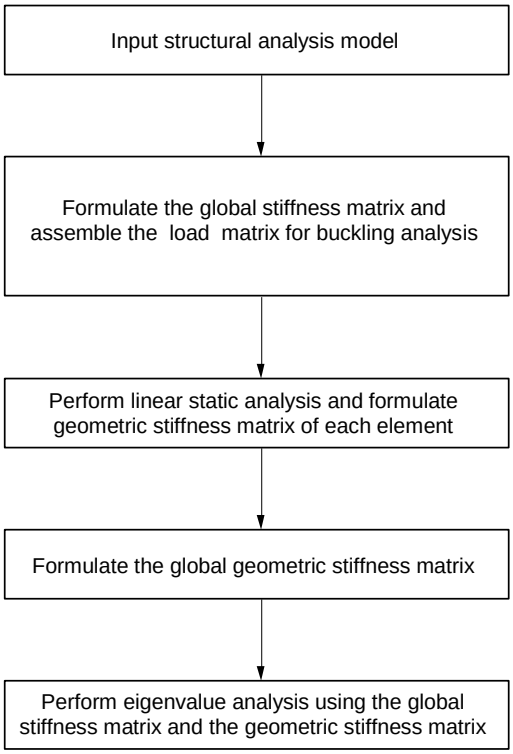

Figure 2.7 Buckling analysis schematics in MIDAS GEN NX

Nonlinear Analysis

Overview of Nonlinear Analysis

When a structure is analyzed for linear elastic behaviors, the analysis is carried out on the premise that a proportional relationship exists between loads and displacements. This assumes a linear material stress-strain relationship and small geometric displacements.

The assumption of linear behaviors is valid in most structures. However, nonlinear analysis is necessary when stresses are excessive, or large displacements exist in the structure. Construction stage analyses for suspension and cable stayed bridges are some of large displacement structure examples. Nonlinear analysis can be classified into 3 main categories.

First, material nonlinear behaviors are encountered when relatively big loadings are applied to a structure thereby resulting in high stresses in the range of nonlinear stress-strain relationship. The relationship, which is typically represented as in Figure 2.8, widely varies with loading methods and material properties.

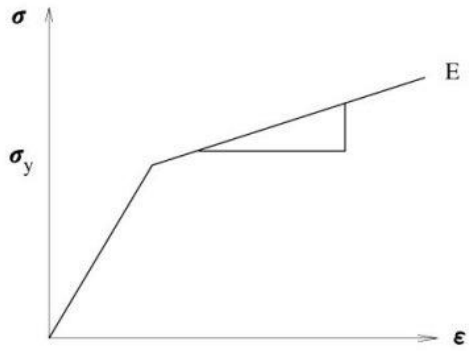

Figure 2.8 Stress-strain relationship used for material nonlinearity

Second, a geometric nonlinear analysis is carried out when a structure undergoes large displacements and the change of its geometric shape renders a nonlinear displacement-strain relationship. The geometric nonlinearity may exist even in the state of linear material behaviors. Cable structures such as suspension bridges are analyzed for geometric nonlinearity. A geometric nonlinear analysis must be carried out if a structure exhibits significant change of its shape under applied

loads such that the resulting large displacements change the coordinates of the structure or additional loads like moments are induced (See Figure 2.9).

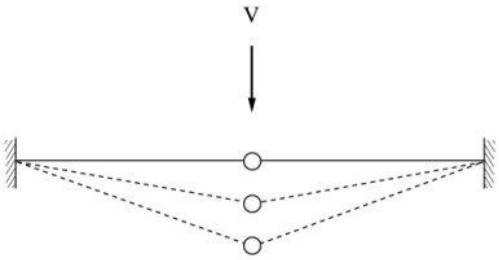

(a) Change in structural stiffness due to large displacement

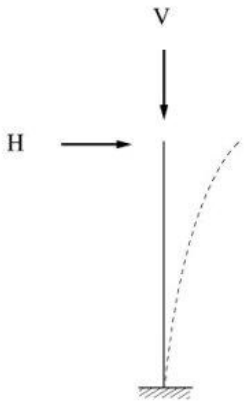

(b) Additional load induced due to displacement

Figure 2.9 Structural systems requiring geometric nonlinear analyses

Third, boundary nonlinearity of a load-displacement relationship can occur in a structure where boundary conditions change with its structural deformations due to external loads. An example of boundary nonlinearity would be compression-only boundary conditions of a structure in contact with soil foundation.

MIDAS GEN NX contains such nonlinear analysis functions as boundary nonlinear analysis using nonlinear elements (compression/tension-only elements) and large displacement geometric nonlinear analysis.

Geometric Nonlinear Analysis

Small displacement (ε_{ij}) used in linear analysis is given below under the assumption of small rotation.

$$\varepsilon_{ij} = \frac{1}{2}\left(u_{i,j} + u_{j,i}\right)$$

"*u*" represents displacement and "," represents the differentiation of the first subscript coordinate. When a large displacement occurs as shown in Figure 2.10, the structural deformation cannot be expressed with small strain any longer. Large displacement can be divided into rotational and non-rotational components as per the equations below. *F* , *R* and *U* represent deformation tensor, rotation tensor and stretch tensor respectively. *U* determines the deformation of a real structure.

$$F = RU,\ \varepsilon = f(U)$$

Accurate strain can be calculated from the above equations after eliminating the rotational component. When the magnitude of rotation is large, accurate deformation-displacement relationship cannot be found initially. That is, geometric nonlinearity is introduced because the deformations change according to the displacements calculated from the linear analysis.

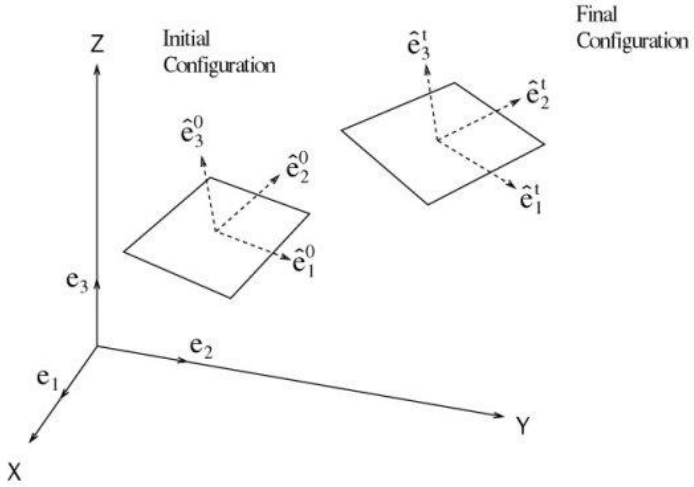

Figure 2.10 Geometric nonlinearity due to large displacement

MIDAS GEN NX uses the Co-rotational method for geometric nonlinear analysis, and its basic concept and analysis algorithm are as follows: This method considers geometric nonlinearity by using the strain in the Co-rotational coordinate system, which moves with the rotation of the element being deformed. The deformation-displacement relationship in the Co-rotational coordinate system can be expressed as a matrix equation $\hat{e} = \hat{B}\hat{u}$, and the deformation-displacement relationship matrix used in linear analysis can be applied. That is, the element's stability and converging ability of linear analysis are maintained even geometric nonlinearity concepts are introduced. Maintaining such superior characteristics is most advantageous for nonlinear analysis.

Displacement $\hat{u}$ in the Co-rotational coordinate system is calculated by the equation, $\hat{u} = \{e_1, e_2, e_3, \hat{e}_1, \hat{e}_2, \hat{e}_3\}$, and the infinitesimal displacement $\delta\hat{u}$ is "linearized" and then expressed as $\delta\hat{u}=T\delta u$. In the case of a linear elastic problem in the Co-rotational coordinate system, the internal element force $\hat{p}^{int}$ is obtained from

$$\hat{p}^{\text{int}} = \int_{dv} B^T \hat{\sigma} dV_0$$

where, $\hat{\sigma}$ is the stress expressed in the Co-rotational coordinate system, and the increment of the above equation becomes

$$\delta\hat{p}^{\text{int}} = (K + \hat{K}_{\sigma})\delta\hat{u}$$

In the above equation, $\hat{K}_{\sigma}$ is the geometric stiffness matrix or initial stress stiffness matrix. The following nonlinear equilibrium equation can be obtained using the equilibrium relationship between the internal and external forces, $p^{ext} - p^{\text{int}} = 0$.

$$(\hat{K} + \hat{K}_{\sigma})\hat{u} = p^{ext}$$

Newton-Raphson and Arc-length methods are used for finding solutions to the nonlinear equilibrium equations. The Newton-Raphson method, which is a load control method, is used for typical analyses. For those problems such as Snap-through or Snap-back, the Arc-length method is used.

MIDAS GEN NX permits the use of truss, beam and plate elements for geometric nonlinear analyses. If other types of elements are used, the stiffness is considered, but not the geometric nonlinearity.

Newton-Raphson iteration method

In the geometric nonlinear analysis of a structure being subjected to external loads, the geometric stiffness is expressed as a function of the displacement, which is then affected by the geometric stiffness again. The process requires repetitive analyses. The Newton-Raphson method is a widely used method, which calculates the displacement in equilibrium with the given external load as shown in Figure 2.11. The stiffness matrix is rearranged in each cycle of repetitive calculations to satisfy equilibrium with the load given in the equilibrium equation of load-displacement. A solution within the allowable tolerance is obtained using the stiffness matrices through the process of iteration.

$$(K + K_{\sigma})u = p, K_T u = p$$
$$K_T = K + K_{\sigma}, K_{\sigma} = f(u)$$
$$K_T(u_{m-1})(u_{m-1} + \Delta u_m) = R_m$$

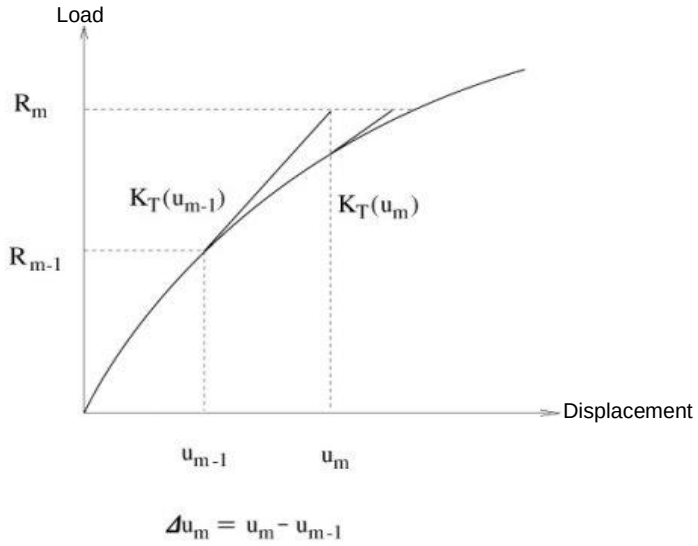

Figure 2.11 Newton-Rapson Method

Expanding the left side of the above equation by Taylor series, ($y(x_n + h) = y(x_n) + y'(x_n)h$), we obtain

$$K_T(u_{m-1})(u_{m-1} + \Delta u_m) = K_T(u_{m-1})u_{m-1} + \frac{dR}{du_{m-1}}\Delta u_m$$

The relationship of $\frac{dR}{du_{m-1}} = K_T(u_{m-1})$ and $R_m - R_{m-1} = R^R$ are substituted into the above equation and rearranged to obtain the following:

$$K_T(u_{m-1})\Delta u_m = R_m - R_{m-1} = R^R \quad (R^R : \text{Residual Force})$$

The process of analysis is illustrated in the above diagram. Once Δu_m is calculated, the displacement is adjusted by $u_m = u_{m-1} + \Delta u_m$. To proceed to the next iterative step, a new tangential stiffness $K_T(u_m)$ and the unbalanced load $R_{m+1} - R_m$ are calculated, and the adjusted displacement u_{m+1} is obtained.

The iterative process is continued until the magnitude of an increment in displacement, energy or load in a step is within the convergence limit.

Arc-length iteration method

In a general iterative process, the calculated value for a displacement increment can be excessive if the load-displacement curve is close to horizontal. If the load increment remains constant, the resulting displacement can be quite excessive. The Arc-length method resolves such problems, and Snap-through behaviors can be analyzed similar to using the displacement control method. Also, the Arc-length method can analyze even the Snap-back behaviors, which the displacement control method cannot analyze (See Figure 2.12 (b)).

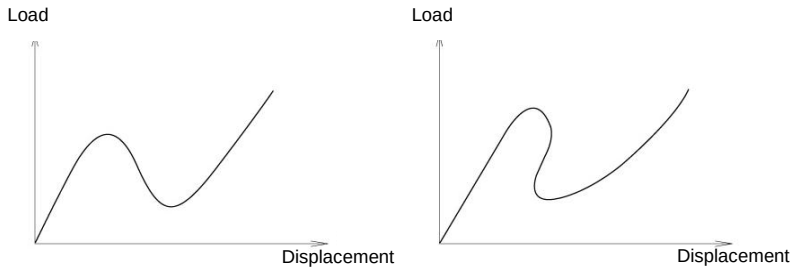

(a) Snap-through (b) Snap-back

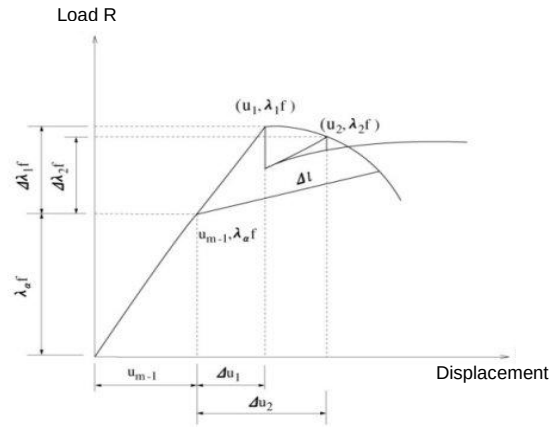

(c) Concept of Arc-Length Method

Figure 2.12 Arc-Length Method

In the Arc-length method, the norm of incremental displacements is restrained to a pre-defined value. The magnitude of the increment is applied while remaining unchanged in the iterative process, but it is not fixed at the starting time of increments. The following process is observed in order to determine the magnitude of the increment: (Figure 2.12 (c)) We define the external force vector at the beginning of increments as R_{m-1} and the increment of external force vector as $\Delta\lambda_i f$. The unit load f is multiplied by the load coefficient $\Delta\lambda_i$ and changed at every step of iteration.

$$K_T(u_{i-1})\delta u_i = \Delta R_i^R$$
$$\delta u_i = K_T\left(u_{i-1}\right)^{-1}\left(\Delta\lambda_i f + f_{\text{int}}\left(u_{m-1}\right) - f_{\text{int}}\left(u_i\right)\right)$$

The solutions to the above equations can be divided into the following two parts, and the incremental displacement can be found as below.

$$\delta u_i^I = K_T\left(u_{i-1}\right)^{-1}\left(f_{\text{int}}\left(u_{m-1}\right) - f_{\text{int}}\left(u_i\right)\right),\ \delta u_i^{II} = K_T\left(u_{i-1}\right)^{-1} f$$
$$\delta u_i = \delta u_i^I + \Delta\lambda_i \delta u_i^{II}$$

MIDAS GEN NX finds the load coefficient $\Delta\lambda_i$ by using the spherical path whose constraint condition equation is as follows:

$$\Delta u_i^T \Delta u_i = \Delta l^2$$

Δl represents the displacement length to be restrained, and the equation $\Delta u_i = \Delta u_{i-1} + \delta u_i$ is substituted into the above equation to calculate the load coefficient $\Delta\lambda_i$ as below.

$$a_1\Delta\lambda^2 + a_2\Delta\lambda + a_3 = 0$$
$$\Delta\lambda_i = \frac{-a_2 + \sqrt{a_2^2 - 4a_1a_3}}{2a_1}$$
$$a_1 = \left(\delta u_i^{II}\right)^T \delta u_i^{II}$$
$$a_2 = 2\left(\delta u_i^I\right)^T \delta u_i^{II} + 2\left(\Delta u_{i-1}\right)^T \delta u_i^{II}$$
$$a_3 = 2\left(\Delta u_{i-1}\right)^T \delta u_i^I + \left(\delta u_i^I\right)^T \delta u_i^I + \left(\Delta u_{i-1}\right)^T \Delta u_{i-1} - \Delta l^2$$

Generally, two solutions exist from the above equations. In the case of complex number solutions, linear equivalent solutions of the spherical path method are used. In order to determine which one of the real number solutions is to be used, the angle θ formed by the incremental displacement vectors of the preceding and present steps of iteration is calculated and used as per the equation below.

$$\cos\theta = \frac{\left(\Delta u_{i\text{-}1}\right)^T \delta u_i}{\left\|\Delta u_{i\text{-}1}\right\|\left\|\delta u_i\right\|}$$

If the solutions contain one negative and one positive values, the positive value is selected. If both solutions produce acute angles, the solution close to the linear solution $\Delta\lambda_i = -a_3/a_2$ is used.

P-Delta Analysis

The P-Delta analysis option in MIDAS GEN NX is a type of Geometric nonlinearity, which accounts for secondary structural behavior when axial and transverse loads are simultaneously applied to beam or wall elements. The P-Delta effect is more profound in tall building structures where high vertical axial forces act upon the laterally displaced structures caused by high lateral forces.

Virtually all design codes such as ACI 318 and AISC-LRFD specify that the P-Delta effect be included in structural analyses to account for more realistic member forces.

Refer to “Analysis> P-Delta Analysis Control" of On-line Manual.

The P-Delta analysis feature in MIDAS GEN NX is founded on the concept of the numerical analysis method adopted for Buckling analysis. Linear static analysis is performed first for a given loading condition and then a new geometric stiffness matrix is formulated based on the member forces or stresses obtained from the first analysis. The geometric stiffness matrix is thus repeatedly modified and used to perform subsequent static analyses until the given convergence conditions are satisfied.

As shown in Figure 2.13, static loading conditions are also required to consider the P-Delta effect for dynamic analyses.

The concept of the P-Delta analysis used in MIDAS GEN NX is shown below.

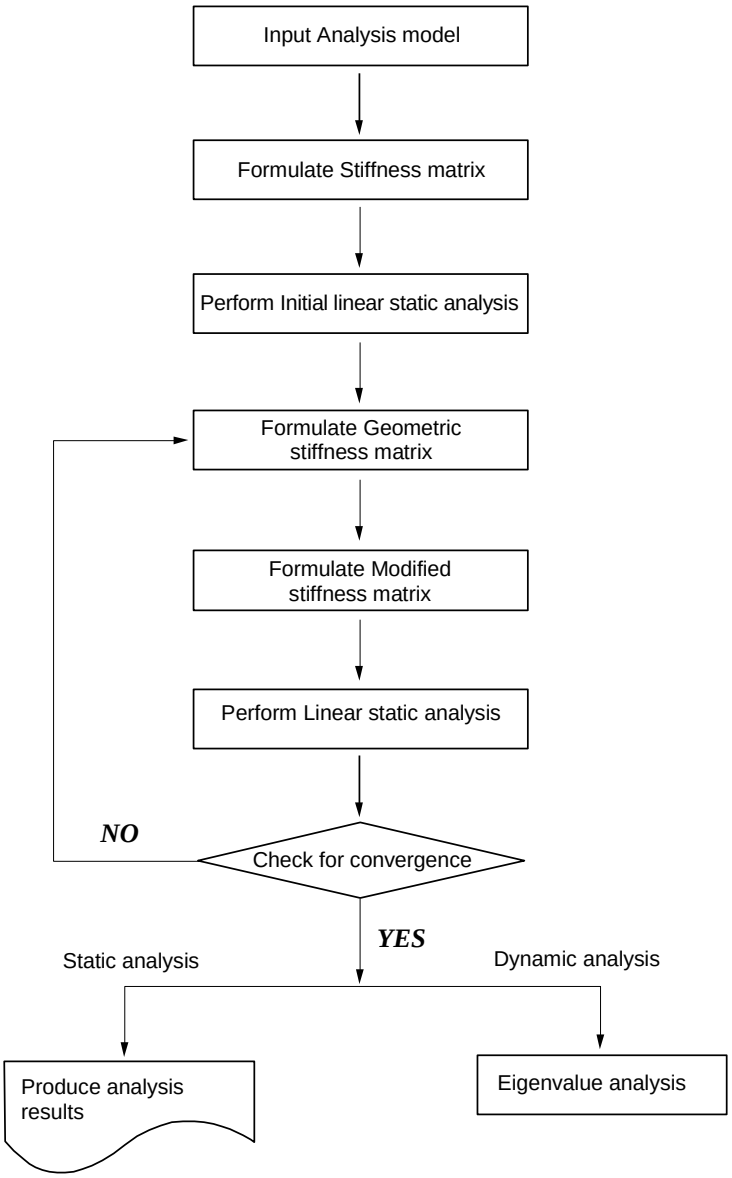

Figure 2.13 Flow chart for P-Delta analysis in MIDAS GEN NX

When a lateral load acts upon a column member thereby resulting in moments and shear forces in the member, an additional tension force reduces the member forces whereas an additional compression force increases the member forces. **Accordingly, tension forces acting on column members subjected to lateral loads increase the stiffness pertaining to lateral behaviors while compression forces have an opposite effect on the column members**.

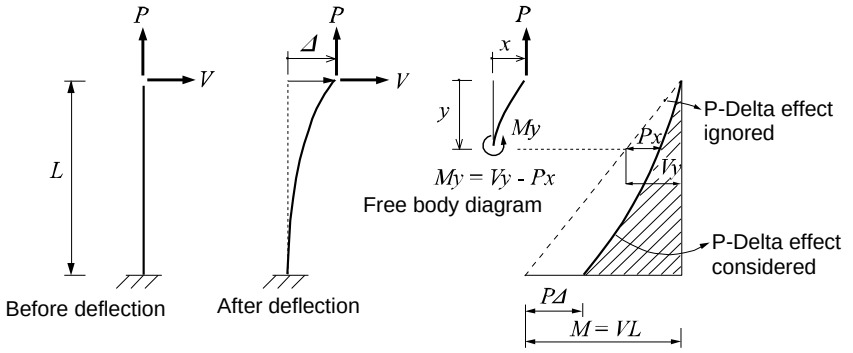

(a) Column subjected to tension and lateral forces simultaneously

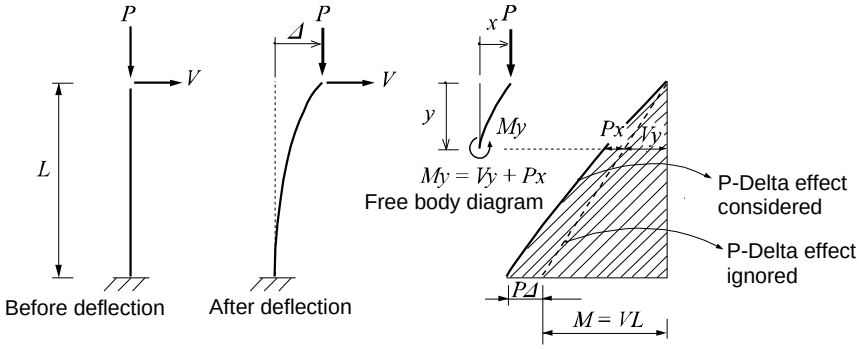

(b) Column subjected to compression and lateral forces simultaneously

Figure 2.14 Column behaviors due to P-Delta effects

If the P-Delta effect is ignored, the column moment due to the lateral load alone varies from *M=0* at the top to *M=VL* at the base. The additional tension and compression forces produce negative and positive P-Delta moments respectively. The effects are tantamount to an increase or decrease in the lateral stiffness of the column member depending on whether or not the additional axial force is tension or compression.

Accordingly, the lateral displacement can be expressed as a function of lateral and axial forces.

$$\Delta = V / K\ ,\ K = K_0 + K_G$$

K_O here represents the intrinsic lateral stiffness of the column and K_G represents the effect of change (increase/decrease) in stiffness due to axial forces. Formulation of geometric stiffness matrices for truss, beam and plate elements can be found in Buckling Analysis.

The P-Delta analysis can be summarized as follows:

1st step analysis

$\Delta_1 = V/K_O$

2nd step analysis

$\Delta_2 = f(P,\Delta_1),\ \Delta = \Delta_1 + \Delta_2$

3rd step analysis

$\Delta_3 = f(P,\Delta_2),\ \Delta = \Delta_1 + \Delta_2 + \Delta_3$

4th step analysis

$\Delta_4 = f(P,\Delta_3),\ \Delta = \Delta_1 + \Delta_2 + \Delta_3 + \Delta_4$

.
.
.

nth step analysis

$\Delta_n = f(P,\Delta_{n-1}),\ \Delta = \Delta_1 + \Delta_2 + \Delta_3 + ... + \Delta_n$

After obtaining Δ_1 from the 1st step analysis, the geometric stiffness matrix due to the axial force is found, which is then added to the initial stiffness matrix to form a new stiffness matrix. This new stiffness matrix is now used to calculate Δ_2 reflecting P-Delta effects, and the convergence conditions are checked. The convergence conditions are defined in "P-Delta Analysis Control", which are Maximum Number of Iteration and Displacement Tolerance. The above steps are repeated until the convergence requirements are satisfied.

Note that the P-Delta analysis feature in MIDAS GEN NX produces very accurate results when lateral displacements are relatively small (within the elastic limit).

The static equilibrium equation for P-Delta analysis used in MIDAS GEN NX can be expressed as

$$[K]\{u\}+[K_G]\{u\}=\{P\}$$

where,

$[K]$: Stiffness Matrix of pre-deformed model

$[K_G]$: Geometric stiffness matrix resulting from member forces and stresses at each step of iteration

$\{P\}$: Static load vector

$\{u\}$: Displacement vector

P-Delta analysis in MIDAS GEN NX premises on the following:

- Geometric stiffness matrices to consider P-Delta effects can be formulated only for truss, beam and wall elements.
- Lateral deflections (bending and shear deformations) of beam elements are considered only for "Large-Stress Effect" due to axial forces.
- P-Delta analysis is valid within the elastic limit.

In general, it is recommended that P-Delta analysis be carried out at the final stage of structural design since it is a time-consuming process in terms of computational time.

Analysis using Nonlinear Elements

Nonlinear analysis in MIDAS GEN NX is applied to a static analysis of a linear structure in which some nonlinear elements are included. The nonlinear elements that can be used in such a case include tension-only truss element, hook element, cable element, compression-only truss element, gap element and tension/compression-only of Elastic Link. The static equilibrium equation of a structural system using such nonlinear elements can be written as

<Eq. 1>

$$[K + K_N]\{U\} = \{P\}$$

K : Stiffness of linear structure
K_N : Stiffness of nonlinear elements

The equilibrium equation containing the nonlinear stiffness, K_N, in <Eq. 1> can be solved by the following two methods:

Refer to "Include Inactive Elements of Analysis>Main Control Data" of On-line Manual.

The first method seeks the solution to the equation by modifying the loading term without changing the stiffness term. The analysis is carried out by the following procedure:

If we apply the stiffness of nonlinear elements at the linear state to both sides of the equation, and move the stiffness of nonlinear elements to the loading term, <Eq. 2> can be derived.

<Eq. 2>

$$[K + K_L]\{U\} = \{P\} + [K_L - K_N]\{U\}$$

K_L : Stiffness of nonlinear elements at the linear state

In <Eq. 2>, the linear stiffness of the structure and the stiffness of nonlinear elements at the linear state always remain unchanged. Therefore, static analysis of a structure containing nonlinear elements can be accomplished by repeatedly modifying the loading term on the right side of the equation without having to repeatedly recompose the global stiffness or decompose the matrix. Not only does this method readily perform nonlinear analysis, but also reducing analysis time is an advantage without the reformation process of stiffness matrices where multiple loading cases exist.

The second method seeks the solution to the equation by iteratively re-assembling the stiffness matrix of the structure without varying the loading term following the procedure below.

A static analysis is performed by initially assuming the stiffness of nonlinear elements in <Eq. 1>. Using the results of the first static analysis, the stiffness of nonlinear elements is obtained, which is then added to the stiffness of the linear structure to form the global stiffness. The new stiffness is then applied to carry out another round of static analysis, and this procedure is repeated until the solution is found. This method renders separate analyses for different loading conditions as the stiffness matrices for nonlinear elements vary with the loading conditions.

The above two methods result in different levels of convergence depending on the types of structures. The first method is generally effective in analyzing a structure that contains tension-only bracings, which are quite often encountered in building structures. However, the second method can be effective for analyzing a structure with soil boundary conditions containing compression-only elements.

Stiffness of Nonlinear Elements (K_N)

MIDAS GEN NX calculates the stiffness of nonlinear elements by using displacements and member forces resulting from the analysis. The nonlinear stiffness of Truss, Hook and Gap types is determined on the basis of displacements at both ends and the hook or gap distance. The nonlinear stiffness of cable elements is obtained from the resulting tension forces.

The nonlinear stiffness of tension/compression–only elements such as Truss, Hook and Gap types can be determined by <Eq. 3>. Whereas, stiffness changes for tension-only cable elements need to be considered according to the changes of tension forces in the members. The nonlinear stiffness is calculated by determining the effective stiffness, which is expressed in <Eq. 4>.

<Eq. 3>

$$K_N = f(D-d)$$

D : Initial distance (Hook or Gap distance)
d : Change in member length resulting from the analysis

<Eq. 4>

$$K_{eff} = \frac{1}{1/K_{sag} + 1/K_{elastic}} = \frac{EA}{L\left(1 + \frac{W^2 L^2 EA}{12T^3}\right)}$$

$$K_{sag} = \frac{12T^3}{W^2 L^3} \ , \ K_{elastic} = \frac{EA}{L}$$

W : Weight density per unit length of cable

T : Tension force in cable

Since the nonlinear elements used in MIDAS GEN NX do not reflect the large-displacement effect and material nonlinearity, some limitations for applications are noted below.

1. Material nonlinearity is not considered.
2. Nonlinearity for large displacements is not considered.
3. Instability due to loadings may occur in a structure, which is solely composed of nonlinear elements. The use of nodes composed of only nonlinear elements are not allowed.
4. Element stiffness changes with changing displacements and member forces due to applied loadings. Therefore, linear superposition of the results from individual loading cases are prohibited.
5. In the case of a dynamic analysis for a structure, which includes nonlinear elements, the stiffness at the linear state is utilized.

The analysis procedure for using nonlinear elements is as follows:

1. Using the linear stiffness of the structure and the stiffness of nonlinear elements at the linear state, formulate the global stiffness matrix and load vector.
2. Using the global stiffness matrix and load vector, perform a static analysis to obtain displacements and member forces.
3. Re-formulate the global stiffness matrix and load vector.
4. If the method 1 is used, where the analysis is performed without changing the stiffness term while varying the loading term, the nonlinear stiffness is computed by using the displacements and member forces obtained in Step 2, which is then used to reformulate the loading term. If the method 2 is used, where the analysis is performed with changing the stiffness term, the

stiffness of nonlinear elements is computed first by using the resulting displacements and member forces, which is then used to determine the global stiffness matrix.

5. Repeat steps 2 and 3 until the convergence requirements are satisfied.

Pushover Analysis (Nonlinear Static Analysis)

Overview

Pushover analysis is one of the performance–based design methods, recently attracting practicing structural engineers engaged in the field of seismic design. The objective of a performance-based design is achieved after the user and the designer collectively select a target performance for the structure in question. The engineer carries out the conventional design and subsequently performs a pushover (elasto-plastic) analysis to evaluate if the selected performance objective has been met.

When equivalent static design loads are computed in a typical seismic design, the method illustrated in Figure 2.15 is generally used. The engineer applies appropriate response force modification factors (R) to compute the design loads and ensures that the structure is capable of resisting the design loads. The significance of using the R factors here is that the structure exhibits inelastic behaviors during an earthquake. That is, the structure is inflicted with material damage due to the earthquake loads. Depending on the energy absorption capability of the structure, the response force modification factors vary. The design method described herein is relative to loads and as such it is termed as "force-based design method". However, a simple comparison of the strengths cannot predict the true behavior of a structure. As a result, it is highly likely that a structure may be designed without a clear knowledge of the structural performance characteristics.

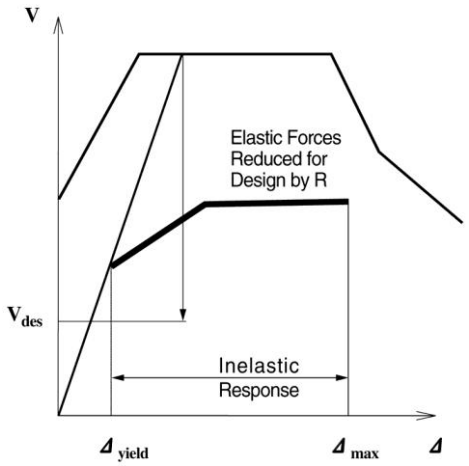

Figure 2.15 Calculation of earthquake loads as per force-based design method

Where a performance-based design method is adopted, the project owner and the engineer pre-select a target performance. This reflects the intent of the project team to allow an appropriate level of structural damage or select the level of energy absorption capability due to anticipated seismic loads in a given circumstance. In order to achieve the objective, we need to be able to predict the deformation performance of the structure to the point of ultimate failure. The eigenvalues change with the level of energy absorption capability. If the performance criteria are evaluated on the basis of the structure's displacements, it is termed as "displacement-based design method".

Where pushover analysis is carried out as one of the means of evaluating the structure's deformability, a load-displacement spectrum is created as illustrated in Figure 2.16. A demand spectrum is also constructed depending on the level of energy absorption capability of the structure. The intersection (performance point) of the two curves is thus obtained. If the point is within the range of the target performance, the acceptance criteria are considered to have been satisfied. That is, the performance point is evaluated against the acceptance criteria or vice versa.

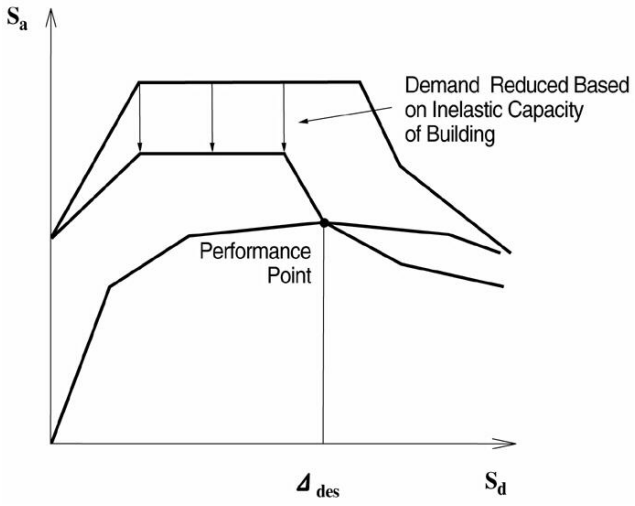

Figure 2.16 Seismic design by performance-based design method

Analysis Method

The project owner and the engineer determine the target performance of a structure at least after having met the requirements of the building and design codes. Several analysis methods exist in assessing the structural performance, namely, Linear Static, Linear Dynamic, Nonlinear Static and Nonlinear Dynamic procedures. MIDAS GEN NX employs pushover analysis, which is a nonlinear static analysis method, generally used for the structures whose dynamic characteristics of higher modes are not predominant. Pushover analysis can incorporate material and geometric nonlinearity. MIDAS GEN NX adopts and applies simplified elements to reflect the nonlinear material characteristics, which are based on "Element model" (Stress-Resultant stress approach) using the load-displacement relationship of the member sections.

Pushover analysis creates a capacity spectrum expressed in terms of a lateral load-displacement relationship by incrementally increasing static forces to the point of the ultimate performance. The capacity spectrum is then compared with the demand spectrum, which is expressed in the form of a response spectrum to seismic loads, to examine if the structure is capable of achieving the target performance. Accordingly, pushover analysis is often referred to as the second stage analysis, which is subsequently carried out after the initial structural analysis and design.

Pushover analysis can provide the following advantages:

- It allows us to evaluate overall structural behaviors and performance characteristics.
- It enables us to investigate the sequential formation of plastic hinges in the individual structural elements constituting the entire structure.
- When a structure is to be strengthened through a rehabilitation process, it allows us to selectively reinforce only the required members, thereby maximizing the cost efficiency.

Evaluating analysis results premises on whether or not the target performance has been achieved. MIDAS GEN NX follows the proposed procedures outlined in FEMA-273 and ATC-40 to help the engineer evaluate the target performance of the structure as well as individual members.

Element Types used in MIDAS GEN NX

The types of elements that MIDAS GEN NX uses for pushover analysis are 2D beam element, 3D beam-column element, 3D wall element and truss element. The characteristics of each element are noted in the subsequent sections.

- **2D Beam element & 3D Beam-column element**
  Nodal forces and displacements can identically represent the beam element and beam-column element as shown in Figure 2.17.

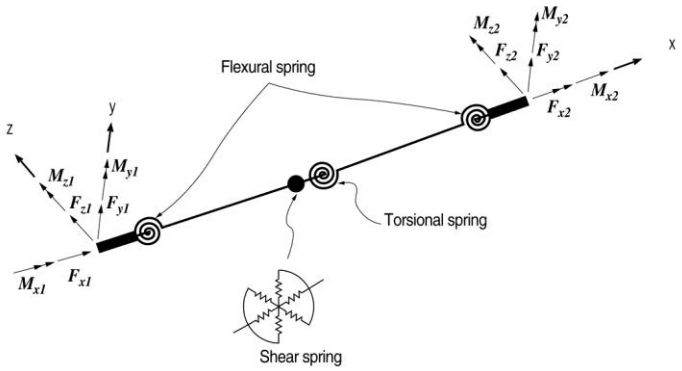

Figure 2.17 Nodal forces and Displacements for 2D Beam element and 3D Beam-column element

The loads and displacements for a beam or beam-column element are expressed as below in order to reflect the effects of biaxial moments in a 3-dimensional space. The expressions can be applied to the beam element provided that there is no presence of axial force.

$$\{P\}^T = \{F_{x1}, M_{x1}, F_{y1}, M_{y1}, F_{z1}, M_{z1}, F_{x2}, M_{x2}, F_{y2}, M_{y2}, F_{z2}, M_{z2}\} \quad (1\text{-a})$$

$$\{u\}^T = \{u_{x1}, \theta_{x1}, v_{y1}, \theta_{y1}, v_{z1}, \theta_{z1}, u_{x2}, \theta_{z2}, v_{y2}, \theta_{y2}, v_{z2}, \theta_{z2}\} \quad (1\text{-b})$$

- **3D Wall element**

  A vertical line element located in the middle connecting the top and bottom rigid beams constitute a wall element as illustrated in Figure 2.18. The middle line element identically behaves like a 3D beam-column element. The top and bottom rigid beams act as rigid bodies in the x-y plane. The moments about the z-axis represent the in-plane bending behavior. The out of plane bending behavior is not considered in the wall element.

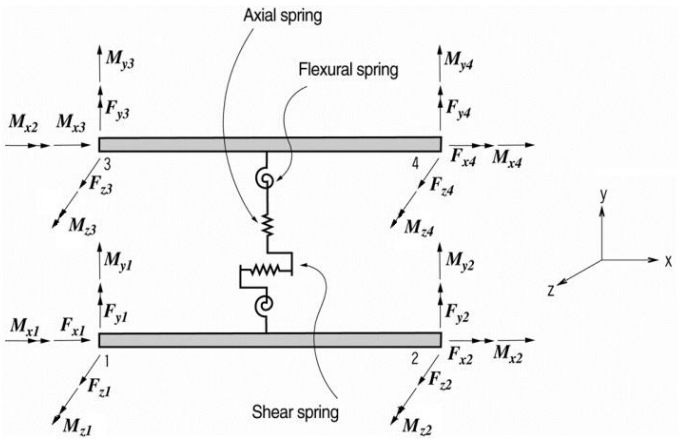

Figure 2.18 Nodal forces and displacements for Wall element

- **Truss element**

  Truss element uses a spring capable of resisting only compression and tension forces acting in the axial (x-dir.) direction.

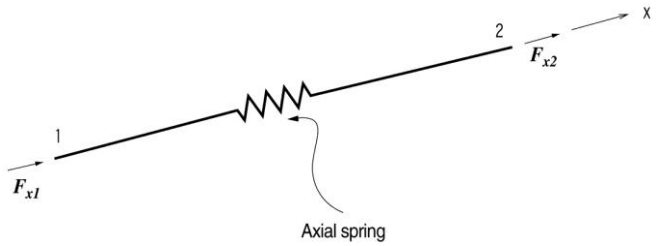

Figure 2.19 Nodal forces for Truss element

Characteristics of Nonlinear Spring

The springs shown in each element do not represent actual spring elements. They are simply noted to convey the concept of the analysis method. This means that plastic deformations occur and are concentrated at the locations of the springs. The nonlinear spring retains the following characteristics:

- **Beam element relates Load-Displacement, Axial force-1 Directional moment-Rotational angle, Shear force-Shear deformation and Torsion-Torsional deformation.**
- **Column and Wall elements relate Load-Displacement, Axial force -2 Directional moments-Rotational angles, Shear force-Shear deformation and Torsion-Torsional deformation.**
- **Truss element relates Load-Displacement**.

The element deformations are expressed in terms of equations by the following methods:

- **Bending deformation spring**

  The sum of the following three terms define the spring deformation angle at a node.

$$\theta=\theta^e+\theta^p+\theta^s \tag{2}$$

  where, θ^e, θ^p and θ^s represent the elastic bending deformation angle, plastic bending deformation angle and the bending deformation angle due to shear respectively. The plastic deformations due to bending moments are assumed to occur and concentrate within the shaded αL zones as shown in Figure 2.20. Accordingly, the flexibility matrix including the plastic deformations and shear deformations can be formulated by the following expressions:

$$f_{11}=\frac{L}{3EI_0}+\frac{\alpha L}{3}\left[\left(3-3\alpha+\alpha^2\right)\left(\frac{1}{EI_1}-\frac{1}{EI_0}\right)+\alpha^2\left(\frac{1}{EI_2}-\frac{1}{EI_0}\right)\right]+\frac{1}{GAL} \tag{3-a}$$

$$f_{12}=f_{21}=-\frac{L}{6EI_0}+\frac{\alpha^2 L}{6}\left(3-2\alpha\right)\left[\left(\frac{1}{EI_1}-\frac{1}{EI_0}\right)+\left(\frac{1}{EI_2}-\frac{1}{EI_0}\right)\right]+\frac{1}{GAL} \tag{3-b}$$

$$f_{22}=\frac{L}{3EI_0}+\frac{\alpha L}{3}\left[\alpha^2\left(\frac{1}{EI_1}-\frac{1}{EI_0}\right)+\left(3-3\alpha+\alpha^2\right)\left(\frac{1}{EI_2}-\frac{1}{EI_0}\right)\right]+\frac{1}{GAL} \tag{3-c}$$

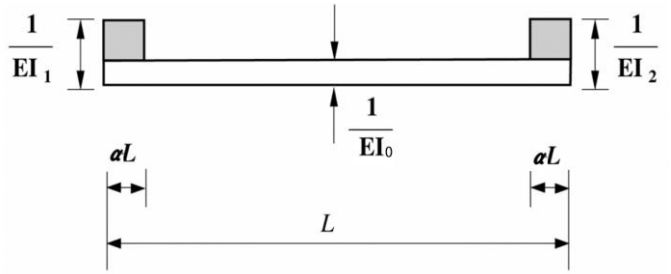

Figure 2.20 Distribution of assumed flexural stiffness

The load-displacement relationship for springs can be arranged as the flexibility matrix equations (4) & (5) below.

$$\{\theta\} = [f]\{M\} \tag{4}$$

where, $[f] = [f]^e + [f]^p + [f]^s$ (5)

The Equation (5) separately presents the flexibility matrices for elastic bending deformation angle, plastic bending deformation angle and the bending deformation angle due to shear as illustrated in Figure 2.21.

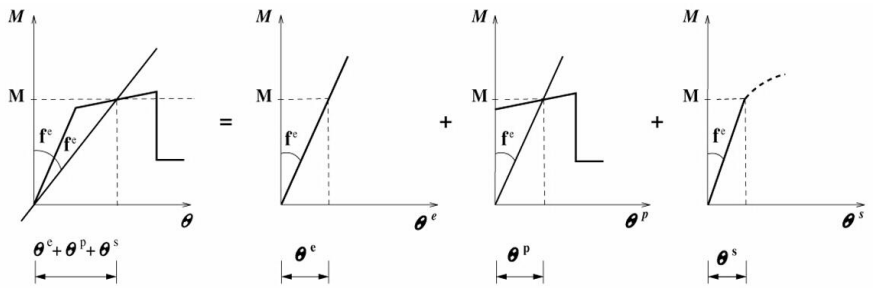

Figure 2.21 Moment-Deformation angle Relationship

- **Axial deformation, Torsional deformation and Shear deformation springs**
  MIDAS GEN NX assumes that axial force, torsional moment and shear force remain constant in a member and that the plastic hinges form at the center of the member for pushover analysis. Thus, their force-deformation relationships can be also expressed similar to the case of bending deformation.

- **Biaxial bending spring**
  In the case of an element subjected to axial force and biaxial moments, the yield moments for the given axial force are separately obtained and then the relationship below is applied.

$$\left(\frac{M_{nx}}{M_{nox}}\right)^{\alpha} + \left(\frac{M_{ny}}{M_{noy}}\right)^{\alpha} = 1.0 \tag{6}$$

  The Equation (6) applies to both reinforced concrete and structural steel members.

Analysis method

Structural stiffness changes as a result of formation of hinges. Lateral displacement increases with reduced stiffness. The loading incrementally increases and the load-displacement relationship is established upon completion of a series of analyses. MIDAS GEN NX uses the following analysis methods:

- **Use of Secant stiffness matrix**
- **Displacement control method**
- **P-Delta and Large deformation effects considered**

The use of the Secant stiffness matrix and Displacement control method provides the advantage of obtaining stable analysis values near the maximum load.

Applied loads

Applied loads must be of lateral forces that can reflect the inertia forces at each floor. Accordingly, it is recommended that at least 2 different types of lateral forces be applied for pushover analysis. MIDAS GEN NX permits 3 types of lateral load distribution patterns. They are the Static load case pattern, Mode shape pattern distribution and Uniform acceleration proportional to the masses at each floor. If a static load case pattern is used for load distribution, the user becomes able to distribute the load in any specific pattern as required.

Capacity spectrum and Demand spectrum

In order to evaluate whether or not the target performance is satisfied, the capacity spectrum and demand spectrum are used. Pushover analysis produces the load-displacement relationship whereas the response spectrum is expressed in terms of accelerations vs. periods. To compare the two spectrums, we need to transform them into the ADRS format, which stands for Acceleration-Displacement Response Spectrum.

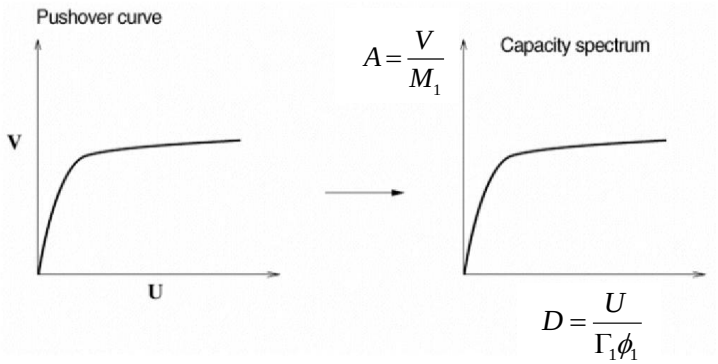

Figure 2.22 Transformation of Load-Displacement into Acceleration-Displacement Spectrum

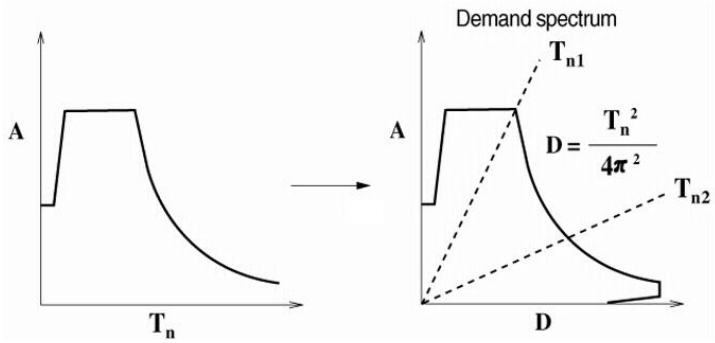

Figure 2.23 Transformation of Acceleration-Period into Acceleration-Displacement Spectrum

The load-displacement relationship is transformed into the acceleration–displacement relationship as illustrated in Figure 2.22 by the following expressions:

$$A = \frac{V}{M_1} \tag{7}$$

$$D = \frac{U}{\Gamma_1 \phi_1} \tag{8}$$

where, the subscript, 1 represents the first mode.

$$\Gamma_1 = \frac{\sum_{j=1}^{N} m_j \phi_{j1}}{\sum_{j=1}^{N} m_j \phi^2_{j1}} \tag{9}$$

$$M_1 = \frac{(\sum_{j=1}^{N} m_j \phi_{j1})^2}{\sum_{j=1}^{N} m_j \phi^2_{j1}} \tag{10}$$

And the response spectrum is transformed as shown in Figure 2.23, using Equation (11).

$$D = \frac{T_n^2}{4\pi^2} A \tag{11}$$

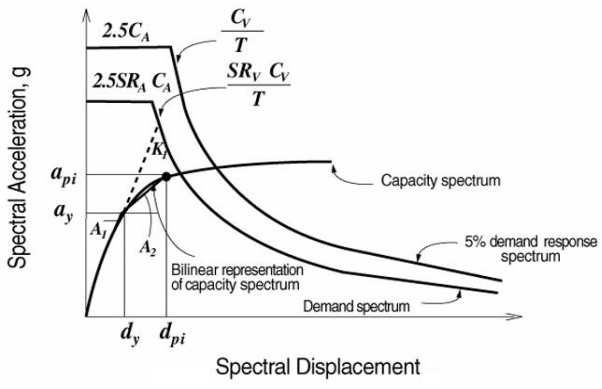

Figure 2.24 Calculation of Demand Spectrum

Calculation of Performance Point

The intersection of the capacity and demand spectrums represents the performance point. When a structure is subjected to a big force such as an earthquake, it undergoes a process of plastic deformations. The magnitude of dissipated energy depends on the extent of plastic deformation or ductility. The magnitude of the demand spectrum, in turn, reduces relative to the increase in magnitude of energy dissipation. The performance point is thus obtained through a process of repeated calculations as illustrated in Figure 2.24. MIDAS GEN NX adopts the Capacity Spectrum Method A (See Figure 2.25) as defined by ATC-40 to find the performance point.

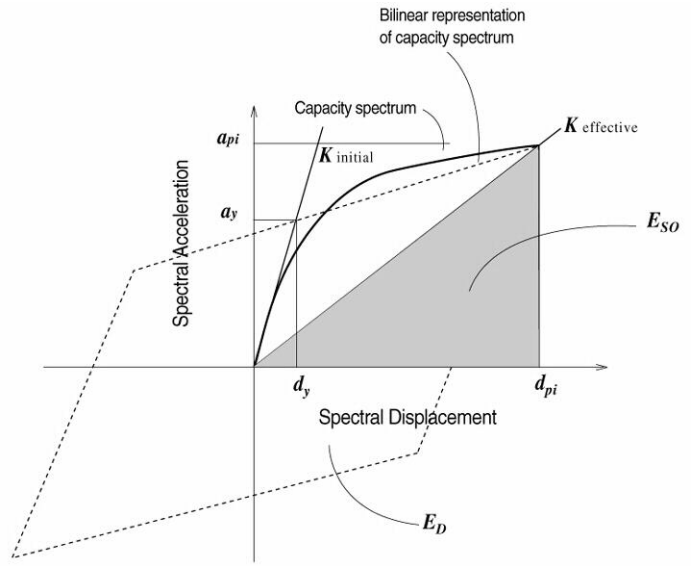

Figure 2.25 Capacity Spectrum Method A of ATC-40

Evaluation of Performance

Once the displacement of the total structure is confirmed to exist within the range of the target performance, the process of evaluating the performance of individual members takes place. MIDAS GEN NX adopts a process similar to the recommended procedures described in FEMA-273 and ATC-40 to evaluate the member performance. These reports classify the target performance into three stages as shown in Figure 2.26. Where the structural performance falls short of the target performance, the engineer improves the strength or ductility of the relevant members.

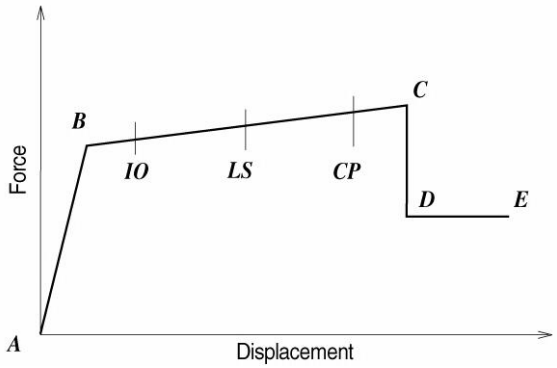

IO = Immediate Occupancy Level
LS = Life Safety Level
CP = Collapse Prevention Level

Figure 2.26 Performance evaluation of members

Procedure for Pushover analysis

1. Complete static analysis and member design
   In order to review the inherent capacity of a structure against seismic loads, first complete the static analysis followed by member design.

2. Input control data for Pushover analysis
   Recall the Design > Pushover Analysis Control dialog box, and specify the maximum number of increment steps, maximum number of (internal) iterations per each increment step and convergence tolerance.

3. Input Pushover Load Case
   Recall the ***Design > Pushover Load Cases*** dialog box, and specify the loading at the initial state prior to the pushover analysis and the Pushover load cases. The initial load may be the dead load on the structure. The pushover load condition may be in the form of Static Load Case, Uniform Acceleration and Mode Shape. Each load pattern can be combined with the initial load.

4. Define Hinge Data
   Recall the ***Design > Define Hinge Data Type*** dialog box, and define the Hinge Data representing the material nonlinearity. You may select the Hinge Types provided in MIDAS GEN NX or the User Type.

5. Assign Hinge Data to the members
   Recall the ***Design > Assign Pushover Hinges*** dialog box, and assign the defined Hinge Data to individual members. In general, moment hinges for beams, axial/moment hinges for columns and walls and axial hinges for bracings are assigned.

6. Perform Pushover analysis
   Carry out the pushover analysis in ***Design > Perform Pushover Analysis***.

7. Check the analysis results
   Upon completing the analysis successfully, click ***Design > Pushover Curve*** to produce the resulting pushover curves. The performance levels of the structure are checked against various design spectrums. We can also check the deformed shapes at each step and the process of hinge formation. The Animate function may be used to animate the process of hinge formation.

Boundary Nonlinear Time History Analysis

Overview

Boundary nonlinear time history analysis, being one of nonlinear time history analyses, can be applied to a structure, which has limited nonlinearity. The nonlinearity of the structure is modeled through General Link of Force Type, and the remainder of the structure is modeled linear elastically. Out of convenience, the former is referred to as a nonlinear system, and the latter is referred to as a linear system. Boundary nonlinear time history analysis is analyzed by converting the member forces of the nonlinear system into loads acting in the linear system. Because a linear system is analyzed through modal superposition, this approach has an advantage of fast analysis speed compared to the method of direct integration, which solves equilibrium equations for the entire structure at every time step. The equation of motion for a structure, which contains General Link elements of Force Type, is as follows:

$$M\ddot{u}(t) + C\dot{u}(t) + (Ks + KN)u(t) = B_p p(t) + B_N(f_L(t) - f_N(t))$$

where,

M : Mass matrix
C : Damping matrix
K_s : Elastic stiffness without General Link elements of Force Type
K_N : Effective stiffness of General Link elements of Force Type
B_p, B_N : Transformation matrices
$u(t), \dot{u}(t), \ddot{u}(t)$: Nodal displacement, velocity & acceleration
$p(t)$: Dynamic load
$f_L(t)$: Internal forces due to the effective stiffness of nonlinear components contained in General Link elements of Force Type
$f_N(t)$: True internal forces of nonlinear components contained in General Link elements of Force Type

The term $f_L(t)$ on the right hand side is cancelled by the nodal forces produced by KN on the left hand side, which correspond to the nonlinear components of General Link of Force Type. Only the true internal forces of the nonlinear components $f_N(t)$ will affect the dynamic behavior. The reason for using the effective stiffness matrix K_N is that the stiffness matrix of K_s alone can become unstable depending on the connection locations of the general link elements of the force type.

Mode shapes and natural frequencies on the basis of mass and stiffness matrices can be calculated through Eigenvalue Analysis or Ritz Vector Analysis. The damping is considered by modal damping ratios.
Using the orthogonality of the modes, the above equation is transformed into the equation of Modal Coordinates as follows:

$$\ddot{q}_i(t) + 2\xi_i\omega_i\dot{q}_i(t) + \omega_i^2 q(t) = \frac{\phi_i^T B_p p(t)}{\phi_i^T M \phi_i} + \frac{\phi_i^T B_N f_L(t)}{\phi_i^T M \phi_i} + \frac{\phi_i^T B_N f_N(t)}{\phi_i^T M \phi_i}$$

where,

ϕ_i : Mode shape vector of the i-th mode

ξ_i : Damping ratio of the i-th mode

ω_i : Natural frequency of the i-th mode

$q(t), \dot{q}(t), \ddot{q}(t)$: Generalized displacement, velocity & acceleration at the i-th mode

The $f_N(t)$ and $f_L(t)$ on the right hand side are determined by the true deformations and the rates of changes in deformations in the local coordinate systems of the corresponding general link elements of the force type. However, the true deformations of the elements contain the components of all the modes without being specific to any particular modes. The above modal coordinate kinetic equation thus cannot be said to be independent by individual modes. In order to fully take the advantage of modal analysis, we assume $f_N(t)$ and $f_L(t)$ at each analysis time step so that it becomes a kinetic equation in the independent modal coordinate system.

First, using the analysis results of the immediately preceding step, the generalized modal displacement and velocity of the present step are assumed; based on these, $f_N(t)$ and $f_L(t)$ for the present step are calculated. Again from these, the generalized modal displacement and velocity of the present stage are calculated. And the deformations and the rates of changes in deformations of the general link elements of the force type are calculated through a combination process. The entire calculation process is repeated until the following convergence errors fall within the permitted tolerance.

$$\varepsilon_q = \max_i \left\{ \frac{q_i^{(j-1)}(n\Delta t) - q_i^{(j)}(n\Delta t)}{q_i^{(j+1)}(n\Delta t)} \right\}$$

$$\varepsilon_{\dot{q}} = \max_i \left\{ \frac{\dot{q}_i^{(j-1)}(n\Delta t) - \dot{q}_i^{(j)}(n\Delta t)}{\dot{q}_i^{(j+1)}(n\Delta t)} \right\}$$

$$\varepsilon_{f_M} = \max_i \left\{ \frac{f_{M,i}^{(j-1)}(n\Delta t) - f_{M,i}^{(j)}(n\Delta t)}{f_{M,i}^{(j+1)}(n\Delta t)} \right\}$$

where,

$$f_{M,i}^{(j-1)}(n\Delta t) = \frac{\phi_i^T B_N f_N^{(j)}(n\Delta t)}{\phi_i^T M \phi_i}$$

Δt : Magnitude of time step
n : Time step
j : Repeated calculation step
i : Mode number

The above process is repeated for each analysis time step. The user directly specifies the maximum number of repetitions and the convergence tolerance in Time History Load Cases. If convergence is not reached, the program automatically subdivides the analysis time interval Δt and begins reanalyzing.

The nonlinear properties of the general link elements of the force type are expressed in terms of differential equations. Solutions to the numerical analysis of the differential equations are required to calculate and correct the internal forces corresponding to nonlinear components in the process of each repetition. MIDAS programs use the Runge-Kutta Fehlberg numerical analysis method, which is widely used for that purpose and known to provide analysis speed and accuracy.

■ Cautions for Eigenvalue Analysis

The boundary nonlinear time history analysis in MIDAS is based on modal analysis, and as such a sufficient number of modes are required to represent the structural response. A sufficient number of modes are especially required to represent the deformations of general link elements of the force type.

A representative example may be the case of the seismic response analysis of a friction pendulum system isolator. In this type of isolator, the internal force of the element's axial direction component is an important factor for determining

the behavior of the shear direction components. Accordingly, unlike other typical seismic response analyses, the vertical modes play an important role. The number of modes must be sufficiently enough so that the sum of the modal masses in the vertical direction is close to the total mass.

When the eigenvalue analysis is used to achieve such objective, a very large number of modes may be required. This may lead to a very long analysis time. If Ritz Vector Analysis is used, the mode shapes and natural frequencies can be found reflecting the distribution of dynamic loads with respect to each degree of freedom. This allows us to include the effects of higher modes with a relatively small number of modes.

For example, in the case of a friction pendulum system isolator, we can select the ground acceleration in the Z-direction and static Load Case Names related to the self weight of the structure in the input dialog box of Ritz Vector analysis. Natural frequencies and mode shapes related mainly to the vertical movement can be obtained. In general, the Ritz Vector analysis is known to provide more accurate analysis results with a fewer number of modes compared to Eigenvalue analysis.

Combining Static and Dynamic Loads

Unlike linear time history analysis, the principle of superposition cannot be applied to nonlinear time history analysis. The analysis results of static loads and dynamic loads cannot be simply combined as if they could occur concurrently. In order to account for the effects of static and dynamic loads simultaneously, the static loads must be applied in the form of dynamic loads, and then a boundary nonlinear time history analysis is carried out. MIDAS GEN NX provides the Time Varying Static Loads functionality, which enables us to input static loads in the form of dynamic loads.

First, we enter the Ramp function of Normal Data Type in Dynamic Forcing Function. Next, we can enter the Static Load Cases pertaining to the vertical direction and previously defined Function Names in Time Varying Static Load. The shape of the Ramp function should be such that the converted static loading is completely loaded and the resulting vibration is sufficiently dampened before the Arrival Time of the ground acceleration. In order to reduce the time that takes to dampen the vibration resulting from the loading of the converted static loads, we may select the option of the 99% initial damping ratio in Time History Load Case. In addition, the static loads are maintained while the ground acceleration is acting.

Effective Stiffness

In a boundary nonlinear time history analysis, the entire structure is divided into linear and nonlinear systems. Nonlinear member forces stemming from the nonlinear system are converted into external dynamic loads acting on the linear system for the analysis. At this point, the linear system alone may become unstable depending on the locations of the general link elements of the force type comprising the nonlinear system. Therefore, modal analysis is carried out after stabilizing the structure using the effective stiffness.

If the structure becomes unstable after removing the general link elements of the force type, appropriate effective stiffness need to be entered to induce the natural frequencies and mode shapes, which closely represent the true nonlinear behavior. The appropriate effective stiffness in this case is generally greater than 0, and a smaller than or equal to the value of the initial stiffness of nonlinear properties is used. The initial stiffness corresponds to the dynamic properties of different element types that will be covered in the latter section; namely, kb for Viscoelastic Damper, k for Gap, Hook and Hysteretic System, and ky & kz for Lead Rubber Bearing Isolator and Friction Pendulum System. The initial stiffness is entered as effective stiffness to carry out linear static analysis or linear dynamic analysis and obtain the response prior to enacting nonlinear behavior. In order to approximate linear dynamic analysis, appropriate Secant Stiffness is entered as effective stiffness on the basis of the anticipated maximum deformation. This is an attempt to closely resemble the behavior of nonlinear link elements in a nonlinear analysis. If the analysis results do not converge, we may adjust the effective stiffness for convergence.

Dynamic Properties of Nonlinear Link Elements of Force Type

MIDAS provides 6 nonlinear boundary elements for boundary nonlinear time history analysis: Viscoelastic Damper, Gap, Hook, Hysteretic System, Lead Rubber Bearing Isolator and Friction Pendulum System Isolator. Their dynamic properties are outlined below.

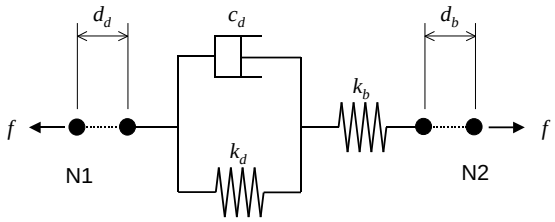

(a) Viscoelastic Damper

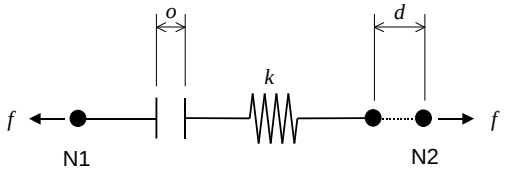

(b) Gap

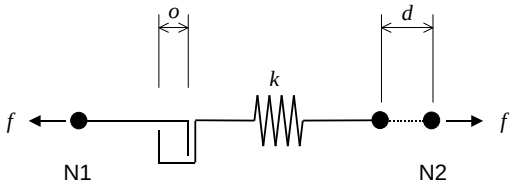

(c) Hook

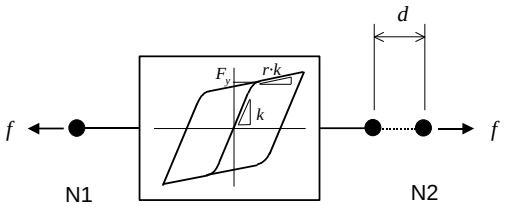

(d) Shear Spring for Hysteretic System & Lead Rubber Bearing isolator

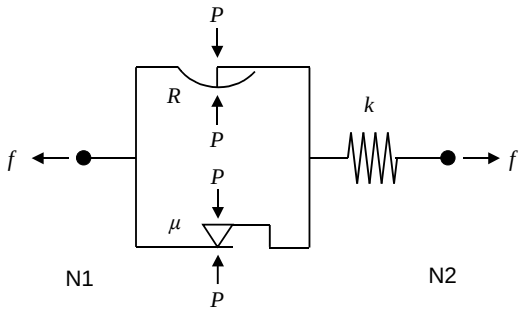

(e) Shear Spring for Friction Pendulum System Isolator

Figure 2.27 Conceptual diagrams of springs for Nonlinear Link Elements

- **Viscoelastic Damper**

Viscoelastic Damper simultaneously retains viscosity, which induces a force proportional to the speed of deformation; and elasticity, which induces a force proportional to deformation. The device increases the damping capability of the structure and thereby reduces the dynamic response due to seismic, wind, etc. The purpose of using the device is to improve structural safety and serviceability.

The representative mathematical models for viscoelastic damper are Maxwell model, which connects a linear spring and a viscosity damper in series; and Kelvin model, which connects both running parallel to each other. MIDAS GEN NX permits modeling the stiffness of the link element using the viscosity damper and the springs of the two models through entering appropriate variables.

The concept of the viscoelastic damper is illustrated in Fig. 2.27 (a). It takes the form of the Kelvin model of a linear spring and a viscosity damper connected in parallel in addition to a bracing with a linear stiffness connecting two nodes. If a connecting member is not present, or if the stiffness of the connecting member is substantially greater than that of the damping device, the connecting member may be defined as a rigid body.

The force-deformation relationship of the element is as follows:

$$f = k_d d_d + c_d sign\left(\dot{d}_d\right)\left|\dot{d}_d\right|^s = k_b d_b$$

$$d = d_d + d_b$$

where,

k_d : Stiffness of viscoelastic damper

c_d : Damping coefficient of viscoelastic damper

k_b : Stiffness of connecting member

s : Exponent defining the nonlinear viscosity damping property of the viscoelastic damper

d : Deformation of element between two nodes

d_d : Deformation of viscoelastic damper

d_b : Deformation of connecting member

sign (.): Sign function

From the above equations, we can model linear viscosity damping linearly proportional to the rate of change in deformation as well as nonlinear viscosity damping exponentially proportional to the rate of change in deformation.

If we wish to model viscoelastic damper with the Maxwell model, we simply enter 0 for kd and specify the stiffness kb for the connecting member only.

- **Gap**

Similar to other boundary elements, Gap consists of 6 springs. The deformations of the node N2 relative to the node N1 for all 6 degrees of freedom in the element coordinate system can be represented. If the absolute values of the negative relative deformations become greater than the initial gaps in the springs, the stiffnesses of the corresponding springs will be activated. The spring in the axial direction only may be used to represent the compression-only element, which is used to model contact problems.

All the 6 springs are independent from one another and retain the following force-deformation relationship:

$$f = \begin{cases} k(d+o) & \text{if } d+o<0 \\ 0 & \text{otherwise} \end{cases}$$

where,

k : Stiffness of gap spring
o : Initial gap
d : Deformation of spring in the element coordinate system

- **Hook**

Similar to other boundary elements, Hook consists of 6 springs. The deformations of the node N2 relative to the node N1 for all 6 degrees of freedom in the element coordinate system can be represented. If the absolute values of the positive relative deformations become greater than the initial slippage distances in the springs, the stiffnesses of the corresponding springs will be activated. The spring in the axial direction only may be used to represent the tension-only element, which is used to model such components as wind bracings, hook elements, etc.

All the 6 springs are independent from one another and retain the following force-deformation relationship:

$$f = \begin{cases} k(d-o) & \text{if } d-o>0 \\ 0 & \text{otherwise} \end{cases}$$

where,

k : Stiffness of hook spring
o : Initial slippage distance
d : Deformation of spring in the element coordinate system

- **Hysteretic System**

Hysteretic system consists of 6 independent springs having the properties of Uniaxial Plasticity. The system is used to model Energy Dissipation Device through hysteretic behavior. Classically, Metallic Yield Damper can be modeled, which is used to protect the primary structure by plastically deforming ahead of adjacent members. The metallic yield damper is relatively stiffer than the primary structure but has lower yield strength.

The force-deformation relationship of Hysteretic System is as follows:

$$f = r \cdot k \cdot d + (1-r) \cdot F_y \cdot z$$

where,

k : Initial elastic spring stiffness
F_y : Yield strength
r : Ratio of post-yield stiffness to elastic stiffness
d : Deformation between two nodes of spring
z : Internal variable for hysteretic behavior

z is an internal hysteretic variable, whose absolute value ranges from 0 to 1. The dynamic behavior of the variable z was proposed by Wen (1976) and defined by the following differential equation:

$$\dot{z} = \frac{k}{F_y}\left[1-|z|^s\left\{\alpha\, sign\left(\dot{d}z\right)+\beta\right\}\right]\dot{d}$$

where,

α , β : Parameters determining the shape of hysteretic curve
s : Parameter determining the magnitude of yield strength transition region
$\dot{d}$: Rate of change in deformation between the spring's two nodes
sign (.): Sign function

α and β are the parameters determining the post-yield behavior. $\alpha+\beta$ >0 signifies Softening System, and $\alpha+\beta$<0 signifies Hardening System. The energy dissipation due to hysteretic behavior increases with the increase in

the closed area confined by the hysteretic curve. In the case of Softening System, it increases with the decrease in the value of (β-α). The change of hysteretic behavior due to the variation of α and β is illustrated in Figure 2.28.

s is an exponent determining the sharpness of the hysteretic curve in the transition region between elastic deformation and plastic deformation, i.e. in the region of yield strength. The larger the value, the more distinct the point of yield strength becomes and the closer is to the ideal Bi-linear Elasto-plastic System. The change of the transition region due to s is illustrated in Figure 2.29.

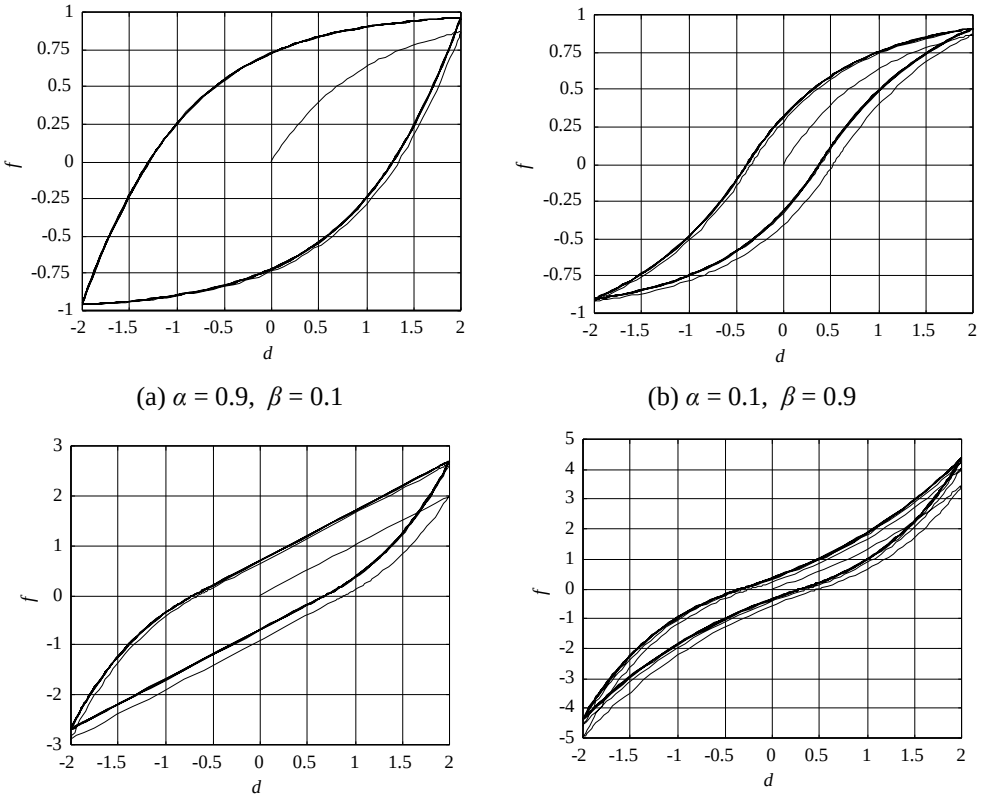

(a) α = 0.9, β = 0.1

(b) α = 0.1, β = 0.9

(c) α = 0.5, β = -0.5

(d) α = 0.25, β = -0.75

Figure 2.28 Force-Deformation relationship due to hysteretic behavior (r = 0, k = Fy = s = 1.0)

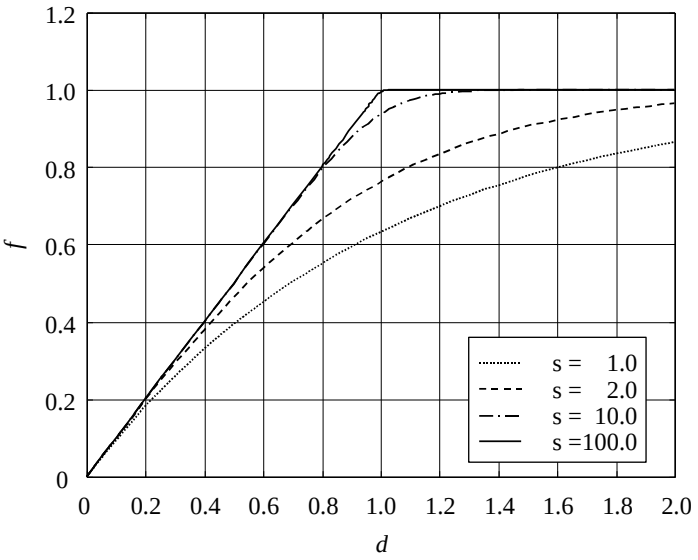

Figure 2.29 Transition region between elastic and plastic deformations (Yield region)

- **Lead Rubber Bearing type Isolator**

  Lead Rubber Bearing type Isolator reduces the propagation of ground acceleration and thereby protects the structure from the ground motion. The isolators are placed between the girders and piers of bridge structures and between the foundations and upper structures of building structures. The lead rubber bearing type isolator of low post-yield stiffness separates the dominant natural frequencies of the structure from the main frequency components of the ground motion. The isolator dissipates the vibration energy within the device through the hysteretic behavior.

  This type of isolator retains the properties of coupled Biaxial Plasticity for the 2 shear deformations and the properties of independent linear elastic springs for the remaining 4 deformations.

  The coupled Force–Deformation relationship for a lead rubber bearing type isolator is noted below.

$$\begin{cases} f_y = r_y k_y \cdot d_y + (1-r_y) F_{y,y} z_y \\ f_z = r_z k_z \cdot d_z + (1-r_z) F_{y,z} z_z \end{cases}$$

where,

k_y, k_z : Initial elastic shear spring stiffnesses in the ECS *y* and *z* directions

$F_{y,y}$, $F_{y,z}$: Yield strengths of shear springs in the ECS y and z directions

r_y, r_z : Ratios of post-yield stiffnesses to elastic stiffnesses of shear springs in the ECS y and z directions

d_y, d_z : Deformations of shear springs between two nodes in the ECS y and z directions

z_y, z_z : Internal variables for hysteretic behaviors of shear springs in the ECS y and z directions

Each of z_y and z_z is an internal hysteretic variable. The SRSS of both values ranges from 0 to 1. The dynamic behavior of the variable z was based on the biaxial plasticity model proposed by Park, Wen, and Ang (1986), which was expanded from the Wen's uniaxial plasticity model (1976). They are defined by the following differential equation:

$$\begin{Bmatrix} \dot{z}_y \\ \dot{z}_z \end{Bmatrix} = \begin{bmatrix} 1 - z_y^2 \left\{ \alpha_y \text{sign}\left(\dot{d}_y z_y\right) + \beta_y \right\} & -z_y z_z \left\{ \alpha_z \text{sign}\left(\dot{d}_z z_z\right) + \beta_z \right\} \\ -z_y z_z \left\{ \alpha_y \text{sign}\left(\dot{d}_y z_y\right) + \beta_y \right\} & 1 - z_z^2 \left\{ \alpha_z \text{sign}\left(\dot{d}_z z_z\right) + \beta_z \right\} \end{bmatrix} \begin{Bmatrix} \frac{k_y}{F_{y,y}} \dot{d}_y \\ \frac{k_z}{F_{y,z}} \dot{d}_z \end{Bmatrix}$$

where,

$\alpha_y, \beta_y, \alpha_z, \beta_z$: Parameters related to the shapes of hysteretic curves of shear springs in the ECS *y* and *z* directions

$\dot{d}_y$, $\dot{d}_z$: Rates of changes in deformations of shear springs between two nodes in the ECS *y* and *z* directions

sign (.): Sign function

If only one nonlinear shear spring exists, the above model becomes identical to the hysteretic system with s=2 in which case the purposes of all the variables and parameters also become identical.

➢ Friction Pendulum System type Isolator

Friction Pendulum System type Isolator is used for the same purpose of using Lead Rubber Bearing type Isolator. Its mechanism of protecting the structure from ground motion through energy dissipation by hysteretic behavior and moving the natural frequencies is identical. The difference is that the friction pendulum system incurs recovery forces through the pendulum curvature radii of the slipping surfaces. By adjusting the radii, we can move the natural frequencies of the total structure to the desired values. Also, energy dissipation due to hysteretic behavior is accomplished through the phenomenon of surface slippage.

This type of isolator retains the properties of coupled Biaxial Plasticity for the 2 shear deformations, the nonlinear property of the Gap behavior for the axial deformation and the properties of independent linear elastic springs for the remaining 3 rotational deformations.

The equation of Force-Deformation relationship of the axial spring of the friction pendulum system type isolator is identical to that of Gap with the initial gap of 0.

$$f_x = P = \begin{cases} k_x d_x & \text{if } d_x < 0 \\ 0 & \text{otherwise} \end{cases}$$

where,

P : Axial force acting on the friction pendulum type isolator

k_x : Linear spring stiffness in the ECS x direction

d_x : Spring deformation in the ECS x-direction

The coupled Force–Deformation relationship for the springs in the shear directions for a friction pendulum system type isolator is noted below.

$$f_y = \frac{|P|}{R_y} d_y + |P| \mu_y z_y \qquad f_z = \frac{|P|}{R_z} d_z + |P| \mu_z z_z$$

where,

P : Axial force acting on the friction pendulum type isolator

R_y, R_z : Pendulum curvature radii of shear springs in the ECS y and z directions

μ_y, μ_z : Friction coefficients of shear springs in the ECS *y* and *z* directions

d_y, d_z : Deformations of shear springs between two nodes in the ECS *y* and *z* directions

z_y, z_z : Internal variables for hysteretic behaviors of shear springs in the ECS *y* and *z* directions

The friction coefficients of the friction surfaces μ_y and μ_z are dependent on the velocities of deformations in the shear directions. They are determined by the equations proposed by Constantinou, Mokha and Reinhorn (1990).

$$\mu_y = \mu_{fast,y} - \left(\mu_{fast,y} - \mu_{slow,y}\right) e^{-r|v|}$$

$$\mu_z = \mu_{fast,z} - \left(\mu_{fast,z} - \mu_{slow,z}\right) e^{-r|v|}$$

$$\text{where,} \begin{cases} v = \sqrt{\dot{d}_y^2 + \dot{d}_z^2} \\ r = \dfrac{r_y \dot{d}_y^2 + r_z \dot{d}_z^2}{v^2} \end{cases}$$

where,

$\mu_{fast,y}$, $\mu_{fast,z}$: Friction coefficients for fast deformation velocities in the ECS *y* and *z* directions

$\mu_{slow,y}$, $\mu_{slow,z}$: Friction coefficients for slow deformation velocities in the ECS *y* and *z* directions

r_y, r_z : Rates of changes in friction coefficients of shear springs in the ECS *y* and *z* directions

$\dot{d}_y$, $\dot{d}_z$: Rates of changes in deformations of shear springs between two nodes in the ECS *y* and *z* directions

Each of z_y and z_z is an internal hysteretic variable. The SRSS of both values ranges from 0 to 1. The dynamic behavior of the variable z was based on the biaxial plasticity model proposed by Park, Wen, and Ang (1986), which was expanded from the Wen's uniaxial plasticity model (1976). They are defined by the following differential equation:

$$\begin{Bmatrix} \dot{z}_y \\ \dot{z}_z \end{Bmatrix} = \begin{bmatrix} 1-z_y^2\left\{\alpha_y \text{sign}\left(\dot{d}_y z_y\right)+\beta_y\right\} & -z_y z_z\left\{\alpha_z \text{sign}\left(\dot{d}_z z_z\right)+\beta_z\right\} \\ -z_y z_z\left\{\alpha_y \text{sign}\left(\dot{d}_y z_y\right)+\beta_y\right\} & 1-z_z^2\left\{\alpha_z \text{sign}\left(\dot{d}_z z_z\right)+\beta_z\right\} \end{bmatrix} \begin{Bmatrix} \frac{k_y}{|P|\mu_y}\dot{d}_y \\ \frac{k_z}{|P|\mu_z}\dot{d}_z \end{Bmatrix}$$

where,

k_y, k_z: Initial shear stiffnesses prior to sliding in the ECS *y* and *z* directions (stiffnesses of link element)

$\alpha_y, \beta_y, \alpha_z, \beta_z$: Parameters related to the shapes of hysteretic curves of shear springs in the ECS *y* and *z* directions

$\dot{d}_y$, $\dot{d}_z$: Rates of changes in deformations of shear springs between two nodes in the ECS *y* and *z* directions

The above model retains the identical form as the lead rubber bearing type isolator except for the fact that the values corresponding to the yield strengths are expressed by the products of the absolute value of the axial force and the friction coefficients. If only one nonlinear shear spring exists, the above model becomes identical to the uniaxial property with s=2.

Inelastic Time History Analysis

■ Overview

Inelastic time history analysis is dynamic analysis, which considers material nonlinearity of a structure. Considering the efficiency of the analysis, nonlinear elements are used to represent important parts of the structure, and the remainder is assumed to behave elastically.

Nonlinear elements are largely classified into Element Type and Force Type. The Element Type directly considers nonlinear properties by changing the element stiffness. The Force Type indirectly considers nonlinear properties by replacing the nodal member forces with loads without changing the element stiffness. MIDAS programs use the Newton-Raphson iteration method for nonlinear elements of the Element Type to arrive at convergence. For nonlinear elements of the Force Type, convergence is induced through repeatedly changing the loads. The two types of nonlinear elements are classified as the Table 2.1. First, beam and general link elements assigned with inelastic hinge properties are classified into the Element Type. Among the general link elements, visco-elastic damper, gap, hook, hysteretic system, lead rubber bearing and friction pendulum system are classified as the Force Type nonlinear elements.

Element Type		Type of Nonlinearity
Beam + Inelastic Hinge		Element
General Link	Spring + Inelastic Hinge	Element
	Visco-elastic Damper	Force
	Gap	Force
	Hook	Force
	Hysteretic System	Force
	Lead Rubber Bearing	Force
	Friction Pendulum System	Force

Table 2.1 Classification of nonlinear elements

The equation of motion or dynamic equilibrium equation for a structure, which contains inelastic elements, can be formulated as below.

$$M\ddot{u} + C\dot{u} + K_S u + f_E + f_F = P$$

where,

M	: Mass matrix
C	: Damping matrix
K_S	: Global stiffness matrix for elastic elements only
u , $\dot{u}$, $\ddot{u}$	: Displacement, velocity and acceleration responses related to nodes
P	: Dynamic loads related to nodes
f_E	: Nodal forces of Element Type nonlinear elements
f_F	: Nodal forces of Force Type nonlinear elements

Direct integration must be used for inelastic time history analysis of a structure, which contains nonlinear elements of the Element Type. If a structure contains nonlinear elements of the Force Type only, much faster analysis can be performed through modal superposition. From this point on, inelastic time history analysis by direct integration is explained.

The MIDAS programs use the Newmark method for the method of direct integration. Iterative analysis by the Newton-Raphson method is carried out in each time step in the process of obtaining the displacement increment until the unbalanced force between the member force and external force is diminished. The unbalanced force is resulted from the change of stiffness in nonlinear elements of the Element Type and the change of member forces in nonlinear elements of the Force Type. The equilibrium equation considered in each iteration step for obtaining response at the time (t+Δt) is as follows:

$$K_{eff} \cdot \delta u = p_{eff}$$

$$K_{eff} = \frac{1}{\beta \Delta t^2} M + \frac{\gamma}{\beta \Delta t} C + K$$

$$p_{eff} = p(t + \Delta t) - f_E - f_F - K_S u - M\ddot{u} - C\dot{u}$$

Where,

K_{eff}	: Effective stiffness matrix
K	: Global tangent stiffness matrix for elastic & inelastic elements
δu	: Incremental displacement vector at each iteration step
p_{eff}	: Effective load vector at each iteration step

β , γ : Parameters related to Newmark method

t , Δt : Time and time increment

The above iterative process constantly updates the internal forces, f_E and f_F, of inelastic elements through state determination. The nodal response becomes updated using the displacement increment vector obtained in each iterative analysis step.

$$u(t+\Delta t) = u(t+\Delta t) + \delta u$$

$$\dot{u}(t+\Delta t) = \dot{u}(t+\Delta t) + \frac{\gamma}{\beta \Delta t}\delta u$$

$$\ddot{u}(t+\Delta t) = \ddot{u}(t+\Delta t) + \frac{1}{\beta \Delta t^2}\delta u$$

The norm by which convergence of iterative analysis is assessed may be displacement, load and energy. One or more of the three can be used to assess the convergence. If no conversion is achieved until the maximum iteration number specified by the user is reached, the time increment, Δt is automatically divided by 2 and the model is reanalyzed. Each norm is defined as follows:

$$\varepsilon_D = \sqrt{\frac{\delta u_n^T \cdot \delta u_n}{\Delta u_n^T \cdot \Delta u_n}}$$

$$\varepsilon_F = \sqrt{\frac{p_{eff,n}^T \cdot p_{eff,n}}{p_{eff,1}^T \cdot p_{eff,1}}}$$

$$\varepsilon_E = \sqrt{\frac{p_{eff}^T \cdot \delta u_n}{p_{eff,1}^T \cdot \delta u_1}}$$

where,

ε_D : Displacement norm

ε_F : Load norm

ε_E : Energy norm

$p_{eff,n}$: Effective dynamic load vector at n-th iterative calculation step

δu_n : Displacement increment vector at n-th iterative calculation step

Δu_n : Accumulated displacement increment vector through n times of iterative calculations

Unlike elastic time history analysis, inelastic time history analysis can not be carried out using the principle of superposition. For example, analysis results from static loads and earthquake loads can not be simply combined to represent the results of those loads acting simultaneously. Instead, such (combined) loads are applied as individual load cases and the loading sequence or the continuity of the load cases can be assigned for analysis.

■ Nonlinear static analysis

Once the effects of mass and damping are excluded from the nonlinear time history analysis, nonlinear static analysis can be performed. Nonlinear static analysis can be used to create initial conditions based on gravity loads for the subsequent nonlinear time history analysis (for lateral loads) or to perform pushover analysis. In creating the initial conditions of the gravity loads, performing nonlinear static analysis can reflect the nonlinear behavior, which may take place in the process. Accordingly, continuity or sequence of applying loads can be maintained to assess the state of nonlinear elements. Pushover analysis is a simple method by which the ultimate strength and the limit state can be effectively investigated after yielding. Especially, this has become a representative analysis method for Performance-Based Seismic Design, PBSD, which has been extensively researched and applied in practice for earthquake engineering and seismic design. This analysis is mainly appropriate for structures in which higher modes are not predominant and which are not influenced by dynamic characteristics.

The method used in nonlinear static analysis is based on the Newton-Raphson method, and it supports the methods of Load control or Displacement control. It is also possible to continually analyze for load cases, which have different control methods. In the load control, the static loads applied by the user are divided into a number of loading steps and loaded. In the displacement control, the user sets a target displacement, which the structure can undergo, and increases the loads until the structure reaches the target displacement. The target displacement can be largely set to Global Control 과 Master Node Control. The Global Control is a method by which loading is increased until the maximum displacement of the structure satisfies the target displacement defined by the user. The displacement has no relation to the direction of the loading. The Master Node Control is a method by which loading is increased until the target displacement at a specific node in a specific direction defined by the user is satisfied. The target displacement in performance based seismic design is generally set by considering the location of a node at which the maximum displacement can possibly occur and its direction. The number of loading steps in the load control or the displacement control is determined by dividing the end time by the time increment.

The loading is applied through Time Varying Static Load in which the user specifies a dummy time function, but it is not used in real analysis. In the case of load control, the load factors linearly increase from 0 to 1 in the process of real analysis. In the case of displacement control, the load factors corresponding to the displacement increments are automatically calculated. The load factors used in a nonlinear static analysis can be saved and reproduced.

■ Inelastic hinge properties

Inelastic hinge properties are a collection of nonlinear behavior characteristics for a beam element or general link elements, which are defined for each of 6 components. The nonlinear behavior characteristics are defined by special rules, which are referred to as hysteresis models. The property of each component can be defined by an independent uni-axial hinge hysteresis model or a multi-axial hinge hysteresis model, which reflects multi-component properties. Inelastic hinge properties are classified into lumped type, distributed type and spring type. Among these different types, the lumped and distributed types are used for beam elements, and the spring type is used for general link elements.

■ Inelastic beam element

Inelastic beam element is a beam element, which is assigned inelastic hinge properties. The inelastic beam element is limited to having a prismatic section whose hinge properties are identical for the single beam element. The stiffness of the inelastic beam element is formalized by the flexibility method. The shape function on which the existing stiffness method is based may differ from the true deformed shape in inelastic analysis. Whereas, the element section force distribution on which the flexibility method is based coincides with the true distribution, which results in much higher accuracy. It has been known that the use of the flexibility method allows us to accurately model with a much less number of elements and as a result, the analysis speed can be much faster.

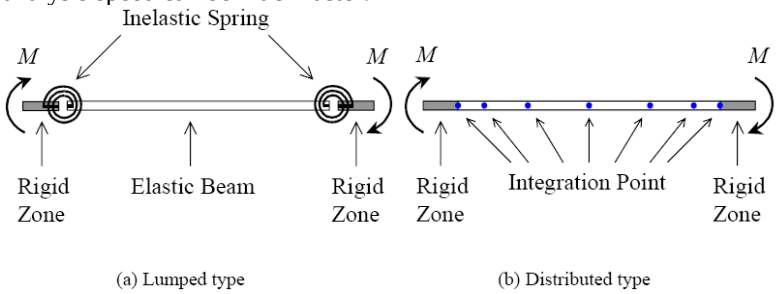

Fig. 2.30 Inelastic beam element

➢ Lumped type hinge

The lumped type hinge is defined by a force-displacement relationship for the axial component and a moment-rotational angle relationship at the ends for the flexural components. The formulation is represented by inserting inelastic translational and rotational springs of non-dimensional 0 lengths, which can deform plastically, into the beam element. The remaining parts

other than the lumped type inelastic hinges are modeled as an elastic beam. The locations for inserting the inelastic springs for axial and flexural deformation components are assigned to the middle and both ends of the beam element respectively.

The stiffness matrix of the beam element, which has been assigned lumped type hinges, is calculated by the inverse matrix of the flexibility matrix. The flexibility matrix of the total element is formulated by adding the flexibility matrices of the inelastic springs and the elastic beam. The flexibility of an inelastic spring is defined by the difference between the tangential flexibility of the lumped type hinge defined by the user and the initial flexibility. The flexibility of the inelastic spring is zero prior to yielding. The tangential flexibility matrix of the inelastic hinge is defined by hysteresis models for uniaxial or multi-axial hinges, which are explained later.

$$F_S = F_H - F_{H0}$$
$$F = F_B + \sum F_S$$
$$K = F^{-1}$$

where,

F_H : Flexibility matrix of inelastic hinge

F_{H0} : Initial flexibility matrix of inelastic hinge

F_S : Flexibility matrix of inelastic spring

F_B : Flexibility matrix of elastic beam

F : Element flexibility matrix of inelastic beam

K : Element stiffness matrix of inelastic beam

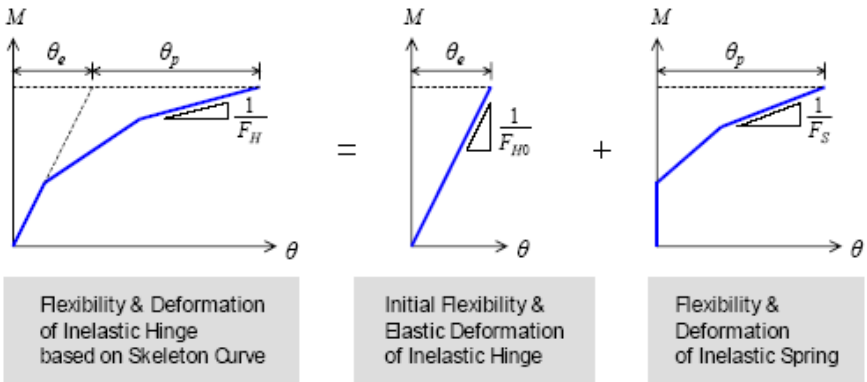

Fig. 2.31 Flexibility of inelastic hinges

The relationship of moment-rotational angle of a flexural deformation hinge is influenced by the end moments as well as by the flexural moment distribution within the member. In order to determine the relationship, the distribution of flexural moment needs to be assumed. The initial stiffness based on assumed moment distribution is shown below.

Deflection Shape	Moment Distribution	Initial Stiffness
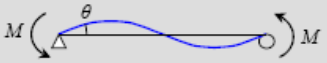	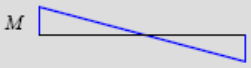	$\frac{6EI}{L}$
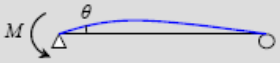	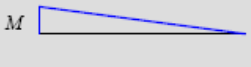	$\frac{3EI}{L}$
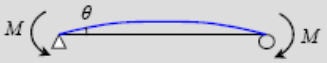	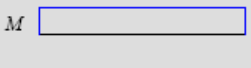	$\frac{2EI}{L}$

Fig. 2.32 Initial stiffness of inelastic hinges relative to flexural deformations (total length=L, flexural stiffness of section=EI)

- **Distributed type hinge**

The distributed type hinge is defined by a force-deformation relationship for the axial component and a moment-curvature rate relationship for the flexural components at the section. The flexibility matrix of a beam element, which has been assigned distributed type hinges, is defined by the following equations and calculated through the Gauss-Lobbatto integration. The flexibility of a section at an integration point in the longitudinal direction is obtained by state determination by the hysteresis models of uni-axial or multi-axial hinges, which are explained later. The stiffness matrix is calculated by the inverse matrix of the flexibility matrix.

$$F = \int_0^L b^T(x) f(x) b(x) dx$$

$$K = F^{-1}$$

where,

$f(x)$: Flexibility matrix of the section at the location x
$b(x)$: Matrix of the section force distribution function for the location x
F : Element flexibility matrix
K : Element stiffness matrix
L : Length of member
x : Location of section

The locations of the integration points are determined by the number of integration points. The distances between the integration points are closer as the points near both ends. A maximum of 20 integration points can be specified. The distributed type hinges for axial and flexural deformations are defined in terms of "force-deformation" and "moment-curvature rate" relationships respectively.

The lumped type hinge is advantageous in that it requires relatively less amount of calculations. Because it arbitrarily assumes the distribution of member forces, inaccurate results may be obtained if the assumption substantially deviates the true distribution. The distributed type on the other hand can reflect the member force distribution more accurately. Its accuracy increases with the increase in the number of hinges. However, it has a drawback of increasing the amount of calculations required to determine the hinge state.

- **Yield strength of beam element**

The yielding of beam elements due to bending is defined as Fig. 4.4. In the case of a structural steel section, the first yielding presumes that the bending stress of the furthermost point from the neutral axis has reached the yield strength. Subsequently, the second yielding presumes that the bending stress over the entire section has reached the yield strength. In the case of a reinforced concrete section, the first yielding presumes that the bending stress of the furthermost point from the neutral axis has reached the cracking stress of concrete. The second yielding presumes that the concrete at the extreme fiber has reached the ultimate strain, and that the stress of reinforcing steel is less than or equal to the yield stress. In the case of steel reinforced concrete composite (SRC) sections, the calculation methods for structural steel and reinforced concrete sections are applied to the concrete filled tube type and the steel-encased type respectively. Where the interaction between axial force and moments needs to be considered, interaction curves are generated by considering the change of neutral axis due to axial force.

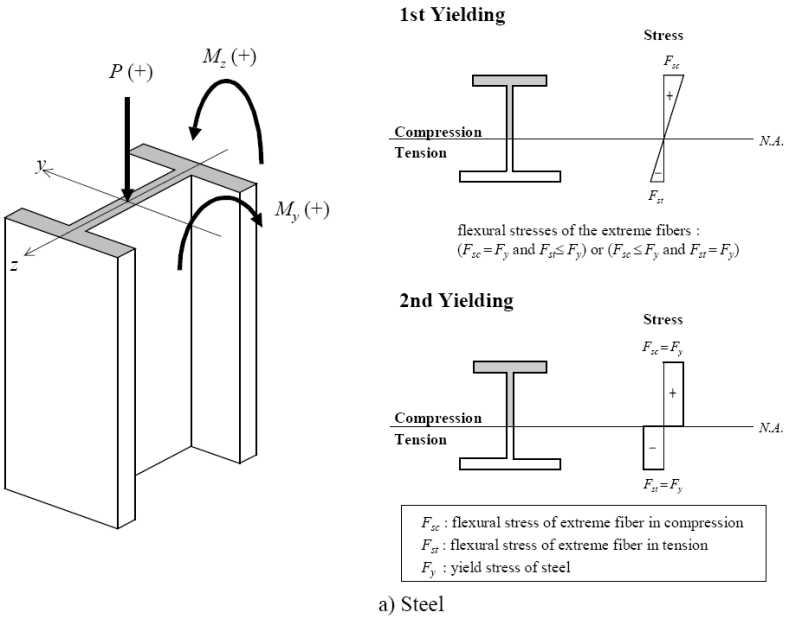

a) Steel

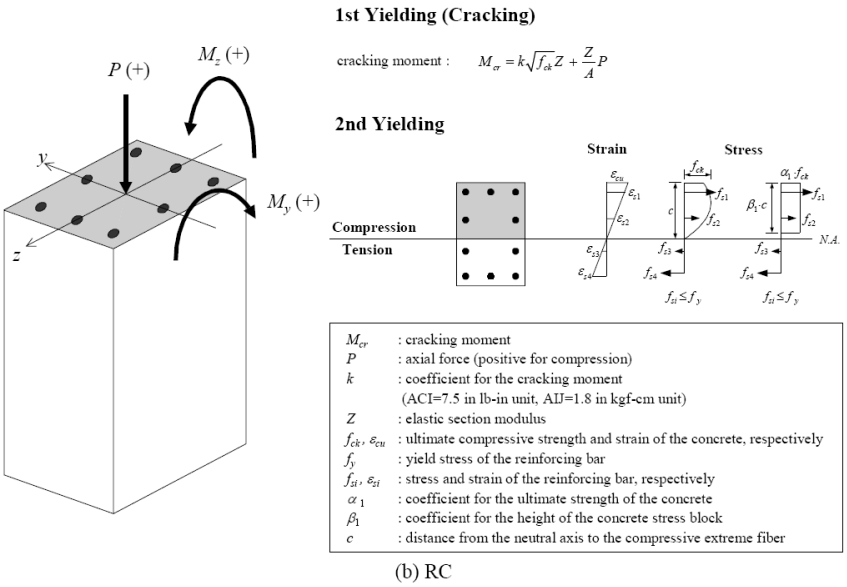

(b) RC

Fig. 2.33 Bases for determining yield strength of beam elements

- **P-M and P-M-M interactions**

A beam element, which is subjected to bending moments and axial force, retains a different yield strength compared to when each component is independently acting on the element, due to interaction. Especially in a 3-dimensional time history analysis, the interaction significantly affects the dynamic response of the structure. A column in a 3-dimensional structure will experience a complex interaction between bending moments about two axes and axial force due to a bi-directional earthquake. The MIDAS programs carry out nonlinear time history analysis reflecting a P-M or P-MM interaction.

A P-M interaction is reflected by calculating the flexural yield strength of a hinge considering the axial force effect. In this case, the interaction of two bending moments is ignored. It is assumed that the axial force independently interacts with each moment in determining the hinge status at each time step.

The yield strength of bending moment is recalculated while reflecting the axial force in the loading case, which satisfies the following three conditions.
1) It must be the first load case among the time history load cases, which are sequenced and analyzed consecutively.
2) Nonlinear static analysis must be performed.
3) Displacement control must be used.
Let us consider an inelastic beam element, which has been assigned hinge properties and for which a P-M interaction is applied. The initial section force is assumed as the combination of the results of linear elastic analysis for all the static load cases included in the time varying static load. The factors used for the combination are defined by the Scale Factors entered in the time varying static load.

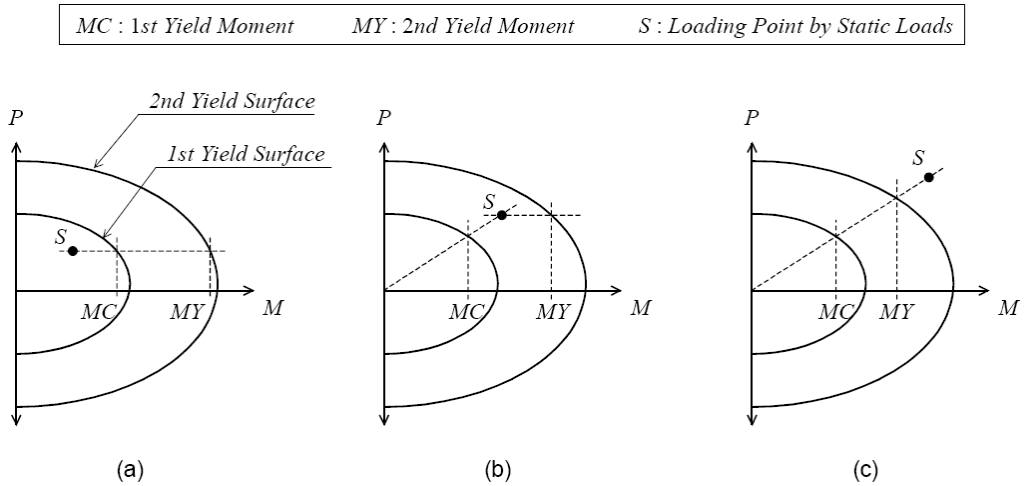

Fig. 2.34 Calculation of bending yield strength by P-M interaction

The yield strength for bending is determined relative to the location of the loading point by static loads on the 2-dimensional interaction curve for the calculated section force as shown in Fig. 2.34. If the loading point exists within the interaction curve, the bending yield strength corresponding to the axial force of the loading point is calculated from the interaction curve. If the loading point exists beyond the interaction curve, the bending yield strength is calculated from the intersection of the yield surface and the straight line connecting the origin and the loading point. The 2-dimensional interaction curves described thus far being idealized will be also used for defining 3-dimensional yield surfaces described in the subsequent section.

A P-M-M interaction can be reflected in a nonlinear time history analysis by using hysteresis models for multi-axial hinges. The hysteresis models for multi-axial hinges represent the interaction of axial force and two bending moments, which is depicted by applying a plasticity theory. State determination is carried out considering the overall combined change of the three components at each time increment. The MIDAS programs support the kinematic hardening type.

- **Approximation of the yield surface**

In order to consider P-M or P-M-M interaction in calculating the yield strength or for state determination of a hinge, a 3-dimentional yield surface needs to be defined from P-M interaction curves. Because it is difficult to construct an accurate yield surface from the rather limited data of P-M interaction curves, the MIDAS programs approximate the P-M interaction

curve and yield surface by a simple equation. First, the P-M interaction curve is approximated by the following equation.

$$\left|\frac{M}{M_{\max}}\right|^{\gamma} + \left|\frac{P - P_{bal}}{P_{\max} - P_{bal}}\right|^{\beta} = 1.0$$

where

M : M_y or M_z in Element Coordinate System - the bending moment component of the loading point

$M_{\max}$: $M_{y,\max}$ or $M_{z,\max}$ in Element Coordinate System – the maximum yield strength for bending about the y- or z- axis

P : Axial force component of the loading point

P_{bal} : P_{bal} ,y or P_{bal} ,z, - Axial force at the balanced failure about the y- or z- axis bending in the element coordinate system, respectively

$P_{\max}$: Axial yield strength – positive (+), negative (-) non symmetry is possible.

γ : An exponent related to P-M interaction surface

β : βy or βz, the exponent related to P-M interaction about the y- or z- axis in the element coordinate system, respectively. Each exponent is allowed to have different values above and below the corresponding Pbal.

An M-M interaction is approximated by the following relationship:

$$\left|\frac{M_y}{M_{y,\max}}\right|^{\alpha} + \left|\frac{M_z}{M_{z,\max}}\right|^{\alpha} = 1.0$$

where,

$M_{y,\max}$: Maximum bending yield strength about y-axis in element coordinate system

$M_{z,\max}$: Maximum bending yield strength about z-axis in element coordinate system

α : An exponent related to interaction curve

For a 3-dimensional yield surface, the equation below, which satisfies the approximated interactions above, is used.

$$f(P,M_y,M_z)=\left\{\left(\frac{M_z}{M_{z,\max}}\right)^{\gamma}+\left\{g_y(M_y,M_z)\right\}^{\frac{\gamma}{a}}\cdot\left(\frac{P-P_{bal,y}}{P_{\max}-P_{bal,y}}\right)^{\beta_y}\right\}^{\frac{a}{\gamma}}$$

$$+\left\{\left(\frac{M_z}{M_{z,\max}}\right)^{\gamma}+\left\{g_z\left(M_y,M_z\right)\right\}^{\frac{\gamma}{a}}\cdot\left(\frac{P-P_{bal,z}}{P_{\max}-P_{bal,z}}\right)^{\beta_z}\right\}^{\frac{a}{\gamma}}=1$$

Where,

$$g_y(M_y,M_z)=\frac{\left(\frac{M_y}{M_{y,\max}}\right)^{a}}{\left(\frac{M_y}{M_{y,\max}}\right)^{a}+\left(\frac{M_z}{M_{z,\max}}\right)^{a}}$$

$$g_z(M_y,M_z)=\frac{\left(\frac{M_z}{M_{z,\max}}\right)^{a}}{\left(\frac{M_y}{M_{y,\max}}\right)^{a}+\left(\frac{M_z}{M_{z,\max}}\right)^{a}}$$

The approximated exponents for interaction curves, βy, βz and γ can be either user defined, or their optimum values can be automatically calculated. The optimum values are found by increasing γ from 1.0 to 3.0 by an increment of 0.1 and calculating the values of βy and βz for a given γ among which the values with the minimum margin of error is selected. The values of βy and βz, each corresponding to P-My and P-Mz interactions respectively, are calculated by equalizing the areas under the above approximated interaction curves and the areas under the real interaction curves, which are calculated from the section and material properties. The margin of error is defined by summing the absolute difference of moment values at the reference interaction points and the real interaction curves at the same axial forces.

There are two 3-dimensional yield surfaces, which exist in the form of a trilinear skeleton curve. Out of convenience, we will call the inner surface and outer surface the first phase yield surface and second phase yield surface respectively. In the case of a reinforced concrete section, the first and second phase yield surfaces correspond to cracking and yielding

respectively. Among the two yield surfaces, the first phase yield surface is approximated as shown in Fig. 2.35. First, the second phase yield surface is approximated by two straight lines, which result in an equal area. Next, the parameters for the approximated first phase yield surface are calculated so that the curve forms tangent to the inclined line of the two straight lines and the original crack curve.

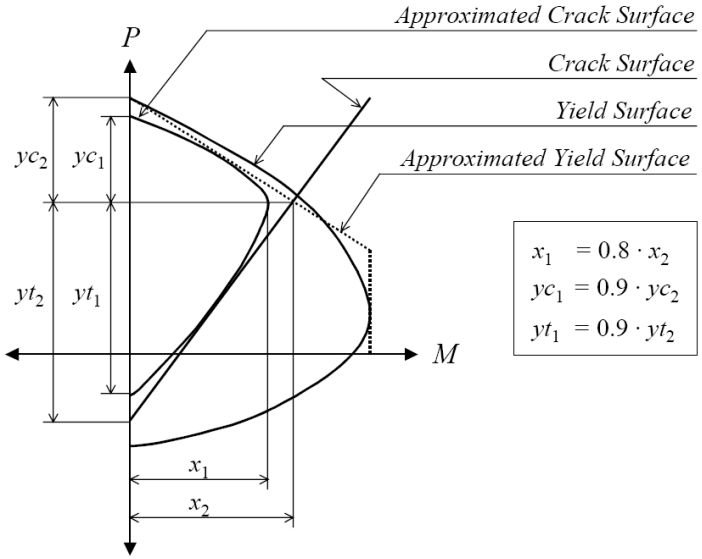

Fig 2.35 Approximation of crack surface of a reinforced concrete section

■ Inelastic general link elements

Inelastic general link elements are assigned inelastic hinge properties, which are used to model specific parts of a structure such as to represent plastic deformations of soils concentrated at a spring. The inelastic properties that can be assigned to the general link elements in the MIDAS programs are limited to the spring type. Such general link elements simply retain only the elastic stiffness for each component. By assigning inelastic hinge properties, they become inelastic elements. The elastic stiffness for each component becomes the initial stiffness in nonlinear analysis.

■ Hysteresis Model for Uni-axial Hinge

A uni-axial hinge is represented by 3 translational and 3 rotational components, which behave independently. The hysteresis models of uni-axial hinges provided in the MIDAS programs are founded on a skeleton curve. They are 6 types, which are kinematic hardening, origin-oriented,

peak-oriented, Clough, degrading tri-linear and Takeda types. All the models except for the Clough type are of basically a tri-linear type. The first and second phase yield strengths and the stiffness reduction factors with positive (+) and negative (-) non symmetry can be defined to represent nonsymmetrical sections or material properties. However, stiffness reduction for the kinematic hardening type does not support non-symmetry due to its characteristics.

In the hysteresis models below, response points represent the coordinates of load-deformation points situated on the path of a hysteresis model. Loading represents an increase in load in absolute values; unloading represents a decrease in load in absolute values; and reloading represents an increase in load in absolute values with the change of signs during unloading. Unloading points represent response points where loading changes to unloading.

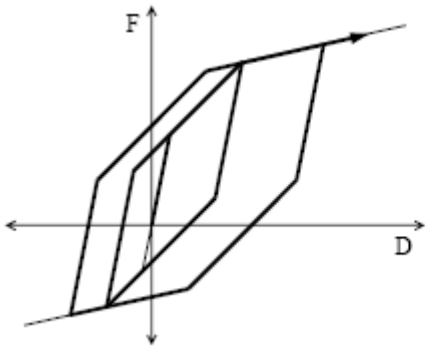

Fig. 2.36 Kinematic hardening hysteresis model

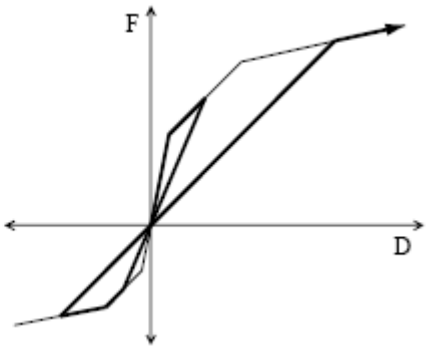

Fig. 2.37 Origin-oriented hysteresis model

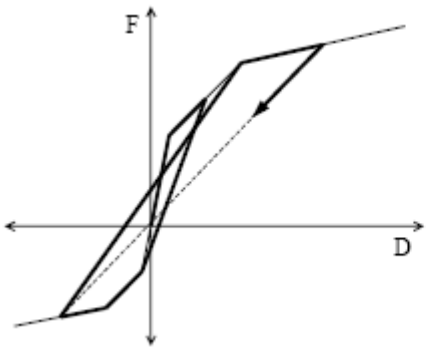

Fig. 2.38 Peak-oriented hysteresis model

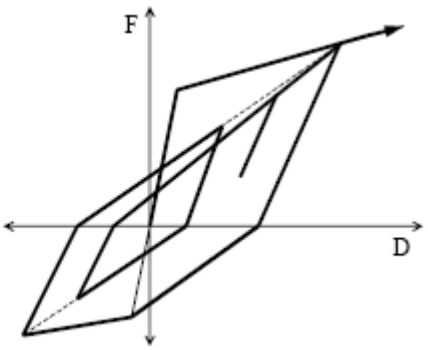

Fig. 2.39 Clough hysteresis model

- **Kinematic Hardening Type**

  Response points at initial loading move about on a trilinear skeleton curve. The unloading stiffness is identical to the elastic stiffness, and the yield strength has a tendency to increase after yielding. This, being used for modeling the Bauschinger effect of metallic materials, should be used with caution for concrete since it may overestimate dissipated energy. Due to the characteristics of the model, stiffness reduction after yielding is possible only for positive (+) and negative (-) symmetry.

- **Origin-oriented Type**

  Response points at initial loading move about on a trilinear skeleton curve. The response point moves towards the origin at the time of unloading. When it reaches the skeleton curve on the opposite side, it moves along the skeleton curve again.

- **Peak-oriented Type**

  Response points at initial loading move about on a trilinear skeleton curve. The response point moves towards the maximum displacement point on the opposite side at the time of unloading. If the first yielding has not occurred on the opposite side, it moves towards the first yielding point on the skeleton curve.

- **Clough Type**

  Response points at initial loading move about on a bilinear skeleton curve. The unloading stiffness is obtained from the elastic stiffness reduced by the

  following equation. As the deformation progresses, the unloading stiffness gradually becomes reduced.

$$K_R = K_0 \left| \frac{D_y}{D_m} \right|^{\beta} \leq K_0$$

  where,

  K_R : Unloading stiffness

  K_0 : Elastic stiffness

  D_y : Yield displacement in the region of the start of unloading

  D_m : Maximum displacement in the region of the start of unloading (Replaced with the yield displacement in the region where yielding has not occurred)

β : Constant for determining unloading stiffness

When the loading sign changes at the time of unloading, the response point moves towards the maximum displacement point in the region of the progressing direction. If yielding has not occurred in the region, it moves towards the yielding point on the skeleton curve. Where unloading reverts to loading without the change of loading signs, the response point moves along the unloading path. And loading takes place on the skeleton curve as the loading increases.

➢ **Degrading Trilinear Type**

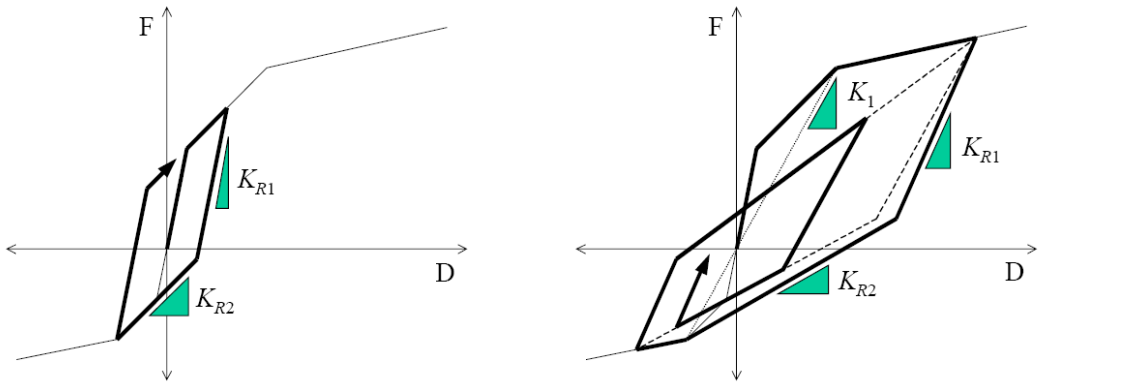

(a) Initial unloading before yielding to uncracked region (small deformation)

(b) Initial unloading before yielding to uncracked region (small deformation) and inner loop

Fig. 2.40 Hysteresis models for trilinear stiffness reduction

Response points at initial loading move about on a trilinear skeleton curve. At unloading, the coordinates of the load-deformation move to a path along which the maximum deformation on the opposite side can be reached due to the change of unloading stiffness once. If yielding has not occurred on the opposite side, the first yielding point is assumed to be the point of maximum deformation. The first and second unloading stiffness is determined by the following equations. As the maximum deformation increases, the unloading stiffness gradually decreases.

$$K_{R1} = b \cdot K_0$$

$$K_{R2} = b \cdot K_C$$

$$b = \frac{1}{K_1}\left\{\frac{F_{M+} - F_{M-}}{D_{M+} - D_{M-}}\right\}$$

where,

K_{R1} : First unloading stiffness

K_{R2} : Second unloading stiffness

K_0 : Elastic stiffness

K_C : First yield stiffness in the region to which the loading point progresses due to unloading

K_1 : Slope between the origin and the second yield point in the region to which the loading point progresses due to unloading

b : Stiffness reduction factor. If unloading takes place between the first and second yield points on the skeleton curve, the value is fixed to 1.0

F_{M+} , F_{M-} : Maximum positive (+) and negative (-) forces respectively

D_{M+}, D_{M-} : Maximum positive (+) and negative (-) deformations respectively

- **Takeda Type**

Response points at initial loading move about on a trilinear skeleton curve. The unloading stiffness is determined by the location of the unloading point on the skeleton curve and whether or not the first yielding has occurred in the opposite region.

If unloading takes place between the first and second yield points on the skeleton curve, the coordinates of the load-deformation progress towards the first yield point on the skeleton curve on the opposite side. If the sign of the load changes in the process, the point progresses towards the maximum deformation point on the skeleton curve in the region of the proceeding direction. If yielding has not occurred in the region, the coordinates will progress towards the first yield point. When the point meets the skeleton curve in the process, it progresses along the skeleton curve.
When unloading takes place in the region beyond the second yield point on the skeleton curve, the coordinates of load-deformation will progress based on the following unloading stiffness.

$$K_{RO} = \left\{ \frac{F_Y + F_C}{D_{Y+} D_C} \right\} \cdot \left(\frac{D_Y}{D_M} \right)^{\beta}$$

where,

K_{RO} : Unloading stiffness of the outer loop

F_C : First yield force in the region opposite to unloading point

F_Y : Second yield force in the region to which unloading point belongs

D_C : First yield displacement in the region opposite to unloading point

D_Y : Second yield displacement in the region to which unloading point belongs

D_M : Maximum deformation in the region to which unloading point belongs

β : Constant for determining the unloading stiffness of the outer loop

If the sign of load changes in the process, the coordinates progress towards the maximum deformation point on the skeleton curve in the region of the proceeding direction. If yielding has not occurred in the region, the coordinates continue to progress without changing the unloading stiffness until the load reaches the first yield force. Upon reaching the first yield force, it progresses towards the second yield point.

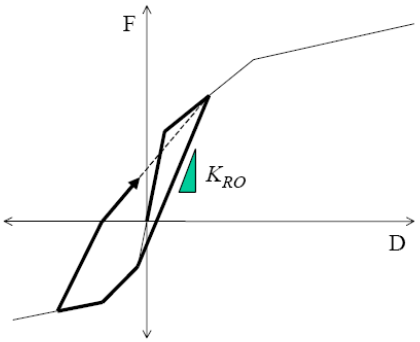

(a) Unloading before yielding to uncracked region (small deformation)

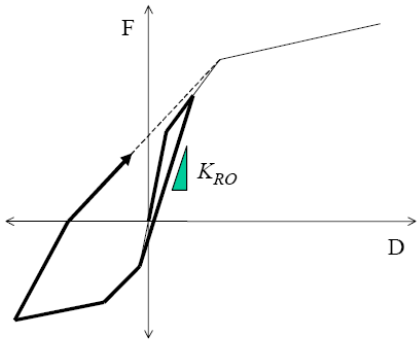

(b) Unloading before yielding to uncracked region (large deformation)

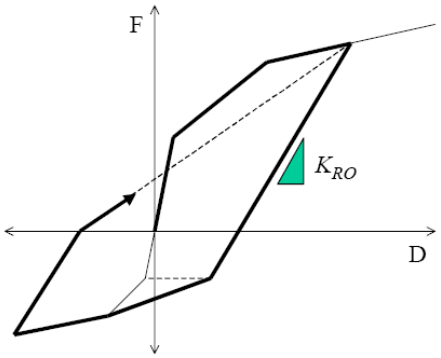

(c) Unloading after yielding to uncracked region

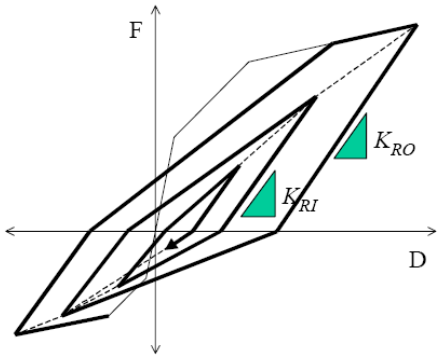

(d) Inner loop by repeated load reversal

Fig. 2.41 Takeda type hysteresis models

Inner loop is formed when unloading takes place before the load reaches the target point on the skeleton curve while reloading is in progress, which takes place after the sign of load changes in the process of unloading. Unloading stiffness for inner loop is determined by the following equation.

$$K_{RI} = \gamma K_{RO}$$

where,

K_{RI} : Unloading stiffness of inner loop

K_{RO} : Unloading stiffness of the outer loop in the region to which the start point of unloading belongs

γ : Unloading stiffness reduction factor for inner loop

In the above equation, β=0.0 for calculating K_{RO} and γ=1.0 for calculating K_{RI} are set if the second yielding has not occurred in the region of unloading. In the case where the sign of load changes in the process of unloading in an inner loop, the load progresses towards the maximum deformation point, if it exists on the inner loop in the region of the proceeding direction. If the maximum deformation point does not exist on the inner loop, the load directly progresses towards the maximum deformation point on the skeleton curve. If the maximum deformation point exists and there exists multiple inner loops, it progresses towards the maximum deformation point, which belongs to the outermost inner loop. Also, if loading continues through the point, it progresses towards the maximum deformation point on the skeleton curve.

■ Hysteresis Model for Multi-axial Hinge

A multi-axial hinge considers interactions between multiple components. This can be used to model a column, which exhibits inelastic behavior subject to an axial force and moments about two axes. Such multi-component interactions can be used to represent complex loading types such as earthquakes. In order to model the interactions more accurately, we may discretize a column into solid elements and analyze the column. However, this type of approach requires a significant amount of calculations. Alternatively, a beam element can be used to reduce the number of elements, which is based on a fiber model. A fiber model separates a beam section by fibers; but a single beam does not need to be advantage of modeling nonlinear behavior more accurately. MIDAS provides hysteresis models of kinematic hardening type by applying the fiber model and plasticity theories for multi-axial hinge.

➢ Kinematic Hardening Type

The hysteresis model of kinematic hardening type for multi-axial hinges follows the kinematic hardening rule, which uses two yield surfaces. This is basically a trilinear hysteresis model of kinematic hardening type for uniaxial hinges, which has been expanded into three axes. Assessing the hinge status and calculating the flexibility matrix thereby depend on the relationship of relative locations of loading points on a given yield surface. The unloading stiffness is identical to the elastic stiffness. The yield surface only changes its location, and it is assumed that the shape and size remain unchanged. If the loading point is located within the first yield surface, an

elastic state is assumed. When the loading point meets the first yield surface and the second yield surface, the first and second yielding are assumed to have occurred respectively.

The flexibility matrix of a hinge is assumed to be the sum of flexibility of three springs connected in a series. The serially connected springs are consisted of one elastic spring and two inelastic springs. Only the elastic spring retains flexibility and the remainder is assumed to be rigid initially. As the loading point comes into contact with each yield surface, the flexibility of the corresponding inelastic spring is assumed to occur. The equation for the flexibility matrix after the N-th yielding is noted below. Here, the terms related to the yield surface are calculated only for the yield surface with which the loading point is currently in contact.

$$F_s = K_{s,(0)}^{-1} + \sum_{i=1}^{N} \frac{a_{(i)} a_{(i)}^T}{a_{(i)}^T K_{s,(i)} a_{(i)}}$$

Where

$$K_{s,(i)} = \begin{bmatrix} k_{1,(i)} & 0 & 0 \\ 0 & k_{2,(i)} & 0 \\ 0 & 0 & k_{3,(i)} \end{bmatrix}$$

$$\frac{1}{k_{n,(i)}} = \left(\frac{1}{r_{n,(i)}} - \frac{1}{r_{n,(i)}} \right) \frac{1}{k_{n,(0)}} \qquad (n = 1,2,3;\ i = 1,2)$$

i : Order of yield surface with which the current loading pointis in contact

F_s : Tangential flexibility matrix of hinge

$a_{(i)}$: Normal vector at the loading point of *i-th* yield surface

$k_{n,(i)}$: *i-th* Serial spring stiffness of *n-th* component (elastic stiffness for i=0)

$r_{n,(i)}$: Stiffness reduction factor at the *i-th* yielding of *n-th* component (1.0 for i=0)

In the above flexibility matrix, Fs, the three components are completely independent as a diagonal matrix in the elastic state. In the state of yield deformation, interactions between the three components take place due to the non-diagonal terms of the matrix.

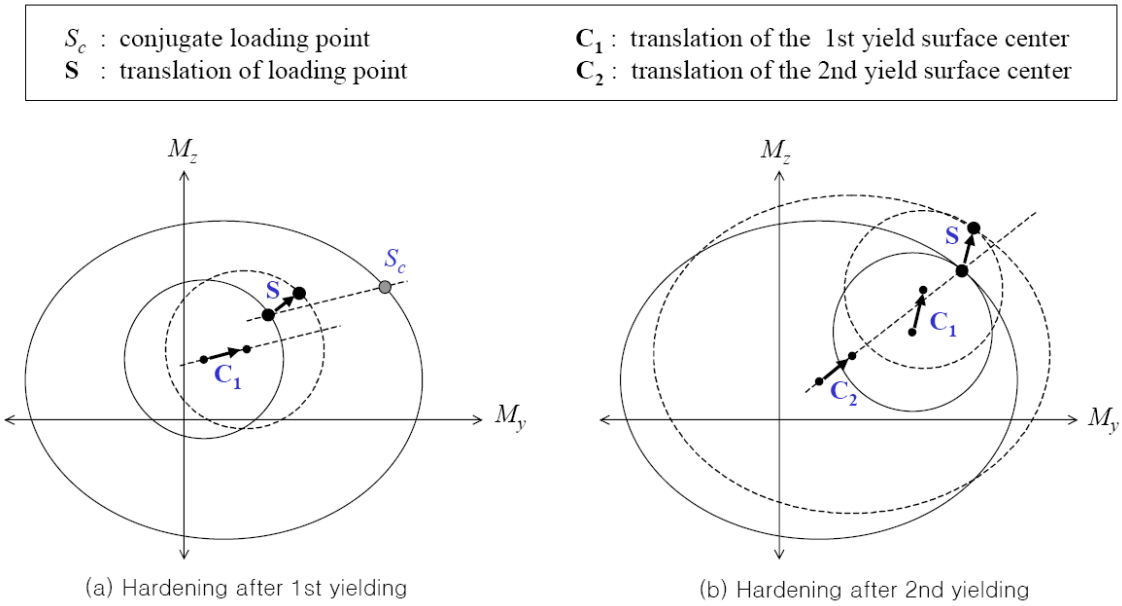

Fig. 2.42 Hardening rule

When the loading point moves to the exterior of the arrived yield surface, the yield surface also moves so as to maintain the contact with the loading point. The direction of the movement follows the hardening rule of deformed Mroz. If the loading point moves towards the interior of the yield surface, it is considered unloading, and the unloading stiffness is identical to the elastic stiffness. The yield surface does not move in the unloading process.

- **Fiber Model**

Fiber Model discretizes and analyzes the section of a beam element into fibers, which only deform axially. When a fiber model is used, the moment curvature relationship of a section can be rather accurately traced, based on the assumption of the stress-strain relationship of the fiber material and the distribution pattern of sectional deformation. Especially, it has the advantage of considering the movement of neutral axis due to axial force. On the other hand, a skeleton curve based hysteresis model has a limitation of accurately representing the true behavior because some behaviors of a beam element under repeated loads have been idealized.

The fiber models in MIDAS assume the following: 1) The section maintains a plane in the process of deformation and is assumed to be perpendicular to the axis of the member. Accordingly, bond-slip between reinforcing bars and concrete is not considered. 2) The centroidal axis of the section is

assumed to be a straight line throughout the entire length of the beam element

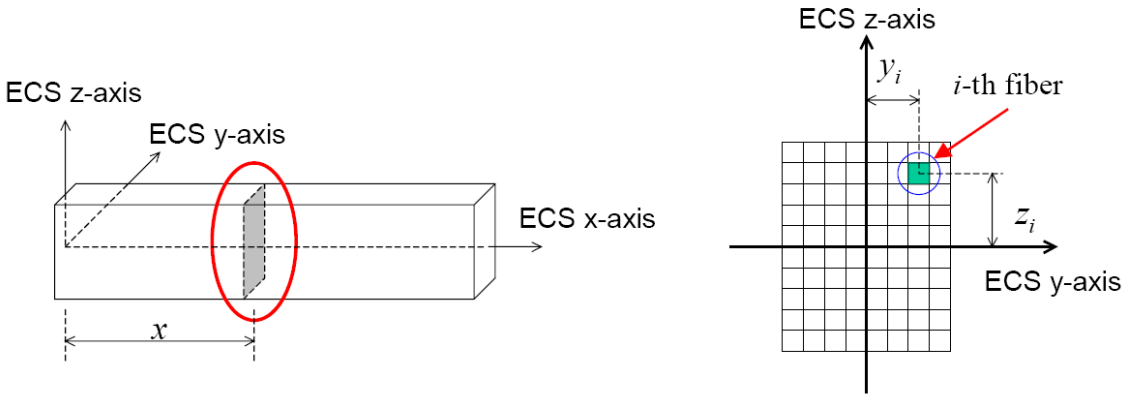

Fig 2.43 Discretization of a section in a fiber model

In a fiber model, the status of fibers is assessed by axial deformations corresponding to the axial and bending deformations of the fibers. The axial force and bending moments of the section are then calculated from the stress of each fiber. Based on the basic assumptions stated above, the relationship between the deformations of fibers and the deformation of the section is given below.

$$\varepsilon_i = \begin{bmatrix} -z_i & -y_i & 1 \end{bmatrix} \begin{Bmatrix} \phi_y(x) \\ \phi_z(x) \\ \varepsilon_x(x) \end{Bmatrix}$$

where,

x : Location of a section

$\phi_y(x)$: Curvature of the section about y-axis in Element Coordinate System at the location x

$\phi_z(x)$: Curvature of the section about z-axis in Element Coordinate System at the location x

$\varepsilon_x(x)$: Deformation of the section in the axial direction at the location x

y_i : Location of the *i-th* fiber on a section

z_i : Location of the *i-th* fiber on a section

ε_i : Deformation of the *i-th* fiber

The properties of nonlinear behavior of a section in a fiber model are defined by the stress-strain relationship of nonlinear fibers. MIDAS provides steel

and concrete material fiber models, and their constitutive models are explained below.

(1) Steel fiber constitutive model

Steel fiber constitutive model basically retains the curved shapes approaching the asymptotes defined by the bilinear kinematic hardening rule. The transition between two asymptotes corresponding to the regions of each unloading path and strain-hardening retains a curved shape. The farther the maximum deformation point in the direction of unloading is from the intersection of the asymptotes, the smoother the curvature becomes in the transition region. The constitutive model is thus defined by the equation below.

$$\hat{\sigma} = b \cdot \hat{\varepsilon} + \frac{(1-b) \cdot \hat{\varepsilon}}{(1+\hat{\varepsilon}^R)^{1/R}}$$

where,

$$\hat{\varepsilon} = \frac{\varepsilon - \varepsilon_r}{\varepsilon_0 - \varepsilon_r}$$

$$\hat{\sigma} = \frac{\sigma - \sigma_r}{\sigma_0 - \sigma_r}$$

$$R = R_0 - \frac{a_1 \cdot \xi}{a_2 + \xi}$$

ε : Strain of steel fiber

σ : Stress of steel fiber

(ε_r σ_r) : Unloading point, which is assumed to be (0, 0) at the initial elastic state

(ε_0, σ_0): Intersection of two asymptotes, which defines the current loading or unloading path

b : Stiffness reduction factor

R_0, a_1, a_2 : Constants

ξ : Difference between the maximum strain in the direction of loading or unloading and ε_0 (absolute value)

However, the initial value of the maximum strain is set to ±(Fy/E). (refer to Fig 2.43)

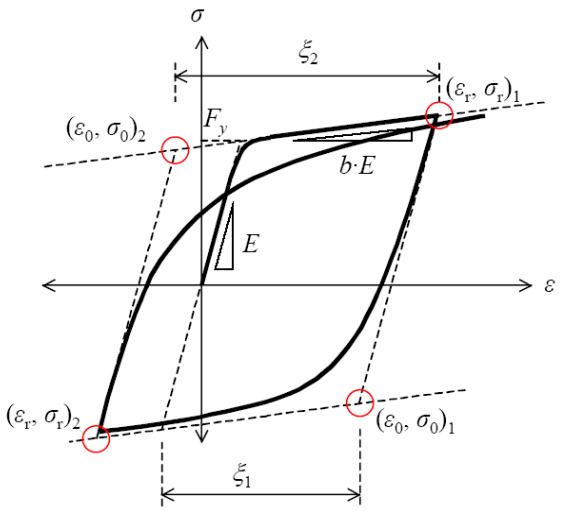

Fig. 2.44 Steel fiber constitutive model

(2) Concrete fiber constitutive model

MIDAS uses the equation of envelope curve proposed by Kent and Park (1973) for the concrete fiber constitutive model of concrete under compression. Tension strength of concrete is ignored. The equation of the envelope curve for compression is noted below. This is a well known material model for considering the effect of increased compression strength of concrete due to lateral confinement.

$$\sigma_c = \begin{cases} Kf_c' \left[2\left(\frac{\varepsilon}{\varepsilon_0}\right) - \left(\frac{\varepsilon}{\varepsilon_0}\right)^2 \right] & \text{for } \varepsilon \le \varepsilon_0 \\ Kf_c' \left[1 - Z(\varepsilon - \varepsilon_0)\right] \ge 0.2Kf_c' & \text{for } \varepsilon_0 \le \varepsilon \le \varepsilon_u \end{cases}$$

where,

ε : Strain of concrete fiber

σ : Stress of concrete fiber

ε_0 : Strain at maximum stress

ε_u : Ultimate strain

K : Factor for strength increase due to lateral confinement

Z : Slope of strain softening

f_c' : Compressive strength of concrete cylinder (MPa)

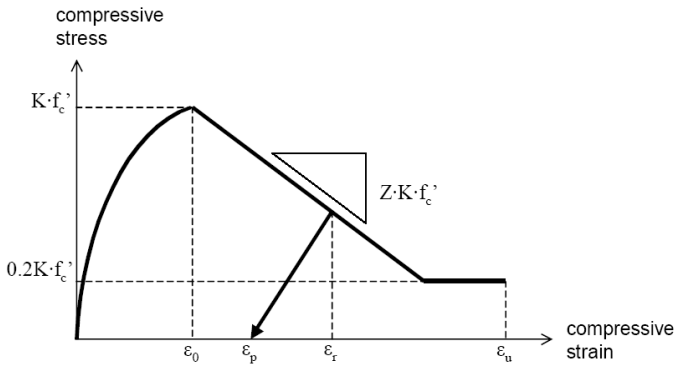

Fig. 2.45 Concrete fiber constitutive model

The concrete, which has exceeded the ultimate strain, is assumed to have arrived at crushing, and as such it is considered unable to resist loads any longer. Kent and Park suggested the following equation in order to calculate the parameters defining the above envelope curve for a rectangular column section.

$$\varepsilon_0 = 0.002K$$

$$K = 1 + \frac{p_s f_{yh}}{f_c^{'}}$$

$$Z = \frac{0.5}{\frac{3 + 0.29 f_c^{'}}{145 f_c^{'} - 1000} + 0.75\rho_s \sqrt{\frac{h^{'}}{S_h}} - 0.002K}$$

where,

f_{yh} : Yield strength of stirrups

p_s: Reinforcing ratio of stirrups = Volume of stirrups / Volume of concrete core

$h^{'}$: Width of concrete core (longer side of a rectangle)
(The range of the concrete core is defined as the outer volume encompassing the stirrups.)

S_k : Spacing of stirrups

Scott et al (1982) proposed the following equation of ultimate strain for a laterally confined rectangular column.

$$\varepsilon_u = 0.004 + 0.9\rho_s(f_{yh}/300)$$

When unloading takes place on the above envelope curve, the unloading path is defined by the equations below, pointing towards a point (εp, 0) on the strain axis. When the strain reaches this point, it moves to the tension zone following the strain axis.

$$\frac{\varepsilon_p}{\varepsilon_0} = 0.145 \cdot \left(\frac{\varepsilon_r}{\varepsilon_0}\right)^2 + 0.13 \cdot \left(\frac{\varepsilon_r}{\varepsilon_0}\right) \qquad for\left(\frac{\varepsilon_r}{\varepsilon_0}\right) < 2$$

$$\frac{\varepsilon_p}{\varepsilon_0} = 0.707 \cdot \left(\frac{\varepsilon_r}{\varepsilon_0} - 2\right) + 0.834 \qquad for\left(\frac{\varepsilon_r}{\varepsilon_0}\right) \geq 2$$

ε_r : Strain at the start of unloading

ε_p : Strain at the final point of the unloading path

If the compressive strain increases again, the load follows the previous unloading path and reaches the envelop curve.

Hysteresis Model for Multi-linear Hinge

(1) Multi-Linear Elastic Type

Overview of Hysteresis

Multi-Linear Elastic Type Hysteresis is nonlinear but elastic. The force-displa cement relationship of the skeleton curve is defined by a multi-linear curve. Ir respective of loading and unloading, no hysteresis loop is generated in Multi-Linear Elastic Type, and the force-displacement relationship exists only on th e skeleton curve.

The curve can be symmetrically or unsymmetrically defined. The types of co rresponding elements include lumped hinge, distributed hinge, spring and trus s elements.

Definition of Skeleton Curve

■ ***Force-Displacement Curve***

The skeleton curve is defined by the force-displacement relationship defined by the user. The following restrictions apply to defining the force-displaceme

nt curve:

- ***Force-Displacement Curve*** has no limitation on the number of data.
- The initial value must be set to (0,0).
- No identical values can be used for ***Displacements***, and the force-displacem ent data are arranged in reference to the displacements.
- The signs of force and displacement must be the same at all times.
- A negative slope is not permitted in ***Force-Displacement Curve*** except for t he final value. As such, the forces must gradually increase on the positive sid e and decrease on the negative side except for the last points on the curve. No fluctuation is permitted.

Rules for Hysteresis of Multi-Linear Elastic Type

The rules for hysteresis of Multi-Linear Elastic Type are identical to those of Elastic Tetralinear Type.

(2) Multi-Linear Plastic Kinematic Type

Overview of Hysteresis

Multi-Linear Plastic Kinematic Type Hysteresis is defined on multi-linear ske leton curves based on the kinematic hardening rules. The curve can be symm etrically or unsymmetrically defined. The types of corresponding elements in clude lumped hinge, distributed hinge, spring and truss elements.

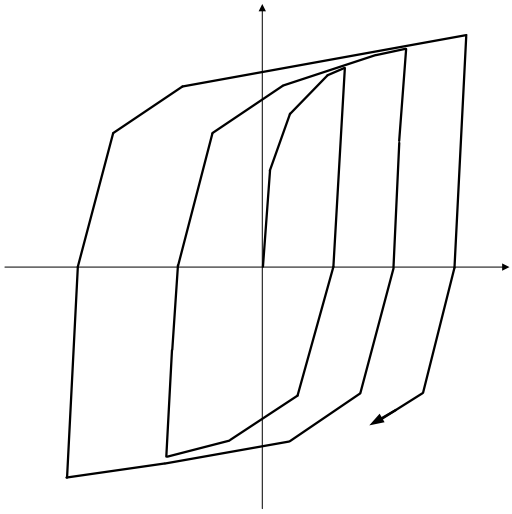

Figure 2.46 Multi-Linear Plastic Kinematic Hysteresis Model

Definition of Skeleton Curve

■ ***Force-Displacement Curve***

The skeleton curve is defined by the force-displacement relationship defined by the user. The following restrictions apply to defining the force-displacement curve:

- ***Force-Displacement Curve*** has no limitation on the number of data.
- At least one data point must be defined on both the positive and negative sides, and the numbers of data on the positive and negative sides must be identical.
- The initial value must be set to (0,0).
- No identical values can be used for ***Displacements***, and the force-displacement data are arranged in reference to the displacements.
- The signs of force and displacement must be the same at all times.
- A negative slope is not permitted in ***Force-Displacement Curve***. As such, the forces must gradually increase on the positive side and decrease on the negative side. No fluctuation is permitted.

Rules for Hysteresis of Multi-Linear Plastic Kinematic Type

1. In the case of $\left|P_{pl}^{(\pm)}\right| < \left|P1^{(\mp)}\right|$, the hysteresis curve for Multi-Linear Plastic Kinematic Type follows the conventional kinematic hardening rules.

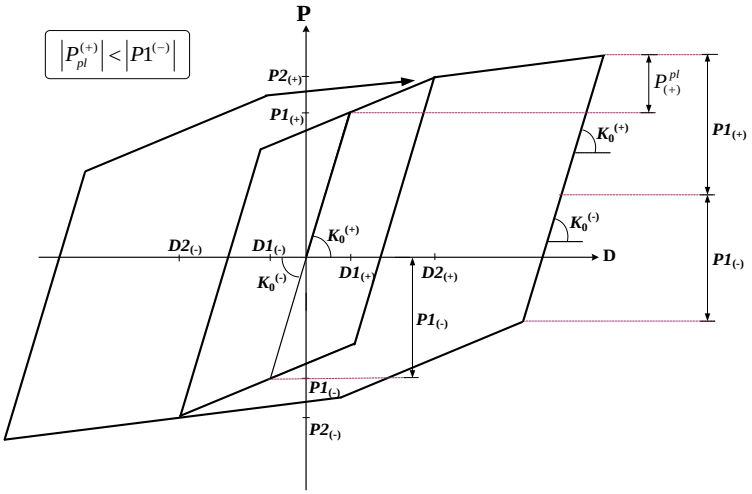

Figure 2.47 Rules for Hysteresis of Multi-Linear Plastic Kinematic Type

2. In the case of $\left|P_{pl}^{(\pm)}\right| > \left|P1^{(\mp)}\right|$, when the force is unloaded on the skeleton curve, the unloading takes place backward at a slope of K0 by the magnitude of ***P1*****(+)** or ***P1*****(-)** (Rule:1). It is then directed towards the point of unloading by the magnitude of the first yielding displacement, ***D1*****(-)** or ***D1*****(+)**, on the opposite side until the restoring force becomes 0 (Rule:2). Once the restoring force exceeds 0, the kinematic hardening rules apply.

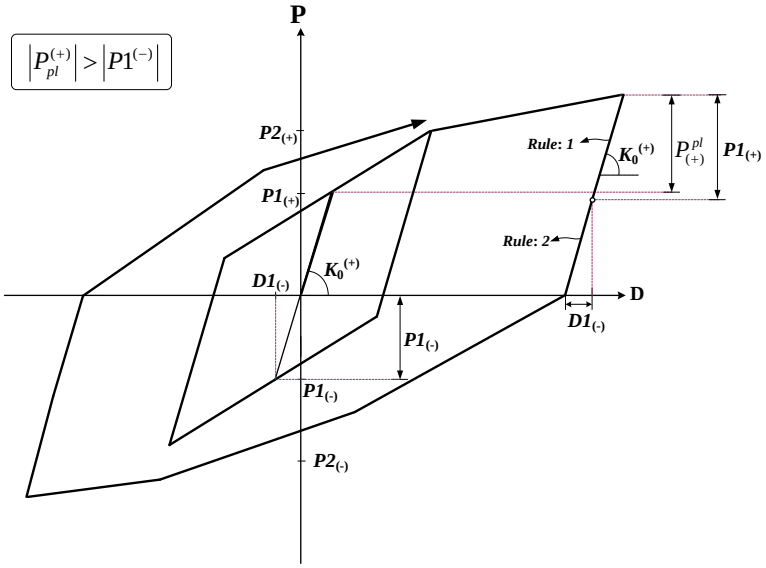

Figure 2.48 Rules for Hysteresis of Multi-Linear Plastic Kinematic Type

(3) Multi-Linear Elastic Type

Overview of Hysteresis

Multi-Linear Plastic Takeda Type Hysteresis is a multi-linear stiffness degradation model. The curve can be symmetrically or unsymmetrically defined. The types of corresponding elements include lumped hinge, distributed hinge, spring and truss elements.

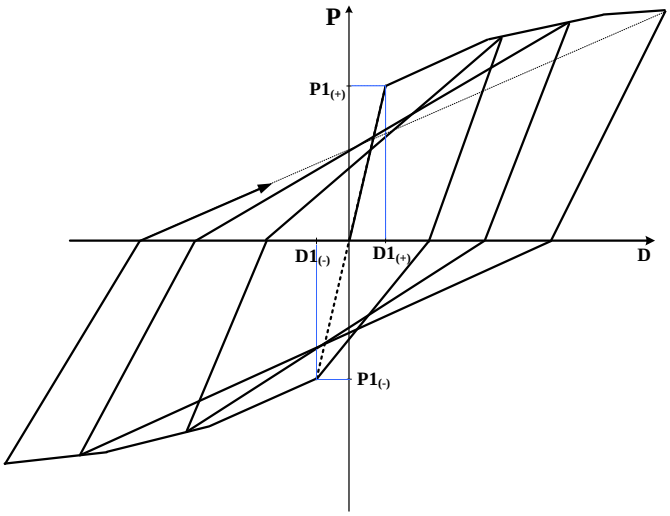

Figure 2.49 Multi-Linear Plastic Takeda Hysteresis Model

Definition of Skeleton Curve

The nonlinear characteristics of the hysteresis model are defined as follows:

■ ***Force-Displacement Curve***

The skeleton curve is defined by the force-displacement relationship defined by the user. The following restrictions apply to defining the force-displaceme nt curve:

- ***Force-Displacement Curve*** has no limitation on the number of data.
- At least one data point must be defined on both the positive and negative si des, and the numbers of data on the positive and negative sides must be identi cal.
- The initial value must be set to (0,0).
- No identical values can be used for ***Displacements***, and the force-displacem ent data are arranged in reference to the displacements.
- The signs of force and displacement must be the same at all times.
- A negative slope is not permitted in ***Force-Displacement Curve***. As such, t he forces must gradually increase on the positive side and decrease on the neg ative side. No fluctuation is permitted.

- ***Unloading Stiffness Parameter* :** β

The stiffness at unloading on the (+) and (-) sides is computed as follows. When $\beta = 0$, the unloading stiffness becomes the same as the elastic stiffness.

$$Kr^{(+)} = K_0 \cdot \left| \frac{D1^{(+)}}{D_{\max}^{(+)}} \right|^{\beta} \le K_0$$

$$Kr^{(-)} = K_0 \cdot \left| \frac{D1^{(-)}}{D_{\max}^{(-)}} \right|^{\beta} \le K_0$$

where, $D1^{(+)}$, $D1^{(-)}$: Yielding displacements on (+) & (-) sides

$D_{\max}^{(+)}$, $D_{\max}^{(-)}$: Maximum displacements on (+) & (-) sides (Replace with the yielding displacement when yielding has not occurred.)

β : Unloading stiffness parameter ($0 \le \beta \le 1$)

Rules for Hysteresis of Multi-Linear Plastic Takeda Type

1. In the case of $|D_{\max}| < D1$, the curve becomes linear elastic, which retains the elastic slope, K_0, passing though the origin.
2. When D first exceeds $D1_{(\pm)}$ or exceeds the maximum D up to the present, the curve follows the skeleton curve.
3. When the force is unloaded at the state, $D1_{(+)} < D$ or $D < D1_{(-)}$, the curve follows the unloading stiffness at a slope of $Kr^{(+)}$ or $Kr^{(-)}$.
4. D moves towards the D_{max} on the opposite side when the sign of the force changes in the process of unloading. If the opposite side has not yielded, the yielding point becomes the maximum displacement.

(4) Multi-Linear Elastic Type

Overview of Hysteresis

Multi-Linear Plastic Pivot Type Hysteresis (Pivot Hysteresis hereafter) is a multi-linear stiffness degradation model proposed by R. K. Dowell, F. Seible & E. L. Wilson(1998)[1]. Pivot Hysteresis uses multiple pivot points to control the nonlinear relationship of stress-strain or moment-rotation of reinforced concrete members. Thus, this model can accurately depict the stiffness degradation and the pinching effect when unloading takes place.

The curve can be symmetrically or unsymmetrically defined. The types of corresponding elements include lumped hinge, distributed hinge, spring and truss elements.

Definition of Skeleton Curve

The nonlinear characteristics of the hysteresis model are defined as follows:

■ ***Force-Displacement Curve***

The skeleton curve is defined by the force-displacement relationship defined by the user. The following restrictions apply to defining the force-displacement curve:

- ***Force-Displacement Curve*** has no limitation on the number of data.
- At least one data point must be defined on both the positive and negative sides, and the numbers of data on the positive and negative sides must be identical.
- The initial value must be set to (0,0).
- No identical values can be used for ***Displacements***, and the force-displacement data are arranged in reference to the displacements.
- The signs of force and displacement must be the same at all times.
- A negative slope is not permitted in Force-Displacement Curve except for the final value. As such, the forces must gradually increase on the positive side and decrease on the negative side except for the last points on the curve. No fluctuation is permitted.

[1] Robert K. Dowell, Frieder Seible, and Edward L. Wilson, "Pivot Hysteresis Model for Reinforced Concrete Members", ACI STRUCTURAL JOURNAL, n95, 1998, pp.607-617.

■ ***Primary Pivot Point***

The ***Primary Pivot Points***, P_1 and P_3 represent the points towards which the unloading curves are oriented in the Q_1 and Q_3 zones. The ***Primary Pivot Points***, P_1 and P_3 control the degradation of the unloading stiffness caused by the change in deformation or displacement. P_1 and P_3 are located along the extended lines of the initial stiffness on the (+) and (-) sides, which are defined by the yield strengths, **Fy(+) and Fy(-)** and ***Scale Factors***, α_1 and α_2 .

α_1 : Scale Factor used to define the pivot point, P_1 when unloading from the Q_1 side ($\alpha_1 \geq 1$)

α_2 : Scale Factor used to define the pivot point, P_3 when unloading from the Q_3 side ($\alpha_2 \geq 1$)

The ocations of the ***Primary Pivot Points***, P_1 and P_3 move to P_1^* and P_3^* after yielding respectively, whenever the maximum displacement point is renewed by the ***Initial Stiffness Softening Factor***, η . However, when η =0, the locat ions of the ***Primary Pivot Points***, P_1 and P_3 remain unchanged.

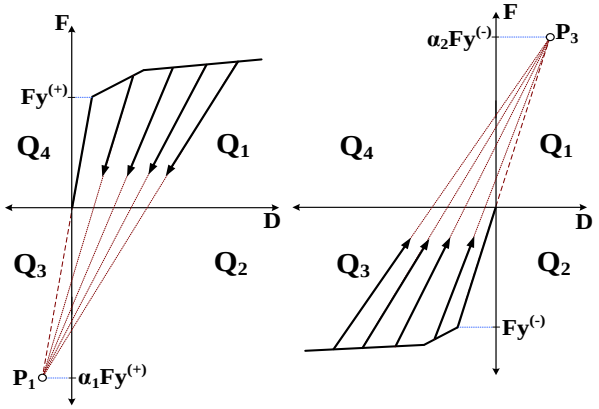

Figure 2.50 Primary Pivot Point

■ ***Pinching Pivot Point***

The ***Pinching Pivot Points***, PP_2 and PP_4 represent the points towards which the unloading curves are oriented in the Q1 and Q3 zones after the restoring force exceeds 0. PP_2 and PP_4 are located on the skeleton curve in the elastic zone on the (+) and (-) sides, which are defined by the yield strengths of the initial stiffness, **Fy(+) and Fy(-)** and **Scale Factors**, β_1 and β_2 .

β_1 : Scale Factor used to define the pivot point, PP_2 when loading on the Q_2 side ($0< \beta_1 \leq 1$)

β_2 : Scale Factor used to define the pivot point, PP_4 when loading on the Q_4 side ($0< \beta_2 \leq 1$)

The locations of the ***Pinching Pivot Points***, PP_2 and PP_4 after yielding will m ove to PP_2^* and PP_4^* respectively, whenever the maximum displacement poin t is renewed by the ***Initial Stiffness Softening Factor***, η . However, when η =0, the ***Pinching Pivot Points***, PP_2 and PP_4 remain unchanged.

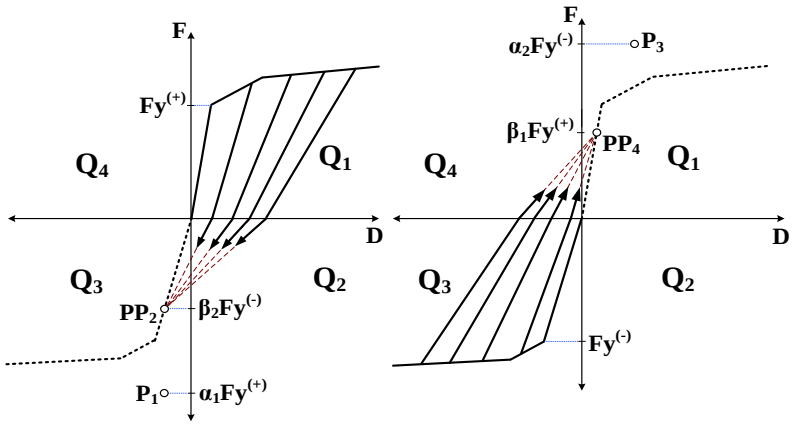

Figure 2.51 Pinching Pivot Point

■ ***Initial Stiffness Softening Factor* : η**

η is an initial stiffness softening factor used to control the initial stiffness de gradation after yielding. After yielding, the ***Primary Pivot Points***, P_1 and P_3 a re relocated to P_1^* and P_3^*, which are located on the lines extended from the maximum displacement points on the (+) and (-) sides respectively. P_1^* and P $_3^*$ are defined by $\mathbf{Fy^{(+)}}$ and $\mathbf{Fy^{(-)}}$, ***Scale Factors***, α_1 and α_2 , and the initial stiff ness softening factor, η .

In addition, the ***Pinching Pivot Points***, PP_2 and PP_4 move to PP_2^* and PP_4^* re spectively. PP2* (or PP4*) is defined by the intersection point of the straight l ine passing through P1* and the origin (or P3* and the origin) and the straigh t line connecting PP2 (or PP4) to the maximum displacement point on (-) side (or (+) side).

■ ***Renewal of Scale Factors***, β_1 and β_2

The ***Pinching Pivot Point Scale Factors***, β_1 and β_2 are renewed after yieldin g under the conditions below.

$$\beta_i^* \begin{cases} = \beta_i & ; D_{\max} \le D_{t1} \\ = \beta_i \cdot \dfrac{F_{\max}}{F_{ti}} & ; D_{\max} > D_{t1} \end{cases}$$

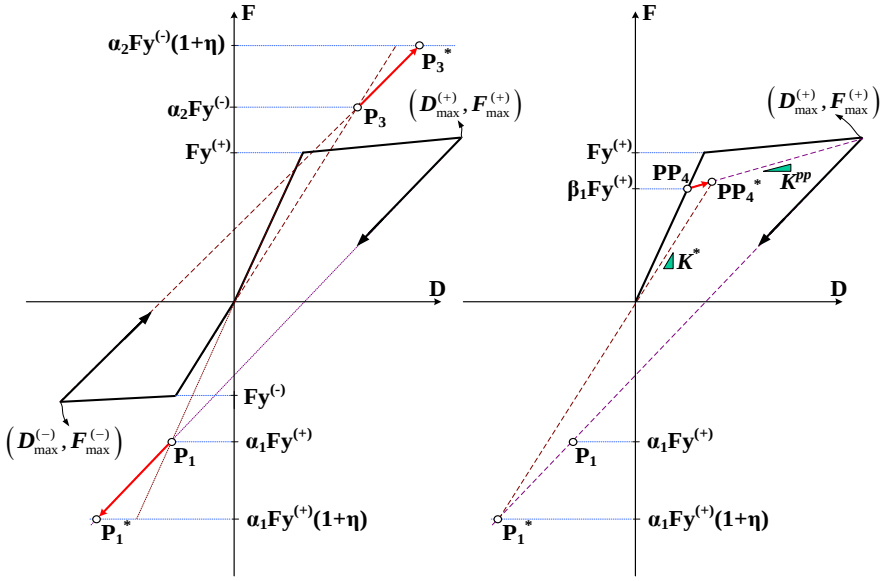

Figure 2.52 Initial Stiffness Softning Factor

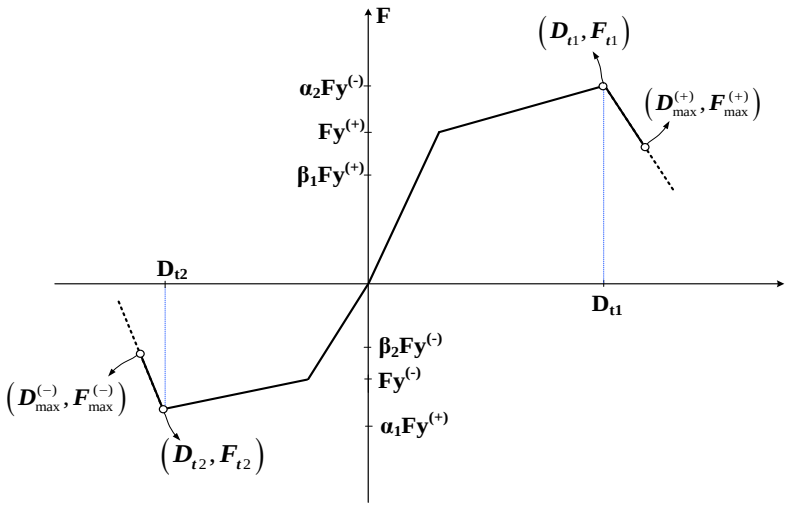

Figure 2.53 Renewal of Scale Factors, β_1 and β_2

Rules for Hysteresis of Multi-Linear Plastic Pivot Type

1. In the case of $|D_{max}| < D1$, the curve becomes linear elastic, which retains the elastic slope, K_o passing the origin. (Rule: 0)
2. i) The curve follows the skeleton curve when the displacement exceeds $D1_{(\pm)}$ for the first time. (Rule: 1)
   ii) When unloading takes place on this straight line, the curve is directed to wards P_1 or P_3. (Rule: 2)
   iii) In the case of reloading before the restoring force reaches 0, the curve c ontinues to follow the same unloading straight line. (Rule: 3) If it reache s the skeleton curve, it follows along the skeleton curve. (Rule: 4)
   iv) When the restoring force exceeds 0, the curve is directed towards PP_2 or PP_4. (Rule: 5)
   v) When PP_2 or PP_4 is exceeded and yielding has not occured, the curve mo ves along the straight line of the elastic slope. (Rule: 6) When yielding t akes place due to large deformation, the curve moves along the skeleton curve. (Rule: 7)

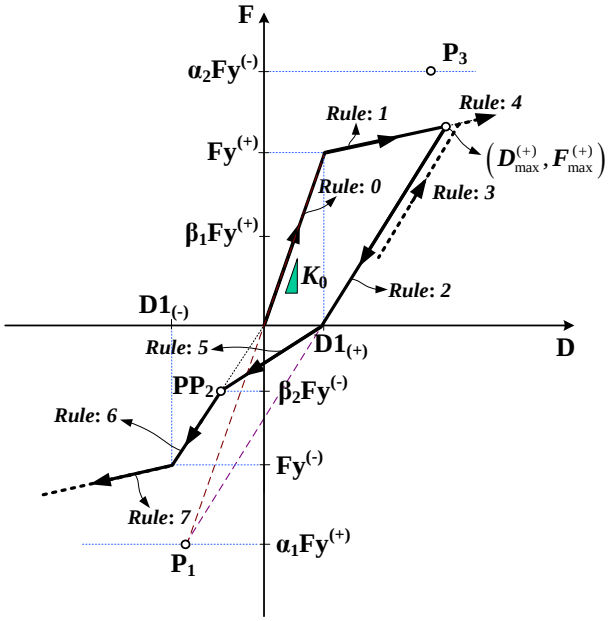

Fig 2.54 Rules for Hysteresis of Multi-Linear Plastic Pivot Type

3. i) When unloading takes place on the skeleton curve after both sides have yielded, the curve moves towards P1 or P3. (Rule: 8) However, it is directed towards the renewed P1* or P3* if η is not equal to 0.

   ii) If the restoring force exceeds 0, the curve is directed towards PP_2 or PP_4. However, it is directed towards the renewed PP_2^* or PP_4^* if η is not equal to 0. (Rule: 9)

   iii) If unloading takes place before reaching PP_2 or PP_4, the curve moves along the straight line passing through the unloading point and P4 (or P2). (Rule:10) If reloading takes place before the restoring force reaches back to 0, the curve moves back towards P3 (or P1). (Rule: 11)

   iv) If the restoring force exceeds 0, the curve moves along the line connecting the point of zero restoring force to P3 (or P1). (Rule: 12) When the curve intersects with a line connecting PP_2 (or PP_4) and $D_{max}^{(-)}$ (or $D_{max}^{(+)}$), it is directed towards $D_{max}^{(-)}$ (or $D_{max}^{(+)}$). (Rule: 13)

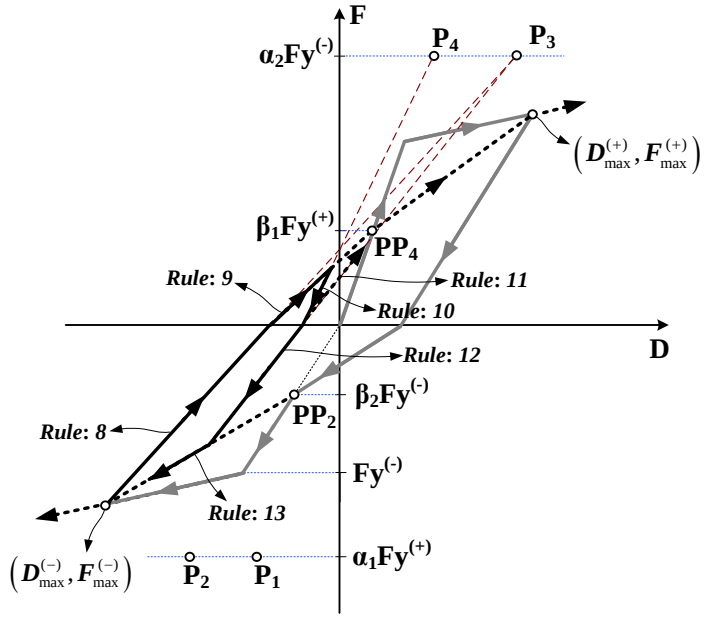

Fig 2.55 Rules for Hysteresis of Multi-Linear Plastic Pivot Type

Material Nonlinear Analysis

A fundamental difference between elastic and plastic material behaviors is that no permanent deformations occur in the structure in elastic behavior, whereas permanent or irreversible deformations occur in the structure in plastic behavior.

Plasticity theory

The components of static plastic strain are constituted by the following assumptions:

- Constitutive response is independent of the rate of deformation.
- Elastic response is not influenced by plastic deformation.
- Additive strain decomposition into elastic and plastic parts is defined by

$$\underset{\sim}{\varepsilon} = \underset{\sim}{\varepsilon}^{e} + \underset{\sim}{\varepsilon}^{p} \qquad (1)$$

where,

$\underset{\sim}{\varepsilon}$: total strains

$\underset{\sim}{\varepsilon}^{e}$: elastic strains

$\underset{\sim}{\varepsilon}^{p}$: plastic strains

And the following basic concepts are used to formulate the equations:

- Yield criteria to define the initiation of plastic deformation
- Flow rule to define the plastic straining
- Hardening rule to define the evolution of the yield surface with plastic str aining

Yield criteria

The yield function (or loading function), F, which defines the limit for the range of elastic response, is as follows (Fig. 2.18):

$$F(\underset{\sim}{\sigma}, \underset{\sim}{\varepsilon}^{p}, \kappa) = \sigma_{e}(\underset{\sim}{\sigma}, \underset{\sim}{\varepsilon}^{p}) - \kappa(\varepsilon_{p}) \le 0 \qquad (2)$$

where,

$\underset{\sim}{\sigma}$: current stresses

σ_e : equivalent or effective stress

κ : hardening parameter which is a function of $\underset{\sim}{\varepsilon}^p$

ε_p : equivalent plastic strain

In classical plasticity theory, a state of stress at which the value of the yield functio n becomes positive is not admissible. When yielding occurs, the state of stress is co rrected by scaling plastic strains until the yield function is reduced to zero. This pro cess is known as the plastic corrector phase or return mapping.

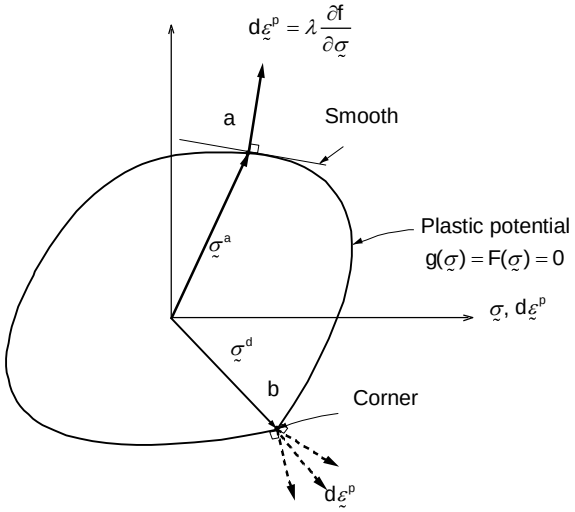

Fig 2.56 Geometric illustration of associated flow rule and singularity

Flow rule

The flow rule defines the plastic straining, which is expressed as follows (Fig 2.5 6):

$$d\underset{\sim}{\varepsilon}^p = d\lambda \frac{\partial g}{\partial \underset{\sim}{\sigma}} = d\lambda \underset{\sim}{\mathbf{b}} \tag{3}$$

where,

$\frac{\partial g}{\partial \tilde{\sigma}}$: the direction of plastic straining

$d\lambda$: plastic modulus which identifies the magnitude of plastic straining

The function g is termed as the ‘plastic potential’ function, which is generally defined in terms of stress invariants. If g=F, it is termed as ‘associated flow rule’, and if g≠F, it is referred to as ‘non-associative flow rule’.

The associated flow rule is adopted for all the yield criteria of MIDAS programs. A s the direction of the plastic strain vector is normal to the yield surface, the above e quation can be expressed as follows:

$$d\underset{\sim}{\varepsilon}^{p} = d\lambda \frac{\partial F}{\partial \underset{\sim}{\sigma}} = d\lambda \underset{\sim}{\mathbf{a}} \tag{4}$$

The corner or the flat surface in Fig 2.56 represents a singular point, which can not uniquely determine the direction of plastic flow. These points require special consi deration.

Hardening rule

The hardening rule defines the expansion and translation of the yield surface with p lastic straining as the material yields.

Depending on the method of defining the effective plastic strain, the hardening rule is classified into ‘strain hardening’ and ‘work hardening’. The strain hardening is d efined by the hypothesis of plastic incompressibility, and as such it is appropriate f or a material model, which is not influenced by hydrostatic stress. Accordingly, wo rk hardening, which is defined by plastic work, is more generally applicable than st rain hardening.

Also, depending on the type of change of yield surface, the hardening rule is classif ied into ‘isotropic hardening’, ‘kinematic hardening’ and ‘mixed hardening’ (Fig. 2. 57).

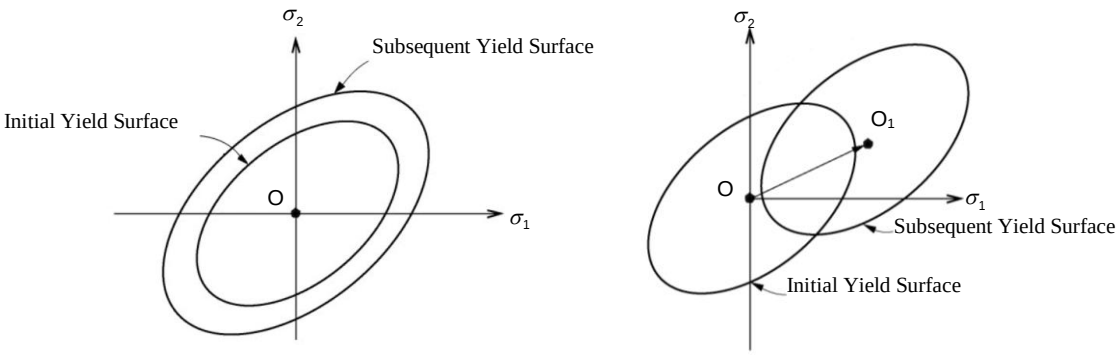

(a) Isotropic hardening rule (b) Kinematic hardening rule

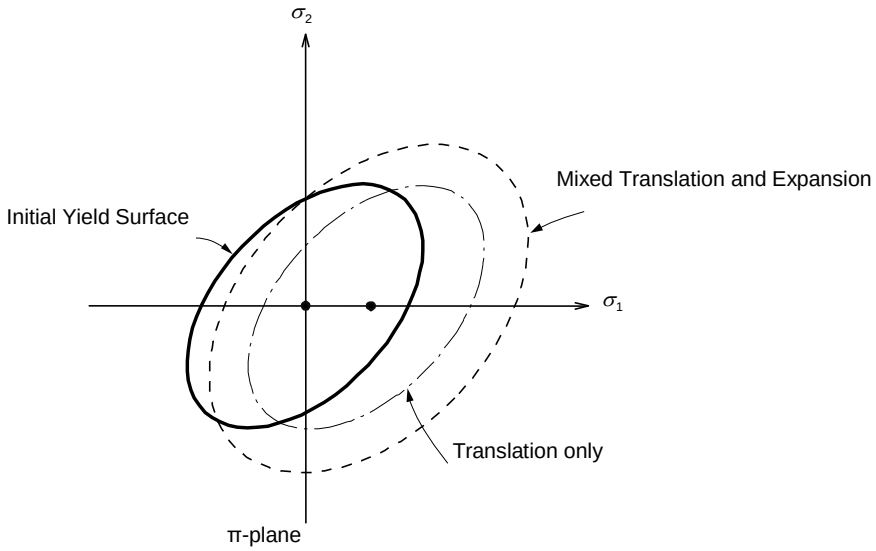

Fig 2.57 Mixed hardening with kinematic hardening

■ Classification by the method of defining the effective plastic strain

1. Strain hardening

The effective plastic strain in strain hardening is defined as follows:

$$d\varepsilon_p = \sqrt{\frac{2}{3}\left(d\underset{\sim}{\varepsilon}^p\right)^T d\underset{\sim}{\varepsilon}^p} = \sqrt{\frac{2}{3}\underset{\sim}{\mathbf{a}}^T\underset{\sim}{\mathbf{a}}}d\lambda \tag{5}$$

The effective plastic strain is derived from transforming the norm of plastic strains to conform to uniaxial strain with the assumption that there is no volumetric plastic deformation. Although this is applicable in principle only to Tresca or von Mises, i t is often applied to other cases because of numerical convenience.

2. Work hardening

The increment of plastic work is as follows:

$$dW_p = \underset{\sim}{\sigma}^T d\underset{\sim}{\varepsilon}^p = d\lambda \underset{\sim}{\mathbf{a}}^T \underset{\sim}{\sigma} \tag{6}$$

In the case of uniaxial strain, the increment of the plastic work is expressed as,

$$dW_p = \sigma_1 d\varepsilon_1 = \sigma_e d\varepsilon_p \tag{7}$$

Hence the effective plastic strain pertaining to work hardening is defined as follow s:

$$d\varepsilon_p = \frac{\underset{\sim}{\mathbf{a}}^T \underset{\sim}{\sigma}}{\sigma_e} d\lambda \tag{8}$$

■ Classification by the types of change of yield surface

1. Perfectly plastic

A perfectly plastic material does not change the yield surface even after plastic def ormation has taken place. The yield function then can be expressed as follows:

$$F\left(\underset{\sim}{\sigma},\kappa\right) = \sigma_e\left(\underset{\sim}{\sigma}\right) - \kappa \tag{9}$$

where,

κ : constant

2. Isotropic hardening

In the case of isotropic hardening, the yield surface expands uniformly as shown in Fig. 2.58(a). The yield function can be expressed as follows:

$$F\left(\underset{\sim}{\sigma},\kappa\right) = \sigma_e\left(\underset{\sim}{\sigma}\right) - \kappa\left(\varepsilon_p\right) \tag{10}$$

3. Kinematic hardening

In the case of kinematic hardening, the size of the yield surface remains unchanged and the center location of the yield surface is shifted as shown in Fig. 2.58(b). The yield function can be expressed as follows:

$$F\left(\underset{\sim}{\sigma},\underset{\sim}{\alpha},\kappa\right)=\sigma_e\left(\underset{\sim}{\sigma}-\underset{\sim}{\alpha}\right)-\kappa \tag{11}$$

where,

$\underset{\sim}{\alpha}$: the center coordinates of yield surface

κ : constant

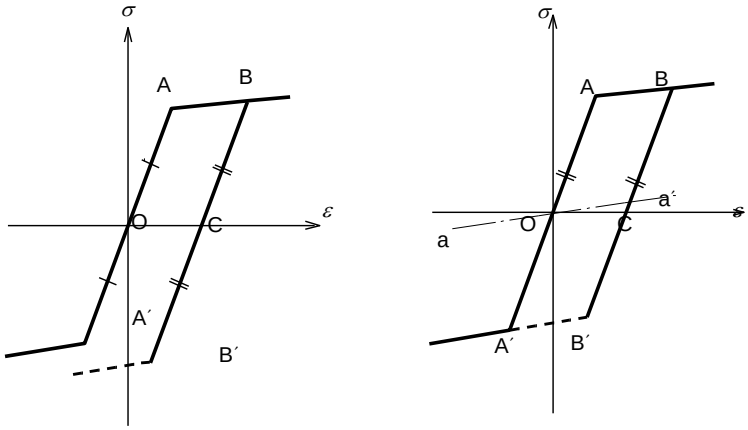

(a) Isotropic hardening (b) Kinematic hardening

Fig. 2.58 Hardening rule in 1-dimension

In kinematic hardening, it becomes important to determine the center coordinates of the subsequent yield surface, $\underset{\sim}{\alpha}$. In order to determine the "kinematic shift", $\underset{\sim}{\alpha}$, there exist Prager's hardening rule, Ziegler's hardening rule, etc.

The Prager's hardening rule can be expressed as,

$$d\underset{\sim}{\alpha}=C_p d\underset{\sim}{\varepsilon}^p=C_p\underset{\sim}{a}d\lambda \tag{12}$$

where,

C_p : Prager's hardening coefficient

This method may present some problems when it is used in the sub space of stress. For example, $d\underset{\sim}{\alpha}$ may not be 0 even any component of stresses is 0, which may no t only present translation of the yield surface. The Ziegler's hardening rule on the o

ther hand assumes that the rate of translation of the center, $d\underset{\sim}{\alpha}$, takes place in the d irection of the reduced-stress vector, $\underset{\sim}{\sigma}-\underset{\sim}{\alpha}$. Hence, it presents no such problem. T his hardening rule is expressed as follows:

$$d\underset{\sim}{\alpha}=d\mu\left(\underset{\sim}{\sigma}-\underset{\sim}{\alpha}\right)=C_z d\varepsilon_p\left(\underset{\sim}{\sigma}-\underset{\sim}{\alpha}\right) \tag{13}$$

where,
C_z : Ziegler's hardening coefficient

4. Mixed hardening
Mixed hardening is a hardening type, which represents the mix of isotropic hardeni ng and kinematic hardening, which is expressed as follows:

$$F\left(\underset{\sim}{\sigma},\underset{\sim}{\alpha},\kappa\right)=\sigma_e\left(\underset{\sim}{\sigma}-\underset{\sim}{\alpha}\right)-\kappa\left(\varepsilon_p\right) \tag{14}$$

? Constitutive equations

Standard plastic constitutive equations are formulated as below. Stress increments a re determined by the elastic part of the strain increments.

That is,

$$d\underset{\sim}{\sigma}=\underset{\sim}{\mathbf{D}}^e\left(d\underset{\sim}{\varepsilon}-d\underset{\sim}{\varepsilon}^p\right)=\underset{\sim}{\mathbf{D}}^e\left(d\underset{\sim}{\varepsilon}-d\lambda\underset{\sim}{\mathbf{a}}\right) \tag{15}$$

where,
$\underset{\sim}{\mathbf{D}}^e$: elastic constitutive matrix

In order to always maintain the stresses on the yield surface, the following consiste ncy condition needs to be satisfied.

$$dF=\frac{\partial F}{\partial\underset{\sim}{\sigma}}^T d\underset{\sim}{\sigma}+\frac{\partial F}{\partial\underset{\sim}{\varepsilon}^p}d\underset{\sim}{\varepsilon}^p+\frac{\partial F}{\partial\kappa}d\kappa=\underset{\sim}{\mathbf{a}}^T\underset{\sim}{\mathbf{D}}^e d\underset{\sim}{\varepsilon}-\left(\underset{\sim}{\mathbf{a}}^T\underset{\sim}{\mathbf{D}}^e\underset{\sim}{\mathbf{a}}+h\right)d\lambda=0 \tag{16}$$

where, h: plastic hardening modulus $\left(=\frac{d\sigma_e}{d\varepsilon_p}\right)$

Accordingly, the rate of infinitesimal stress increments can be obtained as follows:

$$d\underset{\sim}{\sigma} = \underset{\sim}{\mathbf{D}}^e d\underset{\sim}{\varepsilon} - d\lambda \underset{\sim}{\mathbf{D}}^e \underset{\sim}{\mathbf{a}}$$
$$d\underset{\sim}{\sigma} = \left(\underset{\sim}{\mathbf{D}}^e - \frac{\underset{\sim}{\mathbf{D}}^e \underset{\sim}{\mathbf{a}} \underset{\sim}{\mathbf{a}}^T \underset{\sim}{\mathbf{D}}^{eT}}{\underset{\sim}{\mathbf{a}}^T \underset{\sim}{\mathbf{D}}^e \underset{\sim}{\mathbf{a}} + h} \right) d\underset{\sim}{\varepsilon} \qquad (17)$$

When the full Newton-Raphson iteration procedure is used and if a consistent stiffn ess matrix is used, a much faster convergence can be achieved due to the second-or der convergence characteristic of the Newton-Raphson iteration procedure.

$$d\underset{\sim}{\sigma} = \underset{\sim}{\mathbf{D}}^e d\underset{\sim}{\varepsilon} - d\lambda \underset{\sim}{\mathbf{D}}^e \underset{\sim}{\mathbf{a}} - \lambda \underset{\sim}{\mathbf{D}}^e \frac{\partial \underset{\sim}{\mathbf{a}}}{\partial \underset{\sim}{\sigma}} d\underset{\sim}{\sigma}$$
$$d\underset{\sim}{\sigma} = \left(\underset{\sim}{\mathbf{R}} - \frac{\underset{\sim}{\mathbf{R}} \underset{\sim}{\mathbf{a}} \underset{\sim}{\mathbf{a}}^T \underset{\sim}{\mathbf{R}}^T}{\underset{\sim}{\mathbf{a}}^T \underset{\sim}{\mathbf{R}} \underset{\sim}{\mathbf{a}} + h} \right) d\underset{\sim}{\varepsilon} \qquad (18)$$

where,

$$\underset{\sim}{\mathbf{R}} = \left(\underset{\sim}{\mathbf{I}} + d\lambda \underset{\sim}{\mathbf{D}}^e \frac{\partial \underset{\sim}{\mathbf{a}}}{\partial \underset{\sim}{\sigma}} \right)^{-1} \underset{\sim}{\mathbf{D}}^e = \left(\underset{\sim}{\mathbf{I}} + d\lambda \underset{\sim}{\mathbf{D}}^e \underset{\sim}{\mathbf{A}} \right)^{-1} \underset{\sim}{\mathbf{D}}^e$$

? Stress integration

The following two methods can be used for the integration of stresses:

- Explicit forward Euler algorithm with sub-incrementation (Fig. 2.59 & 60)
- Implicit backward Euler algorithm (Fig. 2.61)

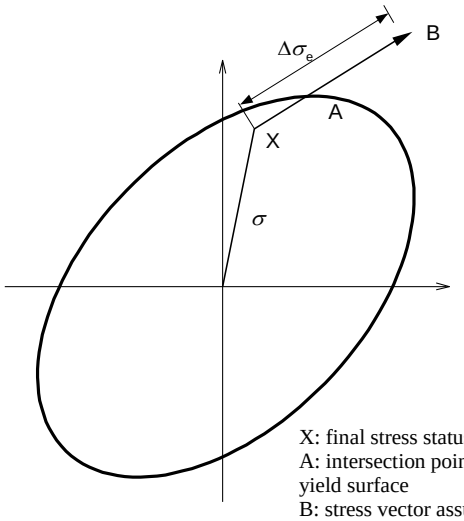

X: final stress status at the previous step
A: intersection point of stress increment and yield surface
B: stress vector assuming elastic straining

(a) Locating intersection point A

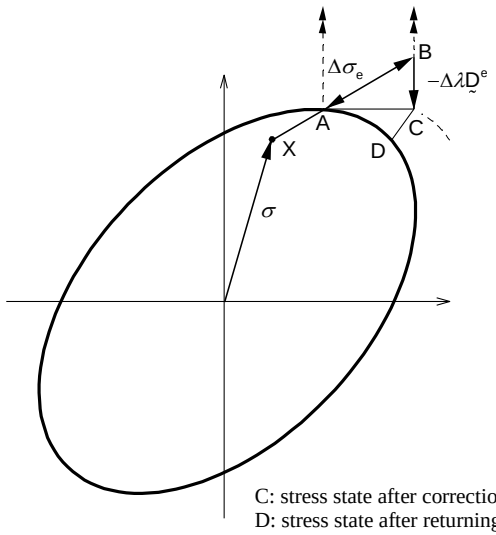

C: stress state after correction
D: stress state after returning the stress to the yield surface artificially

(b) Moving tangentially from A to C and subsequently correcting to D

Fig. 2.59 Explicit forward-Euler procedure

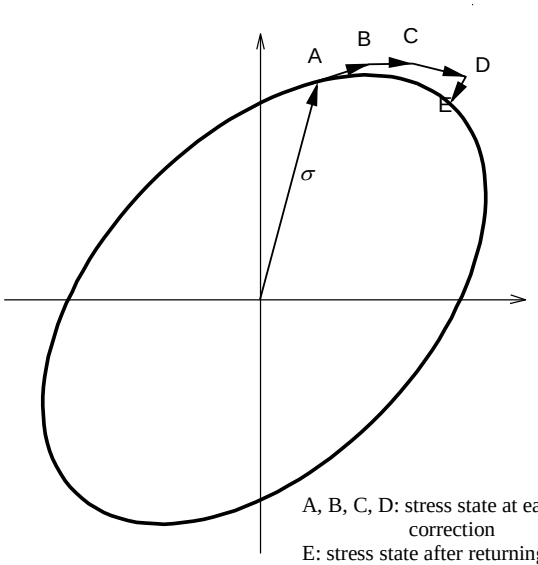

A, B, C, D: stress state at each sub-increment after correction
E: stress state after returning the stress to the yield surface artificially

Fig. 2.60 Sub-incrementation in Explicit forward-Euler procedure

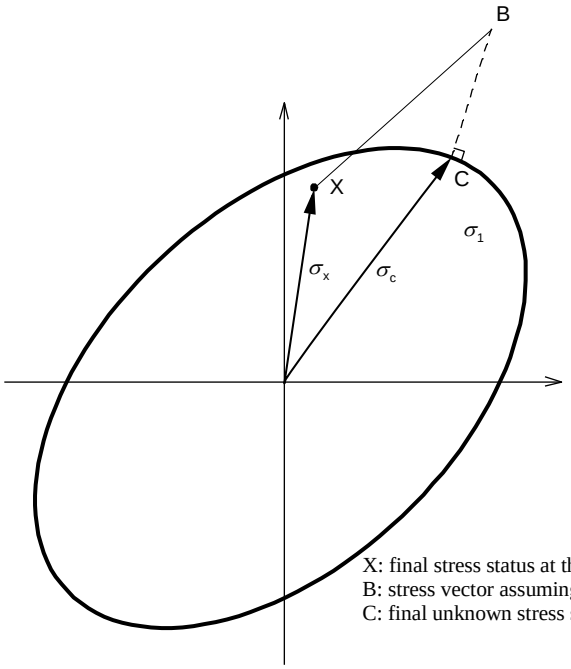

X: final stress status at the previous step
B: stress vector assuming elastic straining
C: final unknown stress state

Fig. 2.61 Implicit backward-Euler procedure

In the Forward-Euler algorithm, the hardening data and the direction of plastic flow are calculated at the intersection point, where elastic stress increments cross the yi eld surface (at point A in Fig. 2.60). Whereas in the Backward-Euler algorithm, the y are calculated at the final stress point (at point B in Fig. 2.61).

The Forward-Euler algorithm is relatively simple, and the stresses are directly integ rated. That is, it need not iterate at the Gauss points, but presents the following dra wbacks:

- It is conditionally stable.
- Sub-increments are required while correcting the stresses to obtain allowa ble accuracy.
- An artificial returning scheme is required to correct the stress state for drif t from the yield surface.

Also, this method does not permit formulating a consistent stiffness matrix.

The Implicit Backward-Euler algorithm is unconditionally stable and accurate with out sub-increments or artificial returning. However for general yield criteria, iterati ons are required at the Gauss points. Because a consistent stiffness matrix can be fo rmulated using this method, even if iterations are performed at the Gauss points, it i s more efficient if the Newton-Raphson iteration procedure is used.

Steps for applying the Explicit forward-Euler procedure

1. Calculate strain increments.

$$d\underset{\sim}{\varepsilon} = \underset{\sim}{\mathbf{B}} d\underset{\sim}{\mathbf{u}} \tag{19}$$

where,

$\underset{\sim}{\mathbf{B}}$: strain-displacement relation matrix

$d\underset{\sim}{\varepsilon}$: the changes of displacements

2. Calculate elastic stresses assuming elastic straining (at point B in Fig. 2.59(a)).

$$d\underset{\sim}{\sigma} = \underset{\sim}{\mathbf{D}}^{e} d\underset{\sim}{\varepsilon}$$
$$\underset{\sim}{\sigma}_{B} = \underset{\sim}{\sigma}_{X} + d\underset{\sim}{\sigma} \tag{20}$$

The Fig. 2.59 should be referenced for the subscripts in the equations above and be low.

3. If the calculated stresses remain on the yield surface, stress correcting is compl eted. If the stresses exist beyond the yield surface, the stresses are returned to t he yield surface by plastic straining.

4. Subsequently, the stresses at the intersection point are calculated. Elastic stress increments are divided into allowable stress increments and unallowable stres s increments; whereas, stresses at the intersection point are calculated by the fo llowing expressions (point A in Fig. 2.59(a)):

$$F\left(\underset{\sim}{\sigma}_X + (1-r)d\underset{\sim}{\sigma}\right) = 0$$
$$r = \frac{F_B}{F_B - F_X} \qquad (21)$$

5. Further straining would cause the stress location to traverse the yield surface. This is approximated by sub-dividing the unallowable stress increments, $rd\underset{\sim}{\sigma}$, into the m number of small stress increments (Fig. 2.60). The number of sub-i ncrements, m is directly related to the magnitude of the error resulted from a o ne step return, which is calculated as,

$$m = \mathrm{INT}\left(8\left(\sigma_{eB} - \sigma_{eA}\right)/\sigma_{eA}\right) + 1 \qquad (22)$$

6. If the final stress state does not lie on the yield surface, the following method o f artificial returning is used to return the stress to the yield stress (point E in Fi g. 2.60).

$$\delta\lambda_C = \frac{F_C}{\underset{\sim}{\mathbf{a}}_C^T \underset{\sim}{\mathbf{D}}^e \underset{\sim}{\mathbf{a}}_C + h}$$
$$\underset{\sim}{\sigma}_D = \underset{\sim}{\sigma}_C - \delta\lambda_C \underset{\sim}{\mathbf{D}}^e \underset{\sim}{\mathbf{a}}_C \qquad (23)$$

Notes

- The shape of the yield surface is corrected using the hardening rule at the en d of each sub-increment.
- Unloading is assumed to be elastic.

Steps for applying the Implicit backward-Euler procedure

The final stress in the Backward-Euler algorithm is calculated by the following equ ation:

$$\underset{\sim}{\sigma}_C = \underset{\sim}{\sigma}_B - d\lambda \underset{\sim}{\mathbf{D}}^e \underset{\sim}{\mathbf{a}}_C \tag{24}$$

The Fig. 2.61 should be referenced for the subscripts.

Since the point C in the equation (24) is unknown, the Newton iteration is used to e valuate the unknowns. Accordingly, a vector, $\underset{\sim}{\mathbf{r}}$, is set up to represent the differenc e between the current stresses and the backward-Euler stresses.

$$\underset{\sim}{\mathbf{r}} = \underset{\sim}{\sigma}_C - \left(\underset{\sim}{\sigma}_B - d\lambda \underset{\sim}{\mathbf{D}}^e \underset{\sim}{\mathbf{a}}_C \right) \tag{25}$$

Now, iterations are introduced in order to reduce $\underset{\sim}{\mathbf{r}}$ to 0 while the final stresses sho uld satisfy the yield criterion, f=0. Using assumed elastic stresses, a truncated Taylo r expansion is applied to the equation (25) to produce a new residual,

$$\underset{\sim}{\mathbf{r}}_n = \underset{\sim}{\mathbf{r}}_o + \dot{\underset{\sim}{\sigma}} + \dot{\lambda} \underset{\sim}{\mathbf{D}}^e \underset{\sim}{\mathbf{a}} \tag{26}$$

where,

$\dot{\underset{\sim}{\sigma}}$: the change in $\underset{\sim}{\sigma}$

$\dot{\lambda}$: the change in $d\lambda$

Setting the above equation to 0, and solving it for $\dot{\underset{\sim}{\sigma}}$, we obtain the following:

$$\dot{\underset{\sim}{\sigma}} = -\underset{\sim}{\mathbf{r}}_o - \dot{\lambda} \underset{\sim}{\mathbf{D}}^e \underset{\sim}{\mathbf{a}} \tag{27}$$

Similarly, a truncated Taylor expansion is applied to the yield function, which resul ts in the following:

$$F_{Cn} = F_{Co} + \frac{\partial F}{\partial \underset{\sim}{\sigma}}^T \dot{\underset{\sim}{\sigma}} + \frac{\partial F}{\partial \varepsilon_p} \dot{\varepsilon}_p = F_{Co} + \underset{\sim}{\mathbf{a}}_C^T \dot{\underset{\sim}{\sigma}} - h\dot{\lambda} = 0 \tag{28}$$

where,

ε_p : effective plastic strain

Hence, $\dot{\lambda}$ is obtained, and the final stress values can be obtained as well.

$$\dot{\lambda} = \frac{F_o - \mathbf{a}^T \mathbf{r}_o}{\mathbf{a}^T \mathbf{D}^e \mathbf{a} + h} \tag{29}$$

? Plastic material models

The following 4 types of general plastic models are used:

- Tresca & von Mises – suitable for ductile materials such as metals, which ex hibit plastic incompressibility (Fig. 2.62).
- Mohr-Coulomb & Drucker-Prager – suitable for materials such as concrete, rock and soils, which exhibit volumetric plastic deformations (Fig. 2.63).

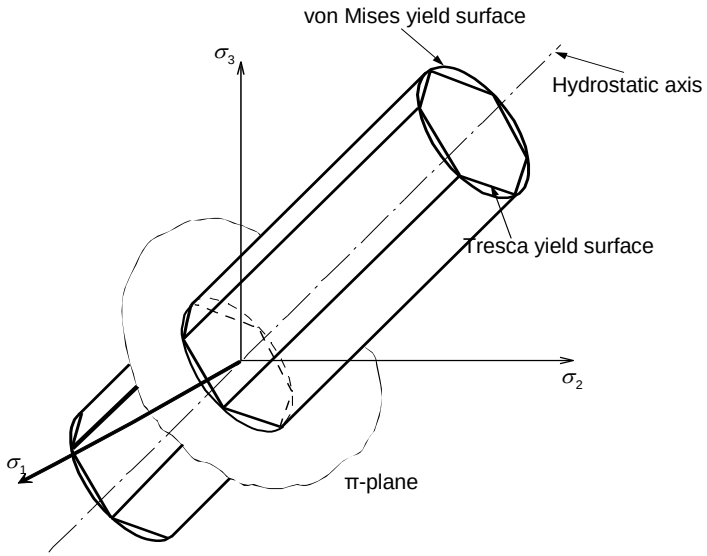

Fig 2.62 Tresca & von Mises yield criteria

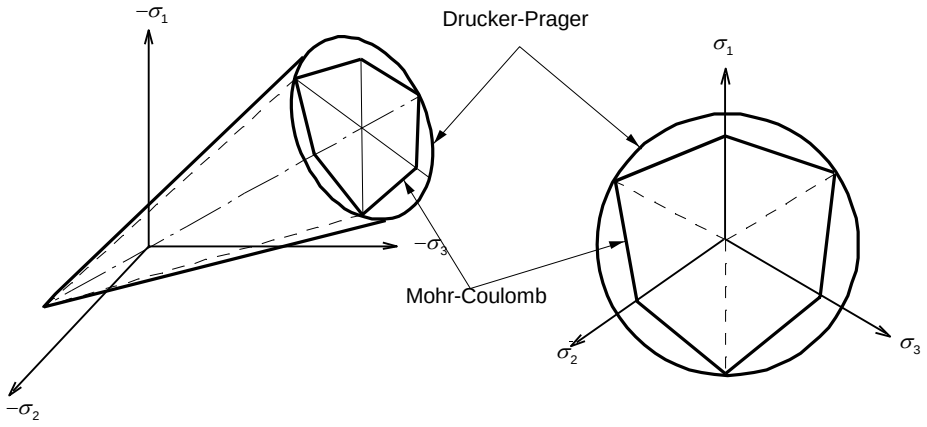

Fig 2.63 Mohr-Coulomb & Drucker-Prager yield criteria

Tresca criterion

The Tresca yield criterion is suitable for ductile materials such as metals, which ex hibit little volumetric plastic deformations. The yielding of a material begins when the maximum shear stress reaches a specified value. So if the principal stresses are $\sigma_1, \sigma_2, \sigma_3$ $(\sigma_1 \geq \sigma_2 \geq \sigma_3)$, the yield function becomes the equation (30).

$$F(\underset{\sim}{\sigma}, \kappa) = \sigma_1 - \sigma_3 - \kappa(\varepsilon_p) \tag{30}$$

Numerical problems arise when the stress point lies at a singular point on the yield surface, which occurs when the lode angle θ approaches $\pm$ 30°. In such cases, the stress integration scheme must be corrected.

Von Mises criterion

The Von Mises criterion is a most widely used yield criterion for metallic materials. It is based on distortional strain energy, and the yield function is expressed as follo ws:

$$F\left(\underset{\sim}{\sigma},\kappa\right)=\sqrt{3J_2}-\kappa\left(\varepsilon_p\right) \tag{31}$$

where,
J2: second deviatoric stress invariant

Mohr-Coulomb criterion

The Mohr-Coulomb criterion is suitable for such materials as concrete, rock and so ils, which exhibit volumetric plastic deformations. The Mohr-Coulomb yield criteri on is a generalization of the Coulomb's friction rule, which is defined by,

$$F\left(\underset{\sim}{\sigma},\kappa\right)=\tau-\left(c-\sigma_n\tan\phi\right) \tag{32}$$

where,

τ : the magnitude of shearing stress
σ_n : normal stress
c : cohesion
ϕ : internal friction angle

The cohesion, c, and the internal friction angle, ϕ, are dependent upon the strain h ardening parameter, κ.

Similar to the Tresca criterion, numerical problems occur when the stress point lies at a singular point on the yield surface. For the Mohr-Coulomb criterion, such num erical problems occur as the lode angle, θ, approaches $\pm 30°$ or at the apex points. Hence, the stress integration scheme must be corrected for the two cases.

Drucker-Prager criterion

The Drucker-Prager criterion is suitable for such materials as soils, concrete and rock, which exhibit volumetric plastic deformations. This criterion is a smooth approximation of the Mohr-Coulomb criterion and is an expansion of the von Mises criterion. The yield function includes the effect of hydrostatic stress, which is defined as follows:

$$F(\underset{\sim}{\sigma},\kappa) = \frac{2\sin\phi}{\sqrt{3}(3-\sin\phi)} I_1 + \sqrt{J_2} - \frac{6c\cos\phi}{\sqrt{3}(3-\sin\phi)} \quad (33)$$

where,
I: first stress invariant

For the Drucker-Prager criterion, Numerical problems occur when the stress point lies at the apex points of the yield surface.

Masonry Model

■ Introduction

Masonry, though a traditional material which has been used for construction for ages, is a complex material. It is a complex composite material, and its mechanical behavior, which is influenced by a large number of factors, is not generally well understood. In engineering practice, many engineers have adopted an elastic analysis for the structural behavior of masonry using rather arbitrary elastic parameters and strengths of masonry. Such analyses can give wrong and misleading results. The proper way to obtain elastic parameters of masonry is through a procedure of homogenization described in the next section.

The effect of nonlinearity (i.e., tensile crack, compressive failure, and so on.) to the behavior of masonry model is very significant and must be accurately taken into account in analyzing the ultimate behavior of masonry structures. Having their own advantages and restrictions, many researches have been conducted, for instance, "Equivalent nonlinear stress-strain concept" of J. S. Lee & G. N. Pande[1], Tomaževic's "Story-Mechanism"[2], the finite element analysis approach of Calderini & Lagomarsino[3], and "Equivalent frame idealization" by Magenes et al.[4]. Thus, in practical application of crack effect to the masonry structure, one must be well aware of unique characteristics of each of the nonlinear models for masonry structure. The main concept of the nonlinear masonry model adopted in the masonry model of MIDAS is based on the line of theory of J.S. Lee & G. N. Pande and described later.

■ Homogenization Techniques in Masonry Structures

Masonry structures can be numerically analyzed if an accurate stress-strain relationship is employed for each constituent material and each constituent material is then separated individually. However, a three-dimension-analysis of a masonry structure involving even a very simple geometry would require a large number of elements and the nonlinear analysis of the structure would certainly be intractable. To overcome this computational difficulty, the orthotropic material properties proposed by Pande et al.[5,6] can be introduced to model the masonry structure in the sense of an equivalent homogenized material. The equivalent material properties introduced in Pande et al. are based on a strain energy concept. The details of the procedure to obtain equivalent elastic parameters based on the homogenization technique are given in the following. The basic assumptions made to derive the equivalent material properties through the strain energy considerations are:

1. Brick and mortar are perfectly bonded
2. Head or bed mortar joints are assumed to be continuous

The second assumption is necessary in the homogenization procedure, and it has be en shown[7] that the assumption of continuous head joints instead of staggered joints, as they appear in practice, does not have any significant effect on the stress states o f the constituent materials.

Let the orthotropic material properties of the masonry panel be denoted by $\bar{E}_x$, $\bar{E}_y$, $\bar{E}_z$, $\bar{\nu}_{xy}$, $\bar{\nu}_{xz}$, $\bar{\nu}_{yz}$, $\bar{G}_{xy}$, $\bar{G}_{yz}$, $\bar{G}_{xz}$, Fig. 2.64. The stress/strain relationship of the homogenized masonry material is represented by

$$\bar{\sigma} = \left[\bar{D}\right]\bar{\varepsilon} \tag{1}$$

or

$$\bar{\varepsilon} = \left[\bar{C}\right]\bar{\sigma} \tag{2}$$

where,

$$\bar{\sigma} = \left\{\bar{\sigma}_{xx}\bar{\sigma}_{yy}\bar{\sigma}_{zz}\bar{\tau}_{xy}\bar{\tau}_{yz}\bar{\tau}_{xz}\right\}^T$$
$$\bar{\varepsilon} = \left\{\bar{\varepsilon}_{xx},\bar{\varepsilon}_{yy},\bar{\varepsilon}_{zz},\bar{\gamma}_{xy},\bar{\gamma}_{yz},\bar{\gamma}_{xz}\right\}^T \tag{3}$$

are the vectors of stresses and strains in the Cartesian coordinate system.

$$\left[\bar{C}\right]=\begin{bmatrix} \frac{1}{\bar{E}_x} & -\frac{\bar{\nu}_{xy}}{\bar{E}_x} & -\frac{\bar{\nu}_{xz}}{\bar{E}_x} & 0 & 0 & 0 \\ -\frac{\bar{\nu}_{yx}}{\bar{E}_y} & \frac{1}{\bar{E}_y} & -\frac{\bar{\nu}_{yz}}{\bar{E}_y} & 0 & 0 & 0 \\ -\frac{\bar{\nu}_{zx}}{\bar{E}_z} & -\frac{\bar{\nu}_{zy}}{\bar{E}_z} & \frac{1}{\bar{E}_z} & 0 & 0 & 0 \\ 0 & 0 & 0 & \frac{1}{\bar{G}_{xy}} & 0 & 0 \\ 0 & 0 & 0 & 0 & \frac{1}{\bar{G}_{yz}} & 0 \\ 0 & 0 & 0 & 0 & 0 & \frac{1}{\bar{G}_{xz}} \end{bmatrix} \quad (4)$$

The details of the derivation of orthotropic elastic material properties of masonry in terms of the properties of the constituents are given in 'Orthotropic Properties of Masonry based on Strain Energy Rule'. In the mathematical theory of homogenization, there has been an issue relating to the sequence of homogenization, if there are more than two constituents. For example, if we homogenize bricks and mortar in head joints first and then homogenize the resulting material with bed joints at the second stage, then the result may not be the same if we had followed a different sequence. However, it has been shown in the case of masonry, the sequence of homogenization does not have any significant influence. Here we present in 'Orthotropic Properties of Masonry based on Strain Energy Rule' equations for equivalent properties if bricks and bed joints are homogenized first. It is noted that, in Pande et al., the equivalent material properties were derived with the brick and the head mortar joint being homogenized first. The equivalent orthotropic material properties derived from the homogenization procedure are used to construct the stiffness matrix in the finite element analysis procedure, and from this, equivalent stress/strains are then calculated. The stresses/strains in the constituent materials can be evaluated through structural relationships, i.e.,

$$\sigma_b = [S_b]\bar{\sigma}$$
$$\sigma_{bj} = [S_{bj}]\bar{\sigma} \quad (5)$$
$$\sigma_{hj} = [S_{hj}]\bar{\sigma}$$

where subscripts b, bj and hj represent brick, bed joint and head joint respectively.

The structural relationships for strains can similarly be established. The structural matrices S are listed in 'Structural Relationship of Masonry'. From the results liste d in Pande et al., it can be shown that the orthotropic material properties are functio ns of

1. Dimensions of the brick, length, height and width
2. Young's modulus and Poisson's ratio of the brick material
3. Young's modulus and Poisson's ratio of the mortar in the head and bed joints
4. Thickness of the head and bed mortar joints

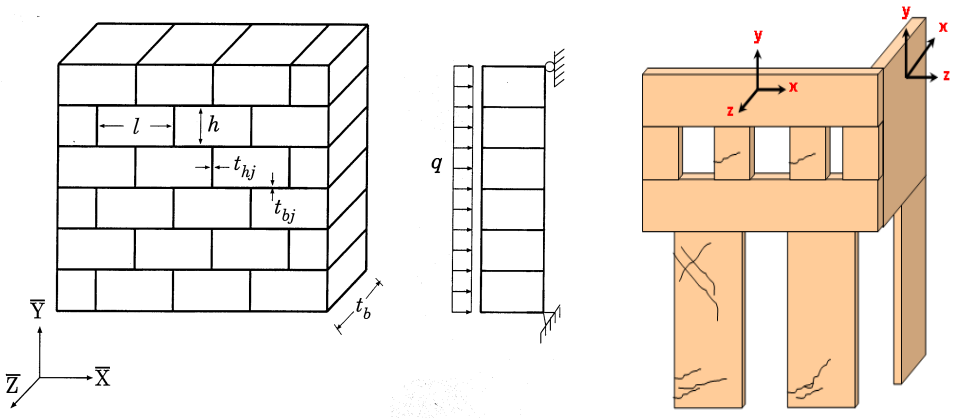

(a) Reference System *(b) Example of local axis rule*

Fig.2.64 Coordinate System used in Masonry Panel

It must be noted that the geometry of masonry has to be modeled with reference to the above figure in which the presented axes are the same as the element local axes of the MIDAS program. Accordingly, it is recommended that the gravity direction be parallel with the element local y direction of the MIDAS program. This is becau

se the homogenization is performed on the local x-y plane. So the generated orthotr opic material properties are also based on the axis system. Since the homogenizatio n is performed only in the local x-y plane, the stiffness in each direction differs fro m each other. It should be also noted that the global axis system of the MIDAS pro gram has no effect on the masonry model. For clarity, the local axes of a three-dim ensional masonry structure is shown in Fig. 2.64(b).

■ Criteria for Failure for Constituents

Failure of masonry can be based on the micromechanical behavior. At every loadin g step, once the equivalent stresses/strains in the masonry structure are calculated, s tresses/strains of the constituent materials can be derived on the basis of the structu ral relationship in eq. (5). The maximum principal stress is calculated in each const ituent level (i.e., Brick, Bed joint, and Head joint) and is compared to the tensile str ength defined by the user. If the maximum principal stress exceeds the tensile stren gth at the current step, the stiffness contribution of the constituent to the whole ele ment is forced to become ineffective. For the nonlinear stress-strain relation of con stituents, even the elastio-perfectly plastic relation could be simulated. This can be numerically implemented by substituting the stiffness of the constituent with very s mall value as $E_i \square zero$ (where the subscript 'i' could be brick, bed joint, or head j oint). If the user sets the 'Stiffness Reduction Factor' as very small value, the maso nry model will behave nonlinearly. By the same reason, if the 'Stiffness Reduction Factor' is set to be a unit value, the masonry model will behave elastically (refer to the figure 2.65 below).

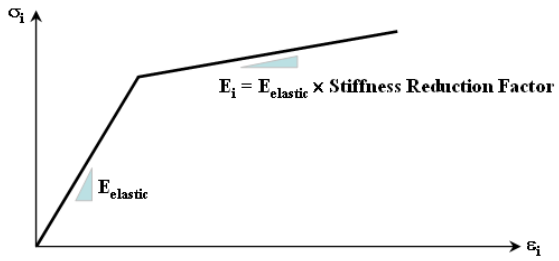

Fig.2.65 Stress-Strain of a constituent of masonry model

In this way, the local failure mode can be evaluated. For better understanding of thi s kind of equivalent nonlinear stress-strain relationship theory, see Lee et al.(1996). Once cracking occurs in any constituent material, the effect is smeared onto the ne ighboring equivalent orthotropic material through another homogenization.
Although there are a number of criteria for the masonry model such as Mohr-Coulo

mb and so on, the masonry model in MIDAS currently determines the tensile failur e referring only to the user-input tensile strength. More advanced failure criteria are developed in the near future based on the abundant research. After the tensile crac ks occur, the crack positions can be traced by post processor of solid stresses.

■ Analysis methods of masonry structures

For the performance assessment of masonry structure, it is generally suggested that the structure needs to be analyzed in both out-of-plane damage and in-plane dama ge concepts.

Firstly, referring to the figure 2.66, the out-of-plane damage which is also called as “first-mode collapse” or “local damage” involves any kinds of local failure such as tensile failure and partial overturn of masonry wall.

For the precise analysis of out-of-plane damage of masonry structure, part of the str ucture is modeled with detailed finite elements such as material nonlinear models a nd interface elements to simulate discrete mortar cracking, interface interaction, sh ear failure, and etc. This type analysis is numerically expensive and difficult to sim ulate real structural response and is not the case in the masonry model of the curren t MIDAS program.

Secondly, in the reference of figure 2.67, the in-plane damage which is also called as “second-mode collapse” means the structural response to the external loading as a whole. MIDAS is providing homogenized nonlinear masonry model for this kind of analysis. Tensile cracks in mortar and brick can be traced with a simply defined nonlinear masonry material model. It should be noted that the nonlinear behavior o f masonry structure is very sensitive to the material properties such as tensile streng th and reduced stiffness after cracking. So proper material properties should be care fully defined by thorough investigation and experimental consideration.

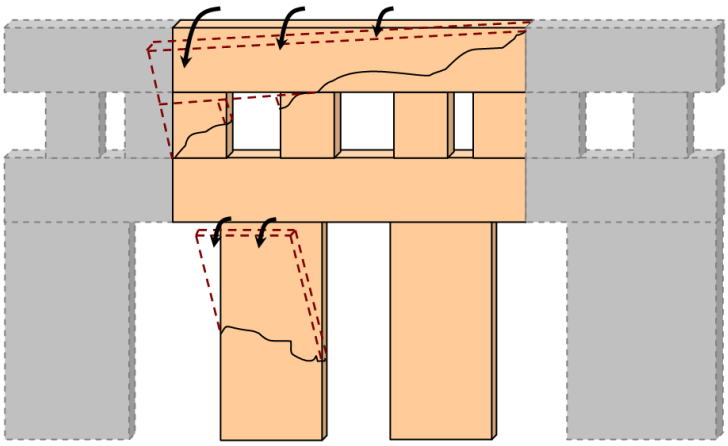

Fig.2.66 Example of out-of-plane damage mechanism

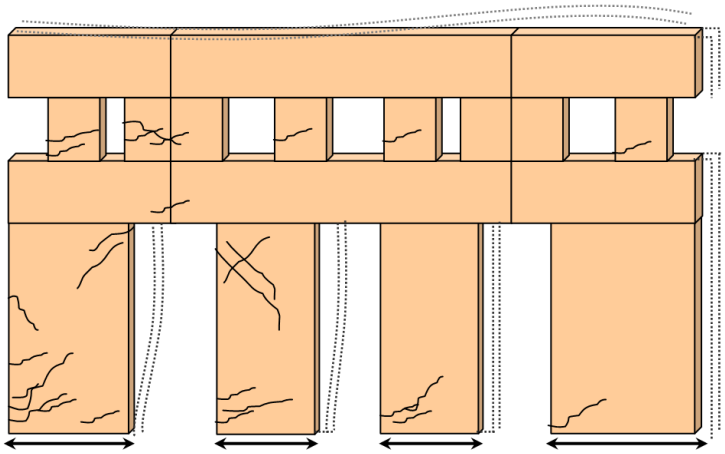

Fig.2.67. Example of in-plane damage mechanism

It is widely recognized that the satisfactory behavior of masonry structure is retaine d only when the out-of-plane damage is well prevented, and the structure shows in-plane reaction as a whole. Although these two types of damage take place simultan eously, the separate detailed analyses are conducted for practical reasons.

■ Importance of nonlinear analysis of masonry model

To appreciate the importance of nonlinear masonry model, as shown in figure 2.68, a two story masonry wall is analyzed linearly and nonlinearly. As suggested by Ma genes[8], the wall model with openings is subjected to in-plane simple pushover load ings. The model has 6m-width and 6.5m-height and is meshed by eight node solid elements.

Firstly, the model is analyzed linearly, which means the stiffness reduction factor is set to be a unit value, '1'. And then, for nonlinear behavior, the stiffness reduction factor is reduced to a very small value of '1.e-10', which leads to elasto-plastic beh avior. The horizontal forces are loaded incrementally over 10 steps, and the cracked deformed shape at the step 8 is presented in figure 2.69. The marked points are rep resenting crack points, and the contour results are based on effective stress results.

In both cases, two models have the same homogenization procedure. The only diffe rence is the reduced stiffness of a constituent at which the crack took place. The for ce-displacement result shown in figure 2.70 gives that the analytic behavior is signi ficantly dependent on the stiffness of the masonry constituents after cracking. The deformation is extracted from the nodal results of the top right point.

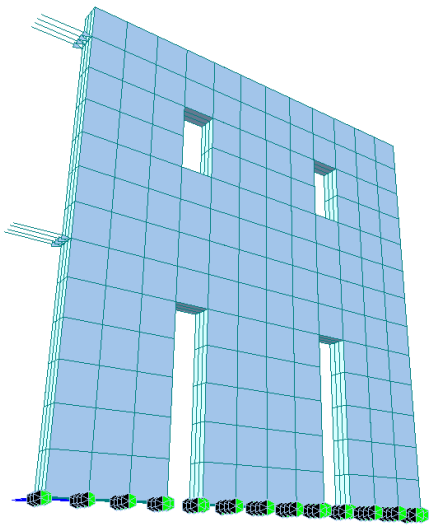

Fig.2.68 Two story masonry wall model

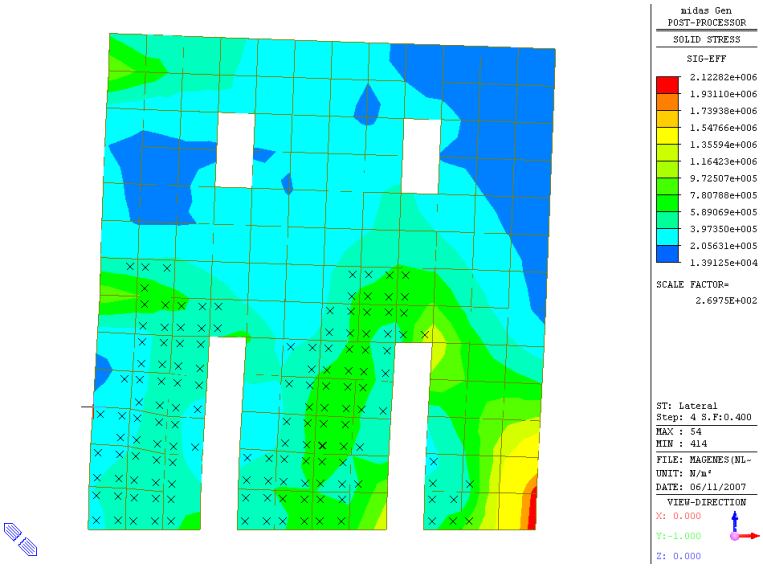

Fig.2.69 Cracked and deformed shape at step 8

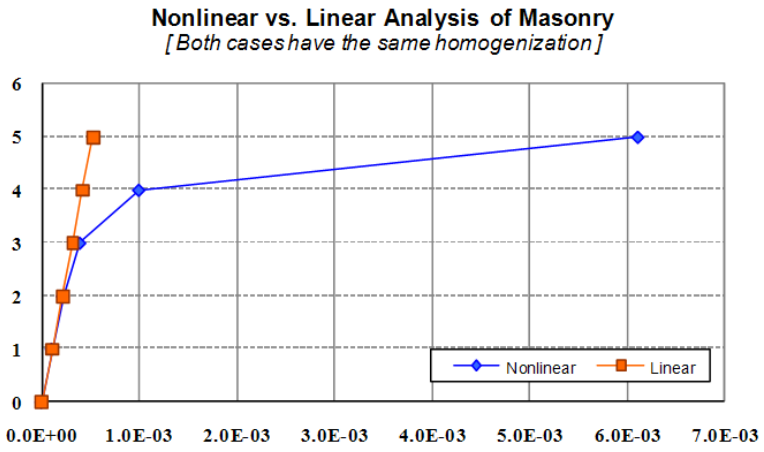

Fig.2.70 Force-deformation results

In the reference of figure 58, the significance of nonlinearity is more convincing if we consider the resultant base shear results. In the figure 2.71, the horizontal axis s hows the pier positions, and the vertical axis represents the resultant shear of each pier divided by the total shear force. In the left pier, the base shear result of the nonl inear masonry model is almost half of that of the linear masonry model. On the co ntrary, in the right pier, the resultant base shear of the nonlinear model is almost twi ce that of the linear masonry model. Also, the overall shear force distribution is quit e different. The linear masonry model shows symmetric force distribution about the mid pier. In the nonlinear masonry model, however, the right pier has the largest sh ear force results. From this consideration, it should be noted that the shear forces af ter crack are shared not by elastic stiffness but by the strength capacity as suggeste d by Magenes(2006).

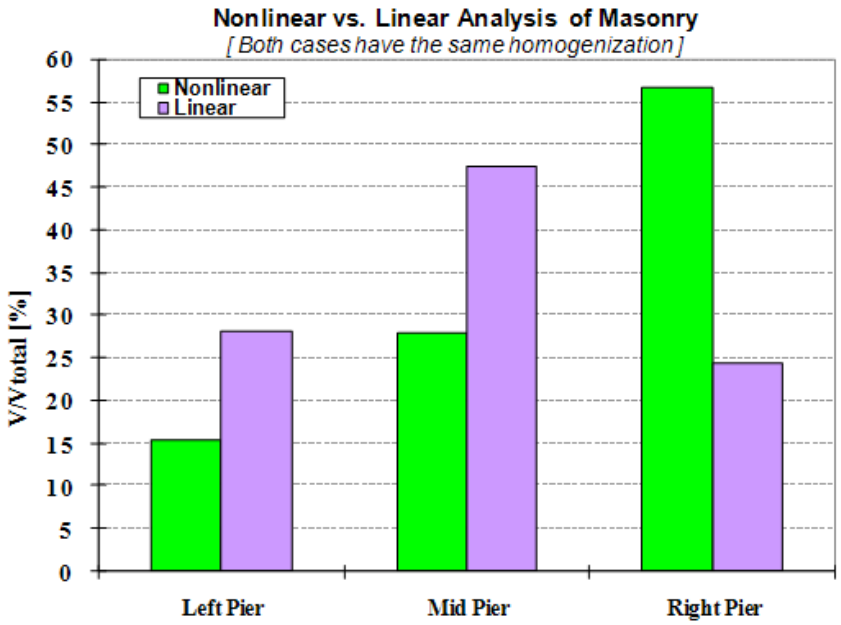

Fig.2.71 Base shear force distribution

■ Orthotropic Properties of Masonry based on Strain Energy Rule

Orthotropic material properties of masonry can be derived employing a strain energy concept, and the details are given in the following. It is noted that homogenization is performed between brick and bed joint first. Similar details can also be obtained when brick and head joint are homogenized first.

Referring to Fig. 2.64, volume fraction of brick and bed joint can be described as

$$\mu_b = \frac{h}{h + t_{bj}}; \qquad \mu_{bj} = \frac{t_{bj}}{h + t_{bj}} \tag{6}$$

where subscript b and bj represent the brick and bed joint respectively. If the brick and bed joint are homogenized in the beginning, the following stress/strain components in the sense of volume averaging can be established:

$$\sigma = \left\{\sigma_{xx}, \sigma_{yy}, \sigma_{zz}, \tau_{xy}, \tau_{yz}, \tau_{zx}\right\}^T$$
$$\varepsilon = \left\{\varepsilon_{xx}, \varepsilon_{yy}, \varepsilon_{zz}, \gamma_{xy}, \gamma_{yz}, \gamma_{zx}\right\}^T \tag{7}$$

where,

$$\sigma_{xx} = \frac{1}{V}\sum_{i=1}^{2}\int_{Vi}\sigma_{xxi}dV_i \tag{8}$$

$$\varepsilon_{xx} = \frac{1}{V}\sum_{i=1}^{2}\int_{Vi}\varepsilon_{xxi}dV_i \tag{9}$$

and i=1 for brick, i=2 for bed joint. For each strain component,

$$\varepsilon_{xxi} = \frac{1}{E_i}\left(\sigma_{xxi} - \nu_i\sigma_{yyi} - \nu_i\sigma_{zzi}\right)$$
$$\varepsilon_{yyi} = \frac{1}{E_i}\left(\sigma_{yyi} - \nu_i\sigma_{xxi} - \nu_i\sigma_{zzi}\right)$$
$$\varepsilon_{zzi} = \frac{1}{E_i}\left(\sigma_{zzi} - \nu_i\sigma_{xxi} - \nu_i\sigma_{yyi}\right)$$
$$\gamma_{xyi} = \frac{\tau_{xyi}}{G_{xyi}}$$
$$\gamma_{yzi} = \frac{\tau_{yzi}}{G_{yzi}}$$
$$\gamma_{xzi} = \frac{\tau_{xzi}}{G_{xzi}} \tag{10}$$

Now the strain energy for each component and 1 layer prism can be denoted as

$$U_{re} = \sum_{i=1}^{2}\frac{1}{2}\int_{Vi}\left(\sigma_{xxi}\varepsilon_{xxi} + \sigma_{yyi}\varepsilon_{yyi} + \sigma_{zzi}\varepsilon_{zzi} + \tau_{xyi}\gamma_{xyi} + \tau_{yzi}\gamma_{yzi} + \tau_{xzi}\gamma_{xzi}\right)dV_i$$
$$U_e = \frac{1}{2}\int_V\left(\sigma_{xx}\varepsilon_{xx} + \sigma_{yy}\varepsilon_{yy} + \sigma_{zz}\varepsilon_{zz} + \tau_{xy}\gamma_{xy} + \tau_{yz}\gamma_{yz} + \tau_{xz}\gamma_{xz}\right)dV \tag{11}$$

where ‘re’ and ‘e’ represent the component and layer prism respectively, and it is obvious that

$$U_{re} = U_e \tag{12}$$

Introduce auxiliary stresses/strains,

$$\begin{aligned}
\sigma_{xxi} &= \sigma_{xx} + A_{xxi} \\
\sigma_{yyi} &= \sigma_{yy} \\
\sigma_{zzi} &= \sigma_{zz} + A_{zzi} \\
\tau_{xyi} &= \tau_{xy} \\
\tau_{yzi} &= \tau_{yz} \\
\tau_{xzi} &= \tau_{xz} + A_{xzi}
\end{aligned} \tag{13}$$

and

$$\begin{aligned}
\varepsilon_{xxi} &= \varepsilon_{xx} \\
\varepsilon_{yyi} &= \varepsilon_{yy} + B_{yyi} \\
\varepsilon_{zzi} &= \varepsilon_{zz} \\
\gamma_{xyi} &= \gamma_{xy} + B_{xyi} \\
\gamma_{yzi} &= \gamma_{yz} + B_{yzi} \\
\gamma_{xzi} &= \gamma_{xz}
\end{aligned} \tag{14}$$

then, from eqs. (8) & (13),

$$\begin{aligned}
\sum_{i=1}^{2} \mu_i A_{xxi} &= 0 \\
\sum_{i=1}^{2} \mu_i A_{zzi} &= 0 \\
\sum_{i=1}^{2} \mu_i A_{xzi} &= 0
\end{aligned} \tag{15}$$

and

$$\sum_{i=1}^{2} \mu_i B_{yyi} = 0$$
$$\sum_{i=1}^{2} \mu_i B_{xyi} = 0$$
$$\sum_{i=1}^{2} \mu_i B_{yzi} = 0 \qquad (16)$$

where, μ_1 and μ_2 represent the volume fraction of brick and bed joint respectively.

From eqs. (10),(14) & (16),

$$E_x = \alpha - \frac{\zeta^2}{\alpha}$$
$$\frac{1}{E_y} = \frac{\mu_b}{E_b} + \frac{\mu_{bj}}{E_{bj}} + 2\chi_b\left(\frac{\nu_{zy}}{E_z} - \frac{\nu_b}{E_b}\right) + 2\chi_{bj}\left(\frac{\nu_{zy}}{E_z} - \frac{\nu_{bj}}{E_{bj}}\right)$$
$$E_z = \alpha - \frac{\zeta^2}{\alpha}$$
$$\frac{1}{G_{xy}} = \sum_i \frac{\mu_i}{G_{xyi}}$$
$$\frac{1}{G_{yz}} = \sum_i \frac{\mu_i}{G_{yzi}}$$
$$G_{xz} = \sum_i \left(\mu\, G_{xzi}\right)$$
$$\nu_{xy} = \chi - \frac{\chi\zeta}{\alpha}$$
$$\nu_{xz} = \frac{\zeta}{\alpha}$$
$$\nu_{zy} = \chi - \frac{\chi\zeta}{\alpha} \qquad (17)$$

where,

$$\alpha = \frac{\mu_b E_b \left(1-\nu_{bj}^2\right) + \mu_{bj} E_{bj} \left(1-\nu_b^2\right)}{\left(1-\nu_b^2\right)\left(1-\nu_{bj}^2\right)}$$

$$\zeta = \frac{\mu_b \nu_b E_b \left(1-\nu_{bj}^2\right) + \mu_{bj} \nu_{bj} E_{bj} \left(1-\nu_b^2\right)}{\left(1-\nu_b^2\right)\left(1-\nu_{bj}^2\right)}$$

$$\chi_b = \frac{\mu_b \nu_b}{1-\nu_b}$$

$$\chi_{bj} = \frac{\mu_{bj} \nu_{bj}}{1-\nu_{bj}}$$

$$\chi = \chi_b + \chi_{bj} \tag{18}$$

and the relationship below can also be established.

$$\nu_{yx} = \nu_{xy} \frac{E_y}{E_x} \tag{19}$$

For the system of masonry panel, the homogenization is applied to the layered mat erial and head joint based on the assumption of continuous head joint. Now, volum e fractions of the constituent materials are

$$\mu_{eq} = \frac{l}{l+t_{hj}}; \qquad \mu_{hj} = \frac{t_{hj}}{l+t_{hj}} \tag{20}$$

where, subscript eq and hj represent layered material and head joint respectively. A s in the previous case, the following stress/strain components in the sense of volum e averaging can be established:

$$\bar{\sigma} = \left\{\bar{\sigma}_{xx}, \bar{\sigma}_{yy}, \bar{\sigma}_{zz}, \bar{\tau}_{xy}, \bar{\tau}_{yz}, \bar{\tau}_{zx}\right\}^T$$

$$\bar{\varepsilon} = \left\{\bar{\varepsilon}_{xx}, \bar{\varepsilon}_{yy}, \bar{\varepsilon}_{zz}, \bar{\gamma}_{xy}, \bar{\gamma}_{yz}, \bar{\gamma}_{zx}\right\}^T \tag{21}$$

Introducing auxiliary stresses/strains,

$$\begin{aligned}
\bar{\sigma}_{xxi} &= \bar{\sigma}_{xx} \\
\bar{\sigma}_{yyi} &= \bar{\sigma}_{yy} + C_{yyi} \\
\bar{\sigma}_{zzi} &= \bar{\sigma}_{zz} + C_{zzi} \\
\bar{\tau}_{xyi} &= \bar{\tau}_{xy} \\
\bar{\tau}_{yzi} &= \bar{\tau}_{yz} + C_{yzi} \\
\bar{\tau}_{xzi} &= \bar{\tau}_{xz}
\end{aligned} \tag{22}$$

And

$$\begin{aligned}
\bar{\varepsilon}_{xxi} &= \bar{\varepsilon}_{xx} + D_{xxi} \\
\bar{\varepsilon}_{yyi} &= \bar{\varepsilon}_{yy} \\
\bar{\varepsilon}_{zzi} &= \bar{\varepsilon}_{zz} \\
\bar{\gamma}_{xyi} &= \bar{\gamma}_{xy} + D_{xyi} \\
\bar{\gamma}_{yzi} &= \bar{\gamma}_{yz} \\
\bar{\gamma}_{xzi} &= \bar{\gamma}_{xz} + D_{xzi}
\end{aligned} \tag{23}$$

where, i=1 & i=2 represent the layered material and head joint respectively. Follow ing the same procedure and defining the following coefficients,

$$\bar{\alpha} = \frac{\mu_{eq} E_y}{1 - \nu_{yz}\nu_{zy}} + \frac{\mu_{hj} E_{hj}}{1 - \nu_{hj}^2}$$

$$\bar{\beta} = \frac{\mu_{eq} E_z}{1 - \nu_{yz}\nu_{zy}} + \frac{\mu_{hj} E_{hj}}{1 - \nu_{hj}^2}$$

$$\bar{\zeta} = \frac{\mu_{eq} \nu_{yz} E_z}{1 - \nu_{yz}\nu_{zy}} + \frac{\mu_{hj} \nu_{hj} E_{hj}}{1 - \nu_{hj}^2}$$

$$\bar{\chi}_{eq} = \frac{\mu_{eq}\left(\nu_{zx} + \nu_{yx}\nu_{zy}\right)}{1-\nu_{yz}\nu_{zy}}$$

$$\bar{\chi}_{hj} = \frac{\mu_{hj}\nu_{hj}}{1-\nu_{hj}}$$

$$\bar{\chi} = \bar{\chi}_{eq} + \bar{\chi}_{hj}$$

$$\bar{\lambda}_{eq} = \frac{\mu_{eq}\left(\nu_{yx} + \nu_{yz}\nu_{zx}\right)}{1-\nu_{yz}\nu_{zy}}$$

$$\bar{\lambda}_{hj} = \frac{\mu_{hj}\nu_{hj}}{1-\nu_{hj}}$$

$$\bar{\lambda} = \bar{\lambda}_{eq} + \bar{\lambda}_{hj} \qquad (24)$$

the orthotropic material properties of the masonry panel are finally derived.

$$\frac{1}{\bar{E}_x} = \frac{\mu_{eq}}{E_x} + \frac{\mu_{hj}}{E_{hj}} + \bar{\lambda}_{eq}\left(\frac{\bar{\nu}_{yx}}{\bar{E}_y} - \frac{\nu_{xy}}{E_x}\right) + \bar{\lambda}_{hj}\left(\frac{\bar{\nu}_{yx}}{\bar{E}_y} - \frac{\nu_{hj}}{E_{hj}}\right) + \bar{\chi}_{eq}\left(\frac{\bar{\nu}_{zx}}{\bar{E}_z} - \frac{\nu_{xz}}{E_x}\right) + \bar{\chi}_{hj}\left(\frac{\bar{\nu}_{zx}}{\bar{E}_z} - \frac{\nu_{hj}}{E_{hj}}\right)$$

$$\bar{E}_y = \frac{\bar{\alpha}\bar{\beta} - \bar{\zeta}^2}{\bar{\beta}}$$

$$\bar{E}_z = \frac{\bar{\alpha}\bar{\beta} - \bar{\zeta}^2}{\bar{\alpha}}$$

$$\frac{1}{\bar{G}_{xy}} = \frac{\mu_{eq}}{G_{xy}} + \frac{\mu_{hj}}{G_{hj}}$$

$$\bar{G}_{yz} = \mu_{eq}G_{yz} + \mu_{hj}G_{hj}$$

$$\frac{1}{\bar{G}_{xz}} = \frac{\mu_{eq}}{G_{xz}} + \frac{\mu_{hj}}{G_{hj}}$$

$$\bar{\nu}_{yx} = \bar{\lambda} - \frac{\bar{\zeta}\bar{\chi}}{\bar{\beta}}$$

$$\bar{\nu}_{yz} = \frac{\bar{\zeta}}{\bar{\beta}}$$

$$\bar{\nu}_{zx} = \bar{\chi} - \frac{\bar{\zeta}\bar{\lambda}}{\bar{\alpha}}$$

$$\bar{\nu}_{zy} = \frac{\bar{\zeta}}{\bar{\alpha}} \qquad (25)$$

■ STRUCTURAL RELATIONSHIP OF MASONRY

Structural relationship of each constituent material with respect to the overall masonry can be established through utilizing auxiliary stress/strain components introduced in Appendix I. Details of each relationship are now deduced.

As in eq. (5), the structural matrix has the following form:

$$[S]=\begin{bmatrix} S_{11} & S_{12} & S_{13} & 0 & 0 & 0 \\ S_{21} & S_{22} & S_{23} & 0 & 0 & 0 \\ S_{31} & S_{32} & S_{33} & 0 & 0 & 0 \\ 0 & 0 & 0 & S_{44} & 0 & 0 \\ 0 & 0 & 0 & 0 & S_{55} & 0 \\ 0 & 0 & 0 & 0 & 0 & S_{66} \end{bmatrix} \tag{26}$$

Solving the auxiliary stress/strain components in eqs. (22) & (23),

$$\begin{aligned} \bar{\sigma}_{yy,hj} &= \bar{\sigma}_{yy} + C_{yy,hj} \\ &= \frac{1}{1-\nu_{hj}\nu_{hj}}\left\{E_{hj}\bar{\varepsilon}_{yy} + \nu_{hj}E_{hj}\bar{\varepsilon}_{zz} + \left(\nu_{hj}+\nu_{hj}^2\right)\bar{\sigma}_{xx}\right\} \\ &= \bar{\sigma}_{xx}\left\{\frac{\nu_{hj}}{1-\nu_{hj}} - \eta\left(\frac{\bar{\nu}_{yx}}{\bar{E}_y} + \frac{\nu_{hj}\bar{\nu}_{zx}}{\bar{E}_z}\right)\right\} + \bar{\sigma}_{yy}\left\{\eta\left(\frac{1}{\bar{E}_y} - \frac{\nu_{hj}\bar{\nu}_{zy}}{\bar{E}_z}\right)\right\} + \bar{\sigma}_{zz}\left\{\eta\left(\frac{\nu_{hj}}{\bar{E}_z} - \frac{\nu_{yz}}{\bar{E}_y}\right)\right\} \end{aligned} \tag{27}$$

where,

$$\eta = \frac{E_{hj}}{1-\nu_{hj}^2} \tag{28}$$

Therefore,

$$S_{hj,21} = \frac{\nu_{hj}}{1-\nu_{hj}^2} - \eta\left(\frac{\bar{\nu}_{xy}}{\bar{E}_y} + \frac{\nu_{hj}\bar{\nu}_{zx}}{\bar{E}_z}\right)$$
$$S_{hj,22} = \eta\left(\frac{1}{\bar{E}_y} - \frac{\nu_{hj}\bar{\nu}_{zy}}{\bar{E}_z}\right)$$
$$S_{hj,23} = \eta\left(\frac{\nu_{hj}}{\bar{E}_z} - \frac{\bar{\nu}_{yz}}{\bar{E}_y}\right) \quad (29)$$

The above equation can be rewritten as follows:

$$S_{hj,21} = \frac{\nu_{hj}}{1-\nu_{hj}} - \bar{\eta}_{hj}\left(\frac{\bar{\nu}_{yx}}{\bar{E}_y} + \frac{\nu_{hj}\bar{\nu}_{zx}}{\bar{E}_z}\right)$$
$$S_{hj,22} = \bar{\eta}_{hj}\left(\frac{1}{\bar{E}_y} - \frac{\nu_{hj}\bar{\nu}_{zy}}{\bar{E}_z}\right)$$
$$S_{hj,23} = \bar{\eta}_{hj}\left(\frac{\nu_{hj}}{\bar{E}_z} - \frac{\bar{\nu}_{yz}}{\bar{E}_y}\right) \quad (30)$$

where,

$$\bar{\eta}_{hj} = \frac{E_{hj}}{1-\nu_{hj}^2} \quad (31)$$

Using the same procedure, the remaining non-zero coefficients can also be derived.

$$
\begin{aligned}
S_{hj,11} &= 1.0 \\
S_{hj,31} &= \frac{\nu_{hj}}{1-\nu_{hj}} - \bar{\eta}_{hj}\left\{\frac{\nu_{hj}\bar{\nu}_{yx}}{\bar{E}_y} + \frac{\bar{\nu}_{zx}}{\bar{E}_z}\right\} \\
S_{hj,32} &= \bar{\eta}_{hj}\left\{\frac{\nu_{hj}}{\bar{E}_y} - \frac{\bar{\nu}_{zx}}{\bar{E}_z}\right\} \\
S_{hj,33} &= \bar{\eta}_{hj}\left\{\frac{1}{\bar{E}_z} - \frac{\nu_{hj}\bar{\nu}_{yz}}{\bar{E}_y}\right\} \\
S_{hj,44} &= 1.0 \\
S_{hj,55} &= \frac{G_{hj}}{\bar{G}_{yz}} \\
S_{hj,66} &= 1.0
\end{aligned}
\tag{32}
$$

Solving for the unknowns A, B, C and D in eqs. (13), (14), (22) and (23), the struct ural matrix for each component can be derived, and the full details will be omitted.

1 J. S. Lee, G. N. Pande, et al., Numerical Modeling of Brick Masonry Panels subject to Lateral Loadings, Computer & Structures, V ol. 61, No. 4, 1996.

2 Tomaževič M., Earthquake-resistant design of masonry buildings, Series on Innovation in Structures and Construction, Vol. 1, Imperial College Press, London, 1999.

3 Calderini, C., Lagomarsino, S., A micromechanical inelastic model for historical masonry, Journal of Earthquake Engineering (in print), 2006.

4 Magenes G., A method for pushover analysis in seismic assessment of masonry buildings, 12th World Conference on Earthquake Engineering, Auckland, New Zealand, 2000.

5 G. N. Pande, B. Kralj, and J. Middleton. Analysis of the compressive strength of masonry given by the equation $f_k = K(f_b')^{\alpha}(f_m)^{\beta}$. The Structural Engineer, 71:7-12, 1994.

6 G. N. Pande, J. X. Liang, and J. Middleton. Equivalent elastic moduli for brick masonry. Comp. & Geotech., 8:243-265, 1989.

7 R. Luciano and E. Sacco. A damage model for masonry structures. Eur. J. Mech., A/Solids, 17:285-303,1998.

8 Guido Magenes, Masonry Building Design in Seismic Areas: Recent Experiences and Prospects from a European Standpoint, *First European Conference on Earthquake Engineering and Seismology*, Paper Number: Keynote Address K9, Geneva, Switzerland, 3-8 September, 2006.

Construction Stage Analysis

Overview

A building structure is typically constructed floor by floor in the case of a reinforced concrete structure or often constructed several floors at a time in the case of a structural steel structure. Even on the same floor, different parts are constructed at different stages. A typical structural analysis entails applying the loads to the completed structure at once. This results in significant discrepancies as the scale of the building increases, especially as the number of stories increases. Regardless of the type of construction, construction dead loads on a particular floor are typically acting on the structure without the presence of the upper floors during the construction. This actually results in completely different column shortenings from the analysis results based on the "full loading on the completed structure". The change of strength gain, creep and shrinkage in the case of reinforced concrete construction compound the discrepancies. MIDAS GEN NX enables the engineer to account for the change of geometries and time dependent material properties during and after the construction.

Each temporary structure at a particular stage of construction affects the subsequent stages. Also, it is not uncommon to install and dismantle temporary supports during construction. The structure constantly changes or evolves as the construction progresses with varying material properties such as modulus of elasticity and compressive strength due to different maturities among contiguous members. The structural behaviors such as deflections and stress re-distribution continue to change during and after the construction due to varying time dependent properties. Since the structural configuration continuously changes with different loadings and support conditions, and each construction stage affects the subsequent stages, the design of certain structural components may be even governed during the construction. Without such construction stage analysis, the conventional analysis will not be reliable.

MIDAS GEN NX considers the following aspects for a construction stage analysis:

- **Time dependent material properties**
  Creep in concrete members having different maturities
  Shrinkage in concrete members having different maturities
  Compressive strength gains of concrete members as a function of time
  Relaxation of pre-stressing tendons if used

- **Conditions for construction stages**
  Activation and deactivation of members with certain maturities
  Activation and deactivation of specific loads at specific times
  Boundary condition changes

The procedure used in MIDAS GEN NX for carrying out a time dependent analysis reflecting construction stages is as follows:

1. Create a structural model. Assign elements, loads and boundary conditions to be activated or deactivated to each construction stage together as a group.

2. Define time dependent material properties such as creep and shrinkage. The time dependent material properties can be defined using the standards such as ACI or CEB-FIP, or you may directly define them.

3. Link the defined time dependent material properties to the general material properties. By doing this, the changes in material properties of the relevant concrete members are automatically calculated.

4. Considering the sequence of the real construction, generate construction stages and time steps.

5. Define construction stages using the element groups, boundary condition groups and load groups previously defined.

6. Carry out a structural analysis after defining the desired analysis condition.

7. Combine the results of the construction stage analysis and the completed structure analysis.

- Refer to "Model> Properties>Time Dependent Material" of On-line Manual.
- Refer to "Model> Properties>Time Dependent Material Link" of On-line Manual.
- Refer to "Load> Construction Stage Analysis Data>Define Construction Stage" of On-line Manual.
- Refer to "Load> Construction Stage Analysis Data>Define Construction Stage" of On-line Manual.
- Refer to "Analysis> Construction Stage Analysis Control, Perform Analysis" of On-line Manual.

Analysis reflecting Erection Sequence

General analysis for a building structure is performed under the assumption that all loads are simultaneously applied to a completed structure. This assumption made everyday, however, is not valid in a real construction sequence because a building is constructed by floor-by-floor or lift-by-lift. Even for the same floor, some different parts may be constructed and loaded in different time frames. As a result, true behaviors of a structure may be considerably different from the analysis based on “instantaneous one-time loading” on an “instantaneously constructed structure”. For instance, girders at high floors of a high-rise building may have considerably large moments. Also, we sometimes note inappropriate vertical load distribution to concrete walls, which is relatively higher compared to the distribution to the adjacent frame. Two main reasons can be deduced to contribute to the behaviors:

1. When all loads are simultaneously applied to a completed structure, discrepancies occur due to the applied loads, which are resisted by the upper floor frame that has not yet been constructed.

2. Differential elastic shortenings of vertical members occur when construction dead loads are applied as the construction progresses.

The following describes the discrepancies caused by the first case:

In a real structure, construction dead loads including self-weights at a given floor do not affect the member forces of the upper floors that are yet to be constructed. In the case of a reinforced concrete structure, vertical members followed by a floor are constructed at a given level, and the subsequent floor is erected after the concrete below has been cured for some time. Deformations due to construction dead loads in columns may have taken place considerably at the lower levels. However, in general analyses, the entire structure is subjected to design loads at the same time. In fact, construction dead loads at a particular floor must not be resisted by the upper structure because the upper floors simply do not exist during the construction.

Figure 254 illustrates a 2-story, 2-D plane, concrete frame structure, comparing analysis results between the conventional and erection sequence analyses. The conventional analysis represents the case where the loads are simultaneously applied to the completed structure. Whereas the erection sequence analysis represents the case where separate analysis models are used according to the erection sequence such that the construction loads are applied in two steps to correspond to the models.

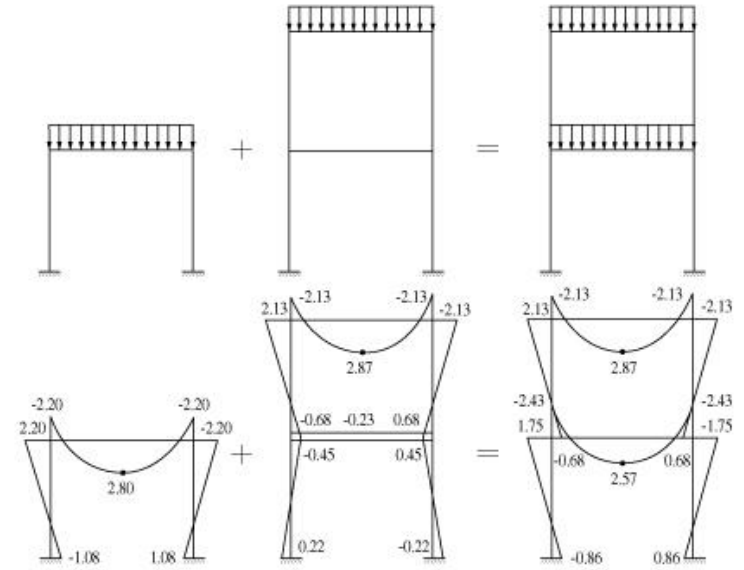

(a) Analysis reflecting Erection sequence

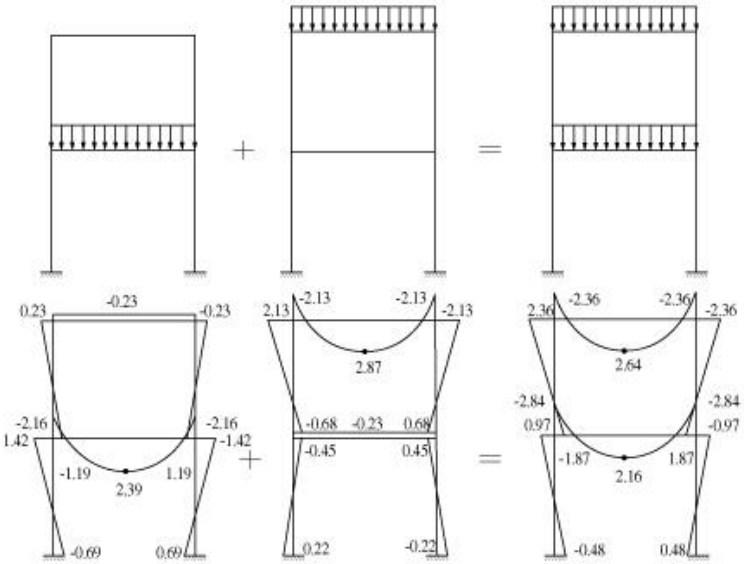

(b) Conventional analysis

Figure 2.72 Comparison of analysis results (moment diagrams) between conventional analysis and erection sequence analysis for a 2-story, 2-D reinforced concrete frame

As summarized in Table 2.5, the erection sequence analysis results show member forces at 90~180% of those obtained from the conventional analysis. In the real construction process, when the construction dead loads are applied to the 1st stage structure, the member forces of the 1st stage structure are not affected by the 2nd stage framing, which is yet to be constructed. In the case of the conventional analysis, however, the non-existing 2nd stage columns restrain the rotational deformations at the first stage. As a result, the columns of the 1st and 2nd stages together sustain the construction loads. This causes the discrepancies between the analyses. Therefore, the conventional analysis method may produce considerable discrepancies in design results.

Ratio
= Erection sequence analysis results / Conventional analysis results x 100%

Description	Bending moment				Displacement	
	1st Stage column (upper end)	1st Stage beam (middle)	2nd Stage column (upper end)	2nd Stage beam (middle)	1st Stage beam (middle)	2nd Stage beam (middle)
Erection sequence analysis	1.75	2.57	2.13	2.87	0.00373	0.00429
Conventional analysis	0.97	2.16	2.36	2.64	0.00301	0.00411
Ratio (%)	180.4	118.5	90.3	108.7	123.9	104.4

Table 2.5 Comparison of analysis results between conventional analysis and erection sequence analysis for a 2-story, 2-D, concrete frame structure

In the case of a structural steel or composite structure, as shown in Figure 2.73**,** the steel frame is erected ahead of placing the steel decks and concrete. Accordingly, the first cause for discrepancies may not be of concern for structural steel and composite structures, which are different from concrete buildings in which each floor is completed at a time.

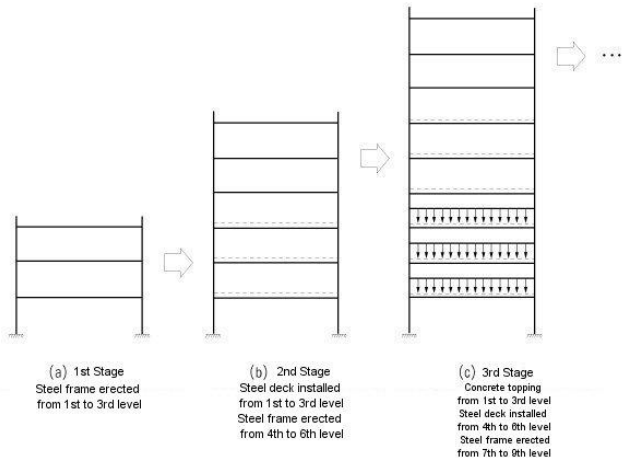

Figure 2.73 Erection sequence of structural steel or composite structure (Building erected in a 3-story lift)

The second cause for discrepancies resulting from the differential shortening of columns is discussed below.

In high-rise concrete buildings, the differential shortening of columns occurs due to elastic shortening, shrinkage and creep under long-term axial loads. The effects of shrinkage and creep on a structure depend on several factors such as concrete strength, construction duration, concrete casting condition, weather condition, etc. In general, the effect of shrinkage is not as extensive as the effects of elastic shortening and creep. It is also very difficult to accurately evaluate the effect of creep in design phase since creep progresses for a long time and depends on many factors.

In general, columns of a building are designed to be similar in their dimensions for the purpose of maintaining simplicity of design and serviceability for occupants, despite their tributary areas are not similar to one another. Therefore, differences in tributary areas for columns result in differential shortenings in columns. Differential shortenings may also occur due to unbalanced axial stiffnesses between contiguous members closely spaced such as columns and walls, which have substantially different axial stiffnesses. In concrete structures, changing stiffness during concrete curing can also contribute to differential shortenings. The effect of differential shortening is significant in tall buildings and may produce additional bending moments and shear forces to beam members. This will in turn affect the columns and other members, which are rigidly connected (moment connected) to the beams.

In order to design beam members for gravity loads in a high-rise building, some may have attempted to avoid excessive moments and shear forces by either artificially restraining the vertical movement of columns or increasing the stiffness of columns. This practice may have been carried out with the belief that shortenings are adjusted during the construction. However, the correction virtually achieves nothing structurally. Additional forces resulting from differential shortenings still remain in the members. If differential shortening is ignored member forces can be substantially underestimated, particularly horizontal member forces.

In order to avoid differential shortening, columns must be designed to proportion to their tributary areas. However, this is not always possible for architectural reasons. Figure 2.74 illustrates a concept of shortening distribution.

For instance, if a unit value is assumed for a concentrated load at each level, story height, modulus of elasticity and cross section area of a 5-story column, the relative vertical displacement of each level becomes 1.0. Figure 2.74 (a) shows a unit load individually applied to the column at each level. The sum of all the displacements is tantamount to the result obtained through a conventional analysis. Figure 2.74 (b) illustrates an erection sequence analysis in which the loads are incrementally applied to individual interim models. A separate analysis is required to calculate the magnitude of vertical length adjustment for "Subsequent" loads such as finish, partition and cladding. In reinforced concrete building construction, floor levels are generally topped (Up to slab) to the architectural levels at each given floor. However, super-elevating floor levels is often adopted in tall building construction to compensate for subsequent vertical displacements.

In steel buildings, differential shortening is often compensated by providing filter plates at column splices on site, as shown in Figure 2.75. Again, the magnitude of compensation will depend on the additional displacements due to subsequent loads.

Elastic axial shortening at floor *n*, as shown in Figure 2.74 (c), is given by

- **Conventional analysis:**

$$\Delta_n = \sum_{k=1}^{n} \frac{L_k}{E_k A_k} \sum_{i=k}^{N} P_i$$

- **Erection sequence analysis:**

$$\Delta_n = \sum_{k=1}^{n} \frac{L_k}{E_k A_k} \sum_{i=n}^{N} P_i$$

- **Displacements due to loads on the current and lower floors (Up to Slab):**

$$\Delta_n = \sum_{k=1}^{n} P_k \sum_{i=1}^{N} \frac{L_i}{E_i A_i}$$

- **Displacements due to loads on the upper floors (Subsequent):**

$$\Delta_n = \sum_{k=1}^{n} \frac{L_k}{E_k A_k} \sum_{i=n+1}^{N} P_i$$

where,

n = n-th floor
N = Number of stories
$L_{i,k}$ = i- or k-th floor story height
$E_{i,k}$ = Modulus of elasticity of column located at the i- or k-th floor
$A_{i,k}$ = Area of column located at the i- or k-th floor
$P_{i,k}$ = Construction load at the i- or k-th floor

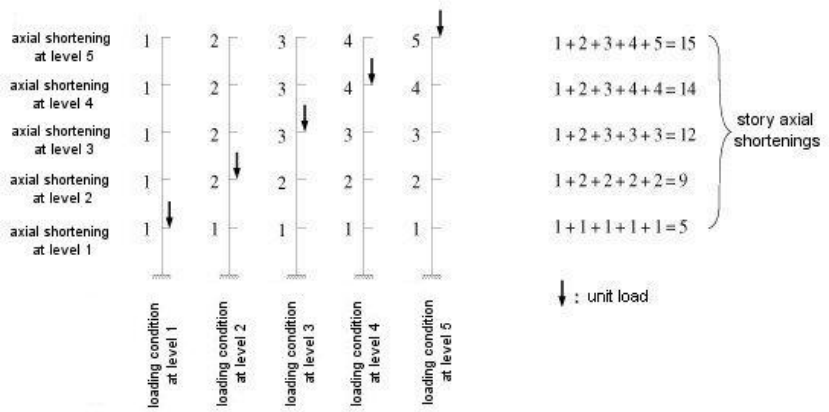

(a) Conventional analysis results

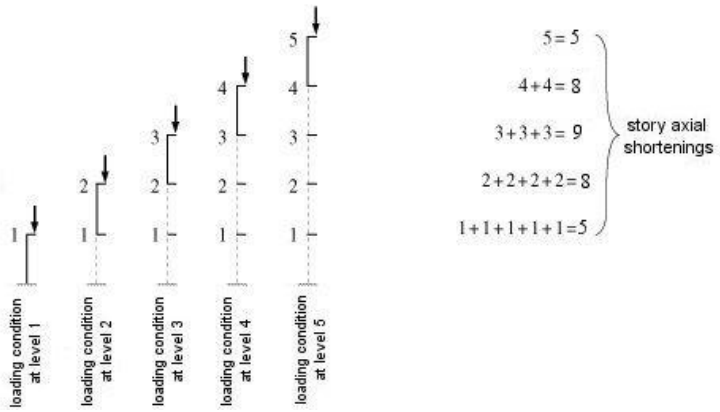

(b) Erection sequence analysis results

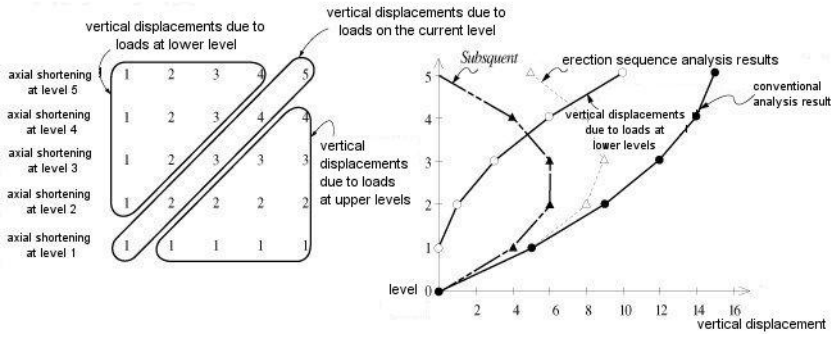

(c) Components of axial shortenings

Figure 2.74 Comparison of column axial shortenings between conventional and erection sequence analyses

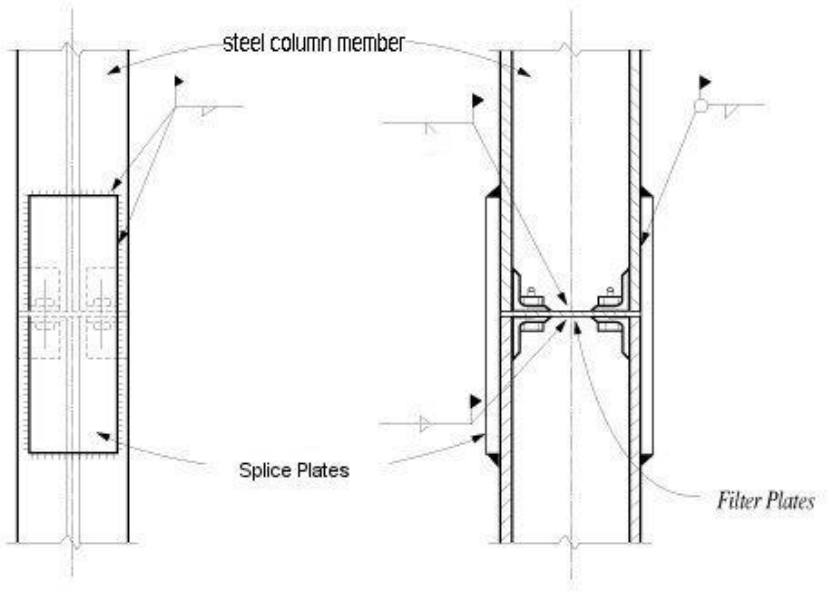

Figure 2.75 Splice detail to correct differential axial shortening in steel column

The erection sequence analysis in MIDAS GEN NX is developed to analytically overcome the practical problems outlined above, and it reflects the true construction stages of a building structure. Construction dead loads are automatically applied to interim structural models that are formulated to represent each stage of construction and subsequently analyzed. Other loads such as superimposed dead loads, live loads and lateral loads, which are applied after the completion of the structural frame, are automatically superimposed according to the user-defined load combinations.

MIDAS GEN NX separates the model into sub-models for each erection stage and assigns corresponding construction dead loads. The results for each stage are then superimposed to carry out the final erection sequence analysis. Analyses for all remaining loads other than the construction dead loads are carried out on the basis of the conventional analysis. Figure 2.76 summarizes the analysis steps.

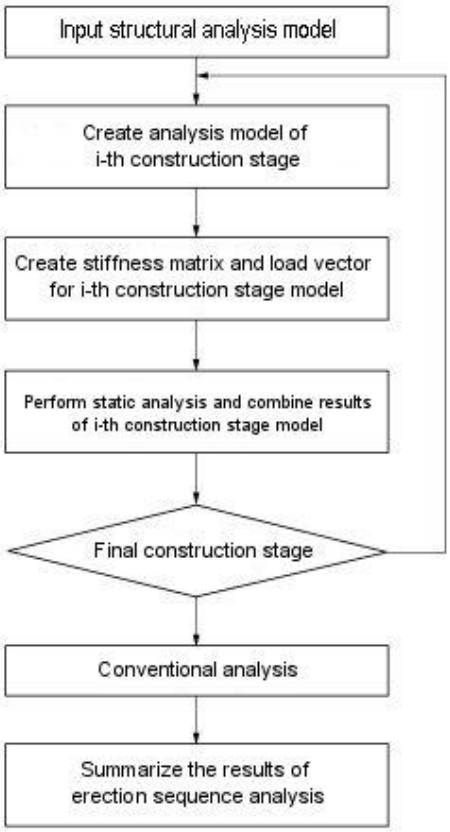

Figure 2.76 Flow chart for erection sequence analysis

Time Dependent Material Properties

MIDAS GEN NX can reflect time dependent concrete properties such as creep, shrinkage and compressive strength gains.

Creep and shrinkage

Creep and shrinkage simultaneously occur in real structures as presented in Figure 2.77. For practical analysis and design purposes, elastic shortening, creep and shrinkage are separately considered. The true elastic strain in the figure represents the reduction of elastic strain as a result of concrete strength gains relative to time. In most cases, the apparent elastic strain is considered in analyses. MIDAS GEN NX, however, is also capable of reflecting the true elastic strain in analyses considering the time-variant concrete strength gains.

Creep deformation in a member is a function of sustained stress, and a high strength concrete yields less creep deformation relative to a lower strength concrete under an identical stress. The magnitudes of creep deformations can be 1.5~3 times those of elastic deformations. About 50% of the total creep deformations takes place within a first few months, and the majority of creep deformations occurs in about 5 years.

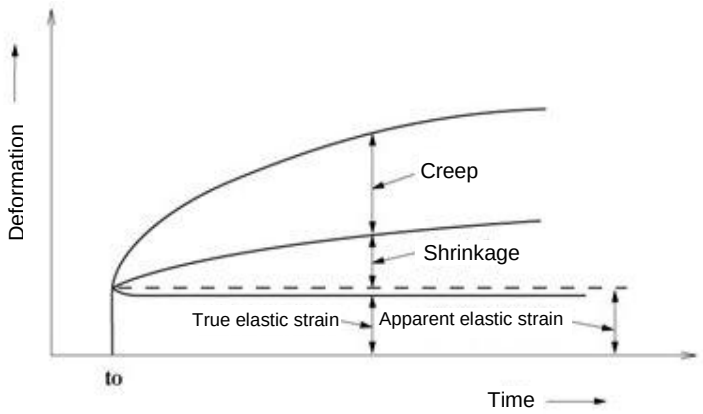

Figure 2.77 Time dependent concrete deformations

Creep in concrete can vary with the following factors:

1. Increase in water/cement ratio increases creep.
2. Creep decreases with increases in the age and strength of concrete when the concrete is subjected to stress.
3. Creep deformations increase with increase in ambient temperature and decrease in humidity.
4. It also depends on many other factors related to the quality of the concrete and conditions of exposure such as the type, amount, and maximum size of aggregate; type of cement; amount of cement paste; size and shape of the concrete mass; amount of steel reinforcement; and curing conditions.

Most materials retain the property of creep. However, it is more pronounced in the concrete materials, and it contributes to the reduction of pre-stress relative to time. In normal concrete structures, sustained dead loads cause the creep, whereas additional creep occurs in pre-stressed/post-tensioned concrete structures due to the pre-stress effects.

If a unit axial stress σ =1 exerts on a concrete specimen at the age t_0, the resulting uniaxial strain at the age t is defined as $J(t,t_0)$.

$$\varepsilon(t) = \varepsilon_i(t_0) + \varepsilon_c(t,t_0) = \sigma \cdot J(t,t_0) \tag{1}$$

where, $J(t,t_0)$ represents the total strain under the unit stress and is defined as Creep Function.

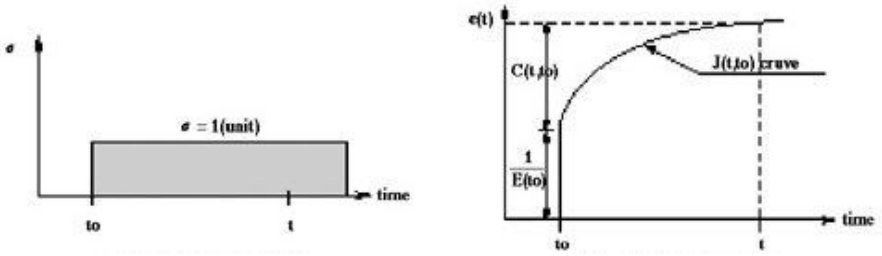

(a) Change in stress with time (b) Change in strain with time

Figure 2.78 Definition of creep function and specific creep

As shown in Figure 2.78, the creep function $J(t,t_0)$ can be presented by the sum of the initial elastic strain and creep strain as follows:

$$J(t,t_0)=\frac{1}{E(t_0)}+C(t,t_0) \tag{2}$$

where, $E(t_0)$ represents the modulus of elasticity at the time of the load application, and $C(t,t_0)$ represents the resulting creep deformation at the age t, which is referred to as specific creep. The creep function $J(t,t_0)$ can be also expressed in terms of a ratio relative to the elastic deformation.

$$J(t,t_0)=\frac{1+\phi(t,t_0)}{E(t_0)} \tag{3}$$

where, $\phi(t,t_0)$ is defined as the creep coefficient, which represents the ratio of the creep to the elastic deformation. Specific creep can be also expressed as follows:

$$\phi(t,t_0)=E(t_0)\cdot C(t,t_0) \tag{4}$$

$$C(t,t_0)=\frac{\phi(t,t_0)}{E(t_0)} \tag{5}$$

MIDAS GEN NX allows us to specify creep coefficients or shrinkage strains calculated by the equations presented in CEB-FIP, ACI, etc., or we may also directly specify the values obtained from experiments. The user-defined property data can be entered in the form of creep coefficient, creep function or specific creep.

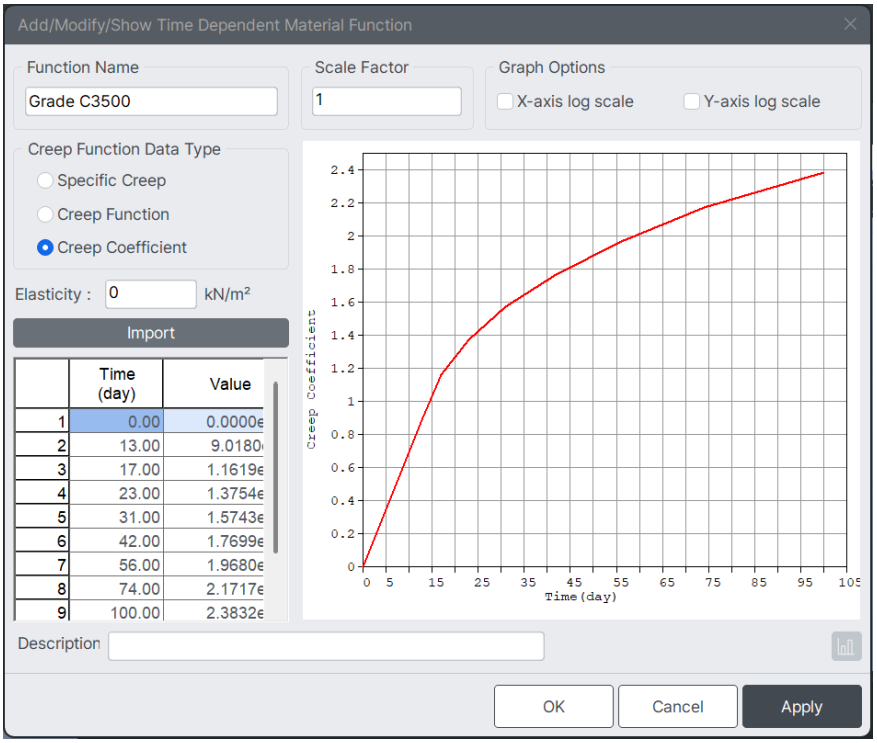

Figure 2.79 Dialog box for specifying user-defined creep coefficients

The creep function widely varies with the time of load applications. Due to the concrete strength gains and the progress of hydration with time, the later the loading time, the smaller are the elastic and creep strains. Figure 2.80 illustrates several creep functions varying with time. Accordingly, when the user defines the creep functions, the range of the loading time must include the element ages (loading time) for a time dependent analysis to reflect the concrete strength gains. For example, if a creep analysis is required for 1000 days for a given load applied to the concrete element after 10 days from the date of concrete placement, the creep function must cover the range of 1010 days. The accuracy of analysis results improves with an increase in the number of creep functions based on different loading times.

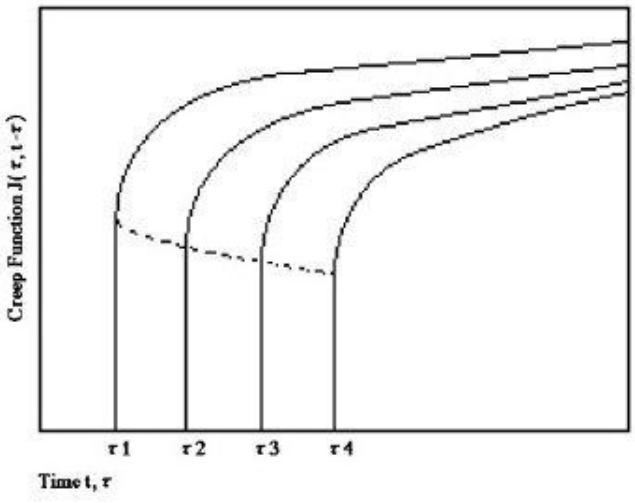

Figure 2.80 Relationship of time and age of loading to creep function

Concrete age at the time of applying sustained load		4~7	14	28	90	365
Creep coefficient	Early strength cement	3.8	3.2	2.8	2.0	1.1
	Normal cement	4.0	3.4	3.0	2.2	1.3

Table 2.6 Creep coefficients for normal concrete

Shrinkage is a function of time, which is independent from the stress in the concrete member. Shrinkage strain is generally expressed in time from t_0 to t .

$$\varepsilon_s(t,t_0) = \varepsilon_{so} \cdot f(t,t_0) \tag{6}$$

where, ε_{so} represents the shrinkage coefficient at the final time; $f(t,t_0)$ is a function of time; t stands for the time of observation; and t_0 stands for the initial time of shrinkage.

Methods of calculating creep

Creep is a phenomenon in which deformations occur under sustained loads with time and without necessarily additional loads. As such, a time history of stresses and time become the important factors for determining the creep. Not only does the creep in pre-stressed and post-tensioned concrete members translate into the increase in deformations, but it also affects the pre-stressing in the tendons, thereby affecting the structural behavior. In order to accurately account for time dependent variables, a time history of stresses in a member and creep coefficients for numerous loading ages are required. Calculating the creep in such a manner demands a considerable amount of calculations and data space. Creep is a non-mechanical deformation, and as such only deformations can occur without accompanying stresses unless constraints are imposed.

One of the general methods used in practice to consider creep in concrete structures is one that a creep coefficient for each element at each stage is directly entered and applied to the accumulated element stress to the present time. Another commonly used method exists whereby specific functions for creep are numerically expressed and integrated relative to stresses and time. The first method requires creep coefficients for each element for every stage. The second method calculates the creep by integrating the stress time history using the creep coefficients specified in the built-in standards within the program. MIDAS GEN NX permits both methods. If both methods are specified for an element, the first method overrides. It is more logical to adopt only one of the methods typically. However, both methods may be used in parallel if a time frame of 20~30 years is selected, or if creep loads are to be considered for specific elements.

If the creep coefficients for individual elements are calculated and entered, the results may vary substantially depending on the coefficient values. For reasonably accurate results, the creep coefficients must be obtained from adequate data on stress time history and loading times. If the creep coefficients at various stages are known from experience and experiments, it can be effective to directly use the values. The creep load group is defined and activated with creep coefficients assigned to elements. The creep loadings are calculated by applying the creep coefficients and the element stresses accumulated to the present. The user directly enters the creep coefficients and explicitly understands the magnitudes of forces in this method, which is also easy to use. However, it entails the burden of calculating the creep coefficients. The following outlines the calculation method for creep loadings using the creep coefficients.

$\varepsilon_c(t,t_0) = \phi(t,t_0)\ \varepsilon(t_0)$: Creep strain

$P = \int_A E(t)\varepsilon_c(t,t_0)dA$: Loading due to creep strain

$\varepsilon(t_0)$: Strain due to stress at time t_0

$\phi(t,t_0)$: Creep coefficient for time from t_0 to t

The following outlines the method in which specific functions of creep are numerically expressed, and stresses are integrated over time. The total creep from a particular time t_0 to a final time t can be expressed as an (superposition) integration of a creep due to the stress resulting from each stage.

$$\varepsilon_c(t) = \int_0^t C(t_0, t-t_0)\frac{\partial\sigma(t_0)}{\partial t_0}dt_0 \tag{7}$$

where, $\varepsilon_c(t)$: Creep strain at time t

$C(t_0, t-t_0)$: Specific creep

t_0 : Time of load application

If we assume from the above expression that the stress at each stage is constant, the total creep strain can be simplified as a function of the sum of the strain at each stage as follows:

$$\varepsilon_{c,n} = \sum_{j=1}^{n-1}\Delta\sigma_j C(t_j, t_{n-j}) \tag{8}$$

Using the above expression, the incremental creep strain $\Delta\varepsilon_{c,n}$ between the stages $t_n - t_{n-1}$ can be expressed as follows:

$$\Delta\varepsilon_{c,n} = \varepsilon_{c,n} - \varepsilon_{c,n-1} = \sum_{j=1}^{n-1}\Delta\sigma_j C(t_j, t_{n-j}) - \sum_{j=1}^{n-2}\Delta\sigma_j C(t_j, t_{n-j}) \tag{9}$$

If the specific creep is expressed in degenerate kernel (Dirichlet functional summation), the incremental creep strain can be calculated without having to save the entire stress time history.

$$C(t_0, t-t_0) = \sum_{i=1}^{m} a_i(t_0)\left[1-e^{-(t-t_0)/\Gamma_i}\right] \tag{10}$$

$a_i(t_0)$: Coefficients related to the initial shapes of specific creep curves at the loading application time t_0

Γ_i : Values related to the shapes of specific creep curves over a period of time

Using the above specific creep equation, the incremental strain can be rearranged as follows:

$$\Delta\varepsilon_{c,n} = \sum_{i=1}^{m}\left[\sum_{j=1}^{n-2}\Delta\sigma_j a_i(t_j)e^{-(t-t_0)/\Gamma_i} + \sigma_{n-1}a_i(t_{n-1})\right]\left[1-e^{-(t-t_0)/\Gamma_i}\right]$$
$$\Delta\varepsilon_{c,n} = \sum_{i=1}^{m} A_{i,n}\left[1-e^{-(t-t_0)/\Gamma_i}\right] \tag{11}$$

where,

$$A_{i,n} = \sum_{j=1}^{n-2}\Delta\sigma_j a_i(t_j)e^{-(t-t_0)/\Gamma_i} + \Delta\sigma_{n-1}a_i(t_{n-1})$$
$$A_{i,n} = A_{i,n-1}e^{-(t-t_{n-1})/\Gamma_i} + \Delta\sigma_{n-1}a_i(t_{n-1})$$
$$A_{i,1} = \Delta\sigma_0 a_i(t_0)$$

Using the above method, the incremental strain for each element at each stage can be obtained from the resulting stress from the immediately preceding stage and the modified stress accumulated to the previous stage. This method provides relatively accurate analyses reflecting the change in stresses. Once we enter necessary material properties without separately calculating creep coefficients, the program automatically calculates the creep. Despite the advantage of easy application, it shares some disadvantages; since it follows the equations presented in Standards, it restricts us to input specific creep values for specific elements.

This method is greatly affected by the analysis time interval. Time intervals for construction stages in general cases are relatively short and hence do not present problems. However, if a long time interval is specified for a stage, it is necessary to internally divide into sub-time intervals to closely reflect the creep effects. Knowing the characteristics of creep, the time intervals should be preferably divided into a log scale. MIDAS GEN NX is capable of automatically dividing the intervals into the log scale based on the number of intervals specified by the user. There is no fast rule for an appropriate number of time intervals. However, the closer the division, the closer to the true creep can be obtained. In the case of

a long construction stage interval, it may be necessary to divide the stage into a number of time steps.

Development of concrete compressive strength

MIDAS GEN NX reflects the changes in concrete compressive strength gains relative to the maturities of concrete members in analyses. The compressive strength gain functions can be defined as per standard specifications such as ACI and CEB-FIP as shown in Figure 2.81, or the user is free to define one directly. MIDAS GEN NX thus refers to the concrete compressive strength gain curves, and it automatically calculates the strengths corresponding to the times defined in the construction stages and uses them in the analysis.

The time dependent material properties (creep, shrinkage and concrete compressive strength gain) defined in Figure 2.81 can be applied in analyses in conjunction with conventional material properties. This linking process is simply necessary for the program's internal data structure.

Refer to "Model> Properties >Time Dependent Material Link" of On-line Manual.

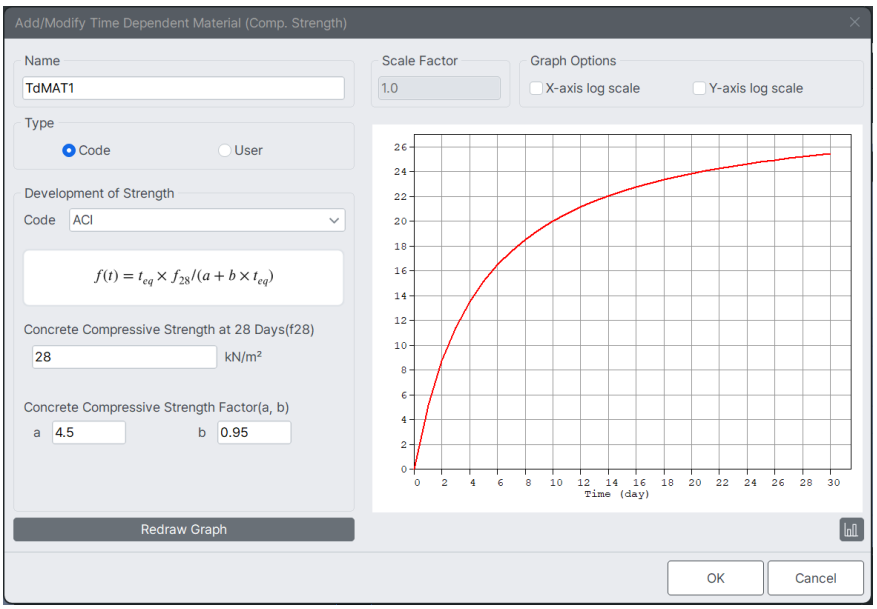

Figure 2.81 Definition of concrete compressive strength gain curve based on standards

Input Process of Time Dependent Material Properties

Time dependent material properties of elements reflecting their maturities are required for construction stage and heat of hydration analyses in which MIDAS GEN NX accounts for creep and shrinkage of concrete. Observe the following steps for entering time dependent material properties:

1. Define the material properties related to creep and shrinkage in ***Model*** > ***Properties*** > ***Time Dependent Material (Creep/Shrinkage)***.

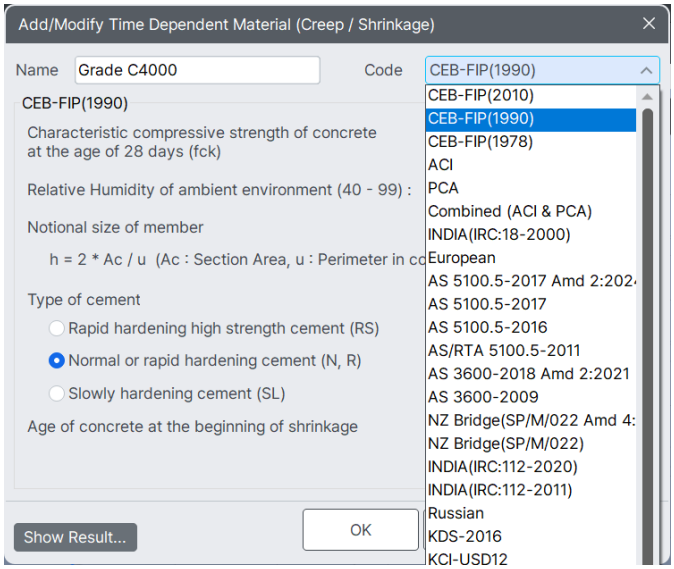

Figure 2.82 Selecting Code for defining material properties

In order to select ***User Defined*** in the ***Code*** field, first define the creep and shrinkage functions in ***Model*** > ***Properties*** > ***Time Dependent Material (Creep/Shrinkage) Function***.

2. Define the time variant modulus of elasticity in ***Model*** > ***Properties*** > ***Time Dependent Material (Comp. Strength)***.

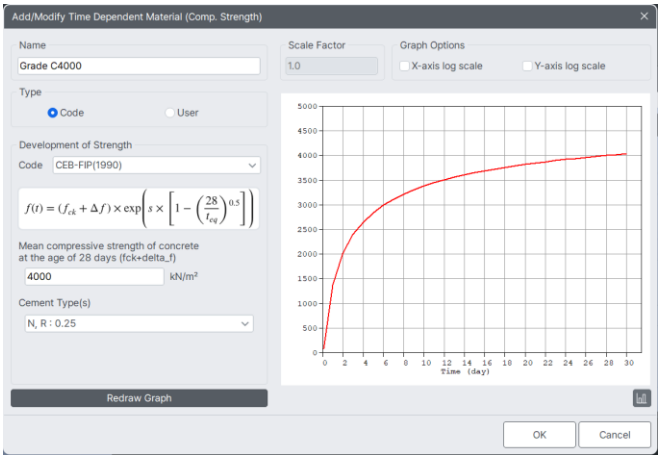

Figure 2.83 Change of modulus of elasticity of concrete

3. Link the time dependent material properties to the general material properties already entered in ***Model*** > ***Properties*** > ***Time Dependent Material Link***.

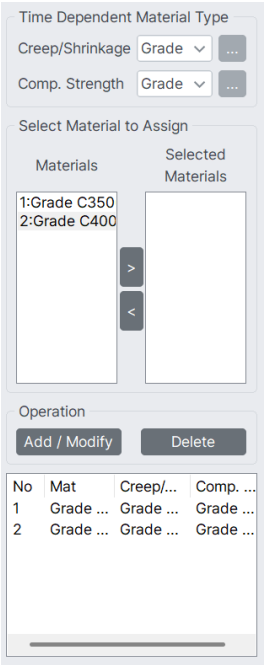

Figure 2.84 Time Dependent Material Link Dialog Bar

Definition and Composition of Construction Stages

MIDAS GEN NX allows us to specify construction stages and their compositions in detail to reflect the true erection sequence of a construction. This is an extremely powerful tool, which can be applied to various construction stage analyses related to different erection methods practiced in building construction.

MIDAS GEN NX defines the three distinct stages, which retain the following characteristics:

- **Base stage**
  When the construction stage is undefined, a general analysis may be performed. If the construction stage is defined, the analysis is disabled; the structural modeling is completed; and the element, boundary and load groups are defined and composed.

- **Construction stage**
  Structural analyses are actually carried out for the construction stages. For each construction stage, relevant element, boundary and load groups are activated.

- **Post-construction stage**
  Being the post-construction stage of the construction, analyses are carried out for the construction stage loads as well as other general loads, response spectrum, etc.

Each construction stage is composed of activated (or deactivated) element, boundary and load groups. By the combination of the three groups with each group defined by the process of activation and deactivation, tremendous flexibility exists in composing the stages.

The following are the contents included in each construction stage:

1. Activation (creation) and deactivation (deletion) of elements with certain maturities (ages)
2. Activation and deactivation of loadings at certain points in time
3. Changes in boundary conditions

The concept of construction stages used in MIDAS GEN NX is illustrated in Figure 2.85. Construction stages can be readily defined by duration for each stage. A construction stage with '0' duration is possible, and the first and last steps are basically created once a construction stage is defined. Activation and deactivation of elements, boundary conditions and loadings are practically accomplished at each step.

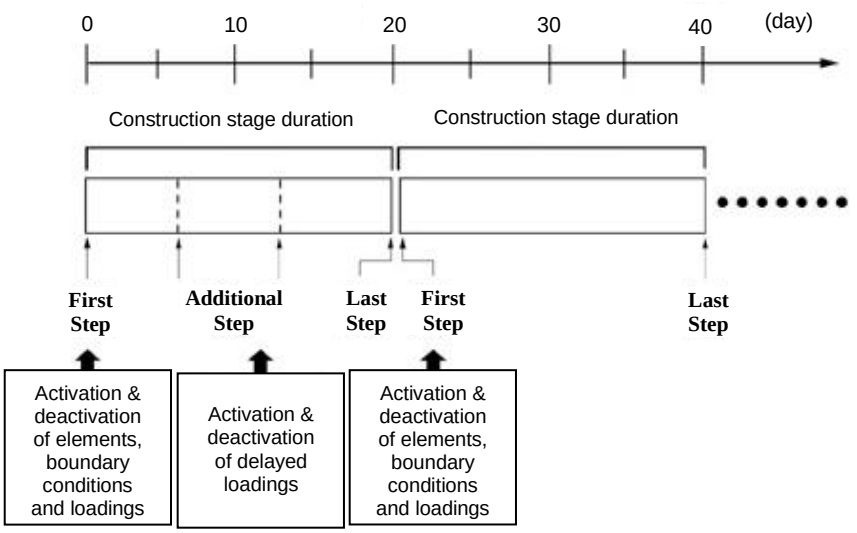

Figure 2.85 Concept of construction stages

Activation and deactivation of changing conditions such as new and deleted elements, boundary conditions and loadings basically take place at the first step of each construction stage. Accordingly, construction stages are created to reflect the changes of structural systems that exist in a real construction relative to the construction schedule. That is, the number of construction stages increase with the increase in the number of temporary structural systems.

Structural system changes in terms of active elements and boundary conditions are defined only at the first step of each construction stage. However, additional steps can be defined within a given construction stage for the ease of analysis to reflect loading changes. This allows us to specify delayed loadings representing, for instance, temporary construction loads while maintaining the same geometry without creating additional construction stages.

If many additional steps are defined in a construction stage, the accuracy of analysis results will improve since the time dependent analysis closely reflects creep, shrinkage and compressive strengths. However, if too many steps are defined, the analysis time may be excessive, thereby compromising efficiency. Moreover, if time dependent properties (creep, shrinkage and modulus of elasticity) are not selected to participate in ***Analysis>Construction Stage Analysis Control Data*** and the analysis is subsequently carried out, the analysis results do not change regardless of the number of steps defined.

Subsequent to activating certain elements with specific maturities in a construction stage, the maturities continue with the passage of subsequent construction stages. The material properties of the elements in a particular construction stage change with time. MIDAS GEN NX automatically calculates the properties by using only the elements' maturities based on the pre-defined time dependent material properties (***Model>Properties>Time Dependent Material***). We are not required to define the changing material properties at every construction stage.

If two elements are activated with an identical maturity in an identical construction stage, the elapsed times for both elements are always identical. However, there are occasions where only selective elements are required to pass the time among the elements activated at the same time. This aging of selective elements is accomplished by using the time load function (***Load>Time Loads for Construction Stage***).

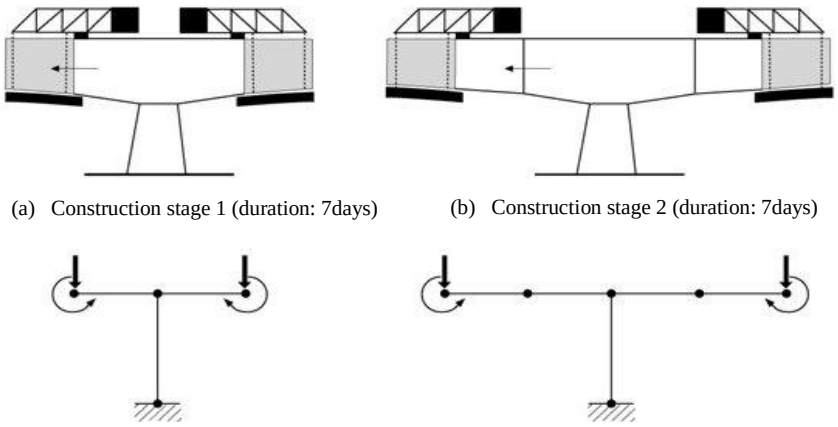

(a) Construction stage 1 (duration: 7days)

(b) Construction stage 2 (duration: 7days)

(c) Analysis model 1

(d) Analysis model 2

Figure 2.86 FCM construction stages and modeling

When specific elements are activated in a construction stage, the corresponding maturities must be assigned to the elements. Creating elements with '0' maturity represents the instant when the fresh concrete is cast. However, a structural analysis model does not typically include temporary structures such as formwork/falsework, and as such unexpected analysis results may be produced if the analysis model includes immature concrete elements. Especially, if elements of '0' maturity are activated, and an analysis is carried out reflecting the time dependent compressive strength gains, significantly meaningless displacements may result due to the fact that no concrete strength can be expected in the first 24 hours of casting. A correct method of modeling a structure for considering construction stages may be that the wet concrete in and with the formwork is considered as a loading in the temporary structure, and that the activation of the concrete elements are assumed after a period of time upon removal of the formwork/falsework.

If new elements are activated in a particular construction stage, the total displacements or stresses accumulated up to the immediately preceding construction stage do not affect the new elements. That is, the new elements are activated with '0' internal stresses regardless of the loadings applied to the current structure.

When elements are deactivated, and 100% stress redistribution is assigned, all the internal stresses in the deactivated elements are redistributed to the remaining structure, and the internal stresses of the elements constituting the remaining structure will change. This represents loading equal and opposite internal forces at the boundaries of the removed elements. On the other hand, if 0% stress redistribution is assigned, the internal stresses of the deactivated elements are not transferred to the remaining structure at all, and the stresses in the remaining elements thus remain unchanged. The amount of the stresses to be transferred to the remaining elements can be adjusted by appropriately controlling the rate of stress redistribution. This flexible feature can be applied to consider incomplete or partial transfer of the stresses in the deactivated elements in a construction stage analysis. A typical example can be a tunnel analysis application. In a tunnel construction stage analysis, the elements in the part being excavated do not relieve the stresses to the remaining support structure all at once. Use of rock bolts or temporary supports may transfer the internal stresses of the deactivated (excavated) elements gradually to the remaining structures of subsequent construction stages. Accordingly, the internal stresses of deactivated elements can be gradually distributed to the interim structures over a number of construction stages.

If “original” is selected while a boundary condition is activated, the boundary condition is activated at the original (undeformed) node location. This is achieved internally by applying a forced displacement to the node in the direction opposite to the displacement of the immediately preceding construction stage. Additional internal stresses resulting from the forced displacement will be accounted for in the structure. Conversely, if the option “deformed” is selected, the node for which the boundary condition is to be activated will be located at the deformed location as opposed to the original location.

In a time dependent analysis reflecting construction stages, the structural system changes and loading history of the previous stages affect the analysis results of the subsequent stages. MIDAS GEN NX thus adopts the concept of accumulation. Rather than performing analyses for individual structural models pertaining to all the construction stages, incremental structural and loading changes are entered and analyzed for each construction stage. The results of the current stage are then added to that of the preceding stage.

If a loading is applied in a construction stage, the loading remains effective in all the subsequent construction stages unless it is deliberately removed. Elements are similarly activated for a given construction stage. Only the elements pertaining to the relevant construction stage are activated as opposed to activating all the necessary elements for the stage. Once-activated elements cannot be activated again, and only those elements can be deactivated.

The loading cases to be applied in a construction stage analysis must be defined as the “construction stage load” type. Even if a number of loading cases exist in a construction stage analysis, their results are combined as a single result as depicted in Figure 2.87. This is because the nonlinearity of time dependent material properties in a construction stage analysis renders a linear combination of load cases impossible. A construction stage analysis produces accumulated analysis results and the maximum/minimum values as shown in Figure 2.87. The results of the construction stage analysis thus obtained can be now combined with the results of the conventional load cases.

We often encounter occasions where intermediary construction stages are structurally significant enough to warrant full investigation. Some special loadings perhaps related to construction activities can be engaged in the analysis. MIDAS GEN NX allows us to specify the “post-construction stage” to an intermediate stage, which can be analyzed as if it was the final completed structure. Once a structure pertaining to a construction stage is designated as the “post-construction stage”, all general load cases can be applied, and various analyses such as time history and response spectrum can be carried out.

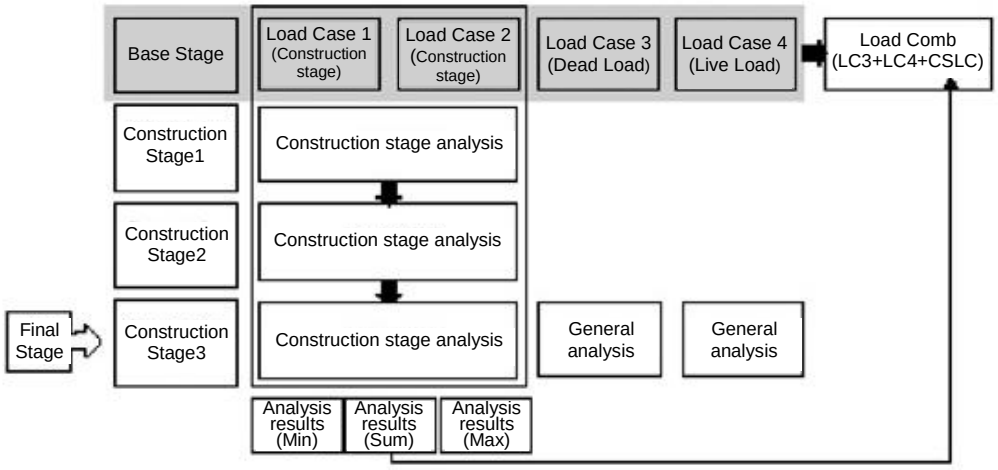

Figure 2.87 Construction stage analysis load combination

Procedure for Construction Stage Analysis

A typical modeling procedure for construction stage analysis is as follows:

1. Model the complete structure except for the boundary and load conditions.
2. Define the element groups in ***Model > Group > Define Structure Group***. Assign the elements that will be activated (constructed) and deactivated (dismantled) at the same time to the defined element groups.
3. Define the boundary groups in ***Model > Group > Define Boundary Group***.
4. Define the load groups in ***Model > Group > Define Load Group***.
5. Compose the construction stages by clicking the Add button in ***Load > Construction Stage Analysis Data > Define Construction Stage***. You may click the Generate button to define a number of construction stages of equal duration followed by clicking the Modify/Show button to compose each construction stage.

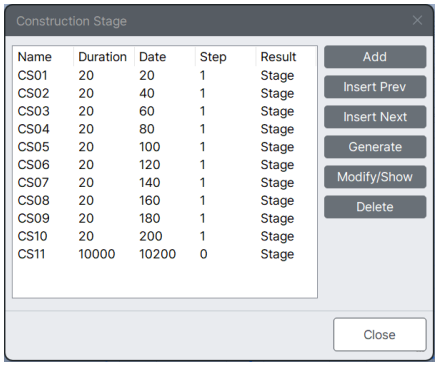

Figure 2.88 Define Construction Stage dialog box

6. In the Compose Construction Stage dialog box, enter the duration of the construction stage and select whether or not to save the analysis results. If loadings are applied with time intervals to the same structural system within the same construction stage, Additional Steps corresponding to the loading times may be defined.

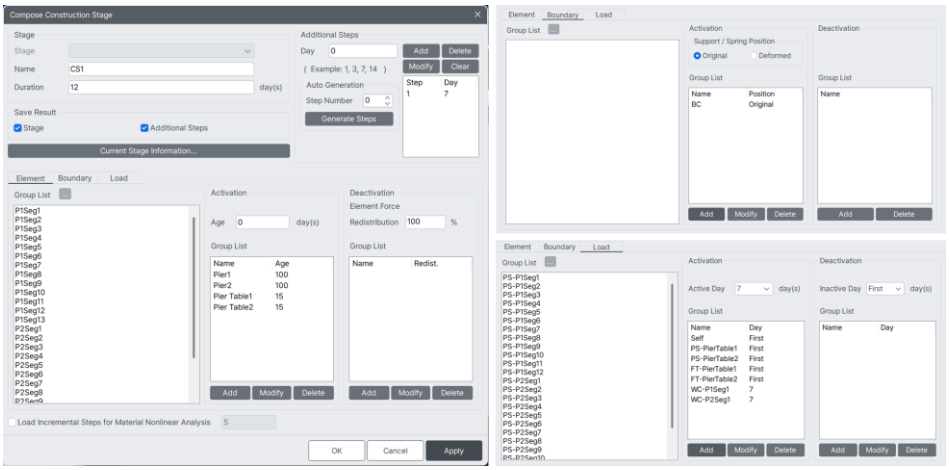

Figure 2.89 Compose Construction Stage dialog box

7. Activate and/or deactivate relevant element groups selected from the ***Group List*** under the ***Element*** tab. The ***Age*** represents the maturity at the start of the stage. The ***Element Force Redistribution*** represents the distribution of the internal forces of the elements being deactivated.

8. Activate and/or deactivate relevant boundary groups selected from the ***Group List*** under the ***Boundary*** tab.

9. Activate and/or deactivate relevant load groups selected from the ***Group List*** under the ***Load*** tab. The ***Active Day*** and ***Inactive Day*** represent the timing of load application and removal respectively.

10. Upon completion of composing construction stages, move around the construction stages in ***Stage Toolbar*** to enter the boundary and load conditions corresponding to the boundary and load groups of each construction stage.

The boundary and load conditions may be input while the corresponding groups are assigned at the same time. It is thus recommended that the boundary and load conditions applied during the construction stages be input in the corresponding construction stages to minimize potential errors.

The above outlines the modeling procedure whereby the user directly defines the construction stages individually. We may also automatically generate all the data necessary for the construction stage analysis using ***Load > Construction Stage Analysis Data > Construction Stage Wizard for Building Structure***. Changes can be made subsequently in Compose Construction Stage.

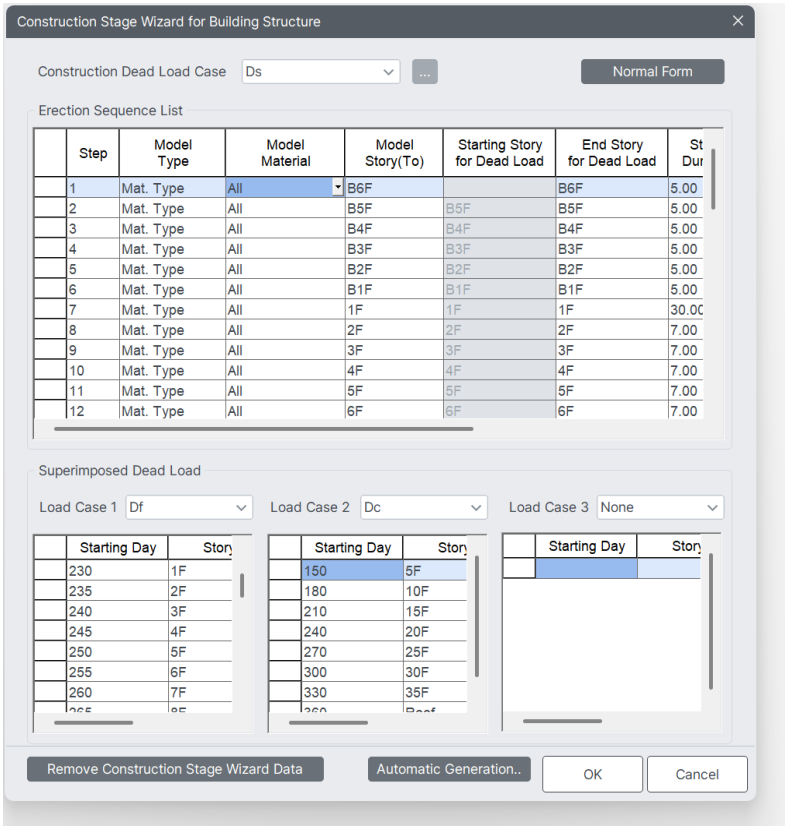

Figure 2.90 Construction Stage Wizard dialog box

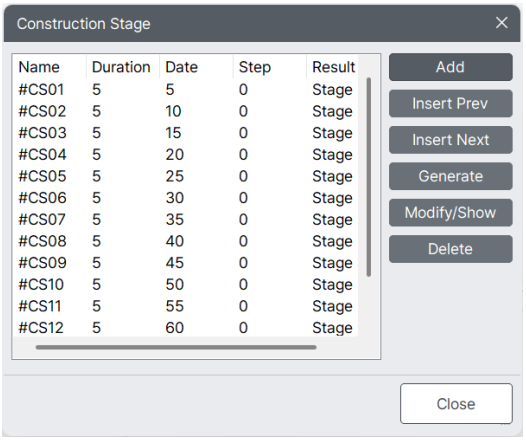

Figure 2.91 Construction stages auto-generated by Construction Stage Wizard

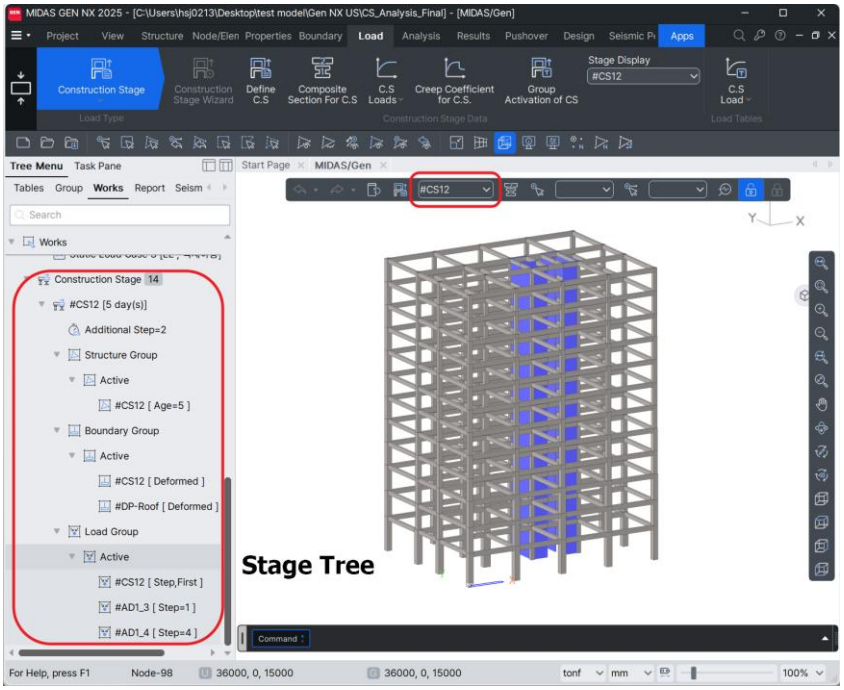

Figure 2.92 Real time display of the changes of structure and load conditions of the construction stages shown in conjunction with Stage Tree

Heat of Hydration Analysis

In a certain concrete structure with considerable mass or where a construction progresses rapidly with a number of construction joints, the rate and amount of heat generation due to hydration are important. Non-uniform thermal expansion and contraction due to heat of hydration and cooling of concrete accompanied by changing constraints create undesirable stresses. The stresses may cause detrimental cracking in the concrete, thereby reducing its strength and durability.

Heat of hydration analysis thus becomes important when casting mass concrete structures. It enables us to predict and control temperature and stress distribution within a structure to avoid potential problems.

Mass concrete structures requiring heat of hydration analysis depend on their dimensions, shapes, cement types and construction conditions. In practice, hydration analyses are normally carried out for slabs or mats in excess of 800~1000mm in thickness and walls confined at bottom in excess of about 500mm.

Surface cracking may develop initially due to the temperature difference between the surface and center. Through-cracks can also develop as a result of contraction restrained by external boundary conditions in the cooling process of high heat of hydration. The heat of hydration analysis is largely classified into several sub-analyses.

It entails temperature distribution analysis for conduction, convection, heat source, etc.; change in modulus of elasticity due to curing and maturity; and stress analysis for creep and shrinkage. The following outlines the various components affecting the analysis.

Heat Transfer Analysis

MIDAS GEN NX calculates changes in nodal temperatures with time due to conduction, convection and heat source in the process of cement hydration. The following outlines pertinent items considered in MIDAS GEN NX and some of the main concepts in heat transfer analysis:

Conduction

Conduction is a type of heat transfer accompanied by energy exchange. In the case of a fluid, molecular movements or collisions and in the case of solid, movements of electrons cause the energy exchange from a high temperature zone to a low temperature zone. The rate of heat transfer through conduction is

proportional to the area perpendicular to heat flux multiplied by the temperature gradient in that direction (Fourier's law).

$$Q_x = -\kappa A \frac{\partial T}{\partial x}$$

where,

Q_x : Rate of heat transfer

A : Area

κ : Thermal conductivity

$\frac{\partial T}{\partial x}$: Temperature gradient

In general, thermal conductivity of saturated concrete ranges between 1.21~ 3.11, and its unit is kcal/h·m·°C . Thermal conductivity of concrete tends to decrease with increasing temperature, but the effect is rather insignificant in the ambient temperature range.

Convection

Convection is another form of heat transfer whereby heat is transmitted between a fluid and the surface of a solid through a fluid's relative molecular motion. Heat transfer by forced convection occurs in the case where a fluid is forced to flow on a surface such that an artificial fluid current is created. If the fluid current is naturally created by a difference in density due to a temperature difference within the fluid thereby inducing a buoyancy effect, the form of heat transfer is referred to as a free convection. Because the fluid's current affects the temperature field in this type of heat transfer, it is not a simple task to determine the temperature distribution and convection heat transfer in practice.

From an engineering perspective, the heat transfer coefficient, h_c is defined to represent the heat transfer between a solid and a fluid, where T represents the surface temperature of the solid, and the fluid flowing on the surface retains an average temperature T_∞ .

$$q = h_c(T - T_\infty)$$

The heat transfer coefficient (h_c) widely varies with the current type, geometric configuration and area in contact with the current, physical properties of the fluid, average temperature on the surface in contact with convection, location and many others, and as such it is extremely difficult to formulate the coefficient. In general, convection problems associated with temperature analyses of mass concrete structures relate to the type of heat transfer occurring between the concrete surface and

atmosphere. Accordingly, the following empirical formula is often used, which is a function of an atmospheric wind speed.

$$h_c = h_n + h_f = 5.2 + 3.2v \quad (m/sec)$$

The unit for heat transfer coefficients (Convection coefficients) is $kcal/m^2 \cdot h \cdot {}^\circ C$.

Heat source

Heat source represents the amount of heat generated by a hydration process in a mass concrete. Differentiating the equation for adiabatic temperature rise and multiplying the specific heat and density of concrete obtain the internal heat generation expressed in terms of unit time and volume. Adiabatic conditions are defined as occurring without loss or gain of heat; i.e., as isothermal.

Internal heat generation per unit time & volume ($kcal/m^3 \cdot h$)

$$g = \frac{1}{24}\rho c K \alpha e^{-\alpha t/24}$$

Equation for adiabatic temperature rise ($^\circ$C)

$$T = K(1 - e^{-\alpha t})$$

where,

T : Adiabatic temperature ($^\circ C$)

K : Maximum adiabatic temperature rise ($^\circ C$)

α : Response speed

t : Time (days)

Pipe cooling

Pipe cooling is accomplished by embedding pipes into a concrete structure through which a low temperature fluid flows. The heat exchange process between the pipes and concrete reduces the temperature rise due to heat of hydration in the concrete, but increases the fluid temperature. The type of the heat exchange is convection between the fluid and pipe surfaces. The amount of the heat exchange is expressed as follows:

$$q_{conv} = h_p A_s (T_s - T_m) = h_P A_s \left(\frac{T_{s,i} + T_{s,o}}{2} - \frac{T_{m,i} + T_{m,o}}{2} \right)$$

h_p : Convection coefficient of fluid in pipes ($kcal / m^2 \cdot h \cdot {}^\circ C$)

A_s : Surface area of a pipe (m^2)

T_s , T_m : Pipe surface and coolant temperatures (${}^\circ C$)

Initial temperature

Initial temperature is an average temperature of water, cement and aggregates at the time of concrete casting, which becomes an initial condition for analysis.

Ambient temperature

Ambient temperature represents a curing temperature, which may be a constant, sine function or time-variant function.

Prescribed temperature

A prescribed temperature represents a boundary condition for a heat transfer analysis and always maintains a constant temperature. The nodes that are not specified with convection conditions or constant temperatures are analyzed under the adiabatic condition without any heat transfer. In a symmetrical model, the plane of symmetry is typically selected as an adiabatic boundary condition.

The basic equilibrium equations shown below are used for heat transfer analysis. Analysis results are expressed in terms of nodal temperatures varying with time.

$$C\dot{T} + (K + H)T = F_Q + F_h + F_q$$

$C = [\int_v \rho c N_i N_j dxdydz]$: Capacitance (Mass)

$K = [\int_v (k_{xx} \frac{\partial N_i}{\partial x} \frac{\partial N_j}{\partial x} + k_{yy} \frac{\partial N_i}{\partial y} \frac{\partial N_j}{\partial y} + k_{zz} \frac{\partial N_i}{\partial z} \frac{\partial N_j}{\partial z}) dxdydz]$: Conduction

$H = [\int_S h N_i N_j dS_h]$: Convection

$F_Q = \int_v N_i Q dxdydz$: Heat load due to Heat Source/Sink

$F_h = \int_S h T_\infty N_i dS_h$: Heat load due to Convection

$F_q = \int_S qN_i dS_q$: Heat load due to Heat Flux

where,

T : Nodal Temperature

ρ : Density

c : Specific heat

$k_{xx}k_{yy}k_{zz}$: Heat conductivity

h : Convection coefficient

Q : Rate of heat flow - Quantity of heat penetrating per unit time

q : Heat flux – Quantity of heat penetrating a unit surface area per unit time

Thermal Stress Analysis

Stresses in a mass concrete at each stage of construction are calculated by considering heat transfer analysis results such as nodal temperature distribution, change in material properties due to changing time and temperature, time-dependent shrinkage, time and stress-dependent creep, etc. The following outlines some important concepts associated with thermal stress analysis and pertinent items considered in MIDAS GEN NX.

Equivalent concrete age based on temperature and time & Accumulated temperature

Change in material properties occurring from the process of maturing concrete can be expressed in terms of temperature and time. In order to reflect this type of phenomenon, equivalent concrete age and accumulated temperature concepts have been incorporated.

Equivalent concrete age is calculated on the basis of CEB-FIP MODEL CODE, and the Ohzagi equation is adopted for calculating accumulated temperature, which bases on a maturity theory.

Equivalent concrete age as per CEB-FIP MODEL CODE

$$t_{eq} = \sum_{t=1}^{n} \Delta t_i \exp[13.65 - \frac{4000}{273 + T(\Delta t_i)/T_0}]$$

t_{eq} : Equivalent concrete age (days)
Δt_i : Time interval at each analysis stage (days)
$T(\Delta t_i)$: Temperature during at each analysis stage (˚C)
T_0 : 1 ˚C

Ohzagi's equation for accumulated temperature

$$M = \sum_{i=1}^{n} \Delta t_i \cdot \beta \cdot \left(T(\Delta t_i) + 10\right)$$

$\beta = 0.0003(\mathrm{T}(\Delta \mathrm{t_i}) + 10)^2 + 0.006(\mathrm{T}(\Delta \mathrm{t_i}) + 10) + 0.55$
M: Accumulated temperature (˚C)
Δt_i : Time interval at each analysis stage (days)
$T(\Delta t_i)$: Temperature during at each analysis stage (˚C)

Concrete compressive strength calculation using equivalent concrete age and accumulated temperature

ACI CODE

$$\sigma_c(t) = \frac{t}{a + bt_{eq}}\sigma_{c(28)}$$

a, b: Coefficients for cement classification
$\sigma_{c(28)}$: 28-day concrete compressive strength

CEB-FIP MODEL CODE

$$\sigma_c(t) = \exp\left\{s\left[1-\left(\frac{28}{t_{eq}/t_1}\right)^{1/2}\right]\right\}\sigma_{c(28)}$$

s : Coefficient for cement classification
$\sigma_{c(28)}$: 28-day concrete compressive strength
t_1 : 1 day

Ohzagi's Equation

$$\sigma_c(t) = \sigma_{c(28)} \cdot y$$

where, $y = ax^2 + bx + c$

$$x = 2.389\ln\left(\frac{M}{3.5}\right) - 1.0$$

a, b, c: Coefficients for cement classification
$\sigma_{c(28)}$: 28-day concrete compressive strength

KS concrete code (1996)

$$\sigma_c(t) = \frac{t}{a + bt_{eq}}\sigma_{c(91)}$$

a, b: Coefficients for cement classification
$\sigma_{c(91)}$: 91-day concrete compressive strength

Deformations resulting from temperature changes

Thermal deformations and stresses are calculated by using the nodal temperature changes at each stage obtained through a heat transfer analysis.

Deformations due to Shrinkage

Additional deformations and stresses develop due to shrinkage after initial curing. MIDAS GEN NX adopts ACI CODE and CEB-FIP MODEL CODE to include the shrinkage effects in thermal stress analyses, which reflect the cement type, structural configuration and time.

Deformations due to Creep

Additional deformations and stresses develop as a result of sustained stresses in concrete structures. MIDAS GEN NX adopts ACI CODE and CEB-FIP MODEL CODE to consider the effects of creep.

Procedure for Heat of Hydration Analysis

1. Select ***Model*** > ***Properties*** > ***Time Dependent Material (Creep/Shrinkage) and Time Dependent Material (Comp. Strength)***, and specify the time dependent material properties. Link the general material properties and time dependent material properties in ***Model*** > ***Properties*** > ***Time Dependent Material Link***.
2. Enter the relevant data required for Heat of Hydration Analysis in the sub-menus of ***Load > Hydration Heat Analysis Data***.
3. Enter the Integration factor, Initial temperature, stress output points and whether or not to consider the effects of creep and shrinkage in ***Analysis*** > ***Hydration Heat Analysis Control***.
4. Select the ***Analysis > Perform Analysis*** menu or click  ***Perform analysis***.
5. Once the analysis is completed, check the results in contours, graphs, animations, etc.

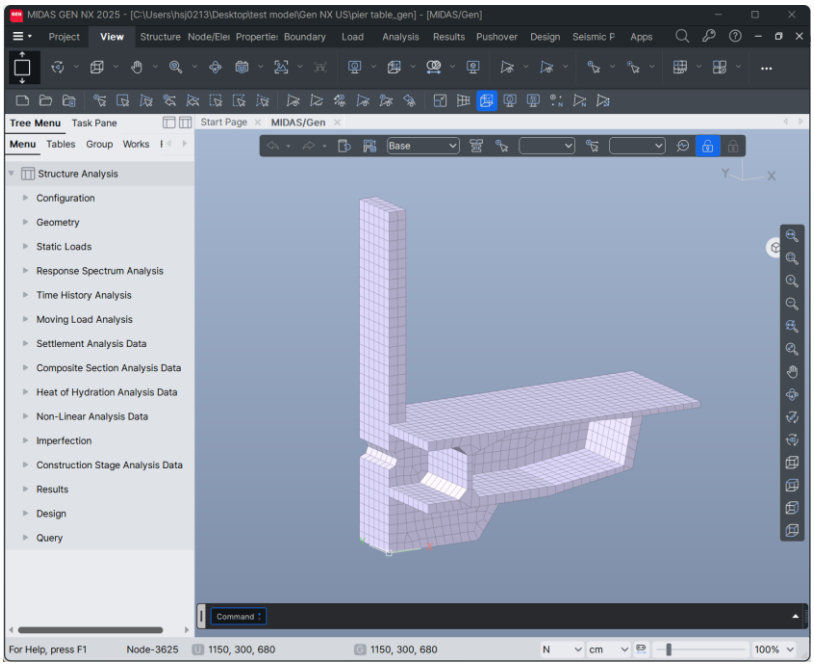

Figure 2.93 Model of a pier cap of an extradosed prestressed concrete box for Heat of Hydration Analysis reflecting the concrete pour sequence

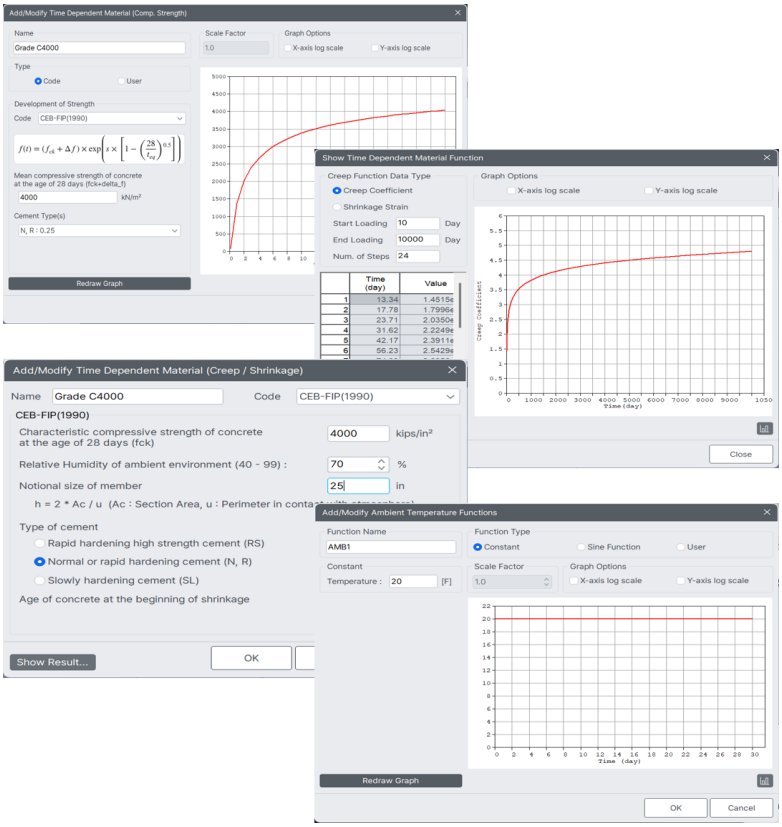

Figure 2.94 Heat properties and time dependent material properties dialog box

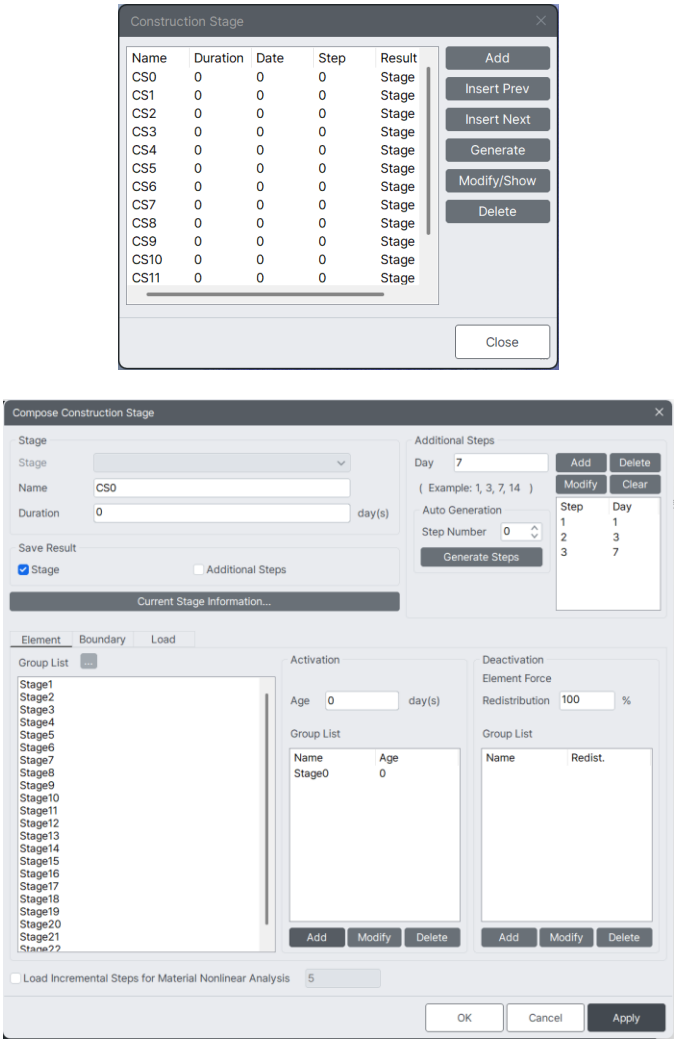

Figure 2.95 Construction Stage dialog box to reflect the concrete pour sequence (Element, boundary and load groups are defined.)

1st Stage

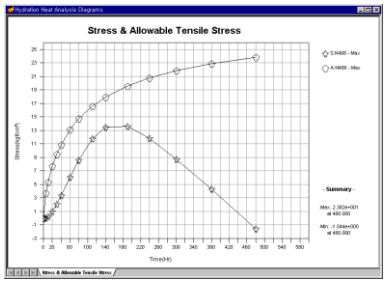

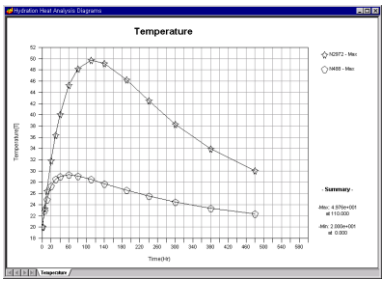

2nd Stage

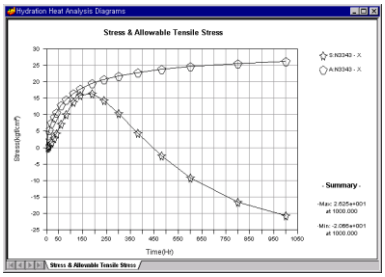

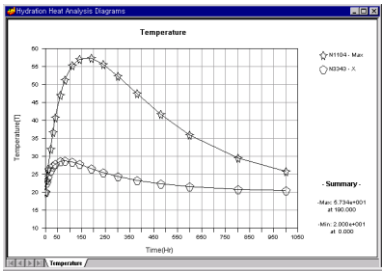

3rd Stage

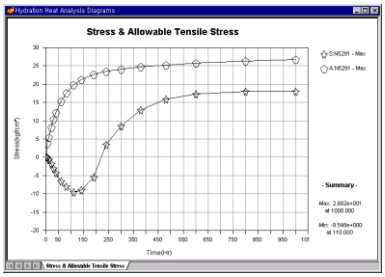

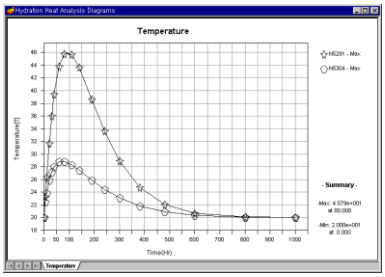

Figure 2.96 Graphs of analysis results for each construction stage

PSC (Pre-stressed/Post-tensioned Concrete) Analysis

Pre-stressed Concrete Analysis

The behaviors of pre-stressed concrete structures depend on the effective pre-stress. When a pre-stressed concrete structure is analyzed, the change of tensions in pre-stressing tendons must be accurately calculated for a load history through every construction stage. Tension losses in Pre-Stressed (PS) tendons occur due to many different factors including the tensioning method.

In the case of pre-tensioning, tension losses are attributed to shrinkage and tendon relaxation before tensioning and elastic shortening, creep, shrinkage, tendon relaxation, loading and temperature after tensioning.

In the case of post-tensioning, tension losses are attributed to frictions between tendons and sheaths, anchorage slip, creep, shrinkage, tendon relaxation, loading and temperature.

MIDAS GEN NX reflects the following tension losses for analyzing pre-stressed concrete structures:

- **Instantaneous losses upon release**
- **Time dependent losses after release**

MIDAS GEN NX uses net cross sections for calculating the section properties such as cross sectional areas and bending stiffness, which account for duct areas deducted from the gross cross sections prior to jacking PS tendons. After tensioning, converted sections are used reflecting the tendon cross sections.

The stiffness of the tendons is relatively larger than the concrete, and it results in the shift of centroid. The eccentricities of the tendons are then calculated relative to the new centroid and their tension forces are calculated.

Rather than modeling PS tendons as truss elements or the like, MIDAS GEN NX treats the tendons as equivalent pre-stressing loads, while the stiffness of the tendons are reflected in the section properties as noted above. The tensions in the tendons, which are used to calculate the equivalent loads must be based on the pre-stress loses at every construction stage caused by various factors.

MIDAS GEN NX adopts the following procedure for analyzing a pre-stressed concrete structure:

1. Model the structure.
2. Activate (create) construction stages by defining time dependent material properties and construction stages followed by defining elements, boundary conditions and loadings for each construction stage.
3. Define the tendon properties; cross sectional area, material properties, ultimate strength, duct diameter, frictional coefficients, etc.
4. Assign the desired tendons to the section and define the tendon placement profile.
5. Define the tensions applied to the tendons and enter the tensions in the appropriate construction stages.
6. Perform the analysis.

- Refer to "Analysis> Construction Stage Analysis Control" of On-line Manual.
- Refer to "Load> Prestress Loads > Tendon Property" of On-line Manual.
- Refer to "Load> Prestress Loads > Tendon Profile" of On-line Manual.
- Refer to "Load> Prestress Loads >Tendon Prestress Loads" of On-line Manual.

Pre-stress Losses

- **Instantaneous losses after release**
  1. Anchorage slip
  2. Friction between PS tendons and sheaths
  3. Elastic shortening of concrete
- **Long-term time dependent losses after release**
  1. Creep in concrete
  2. Shrinkage in concrete
  3. Relaxation of PS tendons

The frictional loss is considered in the post-tensioning but not in the pre-tensioning. The total losses for both instantaneous and long-term losses normally range in the 15~20% of the jacking force. The most important factor for calculating the stresses of PSC (pre-stressed & post-tensioned concrete) members is the final effective pre-stress force P_e in the tendons reflecting all the instantaneous losses and long-term losses. A relationship between P_i and P_e can be expressed as follows:

$$P_e = RP_i$$

R is referred to as the effective ratio of pre-stress, which is generally R=0.80 for pre-tensioning and R=0.85 for post-tensioning.

The following outlines the pre-stress losses considered in MIDAS GEN NX:

Instantaneous losses

1. Loss due to Anchorage slip

When a PS tendon is tensioned and released, the pre-stress is transferred to the anchorage. The friction wedges in the anchorage fixtures to hold the wires will slip a little distance, thus allowing the tendon to slacken slightly. This movement, also known as anchorage take-up, causes a tension loss in the tendon in the vicinity of the anchorage. This phenomenon occurs in both post- and pre-tensioning, and overstressing the tendon can compensate it.

The loss of pre-stress due the anchorage slip is typically limited to the vicinity of the anchorage due to the frictional resistance between the PS tendon and sheath. The effect does not extend beyond a certain distance away from the anchorage.

The tendon length l_{set} in the anchorage zone in Figure 2.97 represents the zone in which tension loss is experienced. The length is a function of the friction; if the frictional resistance is big, the length becomes shorter and vice versa. If we define the anchorage slip as Δl, tendon cross-section area as A_p and modulus of elasticity as E_p, the following equation is established. The equation represents the shaded area in Figure 2.97.

$$\text{Area of triangle } (0.5\Delta P l_{set}) = A_p E_p \Delta l \quad (1)$$

If we further define the frictional resistance per unit length as p, the pre-stress loss ΔP in Figure 2.97 can be expressed as

$$\Delta P = 2pl_{set} \tag{2}$$

From the equations (1) and (2) above, we can derive the equation for l_{set}, which represents the length of the tendon being subjected to pre-stress loss due to anchorage slip.

$$l_{set} = \sqrt{\frac{A_p E_p \Delta l}{p}} \tag{3}$$

Figure 2.97 shows a linear distribution of tension along the length of the tendon for an illustrative purpose. MIDAS GEN NX, however, considers a true nonlinear distribution of tension for calculating the pre-stress loss due to the anchorage slip.

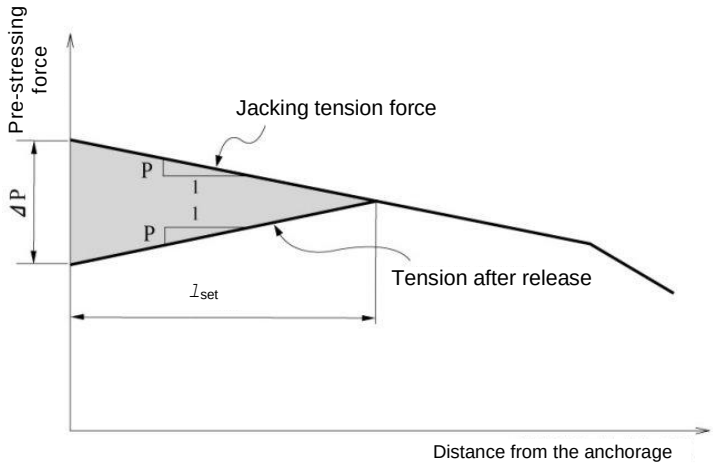

Figure 2.97 Effect on pre-stressing force due to anchorage slip

2. Loss due to friction between PS tendons and sheaths

In post-tensioning, frictions exist between the PS tendon and its sheathing. The pre-stressing force in the tendon decreases as it gets farther away from the jacking ends. The length effect and the curvature effect can be classified. The length effect, also known as the wobbling effect of the duct, depends on the length and stress of the tendon and refers to the friction stemming from imperfect linear alignment of the duct. The loss of pre-stress due to the curvature effect results from the intended curvature of the tendon in addition to the unintended wobble of the duct. Frictional coefficients, μ (/radian) per unit angle and k (/m) per unit length are expressed.

If a pre-stressing force P_0 is applied at the jacking end, the tendon force P_x at a location, l away from the end with the angular change α can be expressed as follows:

$$P_x = P_0 e^{-(\mu\alpha + kl)} \tag{4}$$

Pre-stressing Material			Wobble coefficient, k (/m)	Curvature coefficient, μ (/rad)
Bonded tendons		Wire tendons	0.0033~0.0050	0.15~0.25
		High-strength bars	0.0003~0.0020	0.08~0.30
		7-wire strand	0.0015~0.0066	0.15~0.25
Unbonded tendons	Mastic coated	Wire tendons	0.0033~0.0066	0.05~0.15
		7-wire strand	0.0033~0.0066	0.05~0.15
	Pre-greased	Wire tendons	0.0010~0.0066	0.05~0.15
		7-wire strand	0.0010~0.0066	0.05~0.15

Table 2.7 Friction coefficients k & μ (ACI-318)

3. Loss due to elastic shortening of concrete

As a pre-stress force is transferred to a concrete member, the concrete is compressed. The length of the concrete member is reduced, and the tendon shortens by the same amount thus reducing the tension stress. The characteristics of the elastic shortening differ slightly from pre-tensioning to post-tensioning although the two methods share the same principle.

In the case of a pre-tensioning, an instantaneous elastic shortening takes place as soon as the tendon is released from the anchorage abutments, that is, when the jacking force is applied. This results in a shorter tendon and a loss of pre-tension. As shown in Figure 2.98, the pre-tension (P_j) in the tendon differs from the pre-stressing force (P_i) applied to the concrete member.

In the case of post-tensioning, pre-stressing is directly imposed against the concrete member. The process of elastic shortening is identical to the pre-tensioning method, but the tension force in the tendon is measured after the shortening has already taken place. Therefore, no tension loss occurs as a result of elastic shortening in post-tensioning. MIDAS GEN NX does not consider pre-stress loss due to elastic shortening. As such, when a pre-stress force is specified in a concrete member where a pre-tensioning method is used, the pre-stress load (P_i) must be entered in lieu of the jacking load (P_j).

In a typical post-tensioned member, multiple tendons are placed, stressed and anchored in a pre-defined sequence. A series of concrete elastic shortenings takes place in the same member, and the pre-stress loss in each tendon changes as the pre-stressing sequence progresses. There is no tension loss in the first tendon being stressed in Figure 2.99 (b). When the second tendon is tensioned as shown in Figure 2.99 (c), a tension loss is observed in the first tendon due to the subsequent shortening from the second tensioning. Not only does MIDAS GEN NX account for pre-stress loss due to elastic shortening at every construction stage, but it also reflects all pre-stress losses due to elastic shortenings caused by external forces.

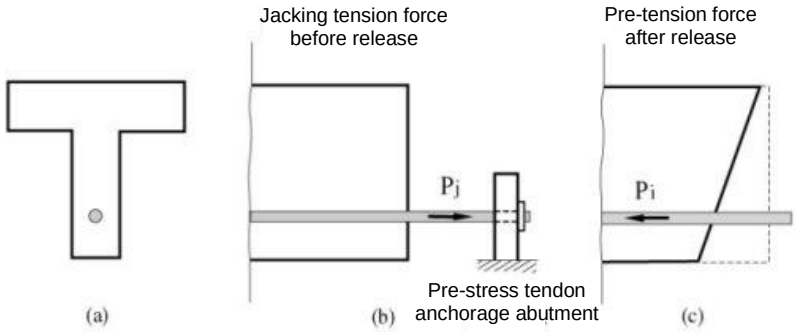

Figure 2.98 Pre-stress loss due to elastic shortening (pre-tensioned member)

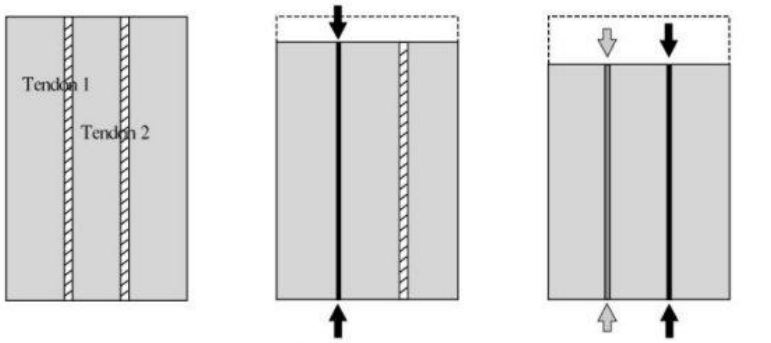

Figure 2.99 Pre-stress losses in multi-tendons due to sequential tensioning (post-tensioned member)

Time dependent losses

Pre-stress losses also occur with time due to concrete creep, shrinkage and PS tendon relaxation. MIDAS GEN NX reflects the time dependent material properties of concrete members and calculates the corresponding creep and shrinkage for all construction stages. It also accounts for pre-stress losses in PS tendons due to the changing member deformation. The pre-stress loss history can be examined for each construction stage by graphs.

Stress relaxation in steel, also termed as creep, is the loss of its stress when it is pre-stressed and maintained at a constant strain for a period of time. Pre-stress loss due to relaxation varies with the magnitude of initial stress, elapsed time in which the stress is applied and product properties. MIDAS GEN NX adopts the Magura[1)] equation for tendon relaxation.

$$\frac{f_s}{f_{si}} = 1 - \frac{\log t}{C}\left(\frac{f_{si}}{f_y} - 0.55\right), \text{ where, } \frac{f_{si}}{f_y} \geq 0.55 \quad (5)$$

f_{si} is initial stress; f_s is the stress after loading for a period of time t; f_y is ultimate stress (0.1% offset yield stress); and C is product-specific constant. C=10 for general steel and C=45 for low relaxation steel are typically used. The above equation assumes that the stress in the tendon remains constant. In real structures, stresses in PS tendons continuously change with time due to creep, shrinkage, external loads, etc., and as such the equation (5) cannot be directly applied. Accordingly, MIDAS GEN NX calculates the change in pre-stress loads in tendons due to all causes except for the relaxation itself for every construction stage and calculates the relaxation loss based on fictitious initial prestress2) for each construction stage.

1) Magura, D.D., Sozen, M.A., and Siess, C.P., "A Study of Stress Relaxation in Pre-stressing Reinforcement," PCI Journal, Vol. 9, No. 2, April 1964.

2) Kan, Y.G., "Nonlinear Geometric, Material and Time Dependent Analysis of Reinforced and Prestressed Concrete Frames", Ph. D. Dissertation, Department of Civil Engineering, University of California, Berkeley, June 1977.

Pre-stress Loads

MIDAS GEN NX converts the pre-stress tendon loads applied to a structure into equivalent loads as described in Figure 2.100 below.

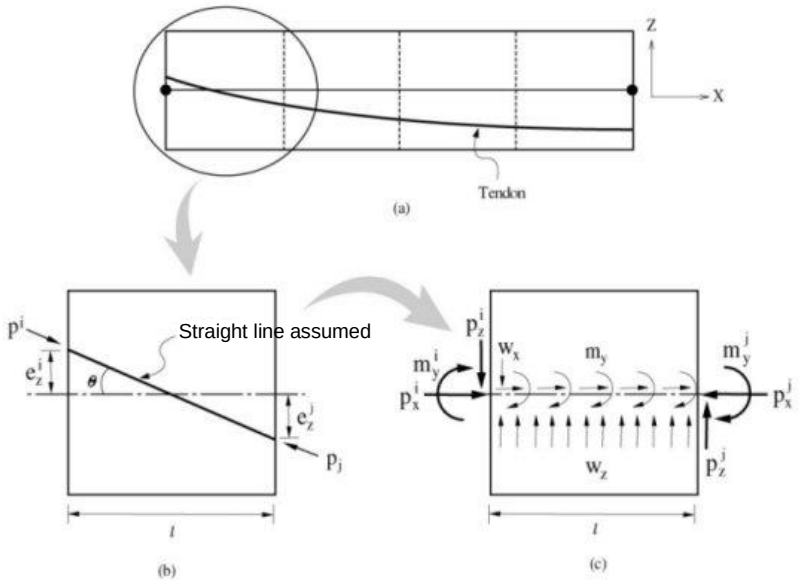

Figure 2.100 Conversion of pre-stress into equivalent loads

Figure 2.100 illustrates a tendon profile in a beam element. 2-Dimension is selected for the sake of simplicity, but the process of converting into equivalent loads in the x-y plane is identical to that in the x-z plane. MIDAS GEN NX divides a beam element into 4 segments and calculates equivalent loads for each segment as shown in Figure 2.100. The tendon profile in each segment is assumed linear. The tension forces p^i and p^j in the tendon are unequal due to frictional loss. 3 Concentrated loads (p_x, m_y, p_z) at each end, i and j, alone cannot establish an equilibrium, and hence distributed loads are introduced for an equilibrium. Equations (1) and (2) are used to calculate the concentrated loads at each end, and Equation (3) and (4) are used to calculate the internal distributed loads.

$$
\begin{aligned}
p_x^i &= p^i \cos\theta \\
p_z^i &= p^i \sin\theta \\
m_y^i &= p_x^i \cdot e_z^i
\end{aligned}
\tag{1}
$$

$$
\begin{aligned}
p_x^j &= p^j \cos\theta \\
p_z^j &= p^j \sin\theta \\
m_y^j &= p_x^j \cdot e_z^j
\end{aligned}
\tag{2}
$$

$$
\begin{aligned}
\sum F_x &= p_x^i + w_x l - p_x^j = 0 \\
\sum F_z &= -p_z^i + w_z l + p_z^j = 0 \\
\sum M_y^j &= m_y^i - p_z^i l + w_z \frac{l^2}{2} + m_y^j + m_y l = 0
\end{aligned}
\tag{3}
$$

$$
\begin{aligned}
w_x &= \frac{p_x^j - p_x^i}{l} \\
w_z &= \frac{p_z^i - p_z^j}{l} \\
m_y &= p_z^i - w_z \frac{l}{2} - \frac{m_y^i + m_y^j}{l}
\end{aligned}
\tag{4}
$$

MIDAS GEN NX calculates time dependent pre-stress losses due to creep, shrinkage, relaxation, etc. for every construction stage as well as other pre-stress losses due to external loads, temperature, etc. First, the change in tension force in the tendon is calculated at each construction stage, and the incremental tension load is converted into equivalent loads, which are then applied to the element as explained above.

Solution for Unknown Loads Using Optimization Technique

Refer to "Results> Unknown Load Factor" of On-line Manual.

In the design of long span structures, we often face a problem where we would seek a solution to unknown loading conditions necessary to satisfy a given design requirement such as shown in Figure 2.101. MIDAS GEN NX is capable of solving this type of problems using an optimization technique by calculating the optimum variables for given constraints and object functions. For constraint conditions, Equality and Inequality conditions are permitted. The types of object functions include the sum of the absolute values ($\sum_{i=1}^{n}|X_i|$), the sum of the squares ($\sum_{i=1}^{n}X_i^2$) and the maximum of the absolute values ($Max(|X_1|,|X_2|,...,|X_n|)$).

Figure 2.101 (a) illustrates a problem of finding jack-up loads in a long span beam. An artificial moment distribution of the beam or initial displacements in the beam may be imposed as a condition.

Figure 2.101 (b) illustrates a problem of finding leveling loads during construction in a long span structure in which a specific deformed shape is imposed as a condition.

Figure 2.101 (c) illustrates a cable stayed bridge having unknown cable tensions under a dead or live load condition. The lateral displacement of the pylon is limited not to exceed a specific value, and the vertical displacements at Points B and C must be positive (+).

The above problems create equality and inequality conditions, and MIDAS GEN NX solves the problems by the optimization technique.

The following describes the analysis procedure for finding the jack-up loads at Points A and B using Equality conditions, as shown in Figure 2.101 (a):

1. Apply a virtual (unit) load at the points of and in the direction of the unknown jack-up loads as shown in Figure 2.101 (a), one at a time. The number of unit load conditions created is equal to the number of the unknown loads.

1. Carry out a static analysis for the design loading condition, which is a uniformly distributed load in this case.

3. Formulate Equality conditions using the constraints imposed.

$$M_{A1}P_1 + M_{A2}P_2 + M_{AD} = M_A$$
$$M_{B1}P_1 + M_{B2}P_2 + M_{BD} = M_B$$

M_{Ai} : Moment at point A due to a unit load applied in the P_i direction
M_{Bi} : Moment at point B due to a unit load applied in the P_i direction
M_{AD} : Moment at point A due to the design loading condition
M_{BD} : Moment at point B due to the design loading condition
M_A : Moment at point A due to the design loading condition and the unknown loads P_1, P_2
M_B : Moment at point B due to the design loading condition and the unknown loads P_1, P_2

4. Using linear algebraic equations, the equality conditions are solved. If the numbers of the unknown loads and equations are equal, the solution can be readily obtained from the matrix or the linear algebra method.

$$\begin{Bmatrix} P_1 \\ P_2 \end{Bmatrix} = \begin{bmatrix} M_{A1} & M_{A2} \\ M_{B1} & M_{B2} \end{bmatrix}^{-1} \begin{Bmatrix} M_A & -M_{AD} \\ M_B & -M_{BD} \end{Bmatrix}$$

The following illustrates an analysis procedure for finding the cable tensions using Inequality conditions of the structure shown in Figure 2.100 (c):

1. Apply a virtual (unit) load in the form of a pre-tension load in each cable. The number of unit load conditions created is equal to the number of the unknown tension loads in the cables.

2. Carry out a static analysis for the design loading condition, which is a uniformly distributed load in this case.

3. Formulate Inequality conditions using the constraints imposed.

$$\delta_{A1}T_1 + \delta_{A2}T_2 + \delta_{A3}T_3 + \delta_{AD} \le \delta_{A1}$$
$$\delta_{B1}T_1 + \delta_{B2}T_2 + \delta_{B3}T_3 + \delta_{BD} \ge 0$$
$$\delta_{C1}T_1 + \delta_{C2}T_2 + \delta_{C3}T_3 + \delta_{CD} \ge 0$$
$$T_i \ge 0 \quad (i = 1,2,3)$$

δ_{Ai} : Lateral displacement at point A subjected to a unit pre-tension loading condition in T_i direction

δ_{Bi} : Lateral displacement at point B subjected to a unit pre-tension loading condition in T_i direction

δ_{Ci} : Lateral displacement at point C subjected to a unit pre-tension loading condition in T_i direction

δ_{AD} : Lateral displacement at point A subjected to the design loading condition

δ_{BD} : Lateral displacement at point B subjected to the design loading condition

δ_{CD} : Lateral displacement at point C subjected to the design loading condition

δ_A : Lateral displacement at point A subjected to the design loading condition and the cable tension load

T_i : Unknown i th cable tension

4. Using the optimization technique, a solution satisfying the inequality conditions is obtained. Numerous solutions to the unknown loads exist depending on the constraints imposed to the Inequality conditions. MIDAS GEN NX finds a solution to Inequality conditions, which uses variables that minimizes the given object functions. MIDAS GEN NX allows us to select the sum of the absolute values, the sum of the squares and the maximum of the absolute values of variables for the object functions. Weight factors can be assigned to specific variables to control their relative importance, and the effective ranges of the variables can be specified.

Comprehensive understanding of a structure is required to use the above optimization technique for finding necessary design variables. Since Equality or Inequality conditions may not have a solution depending on the constraints, selection of appropriate design conditions and object functions are very important.

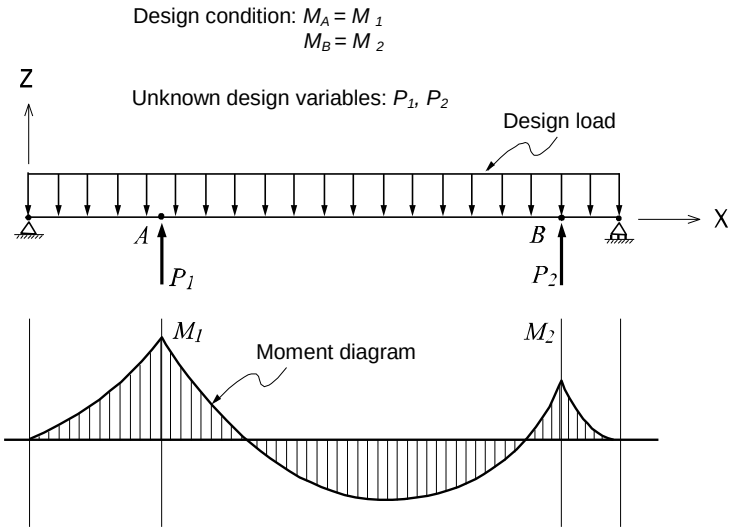

(a) Example of finding the jack-up loads, P_1 and P_2, that cause moment M_1 at point A and moment M_2 at point B under a given uniform loading condition

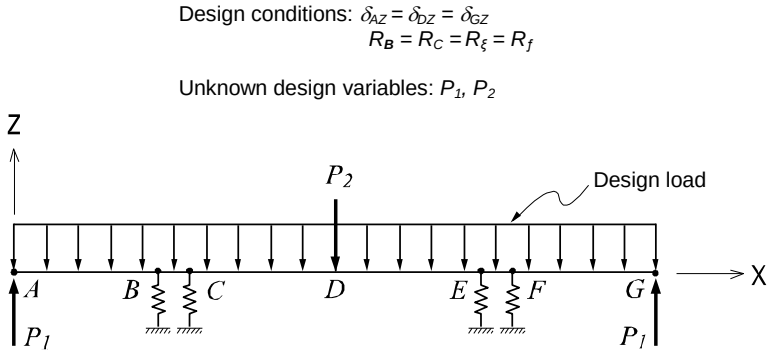

(b) Example of finding the leveling loads, P_1 and P_2, that result in the same vertical displacements at points A, D and G, and the same support reactions at supports B, C, E and F under a given uniform loading condition

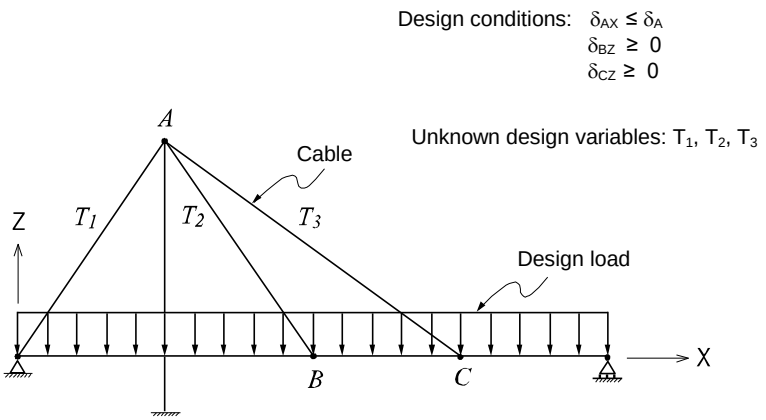

(c) Example of finding the initial cable tension loads, T_1, T_2 and T_3, that limit the lateral displacement at point A less than δ_A, and vertical displacements at points B and C greater than 0 under a given uniform loading condition

Figure 2.101 Examples of finding unknown loads that satisfy various design conditions